The role of γδ T cell subsets in angiotensin II-induced hypertension and vascular injury

Ahmad Usama Mohammad Mahmoud

Division of Experimental Medicine

McGill University

Final thesis submission in May 2022

(A thesis submitted to McGill University in partial fulfillment of the requirements of the degree of PhD Experimental Medicine – Thesis)

Table of Contents

Abstract

Hypertension (HTN), characterized by elevated blood pressure (BP), is the leading risk factor for global disease burden. Investigation of its mechanisms is important for the discovery of novel biomarkers and treatment targets that will allow improving outcomes for patients with HTN. Our laboratory has dedicated much of its activity to the search of new mechanisms that could reveal previously unknown biomarkers and therapies. Among such mechanisms, we and other investigators have focused on immune mechanisms, and have previously shown that both innate (monocytes/macrophages) and adaptive immune cells (T lymphocytes) play an important role in the development of HTN and vascular damage in mouse models. We previously demonstrated that a small subpopulation of T cells considered "innate-like", expressing the γδ T cell receptor (TCR) instead of the conventional αβ TCR, plays a key role in HTN and vascular injury. γδ T cells can be subdivided according to the TCR variant (V) γ subtype that is generally specific for a tissue. A subpopulation of lung and skin γδ T cells that are $V\gamma6^+$ and produce interleukin (IL)-17A was shown to respond promptly to pneumococcal infection and skin inflammation. However, γδ T cell Vγ subtype(s) involved in HTN are still unknown. We hypothesized that $V\gamma6^+$ γδ T cells may play a role in angiotensin (Ang) II-induced HTN.

The objectives of this thesis were 1) to determine the distribution of γ TCR subtypes expressed by γδ T cells in the spleen, mesenteric lymph nodes (MLNs), thoracic aortic (TA) perivascular adipose tissue (PVAT), and mesenteric artery (MA) PVAT upon infusion of Ang II in mice, 2) to investigate the role of $V\gamma6^+$ γδ T cells in Ang II-induced HTN and vascular injury, and 3) to study the contribution of a second candidate, $V\gamma4^+$ γδ T cells, to Ang II-induced BP elevation and vascular damage.

The first study of this thesis showed a differential distribution of γδ T cell Vγ subtypes in lymphoid tissues (spleen and MLNs) compared to PVAT (TA and MA). $V\gamma6^+$ γδ T cells were the most abundant γδ T cell Vγ subtype in both TA and MA PVAT and their frequency was increased by Ang II infusion in the spleen and TA PVAT and tended to augment in MA PVAT.

The second study revealed that the frequency of IL-17 producing effector memory $V\gamma6^+$ γδ T cells was increased in the spleen and tended to be elevated in MA PVAT in Ang II-infused mice compared to control mice. Unexpectedly, blocking of $V\gamma6^+$ γδ T cells in Ang II-infused mice enhanced the early elevation of the systolic and diastolic BP and reduced the MA dilatory response to acetylcholine compared to control Ang II-infused mice.

The third study demonstrated that depletion of TCR $V\gamma4^+$ γδ T cells did not cause any change in Ang II-induced BP elevation or vascular injury in mice.

To conclude, the distribution of γδ T cell Vγ subtypes was different in lymphoid tissues compared to PVATs. $V\gamma6^+$ γδ T cells play a protective role in Ang II-induced HTN and vascular dysfunction. Activation of $V\gamma6^+$ γδ T cells could be a therapeutic approach to control inflammation in Ang II-induced HTN.

Résumé

L’hypertension (HTN) caractérisée par une augmentation de la tension artérielle (TA), est le principal facteur de risque du fardeau mondial résultant de maladies. L'étude de ses mécanismes est importante pour la découverte de nouveaux biomarqueurs et cibles thérapeutiques qui permettront d'améliorer les soins aux patients atteints d'HTN. Notre laboratoire a consacré une grande partie de son activité à la recherche de nouveaux mécanismes qui pourrait révéler des biomarqueurs et des cibles thérapeutiques jusqu'à ce moment inconnus. Parmi ces mécanismes, nous et d'autres chercheurs nous sommes concentrés sur les mécanismes immunitaires et avons auparavant montré que les cellules immunitaires innées (monocytes/macrophages) et adaptatives (lymphocytes T) jouent un rôle important dans le développement de l’HTN et des lésions vasculaires dans des modèles murins. Nous avons précédemment démontré qu'une petite sous-population de cellules T considérées comme "innées", exprimant le récepteur des cellules T (RCT) γδ au lieu du RCT αβ conventionnel, joue un rôle clé dans l'HTN et les lésions vasculaires. Les lymphocytes T γδ peuvent être subdivisés selon le sous-type de variant (V) du RCT γ qui est généralement spécifique d'un tissu. Il a été démontré qu'une sous-population de lymphocytes T γδ $V\gamma6^+$ pulmonaires et cutanés produisant l'interleukine (IL)-17A répondait rapidement à une infection à pneumocoques ou à une inflammation cutanée. Cependant, le ou les sous-types Vγ des lymphocytes T γδ impliqués dans l'HTN sont encore inconnus. Nous avons émis l'hypothèse que les lymphocytes T γδ $V\gamma6^+$ pourraient jouer un rôle dans l'HTN induite par l'angiotensine (Ang) II.

Les objectifs de cette thèse étaient: 1) de déterminer la distribution des sous-types de RCT γ exprimés par les cellules T γδ dans la rate, les ganglions lymphatiques mésentériques (GLM), le

tissu adipeux périvasculaire (TAPV) de l'aorte thoracique (AT) et des artères mésentériques (AM) après infusion d'Ang II chez des souris. 2) Déterminer le rôle des cellules T γδ Vγ6$^+$ dans l'HTN et les lésions vasculaires induites par l'Ang II. 3) Étudier la contribution d'un deuxième candidat, les cellules T γδ Vγ4$^+$, dans l'élévation de la TA et les dommages vasculaires induits par l'Ang II.

La première étude de cette thèse a montré une distribution différentielle des sous-types Vγ des lymphocytes T γδ dans les tissus lymphoïdes (rate et GLM) par rapport au TAPV (AT et AM). Les lymphocytes T γδ Vγ6$^+$ étaient le sous-type de Vγ de lymphocytes T γδ le plus abondant dans les TAPV de L'AT et des AM, et leur fréquence était augmentée dans la rate et le TAPV de l'AT par la perfusion d'Ang II, et tendait à être plus élevée dans le TAPV des AM.

La deuxième étude a révélé que la fréquence des cellules T γδ mémoires effectrices Vγ6$^+$ produisant l'interleukine (IL)-17 était augmentée dans la rate, et tendait à être élevée dans le TAPV des AM chez les souris infusées à l'Ang II par rapport aux souris témoins. De manière inattendue, le blocage des cellules T γδ Vγ6$^+$ chez les souris infusées à l'Ang II a exagéré le début de l'élévation de la TA systolique et diastolique et a réduit la réponse dilatatrice des AM à l'acétylcholine par rapport aux souris témoins infusées avec l'Ang II.

La troisième étude a démontré que la déplétion des lymphocytes T γδ Vγ4$^+$ n'a causé aucun changement dans l'élévation de la TA ou des lésions vasculaires induites par l'Ang II chez des souris.

Pour conclure, la distribution des sous-types Vγ de cellules T γδ était différente dans les tissus lymphoïdes par rapport aux TAPV. Les lymphocytes T γδ Vγ6$^+$ jouent un rôle protecteur dans l'HTN et la dysfonction vasculaire induits par l'Ang II. L'activation des cellules T γδ Vγ6$^+$ pourrait être une approche thérapeutique pour contrôler l'inflammation dans l'HTN induite par l'Ang II.

Abbreviations

12/15-LO	12/15-lipoxygenase
AA	Arachidonic acid
αβ T cells	Alpha beta T cells
ABPM	Ambulatory blood Pressure measurement
ACE	Angiotensin-converting enzyme
Ach	Acetylcholine
AF	Alexa fluor
AML1	Acute myeloid leukemia 1
Ang II	Angiotensin II
AOBP	Automated office blood Pressure measurement
APC	Allophycocyanin
APCs	Antigen-presenting cells
APS	Ammonium persulfate
ARB	Angiotensin receptor blocker
Arg1	Arginase 1
AT_1R	Angiotensin type 1 receptor
AT_2R	Angiotensin type 2 receptor
ATP	Adenosine triphosphate
BAT	Brown adipose tissue
BB	Brilliant blue
BeAT	Beige adipose tissue
BK_{Ca}	Calcium-activated potassium channels
BP	Blood Pressure
BSA	Bovine serum albumin
BTN3A1	Butyrophilin subfamily 3, member A1
BUV	Brilliant ultraviolet
BV	Brilliant violet

C	Constant
Ca^{2+}	Calcium ion
cAMP	Cyclic adenosine monophosphate
CCR2	C–C motif chemokine receptor type 2
CCR6	C-C motif chemokine receptor type 6
CD	Cluster of differentiation
CD40L	CD40 ligand
CD62L	CD62 ligand
CDRs	Complementarity-determining regions
CF	Cyanine-based fluorescent dye
cGMP	Guanosine monophosphate
COX	Cyclooxygenases
CTLA-4	Cytotoxic T-lymphocyte-associated antigen 4
CVD	Cardiovascular disease
CXCL16	C-X-C Motif Chemokine Ligand 16
CXCL2	CXC-chemokine ligand 2
CXCR3	C-X-C motif chemokine receptor type 3
CXCR6	C-X-C Motif Chemokine Receptor 6
Cy	Cyanine
CsA	Cyclosporine A
δ	Delta
D	Diversity
DAMPs	Damage-associated molecular patterns
DBP	Diastolic blood Pressure
DC	Detergent compatible
DCs	Dendritic cells
DETCs	Dendritic epidermal T cells
DN	Double-negative
DOCA	Deoxycorticosterone acetate
E13	Embryonic day 13
ECE	Endothelin-converting enzyme

ECM	Extracellular matrix
ECs	Endothelial cells
EDHF	Endothelium-derived hyperpolarizing factor
EDTA	Ethylenediaminetetraacetic acid
EETs	Epoxyeicosatrienoic acids
Egr	Early growth response
EGTA	Ethylene glycol-bis(β-aminoethyl ether)-N,N,N′,N′-tetraacetic acid
eNOS or NOS III	Endothelial nitric oxide synthase
ERK1/2	Extracellular signal-regulated kinase 1/2
ET-1	Endothelin-1
ET_AR	Endothelin type A receptor
ET_BR	Endothelin type B receptor
FasL	Fas ligand
FBS	Fetal bovine serum
FGF2	Fibroblast growth factor 2
FGL2	fibrinogen-like protein 2
FITC	Fluorescein isothiocyanate
FMO	Fluorescent minus one
FOXP3	Forkhead box protein P3
FSC-A	Forward scatter area
FSC-W	Forward scatter wide
γ	Gamma
Gal-1	Galectin-1
γδ T cells	Gamma delta T cells
γδTn cells	Naïve γδ T cells
GITR	Glucocorticoid-induced tumor necrosis factor receptor-related protein
H_2O_2	Hydrogen peroxide
H2S	Hydrogen sulfide
HBPM	Home blood Pressure monitoring
HETEs	Hydroxyeicosatetraenoic acids
HLA-DR	Human leucocyte antigen DR

HMBPP	(E)-4-hydroxy-3-methyl-but-2-enyl pyrophosphate
HR	Heart rate
HTN	Hypertension
Id3	Inhibitor of DNA binding 3
IELs	Intraepithelial lymphocytes
IFN-γ	Interferon-gamma
IGF-1	Insulin-like growth factor 1
iIELs	Intestinal intraepithelial lymphocytes
IK_{Ca}	Intermediate-conductance calcium-activated potassium channels
IL	Interleukin
IL-17RC	IL-17 soluble receptor C
IL-2Rα	IL-2 receptor alpha chain
IMGT	International ImMunoGeneTics information system
iNKT cells	Invariant natural killer T cells
iNOS or NOS II	Inducible nitric oxide synthase
IP	Intraperitoneal
IP-10	IFN-γ–induced protein 10
IP3	Inositol triphosphate
IPP	Isopentenyl pyrophosphate
IsoLG	Isolevuglandin
I-TAC	IFN-inducible T-cell α chemoattractant
iTreg	Induced T regulatory lymphocytes
J	Joining
K^+	Potassium ion
K_{IR}	Rectifying K^+
L-NAME	N^{ω}-Nitro-L-arginine methyl ester
LNs	Lymph nodes
LTs	Leukotrienes
LXs	Lipoxins
M/L	Media-to-lumen ratio
M1 macrophage	Type-1 macrophage (pro-inflammatory)

M2 macrophage	Type-2 macrophage (anti-inflammatory)
MA	Mesenteric artery
mAb	Monoclonal antibody
MAIT cells	Mucosal-associated invariant T cells
MAP	Mean arterial pressure
MAPK	Mitogen-activated protein kinase
MCP-1	Monocyte chemoattractant protein-1
MCSA	Media cross-sectional area
M-CSF	Macrophage-colony stimulating factor
MDSCs	Myeloid-derived suppressor cells
MHC	Major histocompatibility complex
MIG	Monokine induced by IFN-γ interferon
MLC	Myosin light chain
MLCK	Myosin light chain kinase
MLNs	Mesenteric lymph nodes
MMP/TIMPs	Matrix metalloproteinase/tissue inhibitors of metalloproteinases
MMP-2	Matrix metalloproteinase-2
MR	Mineralocorticoid receptor
MR1	MHC-I-related
Na^+	Sodium ion
NADPH	Nicotinamide adenine dinucleotide phosphate
NE	Norepinephrine
NEP	Neutral endopeptidase
NETs	Neutrophil extracellular traps
NFAT	Nuclear factor of activated T cells
NK cells	Natural killer cells
NLR	Neutrophil-to-lymphocyte ratio
nNOS or NOS I	Neuronal nitric oxide synthase
NO	Nitric oxide
non-AOBP	non-automated office blood Pressure measurement
Nrp-1	Neuropillin-1

NSAID	Nonsteroidal anti-inflammatory drug
nTreg	Natural T regulatory lymphocytes
OBPM	Office blood Pressure measurement
PA	Physical activity
PAgs	Phosphoantigens
PAMPs	Pathogen-associated molecular patterns
PB	Peripheral blood
PBS	Phosphate-buffered saline
PE	Phycoerythrin
PerCP	Peridinin chlorophyll-A protein
PGH2	Prostaglandin H_2
PGs	Prostaglandins
PKA	Protein kinase A
PLA2	Phospholipase A_2
PLC	Phospholipase C
PMA	Phorbol 12-myristate 13-acetate
PP	Pulse pressure
Pre-proET-1	Pre-proendothelin-1
ProET-1	Proendothelin-1
PRRs	Pattern recognition receptors
pTα	Pre-Tα
PUFAs	Polyunsaturated fatty acids
PVAT	Perivascular adipose tissue
PWV	Pulse wave velocity
RAAS	Renin–angiotensin–aldosterone system
RAG-1	Recombination activating gene 1
RegIIIγ	Regenerating islet-derived protein 3γ
ROR γt	Retinoid-related orphan receptor gamma t
ROS	Reactive oxygen species
RPMI	Roswell Park Memorial Institute medium
RT-qPCR	Reverse Transcription-quantitative Polymerase Chain Reaction

RUNX1	Runt-related transcription factor 1
RUPP	Reduced uterine perfusion pressure
SBP	Systolic Blood Pressure
SC	Subcutaneously
SDS	Sodium dodecyl sulfate
SDS-PAGE	Sodium dodecyl sulfate polyacrylamide gel electrophoresis
SFM	Serum-free media
sGC	Soluble guanylate cyclase
SK_{Ca}	Small-conductance calcium-activated potassium channels
SNP	Sodium nitroprusside
Sox13	SRY-box transcription factor 13
SSC-A	Side scatter area
SSC-W	Side scatter-wide
SVR	Systemic vascular resistance
TA	Thoracic aortic
TAE	Tris-acetate-EDTA
Tc	Cytotoxic T cell
T_{CM}	Central memory γδ T
TCR	T cell receptor
T_{EM}	Effector memory γδ T
TEMED	Tetramethylethylenediamine
T_{EMRA}	$CD45RA^+$ effector memory T cells
TGF-β1	Transforming growth factor-beta 1
TGF-β	Transforming growth factor-beta
Th	T helper lymphocyte
TLRs	Toll-like receptors
Tm	Melting temperature
TNF-α	Tumor necrosis factor-α
TonEBP	Tonicity-responsive enhancer binding protein
Treg	T regulatory lymphocytes
TXAs	Thromboxanes

UCP1	Uncoupling protein 1
V	Variable
VCAM-1	Vascular cell adhesion molecule 1
VEGF-C	Vascular endothelial growth factor C
VSMCs	Vascular smooth muscle cells
WAT	White adipose tissue
WT	Wild type
γδT1 cells	IFN-γ-producing γδ T cells
γδT17 cells	IL-17-producing γδ T cells

List of tables

CHAPTER I

CHAPTER III

CHAPTER IV

List of figures

CHAPTER I

CHAPTER II

CHAPTER III

CHAPTER IV

CHAPTER V

Contribution of authors

Ahmad U. M. Mahmoud:

- Design of experiments.
- Technical setup for most of the experiments.
- Production, purification, qualification, and quantification of mAbs specific to $V\gamma6^+$ γδ T cells (clones: 1C10-1F7 and 17D1).
- Collection of samples.
- Extra- and intracellular immunofluorescent staining for flow cytometry.
- Blood pressure analysis.
- Myography data analysis (partial).
- Design PCR primers for TCR gamma and delta variable gene segments.
- RT-qPCR.
- Statistical analysis.

Antoine Caillon:

- Design of experiments.
- Technical setup for some of the experiments.
- Flow cytometry data analysis.
- Statistical analysis (partial).

Brandon Shokoples:

- Design and performance of myography experiments.
- Myography data analysis (partial).

Nathanne S. Ferreira:

- Design and performance of myography experiments.

Kevin Comeau:

- Intracellular immunofluorescent staining for flow cytometry.

Robert E. Tigelaar:

- Provided 17D1 hybridoma.

Pablo Pereira:

- Provided mAb specific to $V\gamma7^{+}$ γδ T cells (clone: F2.67).

Yasunobu Yoshikai:

- Provided 1C10-1F7 hybridoma.

Pierre Paradis:

- Design of experiments.
- Supervision of work and evaluation of raw data.

Ernesto L. Schiffrin:

- Originated the study as a PI of CIHR grant.
- Design of experiments.
- Supervision of work and evaluation of raw data.
- Funding of studies.

Acknowledgements

First and foremost, I would like to praise and thank Allah, the almighty, who has granted countless blessings, knowledge, and opportunities to me, so that I have finally been able to accomplish the thesis.

I would like to express my sincerest thanks to several people who were there at every step of the way to help and support me through my PhD.

To my lovely wife and backbone, Tasneem Alghriany, for her love, care, and continued support. It is impossible to adequately thank you for everything you have done during this challenging journey, particularly through the difficult times during COVID-19 lockdown.

To my family, especially my parents, who have always been very supportive of my academic pursuits and desire to pursue my dream.

To Dr. Ernesto L. Schiffrin for his supportive supervision and invaluable guidance throughout my graduate studies.

To Dr. Pierre Paradis for sharing his scientific expertise and academic advice.

To all my colleagues in Dr. Schiffrin's laboratory, for their help, friendship, and support along the way.

To Adriana Cristina Ene, Veronique Michaud, Isabelle Miguel, Christian Young, Yvhans Chéry, Julie Labrèche, and Kathy Forner for their excellent technical support.

To the members of my thesis committees: Dr. Stéphane Richard, Dr. Ciriaco A. Piccirillo, Dr. Jean-François Tanguay, Dr. Donald C. Vinh, Dr. Koren Kathleen Mann, and Dr. Eric Thorin for their constructive comments.

To the Canadian Institutes of Health Research (CIHR), the Lady Davis Institute for Medical Research (LDI), and the Canadian Vascular Network (CVN) for their financial support.

To the Division of Experimental Medicine (EXMD) of McGill University, including Ms. Katrine Couvrette, Ms. Marylin Linhares, and Ms. Bhinesha Seetaram for their administrative assistance.

Statement of originality

In accordance with the guidelines of the Faculty of Graduate and Postdoctoral Studies of McGill University, the research presented in this thesis constitutes original work and collaboration from co-authors that is described in the section of contribution of authors. All chapters of this thesis were written by Ahmad UM Mahmoud and revised by Dr. Ernesto L. Schiffrin. All elements in this thesis represent original scholarship and a distinct contribution to knowledge.

This thesis is the first to show:

- The protective role of a γδ T cell subtype, $V\gamma6^+$ γδ T cells, in a mouse hypertensive model with vascular dysfunction.

- Another γδ T cell subtype, $V\gamma4^+$ γδ T cells, does not affect this hypertensive model.

CHAPTER I: Introduction

Review of the Literature and Research Objectives

1. Introduction

The cardiovascular system consists of the heart, the network of blood vessels (arteries, capillaries, and veins) and in humans approximately 5 liters of blood that is transported through the blood vessels. This system is a dual circulatory system comprising the systemic circulation and the pulmonary circulation. The pulmonary circulation connects the heart with both lungs and allows the cardiac output of deoxygenated blood to pass through the lungs to be reoxygenated. The systemic circulation then transports the oxygenated blood, as well as transfers nutrients, messenger molecules, and cells to peripheral tissues through the network of blood vessels.

The rate at which blood flow delivers these elements into the peripheral tissues is affected by the arterial blood pressure (BP), which results from the cardiac output and the total peripheral resistance. Under physiological conditions, the normal BP that is exerted against arterial walls during systole of the heart, termed a systolic BP (SBP), rises to around 120mm Hg in humans and most animals, whereas the arterial BP generated during diastole of the heart, the diastolic BP (DBP), falls to around 80mm Hg. When BP is constantly at or above the threshold of 140/90mm Hg, the risk of cardiovascular events is increased, and this pathological condition is referred to as hypertension (HTN).

HTN is a multifactorial pathological condition that causes injury to the arterial system and leads to an impaired exchange of essential nutrients and bioactive products at the tissue level, and thereby is a major essential contributor to the development and progression of cardiovascular disease (CVD) that remains the leading cause of morbidity and mortality globally.[1] Uncontrolled HTN has an impact on several organ systems in the human body, and can independently or cooperatively cause CVD and associated complications, such as myocardial infarction, heart

failure, atrial fibrillation, cerebrovascular disease and stroke, chronic kidney disease, and peripheral vascular disease, which are associated with extensive morbidity and mortality.

Despite huge advances in hypertension research, the precise etiology of blood pressure elevation remains complex and not completely understood. It is essential to understand the fundamental mechanisms involved in the initiation and progression of HTN in order to develop more effective therapies. In recent decades, it has become increasingly evident that inflammation and the immune system influence blood pressure regulation and its effects on blood vessels and the kidney. Various innate and adaptive immune cells have been shown to play significant roles in the development and maintenance of HTN in experimental models of hypertension, mainly in rodents. Macrophages and T cells infiltrate and accumulate in the heart, the vasculature, the perivascular fat, and the kidney in the course of hypertension in humans, rats, and mice.[2-5] Hypertensive responses to vasoactive stimuli such as angiotensin II (Ang II), high-salt challenge or environmental stress are blunted in mice lacking lymphocytes, while the adoptive transfer of T cells, but not B cells, restores the blood pressure responses to these triggers.[6-8]. Furthermore, Ang II-induced BP elevation, mesenteric (MA) endothelial dysfunction, and spleen and MA perivascular adipose tissue (PVAT) T cell activation are blunted in *Tcrδ* null mice, which are devoid of gamma delta (γδ) T cells, and in mice injected with a γδ T cell-depleting antibody.[9] All these studies have established the basis for several advances revealing other mechanisms through which innate and adaptive immunity contribute to the pathogenesis of HTN. This thesis attempts to elucidate how small subsets of γδ T cells can influence the BP elevation and vascular dysfunction in Ang II-induced HTN in mice.

In this chapter, a brief introduction about the structural, functional, and mechanical features of arteries and relevant vasoactive factors, and the pathophysiology behind arterial hypertension will be described. Next, the diverse elements of vascular inflammation in context of CVD with focus on T cell subsets will be described in more detail. Our current understanding of the pathophysiological role of γδ T cells in the context of HTN will be presented. The literature review will be followed by three recent studies, respectively chapters III and IV and V, that demonstrate that γδ T cell subsets can participate in the development and maintenance of Ang II-induced HTN. Finally, a general discussion will be provided in chapter VI about the role of γδ T cell subsets in BP regulation, vascular damage, and activation of other T cells in mice with Ang II-induced HTN.

2. The arterial wall

The arterial system is composed of a network of blood vessels called “arteries”. Most arteries in this system carry the cardiac output of oxygenated blood to organs and tissues in the body; the two exceptions are the pulmonary and umbilical arteries, which carry deoxygenated blood to the lungs and placenta, respectively, that can oxygenate it. Alterations in the systemic arterial system harmfully influence the delivery of essential nutrients and oxygen to vital organs and tissues, contributing thus to CVD.

Systemic arteries can be broadly subdivided into elastic or conduit and muscular arteries according to the relative composition of elastic and muscular tissue in the arterial wall structure. Larger arteries, such as the aorta, carotids, epicardial coronary, iliac, and femoral arteries, are elastic whereas smaller ones, which issue from larger arteries, are muscular with a relatively thick muscular medial layer. Under pathological conditions, such as atherosclerosis, large arteries are

affected [10], whereas in HTN, both large and small arteries are affected by remodeling and functional changes.[11 12] A basic understanding of the anatomy and physiology of normal arteries is required to clearly comprehend the pathological alterations in large and small arteries in CVD.

2.1. Normal arterial wall structural features

The arterial wall is a well-organized connective tissue structure that comprises three main layers (or tunicae) that are from the innermost to the outermost: the intima, the media, and the adventitia, with various components of extracellular matrix (ECM) in between and the PVAT that is surrounding it (**Figure I-1**).

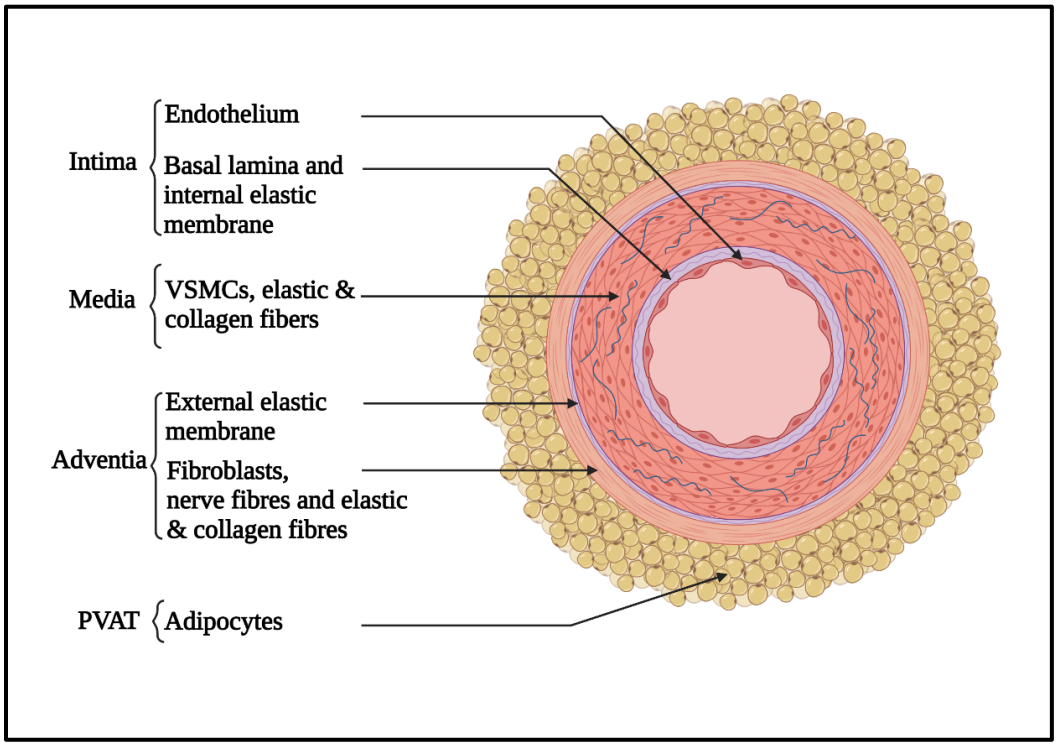

Figure I-1: Transverse section showing normal artery structure.

Created with BioRender.com

2.1.1. Intima

The intima is the inner lining layer of the arterial wall. The intimal layer consists predominantly of a monolayer of squamous endothelial cells (ECs), the endothelium, the basement membrane, then a thin layer of a loose connective tissue, and finally the internal elastic lamina (membrane) that is composed mainly of elastic fibers. The endothelial layer is known to be a highly dynamic organ that is present on all vascular surfaces that are in contact with the blood and could be considered the largest organ in the body.[13] An intact endothelium is crucial for the normal functionality of arteries and other vessels in the vascular tree. The normal endothelium consists of ECs that play a key role in controlling vascular tone by responding to mediators circulating in the blood and sensing mechanical forces generated by flowing blood to release vasoactive factors that act on neighboring vascular smooth muscle cells (VSMCs).[14 15] The integrity of endothelial cell morphology controls the vascular permeability to molecules and cells.[15] During inflammation, for example, alterations can occur in endothelial cytoskeletal structures and inter-endothelial junctions that affect the vascular permeability to macromolecules such as leucocytes.[16 17] The following layer, the basement membrane or basal lamina, is a connective tissue that provides anchoring support for the endothelium and acts as a boundary between the endothelium and the underlying elastic connective tissue. The outermost layer of the intima, internal elastic lamina, contains a small amount of elastic and collagen fibers that provide further flexibility and rigidity, respectively, to the arterial wall.[18 19]

2.1.2. Media

The following layer of the arterial wall is the media that consists predominantly of VSMCs surrounded by ECM components, which include elastin, collagen fibers and fibronectin. VSMCs are responsible for regulating the arterial tone and controlling the BP via vasodilation and vasoconstriction processes. The polarization state of VSMCs that regulates the contractility of the artery is altered by vasoactive mediators produced by ECs and/or those circulating in the bloodstream as well as autonomous nervous system nerves innervating blood vessels and products generated in PVAT. The interplay of ion channels on the plasma membrane of VSMCs also plays an important role in modulating the vascular tone of arteries.[20 21] ECM components are deposited by VSMCs in the arterial media and account for the passive mechanical properties of the arteries. Myogenic tone, that is the contractile response of vessels to increases in intraluminal pressure, may be an important player in the development of HTN, since it may be exaggerated in humans and animals susceptible to HTN. Indeed, VSMCs also regulate the arterial diameter by sensing and responding to mechanical stresses applied to the arterial wall through their tight association with ECM components in a process known as cellular mechanotransduction.[22 23]

Elastic fibers of the media provide the arteries with the elasticity to expand and recoil to reduce the high BP induced by cardiac output during ventricular contraction. Collagen fibers are deposited and circumferentially aligned to limit arterial wall distension when exposed to excessive pressures, provide support to the arterial wall structure, and prevent vascular rupture.[19 24] According to the artery type, the media contains varying amounts of elastic and collagen fibers.[25] The largest arteries in the body, also known as elastic arteries or conduit arteries, contain a large amount of elastic and collagen fibers in the media. Furthermore, fibronectin is a key regulator of

vascular remodeling by controlling the deposition, organization and stability of other ECM molecules.[26]

In contrast, the small arteries, which are also known as muscular arteries or distributing arteries and gradually branch out from conduit arteries, contain less amount of the fibrous connective tissue in the media. These are the source of most of the energy dissipation that results in peripheral resistance, and are accordingly also known as resistance arteries, especially the smaller ones with a lumen diameter under 300 microns.

The media of resistance arteries is comprised mainly of VSMCs that are extensively innervated by sympathetic nerves, and elastic fibers. Consequently, resistance arteries are able to regulate blood flow through arterial constriction and dilation as a result of vascular myogenic responses and upon sympathetic activity modulation.[27 28]

2.1.3. Adventitia

The adventitia is the outermost layer of the arterial wall that surrounds the tunica media. It consists mainly of fibroblasts that produce ECM components such as collagen and elastin.[18 29] The high collagen content in the adventitia plays a protective role against vascular rupture in extremely high pressure conditions.[24] Besides the structural support role for blood vessels, adventitial fibroblasts have been more recently recognized to be involved in vascular inflammation. In response to vascular stresses, adventitial fibroblasts are activated to produce reactive oxygen species (ROS), growth factors and vasoactive mediators that, collectively, influence medial VSMC proliferation, vascular tone, and the recruitment of circulating inflammatory cells to the arterial wall.[30-32]

The adventitia is the most complex compartment in the arterial wall structure as it contains a wide range of cells besides adventitial fibroblasts, including resident progenitor cells and immunomodulatory cells. These resident adventitial cells are often the first to be reprogrammed and activated to then regulate the tone and structure of the arterial wall.[29] In addition to fibroblasts, the adventitia contains a network of small blood vessels known as vasa vasorum that provide nourishment and oxygen to the adventitia and media.[19] This region also contains non-myelinated nerve endings that regulate the VSMC tone in the media.[33]

2.1.4. The extracellular matrix

A substantial component of the arterial wall is the ECM that is predominantly synthesized and organized by VSMCs. The vascular ECM does not only define the arterial mechanical properties but also influences the regulation of immune cell activation and modulation of the effects of growth factors and other stimuli on the vascular tone.[34] Under physiological conditions, the ECM structure is constantly maintained through a careful equilibrium between synthesis, deposition, and degradation. Alterations in the arterial ECM play a critical role in the pathogenesis of some CVDs, including HTN and atherosclerosis.[35 36]

The vascular ECM molecular composition varies depending on the nature, size and position of the artery in the arterial tree.[37-39] The ECM is a non-cellular component that mainly comprises many fibrous proteins such as elastin fibers and various types of collagen fibers, which are connected to the vascular wall cells via glycoproteins such as fibronectin.[39] Elastin fibers amply exist in the wall of large elastic arteries, and to a much lesser extent in smaller muscular arteries.[40] Crosslinking between elastin fibers affords its key function, elasticity, which is required in large

arteries to withstand the high pulsatile pressure generated by the systole of the heart.[41-43] As opposed to elastin fibers, collagen fibers confer rigidity and tensile strength to the arterial wall. As the pressure in the artery increases, collagen fibers are deposited and circumferentially distributed to support wall stress and limit arterial wall distension.[44 45] Type I and type III collagen are the most abundant collagen subtypes found in the normal arterial wall.[46 47] Along with these collagens albeit to a lesser extent, collagen type IV and V are also found in the ECs and VSMCs basement membranes.[48] The glycoprotein fibronectin is another ECM component that plays a pivotal role in interactions between other ECM components and vascular cells, and is a major determinant of the rigidity of the arterial wall.[49 50]

2.1.5. The perivascular adipose tissue

The PVAT is a unique adipose tissue which surrounds the outer limits of the adventitia of most blood vessels and has significant roles in vascular physiology and pathophysiology.[51] The quantity and type (white, brown or beige) of the PVAT varies according to the species and the anatomical location. In rodents, the thoracic aorta is surrounded by brown adipose tissue (BAT), while the abdominal aorta is surrounded by a mixture of WAT and brown-like adipose tissue known as beige adipose tissue (BeAT). Smaller arteries such as mesenteric and femoral arteries are surrounded by white adipose tissue (WAT). There is no adipose tissue surrounding the coronary arteries (**Figure I-2**).[52 53] In humans and large experimental animal models, such as pigs and rabbits, all aforementioned arteries are surrounded by PVAT.[52]

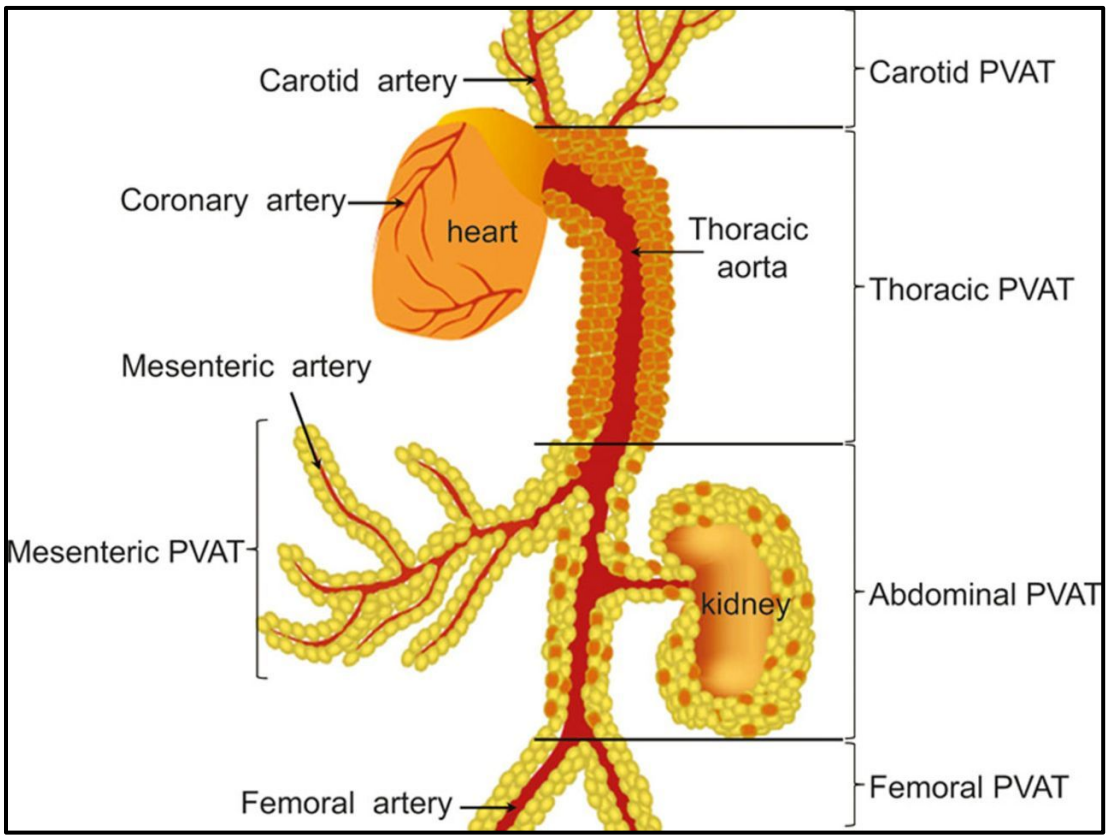

Figure I-2: Types of PVAT. Adapted from Brown et al.[52]

Although the PVAT surrounds most arteries, it has not received appropriate research attention until 1991 when *Soltis* and *Cassis* shed light on the role of PVAT in regulation rat aortic tone by targeting VSMCs.[54] Traditionally, PVAT had long been considered as mechanical support for the vasculature and a lipid-storage depot. However, recent studies have shown that PVAT can also control vascular tone, VSMC proliferation and migration, and thermoregulation, through production and secretion of pro-inflammatory and anti-inflammatory adipokines (e.g., adiponectin, leptin, and omentin), cytokines/chemokines (e.g., interleukin [IL]-6, tumor necrosis factor-α [TNF-α], and monocyte chemoattractant protein-1 [MCP-1]), vasoactive factors (e.g., prostacyclin, Ang 1-7, Ang II, reactive oxygen species [ROS], and methyl palmitate), and gaseous molecules (e.g., nitric oxide [NO] and hydrogen sulfide [H_2S]).[55-58] Adiponectin, prostacyclin, Ang 1–7, NO, H_2S, and methyl palmitate cause vasodilation, whereas, Ang II, ROS, and other yet

unidentified mediators induce vasoconstriction. Thus, PVAT-derived factors collaboratively regulate vascular tone.[59] These factors act in an autocrine fashion on adipocytes, which are the main cell population in the PVAT, or in paracrine fashion to activate or inhibit the adjacent vascular cells such as VSMCs, ECs, fibroblasts, as well as immune cells including T and B cells, macrophages and dendritic cells, or in endocrine fashion to influence the response of many tissues, including the hypothalamus, pancreas, liver, kidney and immune system, to modulate different physiological functions including neuroendocrine function, thermogenesis, blood pressure regulation, and immunity.[52 60 61]

The PVAT possesses important anticontractile effects that are mediated by both endothelium-dependent and endothelium-independent pathways.[62] Under pathological conditions, PVAT secretes more inflammatory adipokines and cytokines that alter PVAT characteristics and its secretion profile, which eventually affects vascular function and contributes to vascular dysfunction.[63 64] In addition to adipocytes, PVAT contains complex dynamic cell populations such as nerve cells, stem cells and a wide spectrum of immune cells that collectively regulate vascular function.[56 65]

2.2. Vascular function

Vascular responses are determined by the interaction and balance between vasoconstrictor and vasodilatory signaling, mediated by various vasoactive factors that target ECs and VSMCs. The outcome of signaling by vasoactive factors determines whether the blood vessel constricts or dilates. Vascular tone refers to the contractile activity of VSMCs. Signaling by a variety of vasoactive factors directly or indirectly influences the intracellular levels of free calcium (Ca^{2+}) in

VSMCs, which as a result determines its contractility. Increased intracellular free Ca^{2+} concentration in VSMCs stimulates calmodulin-dependent activation of myosin light chain kinase (MLCK) that phosphorylates myosin light chain (MLC). Phosphorylation of MLC triggers myosin-actin interactions causing VSMC contraction.[65] In addition to this calcium-dependent mechanism, VSMC contraction is also regulated by calcium-independent pathways, including RhoA-Rho kinase, protein kinase C and mitogen-activated protein kinase (MAPK) signaling, ROS, and actin cytoskeleton reorganization.[66] Emerging evidence also refers to the important role of immune-inflammatory system activation and some types of non-coding RNAs in vascular tone regulation by targeting VSMCs.[67 68] Furthermore, the endothelium is intricately implicated in the regulation of vascular tone. This aspect will be developed in the following section.

2.2.1. Factors released from endothelial cells

The endothelium releases various factors that regulate vascular tone, and consequently control the blood flow through the arteries. These factors include nitric oxide (NO), eicosanoids (e.g., prostacyclin and thromboxane A2), endothelium-derived hyperpolarizing factor (EDHF), and endothelin-1 (ET-1). The main endothelium-derived factors that mediate VSMC relaxation are depicted in **Figure I-3**.

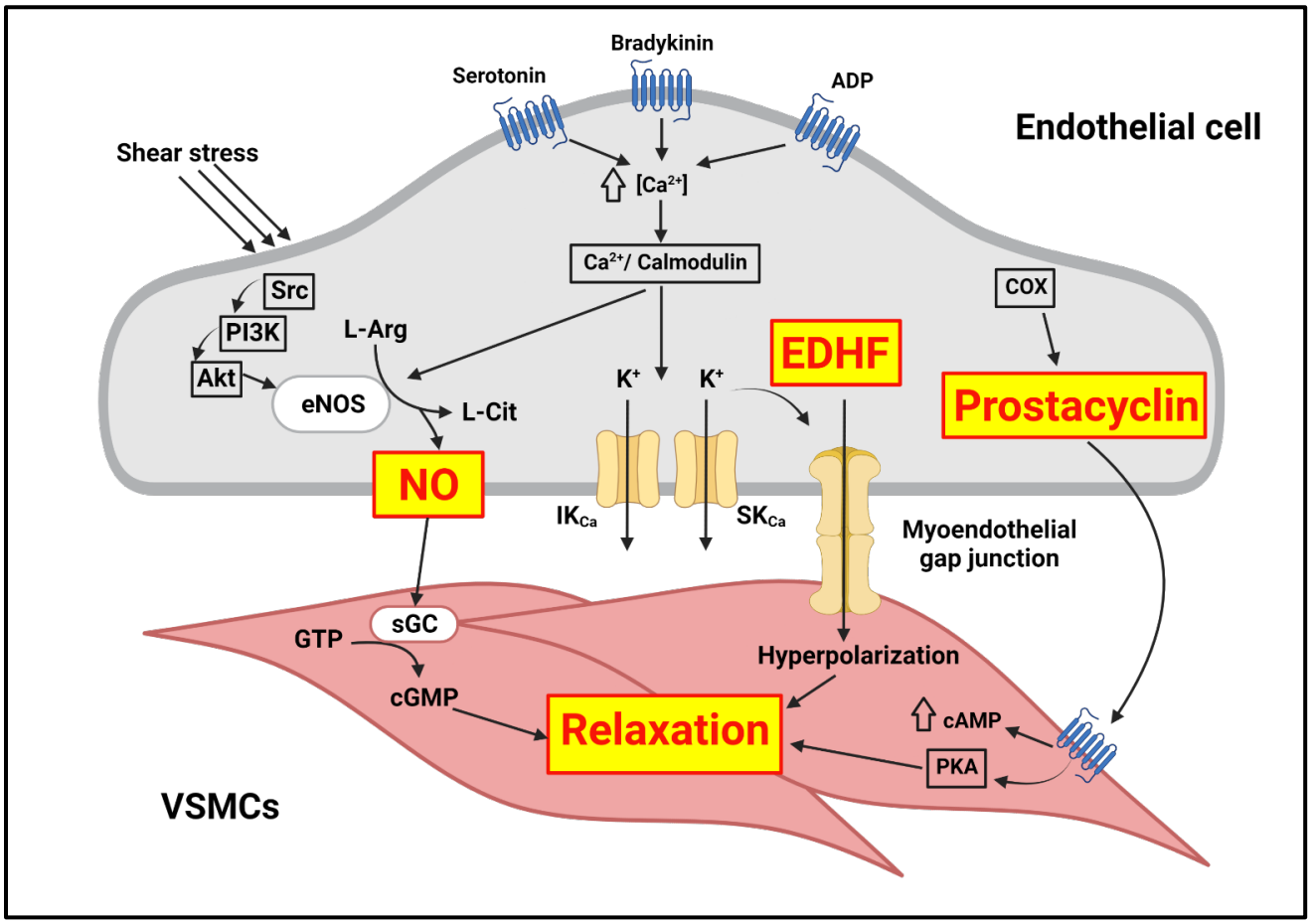

Figure I-3: Endothelium-derived factors that mediate VSMC relaxation.

Created with BioRender.com

2.2.1.1. Nitric oxide

Nitric oxide (NO) is the main vasodilator factor produced by ECs to modulate vascular dilatory tone. In the endothelium, NO is synthesized when the enzyme endothelial NO synthase (eNOS or NOS III) catalyzes the conversion of L-arginine to L-citrulline in a Ca^{2+}-dependent manner.[69] There are two other isoforms of NOS that can also catalyze NO production: neuronal NOS (nNOS or NOS I) and inducible NOS (iNOS or NOS II).[70] During inflammatory responses, iNOS activity is increased in ECs and activated macrophages, which are a major subset of innate immune cells, to produce large amounts of NO.[71-73]

The enzymatic activity of eNOS is regulated by a variety of stimuli through widely different mechanisms. Mechanical stimuli exerted on the EC surface by fluid shear stress and agonists such as acetylcholine (Ach) and bradykinin augment eNOS activity in ECs.[74-76] eNOS is a calcium/calmodulin-dependent enzyme that undergoes phosphorylation at multiple sites, including serine, threonine, and tyrosine residues. eNOS phosphorylation at serine residue 1179 increases eNOS enzymatic activity and NO production.[77] On the other hand, certain inflammatory cytokines such as TNF-α can reduce eNOS activity and NO production in the endothelium.[78-80] Under pathophysiological conditions, the exaggerated production of the vasoactive peptide, endothelin-1, has been shown to downregulate eNOS expression in ECs, resulting in reduction of NO synthesis and causing vasoconstriction.[81 82]

Once formed, NO passively diffuses into the underlying VSMCs to stimulate the activation of soluble guanylate cyclase (sGC), which induces cyclic guanosine monophosphate (cGMP) production.[83] The cGMP prevents Ca^{2+} influx into VSMCs through Ca^{2+} channels, and

consequently the actin-myosin myofilament force sensitivity to Ca^{2+} is decreased, resulting in vasorelaxation.[84 85]

2.2.1.2. Eicosanoids

Eicosanoids are vasoactive mediators originated from the oxidation of 20-carbon polyunsaturated fatty acids (PUFAs), mainly arachidonic acid (AA). There are several subfamilies of eicosanoids, including prostaglandins (PGs), thromboxanes (TXAs), leukotrienes (LTs), hydroxyeicosatetraenoic acids (HETEs), epoxyeicosatrienoic acids (EETs), resolvins, lipoxins (LXs), and eoxins.[86] AA is released from cellular membranes by phospholipase A_2 (PLA_2). It is a substrate for cyclooxygenases (COX)-1 and -2, lipoxygenases, or cytochrome P450 enzymes.[87] COX-1 and-2 catalyze the conversion of AA into prostaglandin H_2 (PGH_2), a vasoconstrictor that can be further enzymatically converted into PGs and TXAs. COX-1 is considered a housekeeping enzyme that is constitutively expressed in most tissues, whereas COX-2 expression is inducible and its activity increases with cell activation, such as during inflammatory responses.[87] The main PG produced in ECs is prostacyclin, (also known as prostaglandin I2 or PGI_2), that stimulates the relaxation of VSMCs by activating adenylyl cyclase to produce cyclic adenosine monophosphate (cAMP). Increased levels of intracellular cAMP activate protein kinase A (PKA) that in turn inhibits the actin-myosin myofilament force sensitivity to Ca^{2+}, leading to VSMC relaxation and vasodilatation.[88 89] ECs can also produce TXAs, (specially TXA_2), which mediates VSMC contraction and subsequently vasoconstriction (**Figure I-4**).[90]

2.2.1.3. Endothelium-derived hyperpolarizing factor (EDHF)

Accumulating evidence since the 1980s has revealed that even after genetic and/or pharmacological manipulations to inhibit the vasodilatory effects of NO and PGI_2, there is residual endothelium-dependent vasorelaxation in response to chemical and/or mechanical stimuli. This phenomenon was particularly present in small resistance arteries. The unknown vasodilatory factor responsible for this effect became known as "endothelium-derived hyperpolarizing factor (EDHF)", since it led to the hyperpolarization of VSMCs and ECs.[91] EDHF is a putative non-NO or PGI_2 mediator that is thought to hyperpolarize and relax VSMCs by directly or indirectly opening of Ca^{2+}-activated potassium (K^+) ion channels on neighboring ECs or through a direct electrical coupling via myo-endothelial gap junctions, which facilitate the communication between ECs and VSMCs.[92 93]

Although the accurate molecular and chemical identity of EDHF has not yet been revealed, several factors have been proposed. EETs, which are products derived from AA metabolism in the cytochrome P450 pathway, generated by ECs show EDHF-like activity in certain vessels by inducing the opening of big-conductance calcium-activated potassium channels (BK_{Ca}) and hyperpolarizing VSMCs.[94 95] The cannabinoid anandamide, another metabolite of AA metabolism, may also act as an EDHF by working through cannabinoid receptors on ECs and VSMCs to hyperpolarize VSMCs.[96] K^+ ions have also been proposed to possess EDHF properties. Activation of EC receptors promotes the opening of small- and intermediate-conductance calcium-activated potassium channels (SK_{Ca} and IK_{Ca}, respectively) in ECs, leading to K^+ efflux and accumulation of K^+ ions in the intercellular space between ECs and VSMCs.[96] Elevation in myo-endothelial K^+ concentration can induce the hyperpolarization and relaxation of VSMCs by activating inwardly rectifying K^+ (K_{IR}) channels and Na^+–K^+-ATPase found in the myo-endothelial gap junctions

between EC and VSMCs.[92 97] Blockers of K^+ channels have been in fact used to investigate their role in regulation of the vascular tone in physiological and pathophysiological conditions.[98 99]

2.2.1.4. Endothelin-1

Endothelin-1 (ET-1) is a potent 21-amino-acid vasoconstrictor peptide, and one of three isoforms belonging to ET peptide family (ET-1, ET-2, and ET-3). ET-1 is the main isoform of ETs expressed and produced in many different tissues, particularly in the vascular endothelium.[100 101] ET-1 expression is induced by several stimuli, including vasoactive peptides such as Ang II[102], lipoproteins[103], inflammation[104], and growth factors[105]. NO[106 107], natriuretic peptides[108 109], and prostaglandins[110 111], and physical stimuli such as physiological fluid shear stress[112 113] are amongst the inhibitory regulators of ET-1 production.

Activation of ECs results in the production of pre-proendothelin-1 (pre-proET-1), which is initially converted to proendothelin-1 (proET-1) and then to the biologically inactive big ET-1.[114 115] The inactive precursors of big ET-1 are cleaved by endothelin-converting enzyme (ECE) to produce mature ET-1 in ECs, both intracellularly and on the cell membrane, and on the surface of adjacent VSMCs.[114] Neutral endopeptidase (neprilysin, NEP) may contribute to the degradation of mature ET-1.[116] Big ET-1 can also be cleaved by the matrix metalloproteinase-2 (MMP-2) to form ET-1 (1-32), which has potent vasoconstriction effects[117], or by the enzyme chymase to yield ET-1 (1-31), which is a weaker vasoconstrictor[118], and can promote several vascular inflammatory responses[119-121]. Mature ET-1 is released mostly abluminally from ECs toward underlying neighboring VSMCs rather than into the vascular lumen.[122-124] Consequently, ET-1 acts locally, in an autocrine and paracrine rather than in an endocrine fashion.

ET-1 acts through its two G-protein-coupled receptors: type A (ET_AR) and type B (ET_BR).[125] In the vascular system, ET_ARs are localized on the VSMCs, whereas ET_BRs are expressed on both ECs and VSMCs.[126] ET receptors are also expressed on cells outside of the vasculature, including certain innate immune cells such as neutrophils and macrophages, cardiomyocytes, and fibroblasts.[127-129] ET-1 binds to ET_AR and ET_BR on VSMCs to activate phospholipase C (PLC), which causes an accumulation of inositol triphosphate (IP3) and intracellular Ca^{2+} and, in turn, stimulates VSMC constriction and proliferation (**Figure I-4**).[130 131]

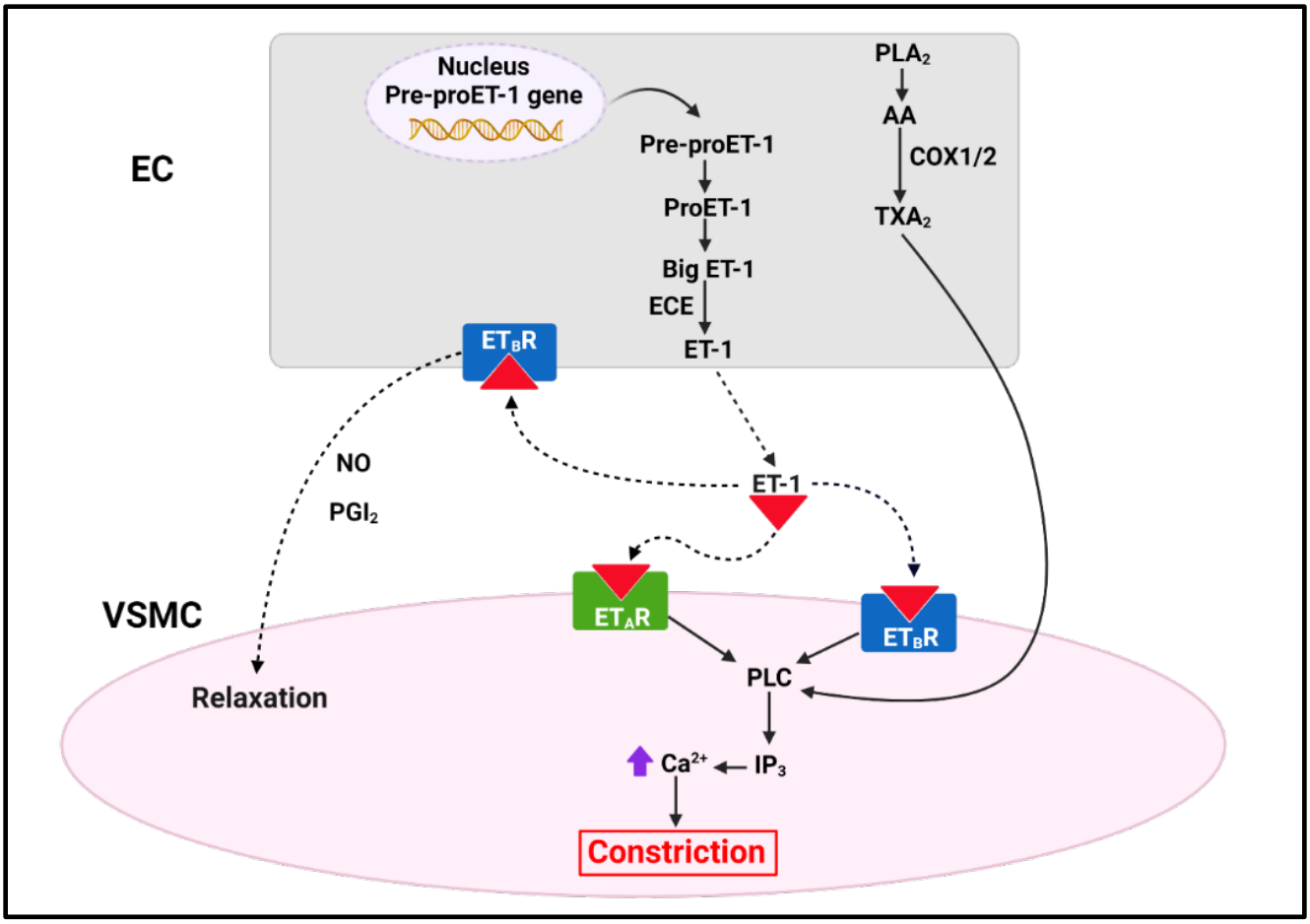

Figure I-4: Endothelium-derived factors that mediate VSMC constriction.

Created with BioRender.com

Conversely, the activation of endothelial ET_BR induces the release of endothelium-derived vasodilators, NO and PGI_2.[132-134] The endothelial ET_BRs also participate in the clearance of circulating ET-1[135], inhibit ECE expression in ECs[136], protect ECs from apoptosis[137], and mediate the reuptake of the extracellular ET-1 by ECs[138].

Beyond its classical vasoconstrictor function, ET-1 has further effects on the vasculature and other tissues. ET-1 is involved in mitogenic effects on VSMCs[139 140], cardiomyocytes[141 142], and glomerular mesangial cells in the kidney[143 144]. ET-1 signaling can stimulate local vascular inflammatory responses independently of BP elevation or systemic inflammation.[145] ET-1 signaling via ET_AR can also interact and synergize with the renin–angiotensin–aldosterone system (RAAS) to augment its effects on the vasculature and other tissues.[146] In several immune cells, ET-1 signaling stimulates the expression and production of various pro-inflammatory mediators and cell migration.[147-150]

2.3. Vascular mechanics

Blood flow and blood pressure generate forces exerted on the arterial wall. Stress refers to the force(s) applied per unit area. Arterial walls are subjected to shear stress due to flowing blood as well as circumferential stress from BP, which represent forces that cause arterial wall deformation.[19] In mechanics, strain is defined as the dimensional difference between the deformed vessel relative to the undeformed vessel.[151] Arterial distensibility is the measure of the arterial elasticity to expand or contract with increasing or decreasing intraluminal pressure.[152] As previously explained, this mechanical feature of arteries is mainly reliant on the structure of the ECM components deposited in the tunica media of VSMCs, and is accordingly different for large

and small arteries. Arterial distensibility or the "stiffness" of different vascular blood vessels can be measured using the stress-strain relationship at different intraluminal pressures.[153] A reduction in arterial distensibility, or an increase in arterial stiffness, has been linked to a variety of CVDs, including HTN and atherosclerosis.[154]

3. Hypertension

3.1. Global burden of hypertension

Hypertension (HTN), or high blood pressure (BP), is one of the most important contributors to CVD and the leading risk factor for morbidity and mortality worldwide. In 2017 and according to a systematic analysis of a study done on participants from 195 countries and territories, high systolic BP was the leading cause for mortality (10.4 million deaths) and disability-adjusted life years (218 million).[155] HTN is also the most expensive part of CVD cost. In 2016-2017, only in the United States, the estimated direct and indirect cost of hypertension was $52.4 billion[156], which was projected to increase to $200.3 billion and to $389.0 billion when taking treatment complications into consideration by 2030[157].

3.2. Blood pressure measurement and assessment

During cardiac left ventricular contraction or systole, the heart pumps blood into the aorta, from where it flows to peripheral arteries, and exerts a higher pressure called systolic blood pressure (SBP). During ventricular relaxation or diastole, the blood stops flowing from the left ventricle into the aorta while it continues to flow to peripheral arteries, and accordingly the

pressure against the arterial walls becomes lower and at the nadir is known as diastolic blood pressure (DBP).

In the 2020 Hypertension Canada guideline for BP diagnosis and assessment, four definitions of high BP were proposed following different forms of BP assessment.[158] The first stated that in automated office BP measurement (AOBP) using automated devices that average multiple readings per session such as BpTRU, a mean systolic BP ≥ 135 mm Hg or diastolic BP ≥ 85 mm Hg is considered high. According to this guideline and another study[159], AOBP is the preferred method of performing office BP measurement (OBPM). The second definition indicated that in non-automated office BP measurement (non-AOBP) using electronic (oscillometric) upper arm devices, a mean systolic BP ≥ 140 mm Hg or diastolic BP ≥ 90 mm Hg is considered high. A mean systolic BP between 130-139 mm Hg or diastolic BP between 85-89 mm Hg is considered high-normal. The third one was based on ambulatory BP measurement (ABPM), with which a mean awake systolic BP ≥ 135 mm Hg or diastolic BP ≥ 85 mm Hg, or a mean 24-hour systolic BP ≥ 130 mm Hg or diastolic BP ≥ 80 mm Hg is considered high. The last definition used home BP monitoring (HBPM), with which a mean systolic BP ≥ 135 mm Hg or diastolic BP ≥ 85 mm Hg is considered high.

3.3. Pathophysiology of hypertension

HTN is a progressive CVD of still unclear etiology, which does not usually cause symptoms.[160] HTN is in majority of cases essential (known also as primary or idiopathic), and the cause of it is unknown[161], while much less frequently, HTN arises secondary to an identifiable cause such as renal dysfunction[162], endocrine tumors[163] or pregnancy[164]. Various organs including

the heart, the vasculature, the kidneys, and the brain, as well as the interaction between different organs, contribute to the pathophysiology of hypertension. Furthermore, genetics, the diet and the environment are all factors that are involved in the development of hypertension.[165] [166] Chronic HTN is characterized by sympathetic nervous system hyperactivity, reduced ability of kidneys to excrete water and sodium, and significantly increased peripheral vascular resistance.[167] In addition to the contribution of the nervous system and the kidneys, structural and functional vascular alterations have essential roles in the development and maintenance of HTN.[168]

3.3.1. Blood pressure and peripheral vascular resistance

Maintenance of BP is essential for appropriate perfusion of tissues and organs. The blood perfusion to vital organs is affected when BP falls to too low levels, as happens in patients with vasodilatory septic shock, which can become a life-threatening condition.[169] BP is mainly affected by the hemodynamic influence of cardiac output and peripheral vascular resistance to blood flow. Essential HTN is typically characterized by increases in peripheral vascular resistance. However, in some types of HTN, increased cardiac output may also lead to BP elevation.[170]

Peripheral vascular resistance (also known as systemic vascular resistance or SVR) is the total resistance to blood flow throughout the systemic vasculature. Resistance to blood flow through an organ regulates the proportion of cardiac output that perfuses the organ.[171] Furthermore, differences in resistance within various organs also affects the percentage of cardiac output supplied to these organs. Hence, the resistance to blood flow is an important determinant of the control of blood volume distribution to different tissues through blood vessels.

Although large artery stiffness is a crucial contributor to increases in peripheral resistance that characterizes BP elevation in isolated systolic HTN and in the elderly, small resistance arteries are, classically, the key determinant of vascular resistance to blood flow, that is enhanced with the reduction of lumen size of these arteries.[39] Resistance arteries with a lumen diameter less than 300 μm are the most important location in the arterial bed of increases in vascular resistance leading to elevated BP.[172] The total vascular resistance to blood flow through a vessel can be assessed by the Hagen–Poiseuille equation as follows:

$$\boldsymbol{R} = \frac{\mathbf{8}}{\boldsymbol{\pi}} \times \frac{\mathbf{V} \times \mathbf{L}}{\boldsymbol{r_i^4}}$$

where R is the vascular resistance, V is the viscosity, L is the vessel length and r_i is the vessel radius. Since resistance is inversely proportional to the fourth power of the vessel radius, a slight reduction in lumen diameter results in a significant increase in vascular resistance. Changes in the structural and functional properties of resistance arteries cause a reduction in arterial lumen size and therefore an increase in vascular resistance. Vascular tone in the walls of resistance arteries is the key regulator of vascular resistance to blood flow through the vascular tree.[20] HTN is associated with increased peripheral vascular resistance as a result of vascular remodeling caused by structural and functional alterations in the walls of resistance arteries.[173]Increased intraluminal pressure in most of small resistance arteries that is associated with functional abnormalities of VSMCs[174-176] sensitizes abluminal VSMCs to constrict in a reflex referred to as myogenic response. Over time, sustained increase in pressure-induced constriction of VSMCs is implicated in blood flow dysregulation to vital organs leading to target organ damage.[177 178]

3.3.2. Pathophysiology of vascular remodeling in arterial hypertension

Arterial tone and stiffness are markedly affected by phenotypic and functional alterations occurring in the arterial walls, which are collectively referred to as vascular remodeling.[11] Alterations in the ratio between media thickness and lumen diameter (media-to-lumen ratio, M/L) and the media cross-sectional area (MCSA) are two main properties that distinguish vascular remodeling in the course of HTN.[179] Vascular remodeling occurs in both large and small arteries in HTN, however, the type of remodeling in each differs (**Figure I-5**).

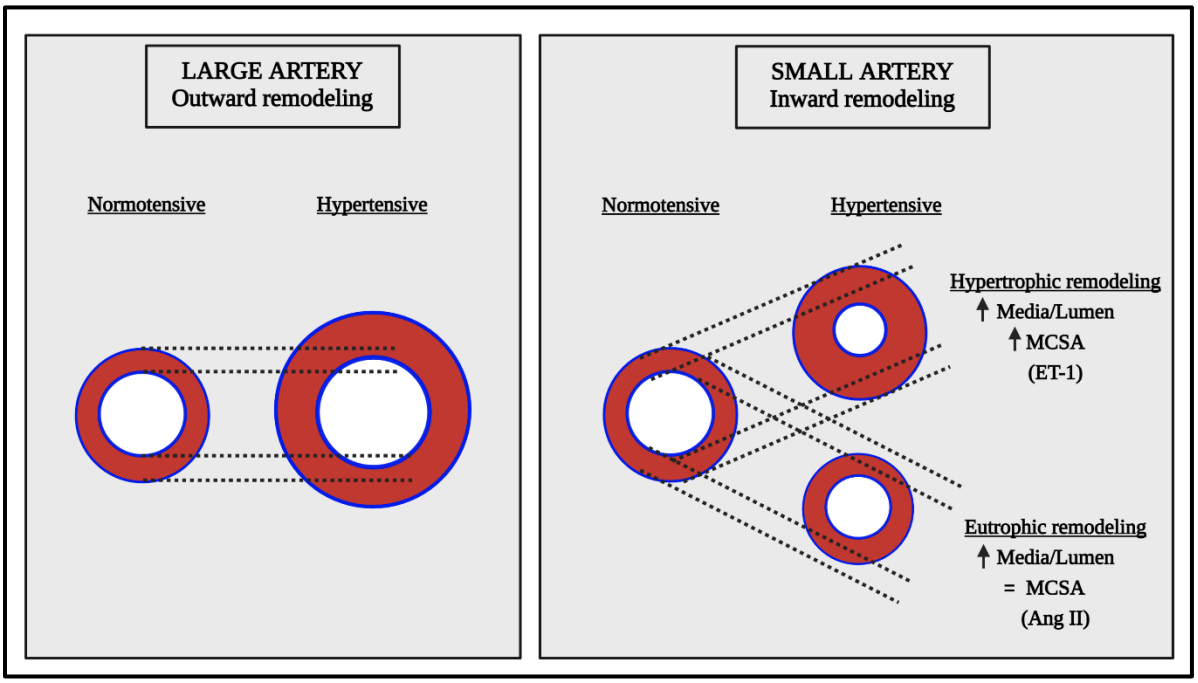

Figure I-5: Schematic diagram illustrating large and small artery remodeling during HTN. Adapted from Schiffrin[179]. Created with BioRender.com

In large arteries, such as the aorta, outward hypertrophic remodeling and arterial stiffness increase with advancing age.[180 181] Outward hypertrophic remodeling of large arteries involves an increase in lumen diameter along with an expansion in cross-sectional area of the media. In HTN, large arteries undergo outward hypertrophic remodeling due to VSMC hypertrophy (increase in

size) and sometimes hyperplasia (increase in number), whereas smaller arteries undergo inward eutrophic remodeling in some forms of HTN such as stage I essential HTN, whereas in severe hypertension, hypertension associated with diabetes mellitus[182], acromegaly[183] or renal artery stenosis[184], remodeling may be hypertrophic.[185-187] Apoptosis of VSMCs may contribute to remodeling of large arteries through compensation or by modulating the growth of muscle cells in the media.[188 189] Besides, changes in the ECM also occur, including elastic fiber fragmentation and collagen and fibronectin deposition by VSMCs, which collectively lead to increased arterial stiffness.[190 191] In the course of HTN, large arteries are prone to several structural and molecular changes in ECs, resulting in endothelial dysfunction.[192 193] The sustained high BP on the stiff large arteries with endothelial dysfunction in the arterial wall results in lumen size expansion, and in turn outward hypertrophic remodeling.[194 195] Large-artery stiffness is associated with less buffering of stroke volume during systolic cardiac contraction and consequently elevated SBP.[196] In addition, stiffening of large arteries is also associated with alterations in the resistance along the arterial tree which in turn affect pulse wave velocity (PWV), pulse pressure (PP) and wave reflection.[197] As PWV and PP are increased in the stiffened large arteries, the wave reflections arrive earlier during systole instead of diastole compared to normal arteries without increased stiffness, which elevates the central SBP in the stiffened aorta.[198-200]

In HTN, small arteries undergo inward remodeling that is characterized by a reduction in lumen diameter. This form of remodeling can be eutrophic in which M/L ratio is increased but there is no change in MCSA, or hypertrophic in which both parameters are increased.[201 202] Eutrophic remodeling predominates in small arteries isolated from experimental rodent models of HTN in which the RAAS is activated[203 204] and from patients with a mild essential HTN[205-207]. Inward eutrophic remodeling may result from a combination of a balance between apoptosis of the

outer periphery of the small artery and inward cell growth, leading to a reduction of the outer diameter of the vessel and decreased lumen diameter without altering the MCSA.[39 208] On the other hand, hypertrophic remodeling is frequently observed in small resistance arteries from severe hypertensive animal models, where the endothelin system is activated[209-211], and in small arteries from patients with secondary HTN[212]. Vascular fibrosis, which is characterized by ECM deposition, especially collagen and fibronectin, is an important aspect of vascular remodeling of small arteries in HTN. Over time, accumulation of ECM components, including collagen[213-215] and fibronectin[216-219], associated with alterations in cell-extracellular fibrillar attachment sites, such as adhesion molecules like integrins[215 220 221] in resistance arteries, collectively contribute to the modulation of arterial wall structure. Alterations in the activity of matrix metalloproteinase/tissue inhibitors of metalloproteinases (MMP/TIMPs) may also contribute to resistance artery remodeling during HTN by promoting ECM remodeling.[216] Furthermore, inflammation plays a crucial role in vascular wall remodeling through oxidative stress to induce pro-inflammatory and pro-fibrotic pathways, and infiltration of immune cells, resulting in abnormal vascular growth, dysfunction and fibrosis.[190 222] All these changes may result in vasoconstriction being turned structurally-based and persistent as a result of ECM remodeling.[190 216]

3.3.3. Angiotensin II and its receptors in HTN

Ang II is one of the key bioactive peptides of the RAAS, which plays a central role in the hemodynamic regulation of BP and in fluid-electrolyte balance.[223] Enzymatic cleavage of the liver-derived angiotensinogen by circulating renin, which is secreted by the juxtaglomerular apparatus in the kidneys, forms the inactive decapeptide Ang I, which in turn is cleaved by angiotensin-converting enzyme (ACE) on the luminal side of endothelial cells in the lung and tissues to generate the octapeptide Ang II. Thereafter, Ang II can undergo further modifications to produce other RAAS peptides, including the heptapeptide Ang III[224], Ang IV[225], and Ang (1-7)[226] that are biologically active on the vascular system. Besides the circulating RAAS, other RAAS components that are tissue-based (local) have been found in the central nervous system, heart, blood vessels, kidneys, adrenal glands, adipose tissue, the lymphatic system, and the gonads.[227-229] Local RAAS components act independently of the circulating RAAS, and are essential for Ang II to mediate its local physiological and pathological effects in these tissue compartments.

Ang II mediates its different effects through binding to its cell-surface receptors. In humans, there are two major distinct subtypes of Ang II receptors: angiotensin type 1 and 2 receptors (AT_1R and AT_2R).[230] Activation of AT_1R mediates the majority of pathophysiological effects of Ang II including, vasoconstriction, endothelial dysfunction, inflammation, growth, fibrosis and remodeling.[231] In rodents, two different genes encode the two AT_1R isoforms: $AT_{1a}R$ and $AT_{1b}R$[232], which are differentially expressed, distributed, and regulated.[233] [234] Mice with combined $AT_{1a}R$ and $AT_{1b}R$ deficiency have lower BP and changes in vascular structure when compared to wild-type (WT) mice[235], implying that these receptors play a role in maintaining physiological vascular function. Although Ang II mediates the most of its effects via AT_1R, in rodents the role of each isoform could be distinct. Mice that are devoid of $AT_{1a}R$, but not $AT_{1b}R$,

exhibit decreased BP compared to WT mice[235 236], and impaired responses to Ang II infusion[237]. This indicates that $AT_{1a}R$ is the principal receptor for regulation of BP in rodents and is responsible for BP elevation in experimental models of Ang II-induced HTN. Furthermore, AT_1R mediates Ang II effects that contribute to the contraction and proliferation of VSMCs[238], and the hypertrophic growth of cardiomyocytes[239 240] and renal epithelial cells[241], which are, collectively, implicated in the onset and development of CVD such as HTN. Ang II also can induce vascular fibrosis by promoting excessive deposition of some ECM components, such as collagen I[242] and fibronectin[204], in VSMCs, and increasing the secretion of transforming growth factor-beta 1(TGF-β1)[242 243] in an AT_1R-dependent mechanism, which in turn enhances collagen synthesis. Interrupting the RAAS through AT_1R blockade or ACE inhibition normalizes the relative content of collagen and integrins in the vascular wall structure of resistance arteries in spontaneously hypertensive rats.[215] Moreover, AT_1R blockade also downregulates the mRNA levels for some ECM components (collagen type I, III and IV, fibronectin and laminin) in small and large arteries in other experimental rat models of arterial HTN.[244]

On the other hand, stimulation of AT_2R is believed to counteract many AT_1R-mediated actions.[245] AT_2R is the predominant Ang II receptor during fetal development[246], whereas AT_1R becomes the dominant one in adults[247]. The effect of Ang II via the AT_2R limits vasocontraction and VSMC growth and proliferation that appears due to AT_1R stimulation.[248 249] In HTN, AT_2Rs are activated and contribute to Ang II-mediated vasodilation in hypertensive rats that are chronically treated with AT_1R blockers[250], and in hypertensive diabetic patients, particularly after treatment with angiotensin receptor blockers[251], suggesting that upregulation of AT_2R participates in BP lowering in the presence of AT_1R blockade. Furthermore, several *in vitro* experiments suggest that Ang II can induce apoptosis, predominantly by signaling via AT_2R.[252] Normotensive

rats infused with Ang II show enhanced apoptotic levels in the thoracic aorta via activation of AT_1R and/or AT_2R.[188] Another *in vivo* study found that treatment with an AT_1R antagonist, losartan, in spontaneously hypertensive rats stimulates aortic VSMC apoptosis, an effect blunted by AT_2R blockade.[253]

3.3.4. Experimental animal model of Ang II-induced hypertension

Several experimental animal models are used to further understand and mimic the heterogeneous etiologies, pathophysiology, complications, and treatment of human HTN. These models of HTN comprise renovascular, renal parenchymal, pharmacologically-induced, environmentally-induced, and genetic models.[254 255] Ang II-induced HTN in rodents is one of the most widely used experimental models to study the pathophysiology of HTN in the presence of an activated RAAS. In this model, HTN is induced by infusion of Ang II using implantable osmotic pumps to deliver the vasoconstrictor peptide at a constant flow rate. Elevation of BP in this model is a cumulative consequence of activation of sympathetic nervous system, increased total peripheral vascular resistance, VSMC contraction, increased aldosterone synthesis, and sodium retention.[256] Ang II-induced HTN is associated with chronic low-grade inflammation, endothelial dysfunction, and inward eutrophic vascular remodeling.[194 222 257] Inflammation of the vasculature in this model is also characterized by enhanced ROS production, infiltration of immune cells, and increased expression of adhesion molecules.[258 259] Renal damage and cardiac hypertrophy are also observed in this model of HTN.[260 261]

4. Vascular inflammation

Vascular inflammation is an important component of immune activation that contributes to the vascular disease that accompanies HTN. Enhanced oxidative stress, and activation of pro-inflammatory signaling pathways, cytokine production, increased expression of chemokines and adhesion molecules, and immune cell infiltration in arteries isolated from hypertensive rodent models are obvious evidence that vascular inflammation plays an essential role in the pathophysiology of HTN.[262]

Vascular inflammation comprises a series of sophisticated and interrelated events that starts with the early activation of the endothelium that is induced by injury, infection, or by stimuli like Ang II.[263] [264] Subsequent events and activation of inflammatory signaling cascades result in an increase in vascular permeability, leukocyte extravasation and tissue regeneration.[257] Under physiological conditions, the inflammatory process is strictly controlled and reversible. Activation and up-regulation of inflammation is followed by a resolution phase to curtail inflammatory responses and restore tissue homeostasis. In contrast, in pathophysiological conditions, inflammatory responses are uncontrolled and persevere leading to tissue damage.

Induction of inflammatory responses that participate in the pathogenesis of vascular disease and the atherosclerotic process has been well described.[265] Over the last two decades, accumulating evidence indicated that the concept of low-grade inflammation in HTN can predispose and accelerate atherosclerosis, and HTN may share similarities with the early stages that are observed in atherosclerosis.[266] In this section, the main cellular and molecular mechanisms that are involved in vascular inflammation will be explained in context of HTN.

4.1. Immune cells in HTN

The discovery of immune cells infiltrating into the vasculature in the course of HTN was the first indication of their significance in the development of HTN and other CVD. In recent years, a large body of evidence from pharmacological and/or genetic targeting of specific immune cell subsets or their effects has increased the knowledge of their role in vascular inflammation in the context of HTN. Various subsets of immune cells can induce vascular injury by generating ROS and activating other pro-inflammatory mediators like cytokines and chemokines.[267-269]

Broadly, the immune system comprises two major branches: the innate and adaptive immune systems, which are closely interrelated.[270] Innate immunity is the first line of host defense that is triggered non-specifically in response to different stimuli, including endogenous damage signals and/or external pathogens. Innate immunity comprises three main components: epithelial and mucous surfaces that provide a barrier against infection and prevent microorganism entrance, phagocytes that engulf and destroy pathogens, and the complement system that enhances the immune response.[271] Innate immune cells include monocytes and macrophages, antigen-presenting cells (APCs) such as dendritic cells, mast cells, basophils, eosinophils, neutrophils, and natural killer (NK) cells. These cells either recognize and respond to pathogen- or damage-associated signals directly or process them as antigens for adaptive immunity activation. In contrast, adaptive (acquired or specific) immunity refers to a highly specialized immune response as a consequence of immunological memory to specific initial immune response(s). T and B lymphocytes are the major cellular components of the adaptive immunity. T cells are responsible for cell-mediated immunity, whereas B cells are involved in the humoral (antibody-mediated) immunity.

Another group of immune cells, such as γδ T cells, invariant natural killer T (iNKT) cells and mucosal-associated invariant T (MAIT) cells, are known as "innate-like" and play a role in bridging the innate and adaptive immune system. These cells are preferentially localized in epithelial and mucosal tissues and respond faster to triggering signals than naïve adaptive immune cells by producing cytokines and cytotoxic effectors.[2] [272] [273] In this thesis, only monocyte/macrophages, APCs, and T cells will be described in the context of CVD. The evidence presented here is not intended to be exhaustive, but rather to provide a broad overview of the literature supporting the significance of different immune cell subsets in the onset and development of HTN. The diverse immune cells and their hematopoietic origin are depicted in **Figure I-6.**

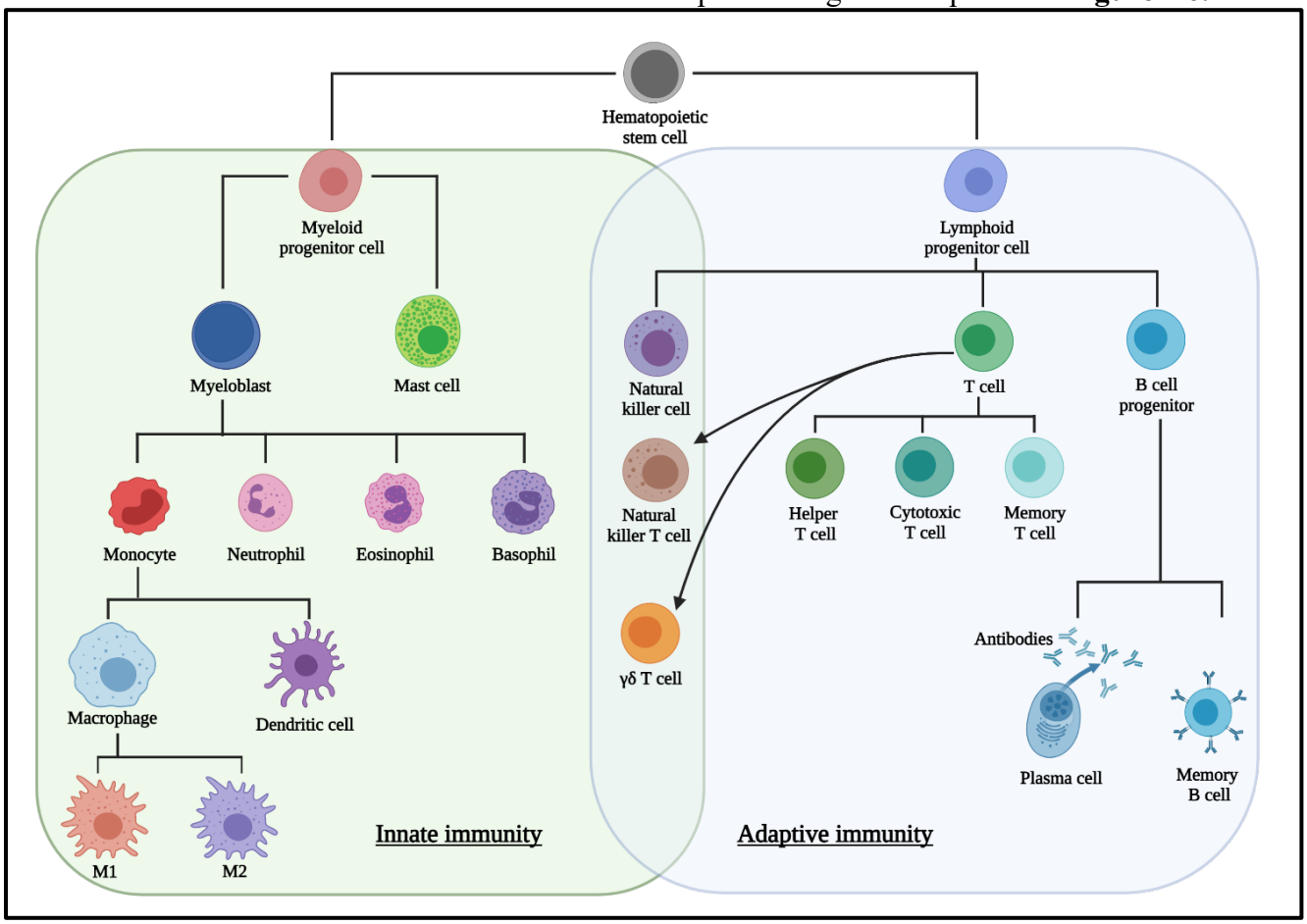

Figure I-6: Cells of the immune system and their hematopoietic origin. Created with BioRender.com

4.2. Innate immune cells in HTN

Monocytes/macrophages, dendritic cells, and neutrophils are the main cellular components that mediate innate immune responses. They express pattern recognition receptors (PRRs) such as Toll-like receptors (TLRs) on their cell surfaces to recognize pathogen-associated molecular patterns (PAMPs), damage-associated molecular patterns (DAMPs), or other antigens derived from injured tissues.[274] Innate immune responses that are mediated by monocytes, macrophages, dendritic cells, and neutrophils may contribute to low-grade inflammation directly or indirectly by stimulating adaptive immune responses mediated by T cells, leading to the development of HTN and end-organ damage.

4.2.1. Monocytes and macrophages

Monocytes are innate immune cells that originate from hematopoietic stem cells in the bone marrow through a series of differentiation phases under the control of macrophage-colony stimulating factor (M-CSF).[275] Following development in the bone marrow, monocytes enter the circulation and act as a systemic reservoir for tissue-specific innate cells. Circulating monocytes are rapidly recruited and attracted to chemical signals “chemokines” that are locally secreted to infiltrate into injured tissues, a process defined as chemotaxis, where they can differentiate into macrophages and/or dendritic cells. Macrophages can be identified by specific expression of various protein markers, including F4/80 (mice), epidermal growth factor module-containing mucin-like receptor 1 (EMR1, human), cluster of differentiation (CD)-11b, CD14, CD68, and Mac-1/Mac-3, depending on the subset of macrophage and the conditions of their local environment[276], whereas dendritic cells mainly express CD11c[277]. Collectively, monocytes,

macrophages, and dendritic cells are implicated in inflammatory responses by implementing phagocytosis, antigen processing and presentation, ROS production, and releasing of inflammatory cytokines.[278]

Monocytes and macrophages are a heterogeneous population of cells with varying degrees of activity that can switch depending on their surrounding microenvironment.[275 279] Similar to human monocytes, murine monocytes are generally divided into inflammatory Ly6C$^+$ monocytes (similar to human CD14$^+$CD16$^-$ classical monocytes), or anti-inflammatory patrolling Ly6C$^-$ monocytes (resemble human CD14^{low}CD16$^+$ non-classical monocytes).[280] In a similar manner to monocytes, macrophages can also show phenotypic and functional diversity that can be switched and adapted according to the needs of the microenvironment.[281] Among the several subsets, two are the most important: M1 and M2 macrophages. Macrophages can be polarized into a pro-inflammatory/killing phenotype (M1) in response to pro-inflammatory cytokines, including interferon (IFN)-γ and TNF-α[282], or towards an anti-inflammatory/wound healing phenotype (M2) in response to IL-4[283] or IL-13[284]. M1 macrophages are characterized by upregulated expression of proteins such as major histocompatibility complex (MHC)-II, CD80, CD86, COX-2, and iNOS. They also produce high levels of ROS and pro-inflammatory cytokines, including TNF-α, MCP-1, IL1-β, IL-6, IL-12, and IL-23, which are collectively promote the initiation of adaptive immune responses.[282 285 286] On the other hand, M2 macrophages express high levels of mannose receptor (CD206) and produce arginase 1 (Arg1)[287] that results in production of polyamines and promotes tissue remodeling and wound healing. M2 macrophages also can produce anti-inflammatory cytokines, such as IL-10, and pro-fibrotic factors, such as the transforming growth factor beta (TGF-β) and insulin-like growth factor 1 (IGF-1), consequently suppressing inflammation and stimulating tissue repair.[288] Inflammatory Ly6C$^+$ monocytes have been postulated to be

progenitors of M1 macrophages, whereas anti-inflammatory Ly6C$^-$ monocytes acquire the phenotype of M2 macrophages.[275 289 290] However, switching of inflammatory Ly6C$^+$ monocyte into M2 macrophage has also been noticed.[291 292] This suggests that differentiation fate of infiltrating monocytes is possibly affected by the neighboring microenvironment.

Ample evidence has revealed that monocytes/macrophages play an important role in HTN and HTN-associated end organ damage.[293 294] The role of monocyte/macrophages in HTN was initially identified using osteopetrotic (Op/Op) mice that are deficient in M-CSF due to a mutation within the colony-stimulating factor 1 (*Csf1*) gene and have accordingly a generalized deficiency of monocyte/macrophage subpopulations and their functions. *Csf1*$^{Op/Op}$ mice exhibit blunted BP elevation, endothelial dysfunction, vascular remodeling, and oxidative stress in response to chronic Ang II infusion[3], when treated with deoxycorticosterone acetate (DOCA)-salt[295], or when they have specific ET-1 overexpression in the endothelium[296], as compared with WT littermates. This finding was extended by Wenzel *et al* using low-dose diphtheria toxin to selectively deplete lysozyme M-positive (LysM$^+$) monocytes transgenically expressing diphtheria toxin receptors. Selective depletion of LysM$^+$ monocytes attenuated Ang II-induced BP elevation, vascular injury, oxidative stress, macrophage infiltration and increased pro-inflammatory mediators.[297] The Ang II hypertensive phenotype was fully restored by adoptive transfer of monocytes, but not neutrophils, from WT mice into LysM$^+$ monocyte-depleted mice. Furthermore, C–C motif chemokine receptor type 2-positive (CCR2$^+$) monocytes have the ability to infiltrate into the surrounding vasculature and contribute to Ang II-induced vascular and renal damage and macrophage infiltration but not BP elevation.[298-300] It has also been reported that mice devoid of macrophage12/15 lipoxygenase (12/15 LO) are significantly resistant to L-NAME- and DOCA/high-salt-induced HTN.[301] The

hypertensive response to L-NAME was restored by adoptive transfer of WT macrophages, effect reversed after depletion of macrophages using clodronate liposomes.

On the other hand, a protective role for macrophages in salt-sensitive hypertensive rats was observed by Machnik *et al.*[302 303]. These authors showed that following high salt intake or DOCA salt treatment, sodium concentration increases in the skin resulting in recruitment of macrophages associated with activation of the osmo-sensitive transcription factor tonicity-responsive enhancer binding protein (TonEBP). Activation of TonEBP induced the recruited macrophages to secrete vascular endothelial growth factor C (VEGF-C) which stimulates subcutaneous lymphatic network restructuring and promotes interstitial Na^+ clearance and water drainage from the skin into the systemic circulation, consequently contributing to mitigate the hemodynamic effects of salt loading.[303 304] Clodronate liposome-mediated depletion of macrophages decreased macrophage infiltration and interstitial Na^+ clearance from the skin, leading to salt-sensitive BP elevation. These opposing roles of monocytes/macrophages may be mediated through different subsets mentioned above. However, the accurate roles of inflammatory vs anti-inflammatory monocytes and M1 vs M2 macrophages in the context of HTN remains to be clarified. Also, more research is still needed to further understand the role of various subsets of T cells on monocyte and macrophage polarization in different hypertensive models.

4.2.2. Dendritic cells

Dendritic cells (DCs) are a subset of innate immune cells highly specialized in antigen presentation, which is an essential step for the activation of adaptive immunity, including T cells. DCs are the most effective APCs. However, other innate immune cells such as macrophages can

also perform antigen presentation function.[305] DCs can activate T cells by two kind of signals: T cell activation signal (also known as signal 1) and T cell co-stimulation signal (often referred to as signal 2)[278]. T cell activation signaling involves presentation of the antigenic peptides via the MHC-I or II molecules on DCs to the TCRs on T cells. The second signal, co-stimulatory signal, that is mediated by interaction between B7 ligands (CD80 and CD86) and CD40 on DCs with CD28 and CD40 ligand (CD40L) on T cells respectively, provides a potent stimulus for full T cell activation and proliferation.[306]

Accumulating evidence indicate that DCs contribute to HTN via their role in T cell activation, (**Figure I-7**).[307-309] Kirabo *et al.* have revealed the mechanism whereby DCs, in particular monocyte-derived DCs, activate T cells under the influence of Ang II or excess salt intake, leading to development of HTN.[307] DCs of hypertensive mice are triggered by Ang II or excess salt to produce high levels of intracellular ROS through activation of the reduced form of nicotinamide adenine dinucleotide phosphate (NADPH) oxidase. ROS induces the formation of isolevuglandin (isoLG) protein adducts, which are highly immunogenic modified proteins that are processed and presented to T cells as neoantigens to induce T cells, particularly $CD8^+$ T cells, activation, proliferation, and production of cytokines such as interferon gamma (IFN-γ) and IL-17A. Importantly, accumulation of isoLG protein adducts promotes DCs to produce large amounts of cytokines, including IL-1β, IL-6, and IL-23. Additionally, adoptive transfer of DCs from hypertensive mice caused a significant BP elevation in the recipient mice in response to a very low "subpressor" dose of Ang II. Another study has shown that activation of renal sympathetic nerves and their release of norepinephrine, promotes activation of DCs and accumulation of isoLG protein adducts in response to chronic angiotensin II infusion, which ultimately leads to T cell activation and causes both renal and vascular inflammation and development of HTN.[310]

In addition to the T cell activation signal, the T cell co-stimulation signal mediated by the interaction between B7 ligands on DCs and CD28 on T cells, has an important role in the development of HTN. Vinh *et al.* showed that pharmacological inhibition of the B7/CD28 axis prevented T cell activation and aortic T cell infiltration and thus blunted Ang II- and DOCA-salt-induced HTN.[311] They also indicated that mice deficient in both CD80 and CD86, ($B7^{-/-}$), are resistant to Ang II-induced HTN, which was restored by engrafting bone marrow from WT mice into $B7^{-/-}$ mice. One the other hand, further research efforts are needed to know whether macrophages have a similar antigen presenting function to activate T cells in the context of HTN.

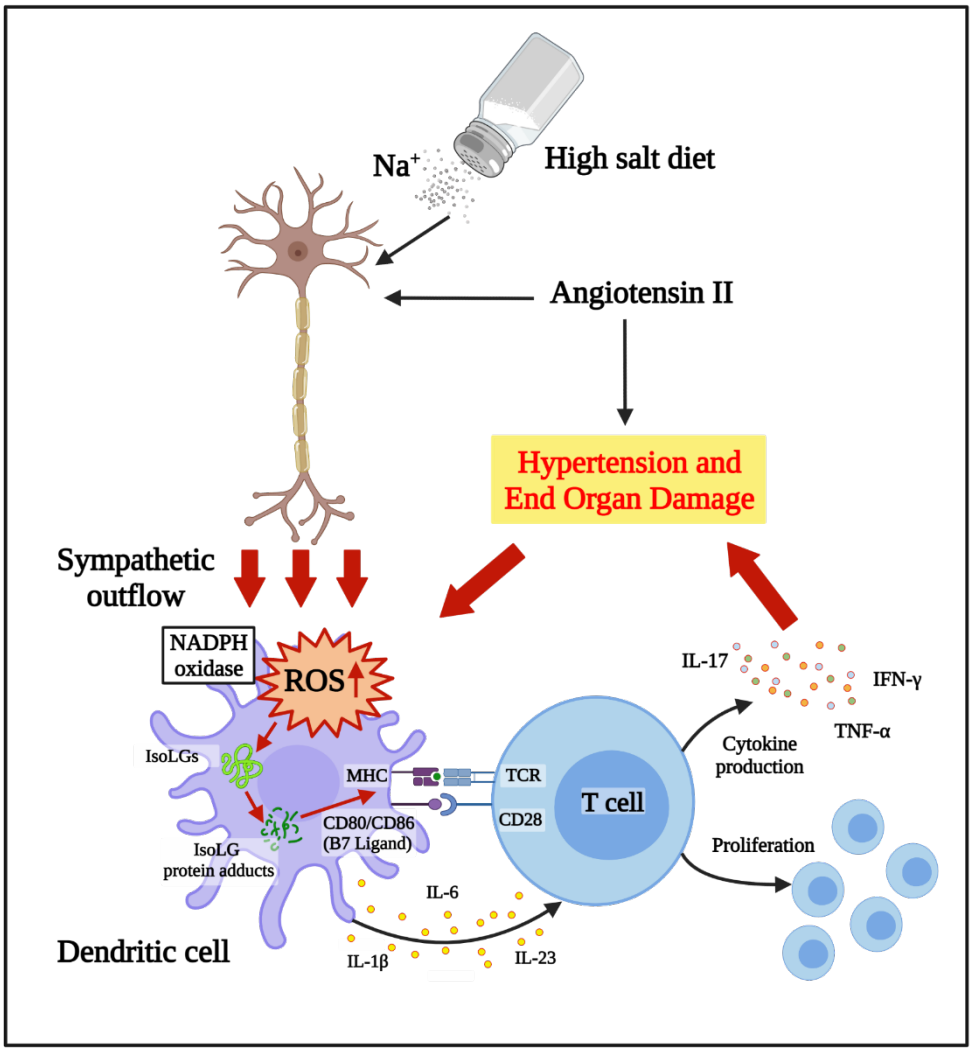

Figure I-7: T cell activation by DC in HTN. Created with BioRender.com

4.2.3. Neutrophils

Neutrophils are polymorphonuclear granulocytes that represent the most abundant type of leukocyte in the circulation. They are effector innate immune cells that are characterized by their function as phagocytic cells, leading to ROS production and release of proteolytic enzymes from their granules. In addition to their antimicrobial effect, neutrophils are also involved in activation of other immune cell types that participate the protection against pathogens.[312] These properties may configure neutrophils to play a role in the immune response. The contribution of neutrophils to some CVD that are characterized by chronic inflammation such as atherosclerosis, myocardial infarction, and ischemic stroke has been indicated.[313] However, their role in other CVDs that are associated with low-grade inflammation such as systemic arterial HTN remains controversial.[314]

There is evidence demonstrating that an increased blood neutrophil count and neutrophil-to-lymphocyte ratio (NLR) are closely correlated with elevated BP and particularly higher in non-dipper hypertensive patients.[315-317] Zhang *et al.* have reported that peripheral blood neutrophil activity (superoxide anion generation and myeloperoxidase activity) was significantly higher in spontaneously hypertensive rats when compared to control rats.[318] Moreover, it has shown that depletion of neutrophils in normotensive mice decreased SBP and reduced endothelial-dependent vasoconstriction.[319] However, these effects were abrogated in the iNOS or IFN-γ knockout mice.[319] From these findings, the correlation between neutrophils and HTN does not necessarily imply causation, but could mean that neutrophils have a role to play in the low-grade inflammation observed in patients with HTN and experimental hypertensive rats. Apparently, neutrophils can also modulate the adaptive immune system through antigen presentation and chemokines/cytokines secretion[312] to promote the pro-inflammatory phenotype, and ultimately leading to development of HTN. Importantly, recent emerging evidence has shown that in patients

with essential HTN, Ang-II promotes ROS production from neutrophils in a dose-dependent manner, and ROS prime neutrophils to expel their nuclear content into the extracellular space and form neutrophil extracellular traps (NETs) in a process called "NETosis", leading to increased thromboinflammation, fibrosis, and endothelial dysfunction that cause target organ damage in essential hypertensive patients. These complications were blunted in hypertensive patients treated with irbesartan, an AT1 receptor blocker (ARB).[320]

4.2.4. Myeloid-derived suppressor cells

Myeloid-derived suppressor cells (MDSCs) are another subset of innate immune cells. They are a heterogeneous population of immature myeloid cells, which seem to have a protective role in HTN and were first described to suppress immune responses in the context of cancer.[321] [322] Shah *et al.* observed an increase in circulating MDSCs and accumulation in the spleen of multiple murine models of experimental HTN, which was associated with blunting of BP elevation, T cell activation, and renal inflammation through the production of hydrogen peroxide (H_2O_2).[323] Chiasson *et al.* demonstrated that adoptive transfer of MDSCs isolated from WT mice into cyclosporine A (CsA)-treated mice after HTN had developed reduced the CsA-induced BP elevation, vascular dysfunction, and renal damage.[324] These findings support the proposition that MDSCs can play an important role suppressing inflammatory cascades associated with the development of HTN.

4.3. Adaptive immune cells in HTN

T and B lymphocytes are the main cellular components of adaptive immunity. These lymphocytes participate in the adaptive immune response by producing pro-inflammatory cytokines and/or cytotoxic mediators or antibodies, leading to the development of chronic inflammatory or auto-immune diseases, which are associated with an increased risk of different forms of CVD, including HTN.[325]

4.3.1. T cells

T lymphocytes are adaptive immune cells that can be distinguished from other lymphocytes, such as B cells and natural killer (NK) cells by the expression of the T cell receptor (TCR) on their cell surface. The TCR is a transmembrane heterodimeric protein that is composed either of alpha and beta (αβ) or gamma and delta (γδ) polypeptide chains. Together, the TCR, the CD3-zeta (ζ-chain, also known as CD247) accessory molecule, and other CD3 molecules (one CD3γ, CD3δ, and two CD3ε chains) form the TCR complex that is responsible for transduction of the activation signal in T lymphocytes.[326 327] During T cell development in the thymus, T cells undergo further differentiation to express $CD4^+$ or $CD8^+$, which are co-receptors for the TCR complex and mediate activation of downstream signaling pathways when the TCR recognizes an antigen presented by APCs. Antigen presentation, co-stimulation and cytokines simulate polarization of the naïve $CD4^+$ T helper (Th0) cells into mainly Th1, Th2, T regulatory lymphocytes (Treg), or Th17 subsets. Each subset produces its own panel of cytokines and performs a specific set of functions[328] (**Figure I-8**). Upon activation, naïve $CD8^+$T cells differentiate into cytotoxic effector T cells.[329]

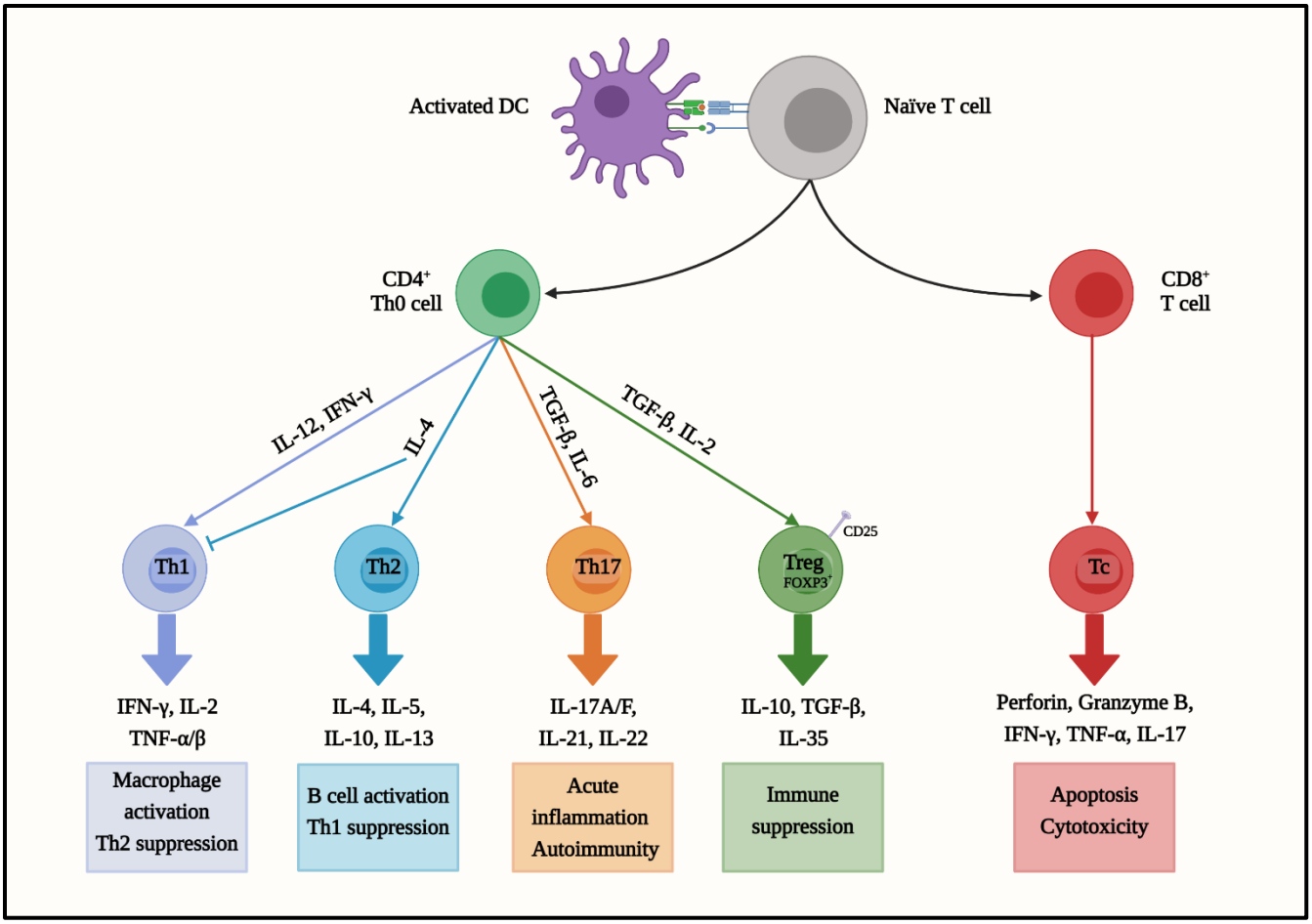

Figure I-8: Various subsets of T lymphocytes, differentiation signals, and their functions. Adapted from Idris-Khodja et al.[328], and created with BioRender.com

Accumulating evidence has demonstrated that T cells play a role in HTN. Ang II-induced HTN, vascular dysfunction, and oxidative stress were shown to be blunted in recombination activating gene-1 (*RAG-1*$^{-/-}$) knockout mice, which are lacking both T and B cells.[6] These hypertensive responses were restored in these immunodeficient mice by the adoptive transfer of T, but not B cells from WT mice. Although this evidence has clearly shown the implication of T cells in the vascular pathology of HTN, the roles played by different T cell subsets in HTN are still an active area of investigation.

4.3.1.1. Effector T helper cells (Th1, Th2 and Th17)

In the presence of cytokines IFN-γ and IL-12, naïve $CD4^+$ T cells polarize towards a more pro-inflammatory Th1 phenotype.[328] [330] [331] Polarized Th1 cells produce pro-inflammatory cytokines IFN-γ, IL-2, TNF-α and TNF-β, and contribute to macrophage activation, cell-mediated defense against intracellular microorganisms, and suppression of Th2 immune responses. On the other hand, IL-4 polarizes naïve $CD4^+$ T cells into Th2 cells, which produce several cytokines, including IL4, IL-5, IL-10, and IL-13. These cytokines suppress Th1 immune responses and activate B cells to produce immunoglobulins. Importantly, IL-4 promotes the production of IL-10, which is an immunomodulatory cytokine that down-regulates IL-12 production and thus limits Th1 immune responses[332] [333], which means that Th1 immune responses are weaker during Th2 polarization and vice versa.

In the context of HTN, several studies have provided evidence that Ang II play a direct role in the modification of Th1/Th2 immune balance.[334] [335] It has been shown that Ang II-infused rats exhibit increased Th1-mediated responses, as indicated by production of Th1 cytokine IFN-γ, and a decline in Th2-mediated responses, as evidenced by production of Th2 cytokine IL-4, in an $AT_{1a}R$-dependent manner.[334] IFN-γ appears to be essential for the initiation of vascular inflammation without affecting BP. Knockout of IFN-γ (*IFN-*$\gamma^{-/-}$) in mice attenuated Ang II-induced vascular dysfunction independently of BP alterations.[336] Absence of chemokine ligand 16 (CXCL16), which interacts with the C-X-C chemokine receptor type 6 (CXCR6, also designated as CD186) that is characteristically expressed on the surface of Th1-type T cells, suppresses infiltration of T cells and macrophages in the kidneys of Ang II-infused mice.[337] Therefore, polarization of Th1/Th2 balance towards Th1-type immune responses may be essential for the

development of HTN. It is important to note, however, that other studies have demonstrated the participation of IL-4 in the progression of HTN and of IFN- γ in regulation of BP in hypertensive rodents.[338 339] This controversy may be due to differences in hypertensive animal models and/or alterations in the relative concentrations of cytokines in these studies.

Th17 cells are a relatively novel subset of $CD4^+$ T helper cells, distinct from Th1 and Th2 subsets by producing the pro-inflammatory cytokine: IL-17A.[340 341] The cytokines TGF-β and IL-6 promote naïve $CD4^+$ T cells polarization towards the Th17 effector phenotype, whereas IL-23 contributes to the full differentiation and maintenance of Th17 cell phenotype. Th17 can differentiate into Treg cells, and Treg cells into Th17, based on the cytokine milieu, as TGF-β can also direct the differentiation of naïve $CD4^+$ T helper cells into Treg cells. Importantly, the presence or absence of IL-6 is a crucial key factor in determining whether naïve $CD4^+$ T helper cells differentiate towards a Th17 or Treg phenotype, respectively. In addition to IL-17A, Th17 cells also produce other pro-inflammatory cytokines, including IL-17F, IL-21, and IL-22 that, collectively, co-operate to trigger acute inflammatory responses against extracellular bacterial and fungal pathogens.[341 342] Furthermore, Th17 cells are important contributors to chronic inflammation associated with inflammatory autoimmune diseases, such as multiple sclerosis, rheumatoid arthritis, systemic lupus erythematosus, inflammatory bowel disease, psoriasis, and asthma.[343-345] IL-17 can mediate potent pro-inflammatory responses by promoting chemotaxis and the infiltration and expansion of neutrophils.[346] Conversely, IL-17 can also exhibit anti-inflammatory responses by reducing the expression of adhesion molecules and chemoattractants on fibroblasts.[347]

Ang II- and DOCA-salt-induced HTN and vascular dysfunction are associated with increased Th17 cell activity and IL-17 production.[348-350] Madhur *et al.* have shown that IL-17a

knockout mice (*IL-17a*$^{-/-}$) infused with Ang II displayed blunted HTN, vascular dysfunction, oxidative stress, aortic T cell infiltration, and aortic collagen deposition and stiffening.[348] A high-salt diet has been demonstrated to promote the activity of Th17 cells via activation of the p38/MAPK pathway in mice and humans.[351] Placental ischemic rats have been shown to have increased numbers of Th17 cells and lower levels of Treg cells compared with control normal pregnant rats.[352] Administration of IL-17 soluble receptor C (IL-17RC), which blocks the IL-17 signaling cascade, in reduced-uterine perfusion pressure (RUPP) rats, an experimental model of preeclampsia, reduced circulating Th17 cells, oxidative stress, and HTN.[353] Together, these findings support the idea Th-17 and IL-17 play a pathophysiological role in HTN and vascular damage.

4.3.1.2. Regulatory T cells

Regulatory T cells (Tregs) are anti-inflammatory T cells that suppress the activity of T effector subsets (including: Th1, Th2, and Th17) and other immune cells. In the presence of both cytokines: TGF-β and IL-2, naïve $CD4^+$ T cells polarize towards Tregs phenotype.[354] Under physiological conditions, $CD4^+$ Tregs develop in the thymus (natural [n]Treg), however, naïve T cells can also be extrathymically stimulated under specialized conditions in the periphery into Tregs (induced [i]Treg).[355] [356] Various subtypes of T cells have been shown to have T cell-suppressive activity, but regulatory activity has been found to be highest in cells expressing CD4, the IL-2 receptor alpha chain (IL-2Rα or CD25), and the transcription factor forkhead box protein 3 (FOXP3).[357] Tregs are also characterized by expression of cytotoxic T-lymphocyte-associated antigen 4 (CTLA-4 or CD152), L-selectin (also known as CD62 ligand [CD62L]), OX40 (CD134),

and glucocorticoid-induced tumor necrosis factor receptor-related protein (GITR).[358] FOXP3 appears to be the key regulator of the pathway of Treg development and function.[359] FOXP3 has been shown to interact with several transcription factors such as nuclear factor of activated T cells (NFAT) and acute myeloid leukemia 1 (AML1, also known as Runt-related transcription factor 1 [RUNX1]), which in turn suppresses expression of genes, like IL-2, that are involved in T cell activation, and upregulates expression of the Treg markers, including CD25 and CTLA-4.[360-362] Importantly, activated $CD8^+$ T cells have also been found to have regulatory functions during inflammatory processes.[363 364]

Tregs exert their immunosuppressant effects through various mechanisms (**Figure I-9**).[267] Tregs are characterized by production of anti-inflammatory cytokines, including IL-10, TGF-β, and IL-35. IL-10 signaling via its receptor suppresses cytokine production by Th1 and Th2 cells, and macrophages, impairs APC function, and enhances cell survival.[267 365] TGF-β can induce generation and function of T suppressor cells in the periphery[366 367]. Nonetheless, it is not required for nTreg activity.[368 369] In addition to its immune-suppressive effects on immune cells, TGF-β can also inhibit proliferation and migration, and induce apoptosis of ECs and VSMCs.[370] In the vasculature, TGF-β has a dual effect in that it can also stimulate vascular fibrosis.[371] IL-35 is a relatively novel anti-inflammatory cytokine that belongs to the IL-12 family, and is known for suppression of Th17 cell development and differentiation.[372]

Tregs express galectin-1 (Gal-1), which can bind with CD45 and other glycoproteins on immune cells and stimulate cell-cycle arrest, apoptosis, and the inhibition of pro-inflammatory cytokine secretion, including IFN-γ and IL-2.[373-375] Furthermore, Tregs can also eliminate activated T effector cells by releasing cytolytic molecules, including granzyme A and B, which induce apoptosis in target cells through mechanisms that are not yet fully understood.[376-378] Tregs

express CD39, which coordinates with CD73 to degrade extracellular pro-inflammatory adenosine triphosphate (ATP) produced during tissue damage and release adenosine, which in turn binds to A2A adenosine receptors and thus mediates T effector cell suppression.[379] [380]

Tregs can also inhibit T effector cell activity by restraining APC-dependent functions, especially those that rely on DCs.[381] *In vitro*, it has been demonstrated that the expression of co-stimulatory molecules on DCs was significantly reduced by co-cultured Tregs through the anti-inflammatory action of TGF-β.[382] Moreover, CTLA-4 that is expressed on the surface of Tregs can block the T effector cell co-stimulation by interacting with B7 ligands (CD80 and CD86) on DCs, which limits expression of these ligands and reduces T effector cell activation.[383] Neuropillin-1 (Nrp-1), which is mostly expressed by Tregs, promotes prolonged interaction between Tregs and DCs, thereby disrupting the interaction of DCs with T effector cells.[384] Tregs also produce fibrinogen-like protein 2 (FGL2) that inhibits DC maturation and proliferation.[385]

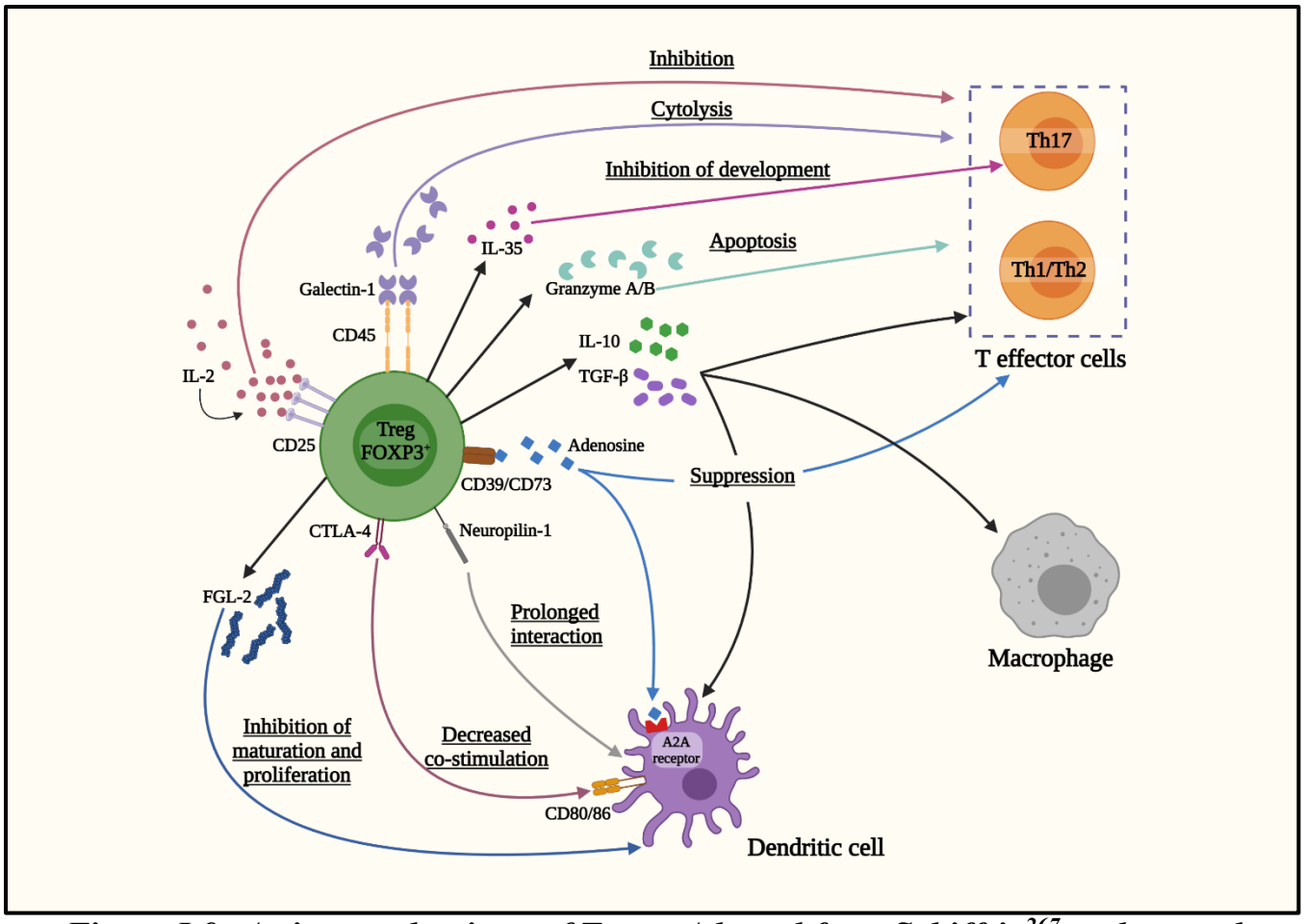

Figure I-9: Action mechanisms of Tregs. Adapted from Schiffrin[267] and created with BioRender.com

The protective role for Tregs during HTN was first identified using consomic rats, a rat model of genetic HTN which had chromosome 2 introgressed from normotensive Brown Norway rats on to hypertensive Dahl salt-sensitive rats.[386] Chromosome 2 bears several pro-inflammatory genes, including those encoding inflammatory mediators such as IL-2, IL-6, vascular cell adhesion molecule 1(VCAM-1 or CD106), fibroblast growth factor 2 (FGF2), and $AT_{1b}R$.[190 387] Consomic rats have been shown to exhibit a reduction in BP and production of pro-inflammatory cytokines compared with Dahl salt-sensitive hypertensive rats, which was associated with enhanced production of anti-inflammatory cytokines, including IL-10 and TGF-β, by Tregs, as well as

promoted aortic FOXP3 expression and increased $CD4^+CD25^+$ and $CD8^+CD25^+$ lymphocytes and their activity.[386] Barhoumi *et al.* reported that adoptive transfer of $CD4^+CD25^+$ Tregs in C57BL/6 mice blunted Ang II-induced HTN, ROS production, endothelial dysfunction, small artery stiffness, infiltration of aortic immune cells, and circulating levels of pro-inflammatory cytokines in the plasma compared with mice infused with Ang II and pretreated with PBS (vehicle).[388] In keeping with this, Kasal *et al.* noted similar protective effects of $CD4^+CD25^+$ Treg adoptive transfer in a mouse model of aldosterone-induced HTN and vascular damage without significant changes in BP.[389] Another study by Kvakan *et al.* demonstrated that Ang II-induced cardiac hypertrophy and fibrosis, cardiac immune cell infiltration, and cardiac electrical remodeling were ameliorated by $CD4^+CD25^+$ Treg adoptive transfer in a BP-independent manner.[390] Moreover, Matrougui *et al.* reported a decrease in Tregs in C57BL/6 mice in response to Ang II infusion.[391] They also observed a reduction in Ang II-induced BP elevation, coronary arteriolar endothelial dysfunction, macrophage activation and infiltration into coronary arterioles and the heart in these hypertensive mice that received intraperitoneal injections of Tregs from control mice.[391] Mian *et al.* found that Ang II-induced microvascular injury and pro-inflammatory polarization in MA PVAT and the renal cortex were exaggerated in *Rag1*$^{-/-}$ mice that received adoptively transferred T cells from Scurfy mice, which are deficient in Tregs due to a mutation in the transcription factor Foxp3 gene, compared with $Rag^{-/-}$ mice given T cells from WT mice.[392]

IL-10 production by Tregs mediates the vascular protective effects in HTN through limiting Ang II-induced vascular damage and oxidative stress. IL-10 KO (*IL 10*$^{-/-}$) mice infused with Ang II had exacerbated endothelial dysfunction and enhanced ROS production compared with WT mice.[393] *Kassan et al.* found that adoptive transfer of Tregs isolated from WT mice into Ang II-infused *IL 10*$^{-/-}$ mice improved endothelial function in resistance arteries, reduced SBP and

NADPH oxidase activity, whereas the transfer of Tregs isolated from IL-10$^{-/-}$ mice had no effect on Ang II-treated WT mice.[394] Taken together, these studies add further evidence supporting that functional Tregs play a potent protective role in the context of HTN via production of the anti-inflammatory cytokine IL-10.

4.3.1.3. Cytotoxic T lymphocytes

Naive CD8$^+$ T cells can be polarized into cytotoxic T cells upon activation by APCs.[395] Similarly to CD4$^+$ T cells, CD8$^+$ T cells can be differentiated into either cytotoxic T cell type 1 (Tc1), Tc2, Tc17, or CD8$^+$ Treg cells.[396] Generally, activated cytotoxic T cells secrete large amounts of pro-inflammatory cytokines such as IFN-γ, TNF-α, and IL-17, and produce cytolytic molecules, including perforin and granzyme B, which together exert a variety of inflammatory functions.[397-399] Perforin is a cytolytic glycoprotein that attaches to target cell membrane, creating a pore through which granzyme B, a serine protease, can enter the cell and trigger apoptosis.[399] Cytotoxic T cells can also induce apoptosis through the Fas ligand (FasL or CD95L) on CD8$^+$ T cells, which binds with its receptor, FAS, on target cells to initiate the apoptotic cascade.[399 400]

Accumulating evidence suggests that cytotoxic CD8$^+$ T cells may play a role in HTN. Trott *et al.* found that mice lacking cytotoxic CD8$^+$ T cells (*CD8*$^{-/-}$ mice) showed a blunted BP elevation in response to Ang II, and were protected against Ang II-induced vascular dysfunction and remodeling as well as microvascular rarefaction in the kidney.[401] In this study, it has also been shown that Ang II caused expansion of an oligoclonal population of CD8$^+$ T cells in the kidney, but not in the spleen or blood vessels, which likely contributed to renal dysfunction and development of HTN.[401] Sun *et al.* revealed that deficiency of mineralocorticoid receptor (MR) in

T cells markedly decreased Ang II-induced BP elevation, vascular and renal damage, and accumulation of interferon IFN-γ-producing T cells, particularly $CD8^+$ T cells, in the aorta and kidney.[402] Treatment of WT mice using eplerenone, which is a selective MR antagonist, mitigated Ang II-induced HTN and accumulation of $CD8^+$ IFN-γ^+ T cells in the kidney and spleen.[402]

Furthermore, Youn *et al.* have observed an increase in the number of cytotoxic $CD8^+$ T cells in hypertensive patients compared with age- and sex-matched normotensive controls.[403] These cells are characterized by increased expression of CD57, an immunosenescence marker, loss of the co-stimulatory surface marker, CD28, and production of excessive amounts of the cytolytic molecules perforin and granzyme B, and the pro-inflammatory cytokines, IFN-γ and TNF-α.[403] This was accompanied with higher levels of tissue-homing chemokines for pro-inflammatory T cells, including C-X-C motif chemokine receptor type 3 (CXCR3, also known as CD183)-binding chemokines, such as monokine induced by IFN-γ interferon (MIG), IFN-γ–induced protein 10 (IP-10), and IFN-inducible T-cell α chemoattractant (I-TAC) in patients with HTN compared to control subjects.[403] Together, these effects could result in ECM remodeling, cell detachment, apoptosis, and T cell-driven inflammation, ultimately leading to development of HTN in humans. In keeping with this, another study by Shen *et al.* demonstrated that granzyme B deficiency, which is produced in large amounts by activated cytotoxic $CD8^+$ T cells, reduced Ang II-induced murine cardiac hypertrophy, fibrosis, and inflammation.[404] Thus, these findings indicate that cytotoxic $CD8^+$ T cells are critical contributors to inflammation and the pathogenesis and development of and HTN.

4.4. Innate-like T lymphocytes in HTN

Innate-like T lymphocytes are a heterogeneous subset of recently discovered T cells that do not fully fit into either direction of the classical innate-adaptive categorization.[405] These cells include some subsets of αβ TCR T lymphocytes, such as CD1-restricted T cells, MHC-I-related (MR1)-restricted MAIT cells, and MHC class Ib-reactive T cells, and NKT cells, as well as γδ TCR T cells.[2 406] Innate-like T lymphocytes also known as "unconventional T cells" because they do not follow the MHC-restricted paradigm, they can recognize non-peptide antigens, have limited TCR diversity compared to conventional T cells, and they tend to reside in non-lymphoid tissues. Moreover, they are poised for a faster response, including proliferation and/or cytokine production, after a recall stimulation with an antigen and activation compared with conventional T cells.[2]

There is evidence that a subset of unconventional T cells, γδ T cells, has a role in Ang II-induced HTN, vascular injury, and T cell activation.[9] These effects will be described in detail in the following section. On the other hand, Kirabo *et al.* have found that NKT cells do not appear to play a role in Ang II-induced HTN.[307] They observed that mice lacking functional NKT cells exhibit similar BP elevation in response to Ang II compared to WT control mice. No role has been identified so far for the other unconventional αβ TCR T cells in HTN.

4.4.1. γδ T cells

γδ T cells are a subset of unconventional T cells that are characterized by expressing γδ TCR instead of conventional αβ TCR and play an essential role in bridging the innate and adaptive immune systems.[2 273 407] These innate-like T cells respond rapidly to pro-inflammatory cytokines IL-1β and IL-23 secreted by innate cells to produce IL-17A that is involved in sustaining BP

elevation and vascular dysfunction.[348] Recently, Caillon *et al.* demonstrated with work in our laboratory a role for these innate-like cells in Ang II-induced HTN, vascular injury, and T cell activation.[9] They observed that Ang II caused an increase in number and activation of γδ T cells in the spleen after 7 days of Ang II infusion. They also showed an accumulation of γδ T cells in MA PVAT at the end of a 14-day Ang II infusion period. Furthermore, Ang II-induced BP elevation, MA endothelial dysfunction, and spleen and MA PVAT T cell activation were blunted in *Tcrδ* null (TCRδ$^{-/-}$) mice, which are devoid of γδ T cells, and in mice injected with a γδ T cell-depleting antibody. However, γδ T cell subtypes involved in HTN are still unknown.

4.4.1.1. γδ T cell discovery

Unlike other subsets of unconventional T lymphocytes (unconventional αβ TCR T cell subsets), whereby the discovery of each remains relatively recent, the first description for a T lymphocyte subset that expresses a TCR different from the classical αβ TCR was by Borst *et al.* more than three decades ago.[408] The step-wise uncovering of the γδ TCR cells started with TCR discovery through cloning of the α and β genes that encode the classical αβ TCR.[409 410] This was associated with demonstration of the role of the "T3 glycoprotein" (CD3 complex) in TCR signal transduction.[411] In 1984, Tonegawa's group uncovered an additional TCR-like gene in mice that was located on a different chromosome than α or β TCRs, but was transcribed by T cells, and they named this novel gene: gamma (γ).[412-414] The molecular structure of TCR delta (δ) was subsequently determined after revealing the genes that encode it.[415 416]

In 1986, Brenner *et al.* were the first to name a T cell subset as "γδ T cells", and they described these cells as a subset of human T lymphocytes expressing novel TCR T3 glycoproteins

(γ and δ subunits), which appeared to be the products of the Tγ and Tδ genes, in the absence of expression of αβ TCRs.[417] Furthermore, Bank *et al.* demonstrated that both of the TCR-γ and -δ proteins were expressed within a single cell, suggesting that these two proteins represent a heterodimer that supports CD3 complex functionality like αβ TCR.[418] In the wake of these important findings, several other studies further defined γδ T cells as a diverse and distinct lineage of T cells.[419] [420] Together, these studies provided robust support for the idea that γδ T cells are structurally and functionally related to αβ T cells, with a separate lymphocyte lineage, and they are non-redundant to αβ T cells, which dramatically changed the understanding and the course of investigations in this field.[421]

4.4.1.2. T cell receptors

4.4.1.2.1.T cell receptor structure and diversity

T lymphocytes can be distinguished from other lymphocytes, such as B cells and NK cells by the expression of the TCR on their cell surface. The TCR is a transmembrane heterodimeric protein that is composed either of αβ or γδ polypeptide chains. Together, the TCR, the CD3-zeta (ζ-chain, also known as CD247) accessory molecule, and other associated invariant CD3 molecules (one CD3γ, CD3δ, and two CD3ε chains) form the TCR protein complex that is responsible for transduction of the activation signal in T lymphocytes (**Figure I-10**).[326] [327] Most of T cells express TCR that consists of the highly variable α and β polypeptide chains, which are encoded by *Tcra/TRA* and *Tcrb/TRB* in mouse/human, respectively, and referred to as αβ T cells. A tiny minority of T cells express alternate TCR formed by the variable γ and δ chains, which are

encoded by *Tcrg/TRG* and *Tcrd/TRD* in mouse/human, respectively, and are referred to as γδ T cells. In this thesis, we will focus on γδ T cells and their subsets.

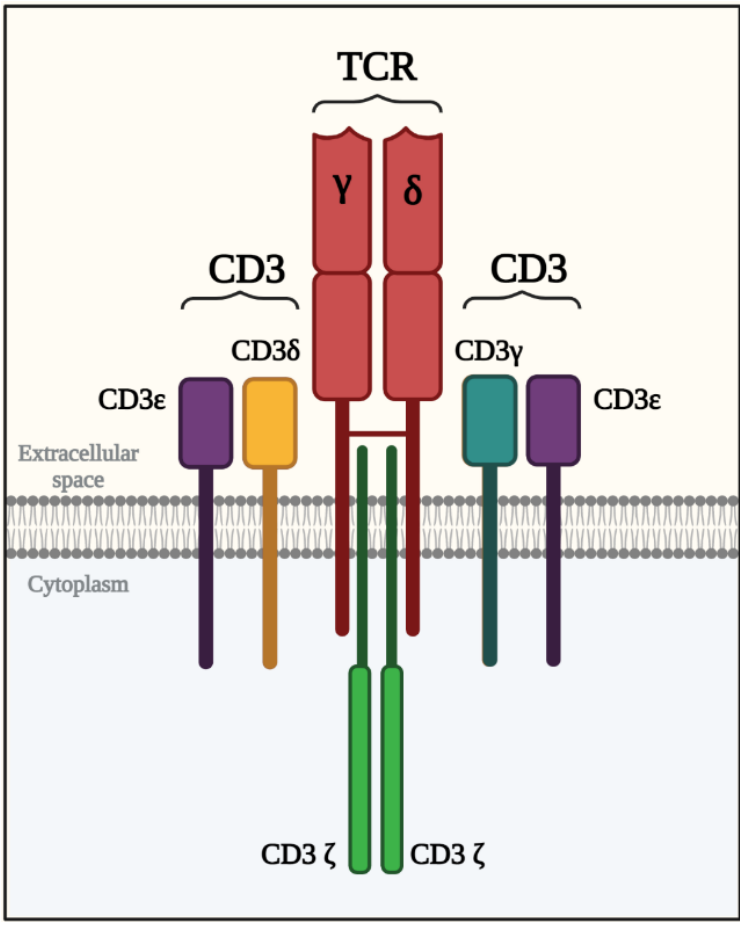

Figure I-10: The γδ TCR complex structure, including associated CD3 proteins. Created with BioRender.com

Each TCR chain comprises two extracellular domains: a variable region and a constant region. The constant region is closer to the cell membrane and is anchored to it via a transmembrane short cytoplasmic tail, while the variable region binds to the antigen binding site. There are three types of TCR gene segments that encode γ chain: variable (V), joining (J), and constant (C). In contrast, the δ chain is encoded by four TCR gene segments: V, J, diversity (D),

and C.[422] The number of TCR gene segments is variable among different species.[423] Importantly, three complementarity-determining regions (CDRs), which are part of the variable domain of both TCR γ- and δ-chains, are forming the antigen binding sites. CDRs, particularly CDR3, are indispensable for the diversity of antigen specificities that are generated by T-lymphocytes through a genetic rearrangement mechanism called V(D)J recombination.[424] V(D)J recombination is a genetic rearrangement mechanism between V, J and D gene segments that occurs with the assistance of RAG-1 and RAG-2 enzymes to separate, shuffle, and rejoin the VDJ gene segments, and thus generate a huge diversity of antigen specificities for TCR during the early stages of T cell maturation in the thymus.[425] In theory, the genetic rearrangement via V(D)J recombination can generate 10^{15} unique rearranged TCRs in mice[326] and 10^{18} TCRs in humans[426]. During the early T cell maturation in ontogeny, TCR γ, δ, and β genes become transcriptionally active before TCR α, and T cells predominantly express γδ TCRs several days prior to T cells expressing αβ TCRs, but from birth onward, the majority of T cells express αβ TCRs.[427]

4.4.1.2.2. Murine γδ TCR nomenclature systems

Various nomenclature systems have been used to identify the mouse TCR variable regions of γ and δ gene segments. For Vγ chains, Heilig & Tonegawa's nomenclature[428] is the most common nomenclature system in the literature and is used by the international ImMunoGeneTics information system (IMGT), which is the global reference in immuno-genetics and immuno-informatics that was created in 1989 by Marie-Paule Lefranc[429]. Garman's nomenclature[430] is another common nomenclature system that also in use in the literature. Furthermore, Arden's[431] and Hayday's[273] are also other nomenclature systems that are not widely used like Heilig &

Tonegawa's and Garman's systems, creating considerable confusion regarding equivalent names for different systems, (Table I-1). Accordingly, it is crucial to determine the nomenclature system used in each study from researcher's side, and on the other hand, attention should be paid to this point from the reader side as well. In this thesis, Heilig & Tonegawa's nomenclature was used to designate Vγ chains. Regarding Vδ chains, IMGT and Elliott's[432] nomenclature systems are the most widely reported nomenclature in the literature compared with Arden's system[431], (Table I-2).

IMGT	**Heilig & Tonegawa[428]**	**Garman[430]**	**Arden[431]**	**Hayday[273]**
TRGV1	Vγ1	Vγ1.1	GV5S1	GV5S1
TRGV2	Vγ2	Vγ1.2	GV5S2	GV5S2
TRGV3	Vγ3	Vγ1.3	GV5S3	GV5S3
TRGV4	Vγ4	Vγ2	GV3S1	GV3S1
TRGV5	Vγ5	Vγ3	GV1S1	GV1S1
TRGV6	Vγ6	Vγ4	GV2S1	GV2S1
TRGV7	Vγ7	Vγ5	GV4S1	GV4S1

Table I-1: Official nomenclature systems for murine Vγ gene segments.

IMGT	Elliott[432]	Arden[431]
TRDV1	Vδ2	DV102S1
TRDV2-1	-	-
TRDV2-2	Vδ4	DV104S1
TRDV3	-	-
TRDV4	Vδ1	DV101S1
TRDV5	Vδ5	DV105S1

Table I-2: Official nomenclature systems for murine Vδ gene segments.

4.4.1.2.3. γδ TCR ligands and antigen recognition

Unlike αβ TCRs which are limited to recognize peptide antigens bound to MHC molecules, γδ TCRs can directly recognize their antigens in their native form, including intact proteins and non-peptide compounds.[433 434] With a few clonal exceptions, γδ TCRs do not necessarily require either antigen processing, MHC-mediated antigen presentation, or co-receptor interaction to recognize their antigens. As a result, mere binding of the γδ TCRs to their cognate antigens is adequate for activation.[435] Furthermore, γδ TCRs have the capacity for both innate and adaptive

ligand recognition via either germline-encoded regions of the TCR, which are similar to PRRs, or via CDR-mediated adaptive antigen binding.[436]

The identification of γδ TCR antigens has been challenging due to a variety of reasons. First, no general restricting molecule has been identified for the γδ TCR. Therefore, the γδ TCR antigens could be, theoretically, any molecule that is expressed on cell surfaces or presents in the surrounding extracellular space. This becomes much more sophisticated when taking into account other molecules, besides proteins which are already very diverse, such as carbohydrates, lipids, and nucleic acids, that could be recognized or at least be involved in the recognition process. Second, affinities for γδ TCR-ligand interactions are substantially lower than for αβ TCR-peptide-MHC interactions, and mostly within the range of ~100 μM.[437] As a result, classical protein biochemistry techniques cannot be applied for low affinity measurements. Alternative methods, such as the generation of blocking antibodies, genetic approaches, or tetramer labelling with known T-cell antigens, are time-consuming and labor-intensive techniques on the one hand, and require a priori knowledge of potential candidates, which introduces bias on the other hand.[437 438] Furthermore, it is challenging to determine whether the recognition of specific antigens via γδ TCRs can be generalized or not, as a number of known antigens can be bound solely by particular clones that have been individually identified.[435] Moreover, the remarkable disparities in TCR sequences and subsets between mice and humans result in difficulty to translate findings in mice, in most cases, into humans, and vice versa. This also makes the assessment of the physiological relevance of many human γδ TCR ligands more difficult because they can only be identified *in vitro*, without the possibility of evaluating their functioning in transgenic mice.[435]

Despite all these obstacles, several and diverse host-cell-derived molecules have been identified since the discovery of γδ T cells as cognate antigens for the γδ TCR. Although the

majority of γδ T cells are not being restricted in recognition to MHC, a considerable number of γδ TCRs have been described that have the capacity to react with MHC or MHC-like molecules.[439-441] In mice, the closely related non-classical MHC class I molecules "T10/T22" have been initially described as ligands that activate specific murine γδ T cell clones.[442 443] Thereafter, it appeared that these molecules can also trigger a significant part of the murine γδ T cell pool in the periphery.[444] Reactivity of γδ TCRs with MHC or MHC-like molecules is largely dependent on the CDRs and particularly on the CDR3δ loop in most cases, which explains the similar antigenic repertoire of different γδ TCR populations, as they could have invariant patterns in their CDR loops.[445] The CD1d molecule, which is known to present lipid antigens to NKT cells, has been proposed as a phospholipid antigen, cardiolipin, of either self or microbial origin for various subsets of splenic and hepatic γδ T cells.[446] Nevertheless, unlike T10 and T22 molecules, no crystallographic data is currently available to validate this interaction in mice. More recently, it has been suggested that peripheral naive γδ T cells could quickly recognize a specific antigen, the algae protein phycoerythrin, which can elicit a rapid immune response that is characterized by producing the pro-inflammatory cytokine IL-17A.[447 448]

In humans, the dominant γδ T cell subset found in peripheral blood expresses a semi-invariant TCR that comprises a restricted Vγ9 rearrangement paired with a more diverse Vδ2 chain. $V\gamma9^{+}V\delta2^{+}$ TCRs can recognize small non-peptidic phosphorylated molecules, called phosphoantigens (PAgs), in a MHC-independent manner.[449 450] However, other studies showed that $V\gamma9^{+}V\delta2^{+}$ T cells are activated by PAgs when presented by the butyrophilin subfamily 3, member A1 (BTN3A1, also known as CD277).[451 452] Several criteria of PAgs are key determinants for their recognition via $V\gamma9^{+}V\delta2^{+}$ TCRs, including their size, resistance to hydrolysis, length of their alkenyl carbon chain, and presence of other chemical groups that affect the chemical structure

of PAgs.[453] [454] On this basis, many synthetic compounds, such as aminobisphosphonates, have been developed to better understand the recognition mechanisms and attempt to manipulate the activity $V\gamma9^{+}V\delta2^{+}$ T cells for therapeutic purposes.[455] [456] Furthermore, other studies have shown that some clones of γδ T cells, like human $V\delta1^{+}$ T cells, are able to recognize lipid-based antigens that are presented in a CD1d-restricted manner.[441] [457] Interestingly, these semi-invariant $V\delta1^{+}$ TCRs seems to recognize CD1d regardless of the presented antigen, suggesting a certain autoreactivity against CD1d-expressing cells. The crystallization of the human $V\delta1^{+}$ TCR complex with the CD1d molecule loaded with a sulfolipid-based antigen, sulfatide, clearly validates the possible interaction of human γδ TCR with CD1d molecules.[458]

4.4.1.3. Development, differentiation, and thymic selection of γδ T cells

αβ- and γδ- T cell lineages are derived from common thymic precursor cells that lack CD4 and CD8 co-receptors ($CD4^{-}CD8^{-}$), which also known as double-negative (DN) thymocytes, before their migration to the periphery. γδ T cells are the first T cell lineage to develop in the thymus to generate discrete γδ T cell effector subsets with distinctive molecular profiles. These subsets migrate from the thymus and preferentially reside in a wide variety of tissues where they can provide a rapid and innate-like source of effector cytokines for pathogen clearance and immunosurveillance.[459] Unlike their αβ T cell counterparts that egress from the thymus as naïve cells, γδ T cells can be pre-programmed for effector cytokine production during their development in the thymus.

During murine T cell development, DN thymocytes, which are common thymic precursors derived from bone marrow hematopoietic progenitor cells and reach the thymic cortex through the

circulation, can be further subdivided, according to their differential CD44 and CD25 expression, into four sequential phenotypic stages: DN1 ($CD44^+CD25^-$), DN2 ($CD44^+CD25^+$), DN3 ($CD44^-CD25^+$), and DN4 ($CD44^-CD25^-$), as depicted in **Figure I-11**. Clonal assays for investigating DN T cell precursors allowed the identification of the late DN2 to DN3 as the developmental stages where αβ- versus γδ-T cell lineage fate is determined.[460] DN2 is an important stage for the initiation of TCR gene rearrangement at the *Tcrd*, *Tcrg*, and *Tcrb* loci, whereas αβ and γδ lineage divergence arises at the DN3 stage, which is a critical selection stage to determine the fate of αβ- or γδ-T cell lineages.[461 462] The pre-TCR complex is formed by assembling of the constant pre-Tα (pTα) and CD3 subunits, resulting in a successful rearrangement of the TCR β. Differentiation of DN3 into DN4 cells and following αβ T cell lineage occur via a process termed as "β-selection", which is a checkpoint to control and produce a functional TCR β chain in a ligand-independent manner.[463-465] Thymocytes that pass β-selection initiate TCR α gene arrangement and expression of CD4 and CD8 to become double positive (DP, $CD4^+CD8^+$), resulting in the surface expression of TCR αβ chains.[466] On the other hand, commitment to γδ T cell lineage requires a γδ TCR genetic rearrangement at a DN3 checkpoint stage in a process known as "γδ-selection". Unlike αβ T cell lineage, thymocytes that pass the γδ-selection checkpoint directly express the γδ TCR/CD3 complex without passing through the pre-TCR complex step.[466] Of note, disruption of TCR gene rearrangement at the *Tcrb* locus, which in turn blocks the expression of pre-TCR complex, leads to the generation of minor subsets of γδ thymocytes that express both CD4 and CD8 co-receptors ($CD4^+CD8^+$), suggesting that the development of γδ T cells is not reliant on either TCR β or TCR α.[467]

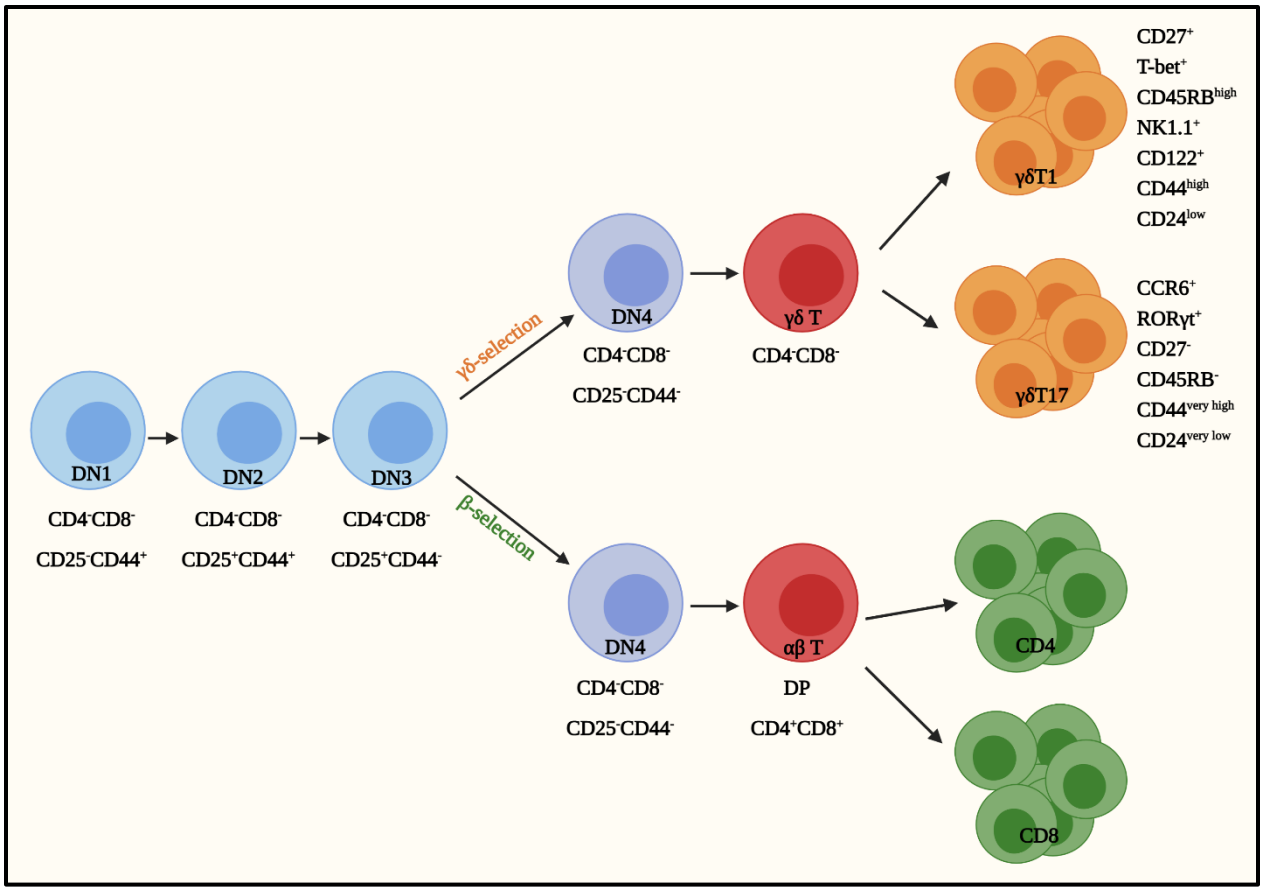

Figure I-11: Development and selection of γδ and αβ T cells in the thymus. Adapted from Qi et al.[468]. Created with BioRender.com

Recent studies have shown opposing perspectives on the models and signals that are involved in γδ T cell development and differentiation in the thymus, particularly on the role of both TCR-dependent and TCR-independent pathways.[469] Two models have emerged from attempts to explain the mechanisms behind αβ/γδ lineage choice: the signal strength "instructive" and stochastic models. The signal strength model proposed that pre-TCR or γδ TCR signaling intensities dictate αβ or γδ T cell lineage choice.[470] This model is based on multiple lines of evidence suggesting that DN cells receiving 'strong' γδ TCR signals commit to the γδ T cell lineage, while those receiving relatively 'weaker' pre-TCR signals are biased to the αβ fate.[471-473] So far, it is not yet clear why pre-TCR signals would be weaker than γδ TCR signals. Notably, the

γδ selection process is associated with increased phosphorylation of extracellular signal-regulated kinase 1/2 (ERK1/2) and induction of the expression of the early growth response (Egr) family of transcriptional factors that target the upregulation of inhibitor of DNA binding 3 (Id3). All of these were identified to be activated by stronger TCR signals, resulting in promoting the adoption of the γδ-fate and its maturation in the thymus besides restricting as well the αβ lineage choice.[466 474] By contrast, the stochastic model suggested that αβ/γδ fate determination occurs before TCR expression via other signals in a TCR-independent manner. In keeping with this, it was observed that TCR^- DN thymocytes with increased expression levels of SRY-box transcription factor 13 (Sox13) and IL-7Rα were directed towards the γδ T cell lineage.[475 476] Nevertheless, γδ T cell development has been also reported in Sox13-deficient mice, suggesting that this transcription factor is dispensable for commitment to the γδ lineage[476], although it could be crucial for the development of some IL-17-producing γδ T cell subsets[477]. Furthermore, Kang *et al.* demonstrated that mice lacking IL-7Rα (*IL-7Rα*$^{-/-}$) exhibited a defective development of γδ T cells due to impaired expression of TCR γ genes, leading to death of γδ lineage cells.[478]

4.4.1.4. Tissue distribution and biological functions of γδ T cell subsets

γδ T cells are significantly less frequent than αβ T cells, and accounting for about 0.5% to 5% of total T lymphocyte population in the peripheral blood and lymphoid tissues in mice and humans. However, they are the most abundant T cell subset at epithelial-rich tissues such as the skin, gut, lung, and reproductive tract, where they can comprise up to 50% of the total T cell population.[479] The exact roles of γδ T cell subsets in tissue physiology and surveillance remain a subject of research and investigation. However, their preferential residence in peripheral tissues

more than lymphoid organs may confer important indications related to their physiology. These clues suggest that γδ T cell subsets may extend their immune responsiveness to the peripheral anatomical locations that are not well covered by αβ T cells and/or B cells.[480 481]

Murine γδ T cells can be subdivided based on their γ chain expression into 7 subsets, from Vγ1 to Vγ7, using the Heilig and Tonegawa's nomenclature system, (Table I-3).[428 469] The development of the γδ T cell subsets starts in the thymus during the fetal period as successive and coordinated waves in the following order: $V\gamma5^+$ cells are produced after embryonic day 13 (E13) to approximately E17, followed by $V\gamma6^+$ cells from E14 to around birth, and last are $V\gamma1^+$, $V\gamma2^+$, and $V\gamma4^+$ cells from E16 onward, as depicted in **Figure I-12**.[463 479 482] Of note, the some $V\gamma7^+$ intestinal intraepithelial lymphocytes supposedly develop extrathymically.[483 484]

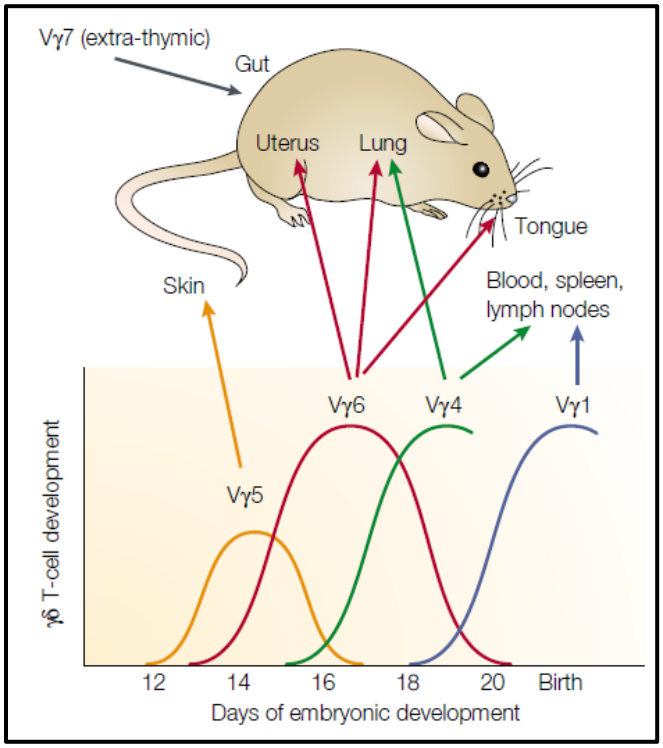

Figure I-12: Different developmental waves of murine γδ T cell progenitor subsets. Adapted from Carding and Egan[479]

	Classify	Common pairs	Tissue resident	Production of cytokines
Murine	Vγ1	Vγ6.3/6.4	skin, lung, colon, liver, PB (Peripheral blood), LNs (Lymph nodes)	IL-4, IFN-γ
	Vγ2	Vδ4	skin, lung, colon, liver, PB	IL-17
	Vγ3	Vδ1	skin, LNs	?
	Vγ4	Vδ4	skin (dermis), lung, colon, liver, PB, LNs	IL-17, IFN-γ
	Vγ5	Vδ1	DETCs (Dendritic epidermal T cells)	IFN-γ, IL-17
	Vγ6	Vδ1	genital tract, tongue, lung, colon, skin (dermis), adipose tissue	IL-17A/F, IL-22
	Vγ7	Vδ4/5/6	IELs (Intraepithelial lymphocytes)	IFN-γ
Human	Vδ1	$Vγ2^+/3^+/4^+/5^+/8^+/9^+$	gut, skin, liver, PB	IL-2, IL-4, IL-10, IL-17, IFN-γ, TNF-α
	Vδ2	$Vγ9^-/9^+$	PB, skin	IL-17, IL-21, IL-24, IFN-γ, TNF-α

Vδ3	Vγ2$^+$/3$^+$/4$^+$	PB, liver	IL-4, IL-10, IL-17, IFN-γ, TNF-α

Table I-3: Characteristics of murine and human γδ T cell subsets. Adapted from Qi *et al.*[468].

Vγ5$^+$ cells, also known as dendritic epidermal T cells (DETCs), pair with the Vδ1 subset of γδ TCR and are exported from the thymus to the epidermis.[485] Under physiological conditions of healthy skin, DETCs secrete some bioactive mediators, including IL-15 and IGF-1, to maintain skin immune homeostasis and enhance wound healing, while under pathological conditions, DETCs undergo morphological alterations that are associated with an increase in the early activation marker, CD69, and release soluble factors that control tissue repair.[486] Moreover, activated DETCs can express a variety of chemokines, including CCL3 and CCL4 chemokines that are essential for macrophage homing and recruitment.[487] Importantly, Vγ5$^+$Vδ1$^+$ T cells mostly produce IFN-γ via activation of the ERK-Egr-Id3-mediated pathway and suppression of the expression of Sox13 and retinoic acid-related orphan receptor-γt (RORγt) transcription factors that are associated with IL-17 production.[488] Nevertheless, other studies have demonstrated that DETCs have also the capacity to produce IL-17 and participate in skin inflammatory responses.[489]

After DETC development, the next functional developmental wave comprises the Vγ6$^+$ cells that are paired with the Vδ1 subset of the γδ TCR. After their development in the thymus, Vγ6$^+$ cells migrate to multiple epithelial-rich tissues, including genital tract, tongue, lungs, colon, and skin, as well as adipose tissue.[490] Vγ6$^+$Vδ1$^+$ T cells that produce IL-17 and other effector

molecules have been shown to drive immune homeostasis and inflammation. Paget *et al*. identified a $CD3^{bright}$ γδ T-cell subset with an effector memory phenotype. These cells rapidly produce IL-17A, but not interferon-γ, and respond promptly and strongly to pneumococcal infection and in the course of skin inflammation. They also showed using single cell sequencing that lung $CD3^{bright}$ γδ T cells were $V\gamma6^+V\delta1^+$ T cells.[491] On the other hand, Simonian *et al.* identified a subset of regulatory IL-22-secreting $V\gamma6^+$ cells that plays a role in the inhibition of αβ T cells and protection against lung fibrosis independently of IL-17 production.[492] Moreover, a seminal study by Kohlgruber *et al.* demonstrated that $V\gamma6^+$ γδ T cells were abundant in lean adipose tissue where they produced IL-17A and TNF, which in turn induced IL-33 production by stromal cells, stimulated the local proliferative expansion of Treg cells, and promoted fat lipolysis and thermogenesis via activating mitochondrial uncoupling protein 1 (UCP1) in brown adipocytes upon cold exposure.[493] Hu *et al.* have shown that $V\gamma6^+$ γδ T cell-derived IL-17F promotes the expression of TGF-β1 in adipocytes via IL-17 Receptor C (IL-17RC) signaling, which in turn enhances fat sympathetic innervation and regulates thermogenesis.[494]

Subsequently, the following functional waves of γδ T cell development generate $V\gamma1^+$, $V\gamma2^+$, $V\gamma4^+$ cells, which preferentially home to the dermis, lung, colon, liver, and lymph nodes as well.[481] [495] $V\gamma1^+$ γδ T cells are typically found in the form of $V\gamma1^+V\delta6.3/6.4^+$ TCR cells that produce IL-4 and IFN-γ.[496] $V\gamma1^+$ γδ T cells have been shown to play a protective role against acute viral myocarditis in mice, as they were reported to be one of the dominant and early producers of IL-4, which is a key mediator for modulating the IFN-γ secretion profile.[497] Furthermore, both $V\gamma1^+$ and $V\gamma4^+$ γδ T cells can produce IFN-γ, TNF-α, TGF-β, and IL-10 upon activation. However, $V\gamma1^+$ γδ T cells are biased to secrete IL-4 and IL-5, while $V\gamma4^+$ γδ T cells preferentially produce IL-17.[498] On the other hand, $V\gamma2^+$ γδ T cells have been shown to recruit neutrophils and worsen

liver fibrosis via secreting IL-17A.[499 500] Interestingly, and in the context of bacterial skin infection, a shift in responding γδ T cell subsets was observed, by which early Vγ1$^+$ and Vγ2$^+$ responders were replaced by a dominant Vγ4$^+$ γδ T cell subset, which enhanced IL-17 production, resulting in bacterial clearance.[501]

Noteworthy, there are two main functional subsets of murine γδ T cells that can commit to effector cytokine production during their development in the thymus and have been extensively described: IFN-γ-producing γδ T cells (γδT1 cells) and IL-17-producing γδ T cells (γδT17 cells).[502] γδT1 cells are characterized by expression of surface markers such as CD27, CD45RB^{high}, CD44^{high}, and CD24^{low} (as well as NK1.1 and CD122 in particular subsets), and also express T-bet, which is the key regulator transcription factor of IFN-γ production in T cells, (**Figure I-11**).[468 481 495 503] γδT1 cells include the fetal and perinatally derived Vγ5$^+$ DETCs, the Vγ1/Vδ6.3$^+$ γδ T cells, and the postnatally generated γδ T cell subsets that express more polyclonal γδ TCRs, mainly Vγ1$^+$ or Vγ4$^+$ cells, which distribute themselves, more systemically, to peripheral lymphoid organs, including spleen and lymph nodes.[481] On the other hand, γδT17 cells are distinguished by expression of surface markers, including C-C chemokine receptor type 6 (CCR6, also known as CD196), CD44$^{very\ high}$, and CD24$^{very\ low}$, lacking however CD27 expression. Moreover, γδT17 cells also express RAR-related orphan receptor gamma t (RORγt), which is the master transcription factor for IL-17 production in T cell subsets, (**Figure I-11**).[468 481 495 503] γδT17 cells comprise the fetal-derived monoclonal and/or oligoclonal Vγ6$^+$ γδ T cells, oligoclonal semi-invariant Vγ4$^+$ γδ T cells, and minor populations of Vγ1$^+$ and Vγ2/3$^+$ γδ T cells that are most notably found in the liver.[481 504] Of note, γδ T cells undergo effector cell differentiation in the thymus that is influenced by TCR signal strength. Strong TCR signaling promotes the IFN-γ effector fate, while γδT17 cells develop upon no/weak TCR signaling (**Figure I-13**).[495] Nevertheless, many studies have identified

a population of uncommitted γδ T cells termed naïve γδ T cells (γδTn cells) in the absence of TCR ligation during murine thymic development. These cells can exhibit adaptive-like behavior as they egress the thymus as naïve cells that require peripheral priming for functional development in the periphery and can establish long-lasting TCR-dependent memory as well (**Figure I-13**).[495 505-507]

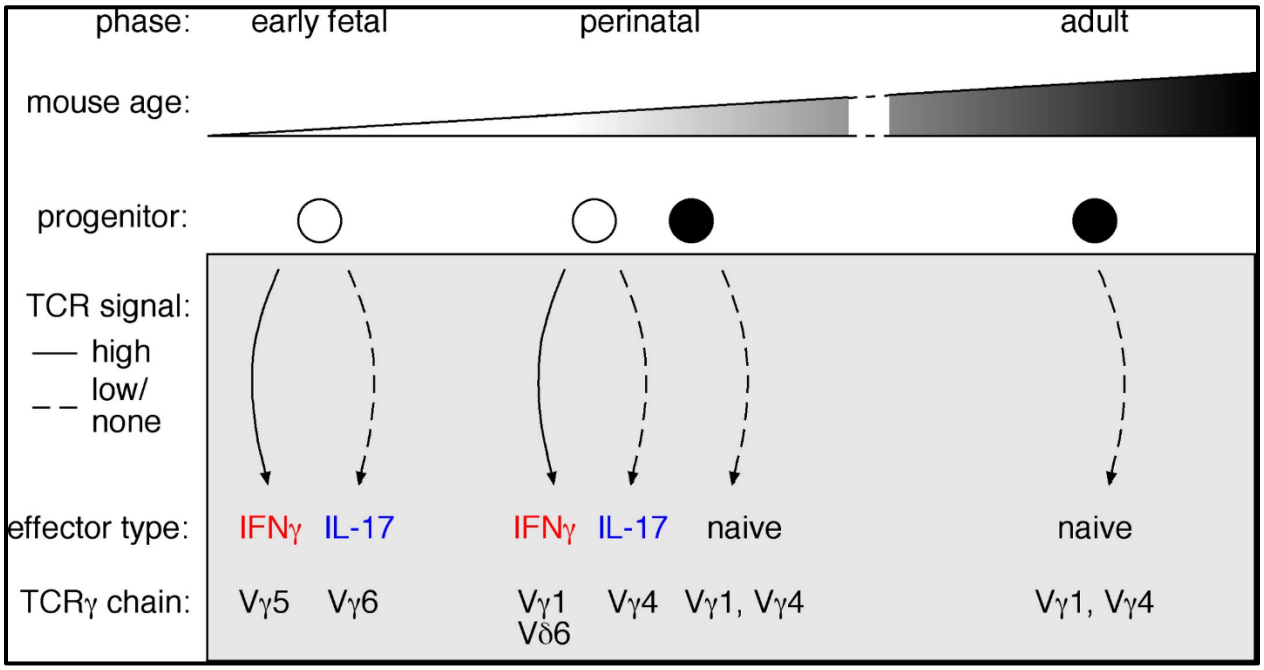

Figure I-13: Thymic development that generates γδ T cells pre-committed to the secretion of IFN-γ or IL-17A throughout murine life span. Adapted from Fiala et al.[495].

Importantly, Vγ4$^+$ γδ T cells share functional characteristics with Vγ6$^+$ γδ T cells as both subsets are the main component of γδT17 cell population.[508] Vγ4$^+$ and Vγ6$^+$ γδ T cells constitute the majority of dermal γδ T cell subsets that are responsible for IL-17 production, which have a detrimental effect in models of skin inflammatory diseases, namely dermatitis and psoriasis.[509-512] Gray *et al.* have observed that *Sox13*$^{-/-}$ mice, which lack Vγ4$^+$ γδ17 T cells, were less susceptible

to imiquimod-induced psoriasis-like skin inflammation.[477] Furthermore, Vγ4$^+$ γδ17 T cells have been observed to be recruited into the uterus and placenta during pregnancy, suggesting a role in tissue surveillance against pathogens.[513] Other studies suggest a deleterious role for IL-17 in pre-eclampsia, preterm birth, and miscarriage.[514] As a result, further investigation is required to understand how γδT17 T cells can protect against infection without causing high-risk inflammation during pregnancy. In bacterial lung infection, Vγ4$^+$ γδ T cells secrete CXC-chemokine ligand 2 (CXCL2) and TNF, which in turn promote neutrophil recruitment and bacterial clearance.[515] In tuberculosis lung infection, Vγ4$^+$ and Vγ6$^+$ γδT17 T cells have been shown to rapidly produce IL-17 and contribute to macrophage aggregation and granuloma formation in response to IL-23 produced by *Mycobacterium tuberculosis*-infected DCs.[516] Interestingly, memory-like γδ T cell responses in the lungs have been identified in mice infected with *Bordetella pertussis*, where lung-resident Vγ4$^+$ γδ T cells, which had expanded during primary infection, proliferated more rapidly, and secreted substantially more IL-17 after pathogen-specific rechallenge, leading to bacterial clearance enhancement.[517]

Vγ7$^+$ γδ T cells represent the majority of murine TCRγδ$^+$ intestinal intraepithelial lymphocytes (iIELs), which mainly home to the intestine and maintain the integrity of the intestinal epithelium.[481] [485] Activated Vγ7$^+$ γδ T cells constitutively secrete several cytokines[518], including IFN-γ, TGF-β, IL-10, and IL-13 as well as cytotoxic mediators[519] such as granzyme A and granzyme B, and antimicrobial peptides like regenerating islet-derived protein 3γ (RegIIIγ)[520], which together play an essential role in the early protection of the intestinal epithelium against microbial invasion and tissue damage.

On the other hand, human γδ T cells can be distinguished based on their δ chain expression into Vδ1, Vδ2, and Vδ3 subsets, (Table I-3).[521] Typically, Vδ1$^+$ cells pair with different Vγ TCR

family members ($V\gamma2^+/3^+/4^+/5^+/8^+/9^+$). $V\delta1^+$ cells are predominantly found in the gut, skin, spleen, and liver. Moreover, they account for about 30% of total γδ T cells in the peripheral blood.[522] $V\delta1^+$ T cells exert their effects via TCR recognition of stress molecules on epithelial cells. Activated $V\delta1^+$ T cells can produce cytokines, including IL-2, IL-4, IL-10, IL-17, IFN-γ, TNF-α, and chemokines, such as CCL3, CCL4, and CCL5, to play an essential role in maintaining the integrity of epithelial tissues and establishing antiviral immunity.[523] [524] Many studies have reported that $V\delta1^+$ T cells play a role in several diseases, such as human immune deficiency virus infection[525], malaria[526], and inflammatory bowel disease[527] through their cytotoxic function and release of cytokines and chemokines.

$V\delta2^+$ T cells are mainly distributed in the circulation and lymphoid organs and are the dominant δ chain subset found in healthy humans. They constitute approximately 50-90% of the total γδ T cell population in peripheral blood.[528] $V\delta2^+$ T cells can be distinguished into two main subsets based on their expression to Vγ9 chain: innate-like ($V\gamma9^+$) and adaptive ($V\gamma9^-$) subsets, $V\delta2^+V\gamma9^+$ T cells being the major subset of $V\delta2^+$ T cells.[529] $V\delta2^+V\gamma9^+$ T cells can be functionally subdivided, based on their surface expression of CD45RA and CD27, into naïve γδ T ($CD45RA^+CD27^+V\delta2^+V\gamma9^+$), central memory γδ T ($T_{CM}$, $CD45RA^-CD27^+V\delta2^+V\gamma9^+$), effector memory γδ T (T_{EM}, $CD45RA^-CD27^-V\delta2^+V\gamma9^+$), and $CD45RA^+$ effector memory γδ T (T_{EMRA}, $CD45RA^+CD27^-V\delta2^+V\gamma9^+$) subsets.[530] Naïve $V\delta2^+V\gamma9^+$ T cells form about 10-20% of the circulating γδ T cells in healthy human adults. T_{CM} γδ T cells are abundant in peripheral blood and have high proliferative capacity with limited effector functions. On the other hand, T_{EM} and T_{EMRA} γδ T cells are fully differentiated subsets that are less common in peripheral blood, but more abundant in tissues and at sites of inflammation. On contrary with T_{CM} γδ T cells, both T_{EM} and

T_{EMRA} γδ T cells exhibit low proliferative capacity with robust effector functions.[530] $V\delta2^+V\gamma9^+$ T cells particularly recognize phosphoantigens, such as isopentenyl pyrophosphate (IPP) and (E)-4-hydroxy-3-methyl-but-2-enyl pyrophosphate (HMBPP), and are rapidly activated to produce pro-inflammatory mediators, including IFN-γ, TNF-α, IL-17, IL-21, and IL-24.[468 531-533]

$V\delta3^+$ T cells are a minor lymphocyte subset in peripheral blood that account for 0.2% of circulating peripheral T cells but are more abundant in the liver and gut, and expand in patients with some chronic viral infections and leukemias. They variably express human leucocyte antigen DR (HLA-DR) and the NK cell-associated receptors NKG2D, CD56 and CD161 but not NKG2A, NKG2C nor CD25.[534] Upon activation, expanded $V\delta3^+$ T cells can only recognize CD1d molecules, but not CD1a, CD1b nor CD1c, and produce Th1, Th2, and Th17 cytokines that control DC maturation into efficient cytokine-producing-APCs.[534] Furthermore, $V\delta3^+$ T cells and B cells reciprocally upregulate the expression of maturation markers, including CD40, CD86, and HLA-DR, and promote IgM but not cytokine secretion by B cells.[535]

5. Experimental design

Many experimental animal models of HTN have been developed to mimic the human forms of HTN. These animal models are the result of pharmacological, genetic, dietary, and surgical manipulations that help to investigate the underlying mechanisms contributing to the development and progression of HTN. Ang II-induced hypertensive mouse model is one of the most frequently used models to understand the pathophysiology of essential HTN associated with an activated RAAS.

In this thesis, we attempted to elucidate how small subsets of γδ T cells can influence the BP elevation and vascular dysfunction in Ang II-induced HTN in mice. We profiled the distribution of γ TCR subtypes expressed by γδ T cells in perivascular adipose tissues and lymphoid tissues upon infusion of Ang II in mice using flow cytometry. Furthermore, flow immunophenotyping has been used to define the phenotype of the two most abundant γ TCR subtypes in PVAT, $V\gamma6^+$ and $V\gamma4^+$ γδ T cells, in WT and Ang II-induced hypertensive mice. We studied the effects of the absence of these two γ TCR subtypes on Ang II-induced BP elevation using telemetry and on MA endothelial dysfunction using pressurized myography.

6. Hypothesis and objectives

We previously demonstrated that γδ T cells play a key role in Ang II-induced HTN and vascular injury.[9] γδ T cells can be subdivided according to the TCR Vγ subtype that is generally specific for a tissue. A subpopulation of lung and skin γδ T cells that are $V\gamma6^+$ and produce IL-17A was shown to respond promptly to pneumococcal infection and skin inflammation.[491] However, γδ T cell Vγ subtype(s) involved in HTN is/are still unknown. We hypothesized that $V\gamma6^+$ γδ T cells may play a role in Ang II-induced HTN and vascular injury.

The main objectives of this thesis include:

1) To determine the distribution of γ TCR subtypes expressed by γδ T cells in the spleen, mesenteric lymph nodes (MLNs), thoracic aortic (TA) perivascular adipose tissue (PVAT), and mesenteric artery (MA) PVAT upon infusion of Ang II in mice.
2) To investigate the role of $V\gamma6^+$ γδ T cells in Ang II-induced HTN and vascular injury.
3) To study the contribution of a second candidate, $V\gamma4^+$ γδ T cells, to Ang II-induced BP elevation and vascular damage.

CHAPTER II: Materials & Methods

7. Materials

7.1. qPCR primer design digital tools

Digital tool	Link
UCSC genome browser	http://genome.ucsc.edu/
MultAlin	http://multalin.toulouse.inra.fr/multalin/
Primer3 v4.0	http://bioinfo.ut.ee/primer3-0.4.0/
Ensembl BLAST/BLAT	http://www.ensembl.org/
mfold tool	http://www.unafold.org

7.2. Chemicals, kits, and reagents

Name	Catalog number	Company and location
Angiotensin II, Human	05-23-0101	Calbiochem®, EMD Millipore Sigma, Oakville, ON, Canada
Bovine Serum Albumin (BSA) Media Grade, Powder	810685	Probumin®, EMD Millipore Sigma, Oakville, ON, Canada
Normal Goat Serum	005-000-121	Jackson ImmunoResearch, West Grove, PA, USA

RNAlater™ Stabilization Solution	AM7021	Thermo Fisher Scientific, Waltham, MA, USA
mirVana™ Isolation Kit	AM1560	Invitrogen, Thermo Fisher Scientific, Waltham, MA, USA
RNeasy® Lipid Tissue Mini Kit	74804	Qiagen, Hilden, Germany
TURBO DNA-*free*™ kit	AM1907	Invitrogen, Thermo Fisher Scientific, Waltham, MA, USA
QuantiTect Rev. Transcription Kit	205311	Qiagen, Hilden, Germany
SsoFast™ EvaGreen® Supermix	1725201	Bio-Rad Laboratories, Hercules, CA, USA
SsoAdvanced Universal SYBR® Green Supermix	1725274	Bio-Rad Laboratories, Hercules, CA, USA
AbSolve™ Glassware Cleaner, 1L	6NE9711	PerkinElmer Inc., Waltham, MA, USA
Gibco™ PBS (1X), pH 7.4	10010049	Thermo Fisher Scientific, Waltham, MA, USA
NAb™ Protein L Spin Kit, 1 mL	89981	Thermo Fisher Scientific, Waltham, MA, USA
NAb™ Protein G Spin Kit, 1 mL	89979	Thermo Fisher Scientific, Waltham, MA, USA
DC™ Protein Assay Kit II	5000112	Bio-Rad Laboratories, Hercules, CA, USA

Tris-Base (Tham®)	T370-500	Fisher Chemical, Thermo Fisher Scientific, Fair Lawn, NJ, USA
Sodium Dodecyl Sulfate (SDS)	L3771	Sigma-Aldrich, Darmstadt, Germany
40% Acrylamide/Bis Solution, 37.5:1	1610148	Bio-Rad Laboratories, Hercules, CA, USA
Ammonium persulfate (APS)	A3678	Sigma-Aldrich, Darmstadt, Germany
N,N,N′,N′-Tetramethylethylenediamine (TEMED)	T9281	Sigma-Aldrich, Darmstadt, Germany
Glycine	G8898	Sigma-Aldrich, Darmstadt, Germany
Glycerol	17904	Thermo Fisher Scientific, Waltham, MA, USA
β-mercaptoethanol (14.3M)	11-102-0493	Fisher Chemical, Thermo Fisher Scientific, Fair Lawn, NJ, USA
Bromophenol blue	B0126	Sigma-Aldrich, Darmstadt, Germany
Laemmli SDS sample buffer, reducing (6X)	J61337	Alfa Aesar, Thermo Fisher Scientific, Haverhill, MA, USA
Precision Plus Protein™ Kaleidoscope™ Prestained Protein Standards (protein ladder)	1610375	Bio-Rad Laboratories, Hercules, CA, USA
Gel-loading tips	2239915	Bio-Rad Laboratories, Hercules, CA, USA

Coomassie Brilliant blue R250	1610400	Bio-Rad Laboratories, Hercules, CA, USA
LIVE/DEAD™ Fixable Aqua Dead Cell Stain Kit	L34957	Invitrogen, Thermo Fisher Scientific, Waltham, MA, USA
DyLight® 650 Conjugation Kit (Fast) - Lightning-Link®	ab201803	Abcam, Cambridge, UK
Alexa Fluor™ 647 Antibody Labeling Kit	A20186	Invitrogen, Thermo Fisher Scientific, Waltham, MA, USA
R-Phycoerythrin Conjugation Kit	PJ31K	ProZyme, Hayward, CA, USA
Phorbol 12-myristate 13-acetate (PMA)	P1585	Sigma-Aldrich, Darmstadt, Germany
Ionomycin calcium salt from *Streptomyces conglobatus*	I0634	Sigma-Aldrich, Darmstadt, Germany
Monensin Solution (1,000X)	420701	BioLegend, San Diego, CA, USA
10% Paraformaldehyde (formaldehyde) aqueous solution	15712	Electron Microscopy Sciences, Hatfield, PA, USA
Saponin	558255	Calbiochem®, EMD Millipore Sigma, Oakville,ON, Canada

UltraComp eBeads™ Compensation Beads	01-2222-42	Invitrogen, Thermo Fisher Scientific, Waltham, MA, USA
BD CS&T research beads	650621	BD Biosciences, Franklin Lakes, NJ, USA
Trypsin Inhibitor, Lyophilized	LS003570	Worthington Biochemical Corporation, Lakewood, NJ, USA
Elastase, Lyophilized	LS002292	Worthington Biochemical Corporation, Lakewood, NJ, USA
Collagenase, Type 2, Lyophilized	LS004176	Worthington Biochemical Corporation, Lakewood, NJ, USA
Collagenase A, Lyophilized	10103586001	Roche, Basel, Switzerland
Hyaluronidase, Lyophilized	H2126	Sigma-Aldrich, Darmstadt, Germany
DL-Norepinephrine (NE) hydrochloride	A7256	Sigma-Aldrich, Darmstadt, Germany
Acetylcholine (Ach) chloride	A6625	Sigma-Aldrich, Darmstadt, Germany
N^{ω}-Nitro-L-arginine methyl ester (L-NAME) hydrochloride	N5751	Sigma-Aldrich, Darmstadt, Germany
Sodium nitroprusside (SNP) dihydrate	71778	Sigma-Aldrich, Darmstadt, Germany
Ethylene Glycol-bis(β-aminoethyl ether)-	ED0077	Bio Basic Inc., Markham, ON, Canada

N,*N*,*N*′,*N*′-Tetra Acetic acid

[EGTA]

7.3. Instruments and materials.

Name	**Catalog number**	**Company and location**
MicroAmp™ Fast Optical 96-Well Reaction Plate, 0.1 mL	4346907	Applied Biosystems®, Thermo Fisher Scientific, Waltham, MA, USA
Repeater® M4 - Positive Displacement Pipette	4982000322	Eppendorf, Hamburg, Germany
Combitips® advanced, 5.0 mL	30089561	Eppendorf, Hamburg, Germany
500 mL Bottle Top Vacuum Filter, 0.22 µm	431118	Corning Life Sciences Inc., Corning, NY, USA
Column Extender for Pierce™ Centrifuge Column	69707	Thermo Fisher Scientific, Waltham, MA, USA
CELLSTAR®96-well plate (flat and transparent bottom)	655180	Greiner Bio-One International GmbH, Kremsmünster, Austria

Cotton-Tip Applicators	807	SafeBasics ™, AMD Medicom®, Montréal, QC, Canada
Systane® Lubricant Eye Ointment	2444062	Alcon, Mississauga, ON, Canada
Baxedin® Antiseptic Solution, Untinted	OMEL0000017	Omega Laboratories, Montréal, QC, Canada
Metzenbaum scissors, straight, 14.5CM	130.100.14	Instrumentarium, Terrebonne, QC, Canada
ALZET® Micro-osmotic pump	Model 1002	Durect, Cupertino, CA, USA
Michel suture clip 7.5X1.75MM	BN507R	AESCULAP® Surgical Instruments, Tuttlingen, Germany
96 well Mini tubes, 1.1 mL	MTS11C	Axygen™, Corning Life Sciences Inc., Corning, NY, USA
40 µm Cell Strainer	352340	Falcon, Corning, Glendale, AZ, USA
70 µm Cell Strainer	352350	Falcon, Corning, Glendale, AZ, USA
70 µm Cell strainer	83.3945.070	Sarstedt, Nümbrecht, Germany
Cell strainer adapter	83.3945.999	Sarstedt, Nümbrecht, Germany
Microtube 5 mL, SafeSeal reaction tube	72.701.400	Sarstedt, Nümbrecht, Germany
PARAFILM® "M"	PM996	Pechiney Plastic Packaging, Inc., Chicago, IL, USA

96-Well Polystyrene Conical Bottom MicroWell™ Plate	249570	Nunc™, Thermo Fisher Scientific, Waltham, MA, USA
Borosilicate capillary glass tubing	G150T-4	Warner Instruments, Holliston, MA, USA
Borosilicate glass capillaries	TW120-4	World Precision Instruments, Sarasota, FL, USA

7.4. Antibodies

Antibody	Fluorochrome	Clone	Catalog number	Company and location
CD45	BV785	30-F11	103149	BioLegend, San Diego, CA, USA
CD3	AF700	17A2	56-0032-82	eBioscience, San Diego, CA, USA
CD3	BUV395	17A2	740268	BD Biosciences, Franklin Lakes, NJ, USA
CD4	PerCP-eFluor710	RM4-5	46-0042-82	eBioscience, San Diego, CA, USA
CD8a	APC-eFluor780	53-6.7	47-0081-82	eBioscience, San Diego, CA, USA

γδ T-Cell Receptor (TCR)	PE-CF594	GL3	563532	BD Biosciences, Franklin Lakes, NJ, USA
TCR Vγ1 and Vγ2	PE	4B2.9	142704	BioLegend, San Diego, CA, USA
TCR Vγ4	BV605	UC3-10A6	742310	BD Biosciences, Franklin Lakes, NJ, USA
TCR Vγ4	PE	UC3-10A6	137706	BioLegend, San Diego, CA, USA
TCR Vγ4	BV421	UC3-10A6	742308	BD Biosciences, Franklin Lakes, NJ, USA
TCR Vγ4	non-conjugated	UC3-10A6	BE0168	Bio X Cell, Lebanon, NH, USA
Armenian hamster IgG isotype control	non-conjugated	Polyclonal (HAMSTER IGG)	BE0091	Bio X Cell, Lebanon, NH, USA
TCR Vγ5	BB700	536	746021	BD Biosciences, Franklin Lakes, NJ, USA
TCR Vγ6	non-conjugated	17D1	-	Gift from Dr. R. Tigelaar, Yale University, New Haven, CT, USA

TCR Vγ6	non-conjugated	1C10-1F7	-	Gift from Dr. Y. Yoshikai, Kyushu University, Fukuoka, Japan
mouse IgG1 isotype control	non-conjugated	MOPC-21	BE0083	Bio X Cell, Lebanon, NH, USA
TCR Vγ7	DyLight650	F2.67	-	Gift from Dr. P. Pereira-Esteva, Pasteur Institute, Paris, France
IgM, μ chain specific	AF488	Polyclonal	312-545-049	Jackson ImmunoResearch, West Grove, PA, USA
IgM, μ chain specific	R-PE	Polyclonal	112-116-075	Jackson ImmunoResearch, West Grove, PA, USA
IgG1	APC	RMG1-1	406610	BioLegend, San Diego, CA, USA
CCR6 (CD196)	PE-Cy7	29-2L17	129816	BioLegend, San Diego, CA, USA
CXCR3 (CD183)	APC	CXCR3-173	126511	BioLegend, San Diego, CA, USA
CXCR3 (CD183)	BV605	CXCR3-173	126523	BioLegend, San Diego, CA, USA

CD69	PE-Cy5	H1.2F3	15-0691-82	eBioscience, San Diego, CA, USA
CD44	BB515	IM7	564587	BD Biosciences, Franklin Lakes, NJ, USA
CD25	BV421	PC61	102043	BioLegend, San Diego, CA, USA
CD25	BV605	PC61	102036	BioLegend, San Diego, CA, USA
CD27	BV605	LG.3A10	563365	BD Biosciences, Franklin Lakes, NJ, USA
Ki-67	BUV395	B56	564071	BD Biosciences, Franklin Lakes, NJ, USA
ROR γt	APC	AFKJS-9	17-6988-80	eBioscience, San Diego, CA, USA
T-bet	PE-Cy7	eBio4B10 (4B10)	25-5825-80	eBioscience, San Diego, CA, USA
IL-17A	APC	eBio17B7	17-7177-81	eBioscience, San Diego, CA, USA
IFNγ	AF488	XMG1.2	53-7311-82	eBioscience, San Diego, CA, USA
CD39	PE-Cy7	Duha59	143806	BioLegend, San Diego, CA, USA

CD73	PE	TY/23	550741	BD Biosciences, Franklin Lakes, NJ, USA
FOXP3	FITC	FJK-16s	11-5773-82	eBioscience, San Diego, CA, USA
IL-22	APC	Polyclonal (Poly5164)	516409	BioLegend, San Diego, CA, USA
IL-10	AF488	JES5-16E3	505013	BioLegend, San Diego, CA, USA
CD16/CD32 (Mouse BD Fc Block™)	non-conjugated	2.4G2	553142	BD Biosciences, Franklin Lakes, NJ, USA

BV: Brilliant violet; **AF:** Alexa fluor; **BUV:** Brilliant ultraviolet; **PerCP:** Peridinin chlorophyll-A protein; **PE:** Phycoerythrin; **CF:** Cyanine-based fluorescent dye; **BB:** Brilliant blue; **APC**: Allophycocyanin; **Cy:** Cyanine; **FITC:** Fluorescein isothiocyanate.

7.5. Hybridoma cell culture reagents and consumables

Name	**Catalog number**	**Company and location**
Falcon® 75cm² rectangular straight neck cell culture flask with vented cap	353110	Corning Life Sciences Inc., Corning, NY, USA

Falcon® 175cm² rectangular straight neck cell culture flask with vented cap	353112	Corning Life Sciences Inc., Corning, NY, USA
Nunc™ EasYFlask™ Cell Culture Flask, 175cm²	159910	Thermo Fisher Scientific, Waltham, MA, USA
Hybridoma-SFM	12045076	Gibco, Thermo Fisher Scientific, Waltham, MA, USA
Fetal Bovine Serum (FBS)	12483020	Gibco, Thermo Fisher Scientific, Waltham, MA, USA
Penicillin-Streptomycin-Amphotericin B Suspension (×100)	161-23181	FUJIFILM Wako Pure Chemical Corporation, Osaka, Japan
Antibiotic-Antimycotic (100X)	15240062	Gibco, Thermo Fisher Scientific, Waltham, MA, USA
Recombinant Human IL-6 (10µg)	206-IL-10	R&D Systems, Minneapolis, MN, USA
RPMI 1640 Medium	11875119	Gibco, Thermo Fisher Scientific, Waltham, MA, USA
HEPES (1 M)	15630080	Gibco, Thermo Fisher Scientific, Waltham, MA, USA
Sodium Pyruvate (100mM)	11360070	Gibco, Thermo Fisher Scientific, Waltham, MA, USA

MEM Non-Essential Amino Acids Solution (100X)	11140050	Gibco, Thermo Fisher Scientific, Waltham, MA, USA
Penicillin-Streptomycin (10,000 U/mL)	15140122	Gibco, Thermo Fisher Scientific, Waltham, MA, USA

7.6. Buffers and solutions

Solution	Recipe
17D1 hybridoma culture medium	(Complete RPMI, 47.2 mL): 40 mL RPMI 1640, 4.8 mL FBS or FCS, 960 µL Hepes (1M), 480µL Sodium Pyruvate (100 mM), 480 µL MEM Non-Essential Amino Acids Solution (100X) and 480 µL Penicillin-Streptomycin (10,000 U/mL)
1C10-1F7 hybridoma culture medium	Hybridoma- serum free medium (SFM) including 1ng/mL recombinant human IL-6, 10% fetal bovine serum (FBS) and Penicillin-Streptomycin-Amphotericin B (1X)
Binding buffer (for antibody purification)	100 mM phosphate and 150 mM sodium chloride dissolved in 500 mL ultrapure H_2O; pH 7.2
IgG Elution buffer	240 mL, pH 2.8
Neutralization buffer	12 mL, 1M Tris-HCl, pH 8.5
Separating (resolving) gel buffer, 500 mL	91 g of Tris-Base dissolved in 300 mL H_2O and pH adjusted to 8.8 with HCl, then completed to 500 mL with H_2O and add 2 grams of SDS

SDS-PAGE 10 % resolving gel (1.5 mm thickness), for 1 gel of 10 mL	In 4.85 mL distilled H_2O, these ingredients added in order: 2.5 mL resolving gel buffer, 2.5 mL 40% acrylamide/Bis 37.5:1, 45 µl 10% APS and 10 µl TEMED
Staking gel buffer, 100 mL	6.05 g of Tris-Base dissolved in 40 mL of H_2O and pH adjusted to 6.8 with HCl, then completed to 100 mL and add 0.4 g of SDS
SDS-PAGE 4 % stacking gel (1.5 mm thickness), for 1 gel of 10 mL	In 2.54 mL distilled H_2O, these ingredients added in order: 1 mL stacking gel buffer, 0.4 mL 40% acrylamide/Bis 37.5:1, 20 µl 10% APS and 4 µl TEMED
SDS-PAGE SDS Running Buffer (10x), 1L	0.25 M Tris base (MW: 121.14 g/mol), 1.92 M Glycine (MW: 75.07 g/mol) and 0.035 M SDS (MW: 288.38 g/mol) dissolved in distilled H_2O until volume is 1 L
50x Tris base, acetic acid and EDTA (TAE) buffer, 1L	242 grams of Tris-base (MW = 121.14 g/mol) dissolved in 700 mL deionized H_2O, then added 57.1 mL of 100 % glacial acid (or acetic acid) and 100 mL of 0.5 M EDTA (pH 8.0), and completed with deionized H_2O to 1L. Finally, pH adjusted to 8.5

7.7. Devices

Name	Model	Company and location
NanoDrop™ ND-1000 spectrophotometer	ND-1000	Thermo Fisher Scientific, Waltham, MA, USA
Benchmark Plus ™ microplate spectrophotometer	-	Bio-Rad Laboratories, Hercules, CA, USA
T-Gradient Thermoblock Thermocycler	-	Biometra® GmbH, Goettingen, Germany
Real-time PCR cycler	Mx3005P	Agilent Technologies, Santa Clara, CA, USA
Fast Real-Time PCR System	7500	Applied Biosystems®, Thermo Fisher Scientific, Waltham, MA, USA
PowerPac™ HC Power Supply (for gel electrophoresis)	1645052	Bio-Rad Laboratories, Hercules, CA, USA
Hybridization oven	-	VWR International, LLC Radnor, PA, USA
ChemiDoc Gel Imaging System	Universal hood II	Bio-Rad Laboratories, Hercules, CA, USA
BD LSRFortessa™ Flow Cytometer	-	BD Biosciences, Franklin Lakes, NJ, USA
BD FACSAria™ III Cell Sorter	-	BD Biosciences, Franklin Lakes, NJ, USA
MS5 Stereo microscope	-	Leica Microsystems, Wetzlar, Germany

M3C Stereo microscope	-	Wild Heerbrugg, Heerbrugg, Switzerland
Pressure servo controller with peristaltic pump	PS-200	Living Systems Instrumentation, St. Albans City, VT, USA
Temperature controller for single chamber	TC-02 and TC-09S	Living Systems Instrumentation, St. Albans City, VT, USA
Perfusion pressure monitor	PM-4	Living Systems Instrumentation, St. Albans City, VT, USA
Video dimension analyzer	VDA-10	Living Systems Instrumentation, St. Albans City, VT, USA
Minipuls® 3 peristaltic pumps	-	Gilson Inc., Middleton, WI, USA
B14 heated water bath with isotemp 2100 circulating pump	-	Thermo Fisher Scientific, Waltham, MA, USA
Needle/pipette puller	750	David Kopf Instruments, Tujunga, CA, USA
PA-C10 radiotelemetry pressure transmitter	-	Data Sciences International, St. Paul, MN, USA

7.8. Software for data acquisition and analysis

Name	Version	Company and location
Clone Manager Basic software	V 9.0	Sci-Ed Software, Westminster, CO, USA
NanoDrop™ ND-1000 software	V 3.8.1	Thermo Fisher Scientific, Waltham, MA, USA
Microplate manager	V 5.2.1	Bio-Rad Laboratories, Hercules, CA, USA
7500 Real-Time PCR Software	V 2.0.1	Applied Biosystems®, Thermo Fisher Scientific, Waltham, MA, USA
Quantity One 1-D Analysis Software	V 4.6.9	Bio-Rad Laboratories, Hercules, CA, USA
FlowJo software	V 10.1	Tree Star Inc., Ashland, OR, USA
SigmaPlot	V 12.5	Systat Software Inc., San Jose, CA, USA

8. Methods

8.1. qPCR primer design and RT-qPCR

In order to know which γδ T cell subtypes are infiltrating studied tissues, the expression profile of γ and δ TCR variable region subtypes and constant regions was examined in mesenteric arteries, which may contain immune cells infiltrating the adventitia. This was done using a previously obtained total RNA sequencing data from mesenteric arteries of 10–12-week-old male mice (The Jackson Laboratory, Bar Harbor, ME, USA) infused or not with Ang II (1000 ng/kg/min, subcutaneously (SC)) using ALZET micro-osmotic pumps (Durect Corporation) for 7 and 14 days. Genes encoding γ and δ TCR variable region subtypes and constant regions expressed in MAs were identified.

In order to profile γδ T cell subtypes by Reverse Transcription-quantitative Polymerase Chain Reaction (RT-qPCR), oligonucleotide primers for RT-qPCR were designed as follows, (**Figure II-1**). mRNA sequences of each candidate gene were downloaded and mapped to the mouse genome GRCm38/mm10 to verify the sequence quality and determine the structure of the gene and the exon junctions using UCSC genome browser gene sorter and blat tools, respectively. The sequences were annotated using Clone Manager Basic software v 9.0 (Sci-Ed Software). Since the sequences of γ and δ TCR variable and constant regions are highly homologous, they were aligned using the MultAlin tool to determine the portions of sequence that are unique for each of them. Thereafter, the design of oligonucleotide primers was planned in a way to be specific and not amplify genomic DNA (genomic proof). Oligonucleotide primers were designed to have a melting temperature (Tm) of 60°C and a 3’ GC clamp using Primer3 v 4.0.

Oligonucleotide primers were first tested using the UCSC genome browser *in silico* PCR and tools to determine whether the expected PCR product is obtained with the UCSC genes but not with the genome assembly. This was also verified using the Ensembl BLAST/BLAT tool. Oligonucleotide primers were also selected that did not have hairpins with a Tm <50°C, and that did not form primer dimers using the mfold tool. All links for primer design tools are listed in Materials section (7.1).

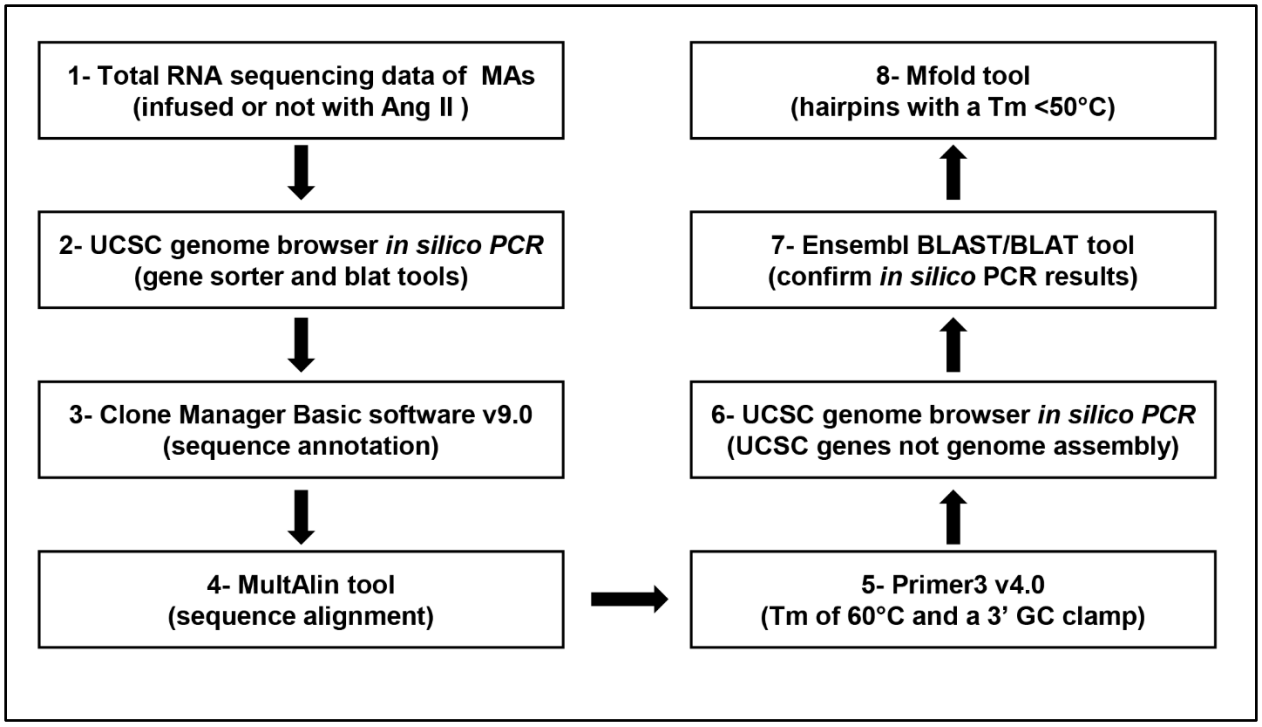

Figure II-1: The workflow of qPCR oligonucleotide primer design

Oligonucleotide primers were validated by RT-qPCR in tissues expected to express these genes, such as thymus, mesenteric arteries with perivascular adipose tissue (MA+PVAT), intestine and skin, to have a PCR efficiency between 95% and 105%, one amplicon with a Tm >80°C in the qPCR dissociation curve, and the right PCR product length using agarose gel electrophoresis, (**Figure II-2**). Thirteen-to-15-week-old male mice were anesthetized with isoflurane 2.5% mixed

with O_2 at 1 L/mL, and blood was collected by cardiac puncture. Pieces of thymus, (MA+PVAT), shaved-skin and small intestine were collected in ice-cold phosphate buffered saline (PBS), transferred in RNAlater™ Stabilization Solution (Thermo Fisher Scientific) and used immediately for RNA extraction or froze in liquid nitrogen and stored at -80°C until used. Total RNA was extracted using mirVana™ Isolation Kit (Thermo Fisher Scientific), except for (MA+ PVAT). Total RNA from (MA+PVAT) was extracted using RNeasy® Lipid Tissue Mini Kit (Qiagen). TURBO DNA-*free*™ kit (Thermo Fisher Scientific) used to eliminate trace quantities of DNA that can interfere with RT-qPCR. The concentration and purity of RNA were assessed with a NanoDrop™ ND-1000 spectrophotometer (Thermo Scientific) and integrity assessed by determining the rRNA and mRNA profiles in agarose gel electrophoresis. One µg of RNA was reverse transcribed with the QuantiTect RT kit (Qiagen) according to the manufacturer's protocol. qPCR was then performed using the SsoFast™ EvaGreen® Supermix (Bio-Rad Laboratories) with the Mx3005P real-time PCR cycler (Agilent Technologies) or using the SsoAdvanced Universal SYBR® Green Supermix (Bio-Rad Laboratories) with the Applied Biosystems® 7500 Fast Real-Time PCR System (Thermo Fisher Scientific). The qPCR conditions for SsoFast™ EvaGreen® Supermix were 2 min at 98°C, followed by 40 cycles of 5 sec at 96°C and 30 sec at 58°C. The qPCR conditions for SsoAdvanced Universal SYBR® Green Supermix were 30 sec at 98°C, followed by 40 cycles of 10 sec at 98°C and 30 sec at 60°C. Amplification products were checked using agarose gel electrophoresis [1.2% RNase-free Tris-Acetate-EDTA (TAE) agarose at 50V then 90V for 25 min then 30 min, respectively].

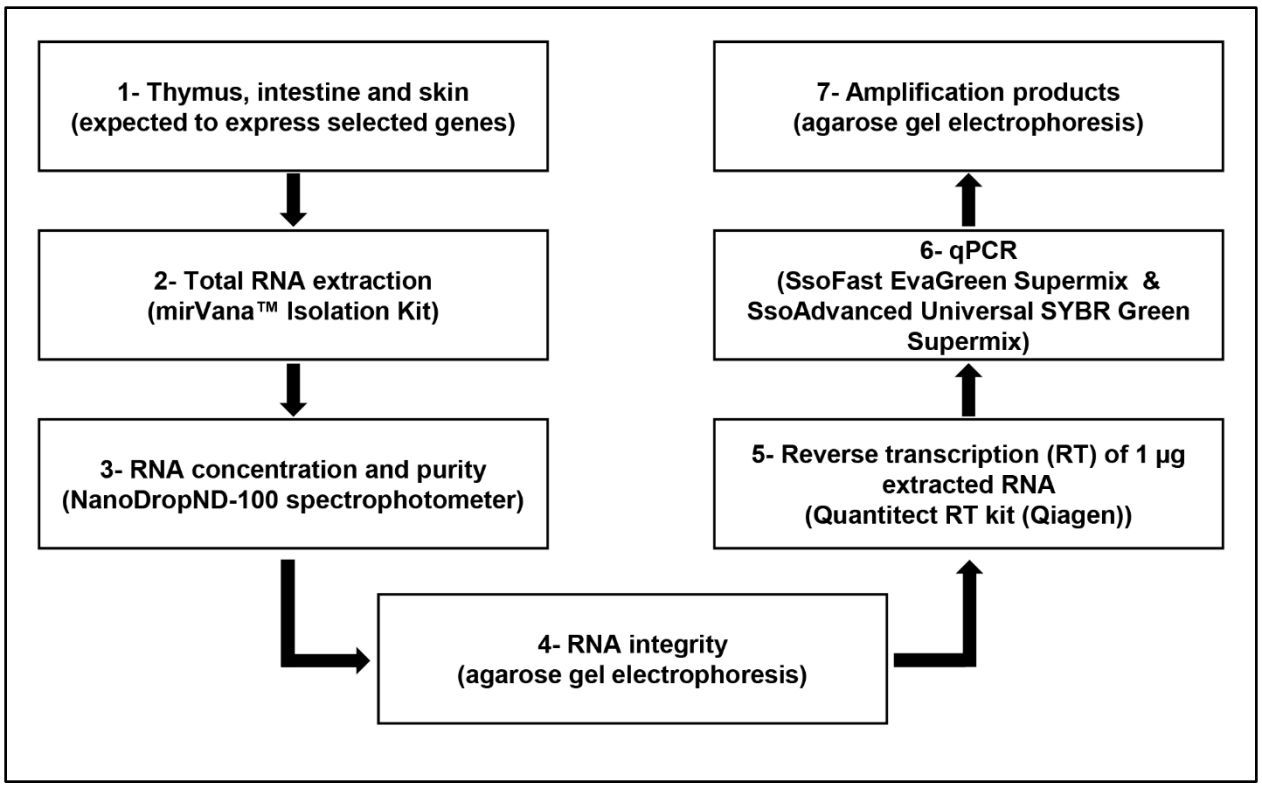

Figure II-2: qPCR oligonucleotide primer validation

8.2. Hybridoma cell culture (17D1 and 1C10-1F7)

Two different hybridomas were used in the TCR Vγ6 study to produce rat IgM anti-mouse TCR Vγ6 (clone 17D1: a gift from Dr. R. Tigelaar, Yale University, USA) and mouse IgG1 anti-mouse TCR Vγ6 (clone 1C10-1F7: obtained through a collaboration with Dr. Y. Yoshikai, Kyushu University, Japan) antibodies. Culturing of 17D1 and 1C10-1F7 hybridomas was carried out based on provider's protocols. Each hybridoma was received frozen in liquid nitrogen. Frozen hybridomas were rapidly thawed (<30 sec.) at 37 °C in a water bath. Inside a laminar flow cabinet, the thawed cells were carefully and slowly diluted in pre-warmed (37 °C) hybridoma culture medium (ingredients of hybridoma culture medium for each hybridoma were mentioned in detail in materials section). The hybridoma suspension was transferred into a 15 mL conical sterile

polypropylene centrifuge tube and centrifuged for 5 minutes at 800 x g at room temperature, the supernatant was then removed carefully without disturbing the hybridoma cell pellet. The cell pellet was suspended in 10 mL pre-warmed hybridoma culture medium and centrifuged for 5 minutes at 800 x g at room temperature. The supernatant was then discarded without disturbing the hybridoma cell pellet. The cell pellet was resuspended in 10 mL pre-warmed hybridoma culture medium, transferred to T-75 cell culture flask (maintenance flask) and incubated in cell culture incubator (37 °C, 5% CO_2). The hybridomas were cultured in maintenance flasks until they reached the appropriate density that was appropriate for antibody production (20 million cells/ production flask). T-175 cell culture flasks (production flask) were filled with 20 mL hybridoma culture medium without FBS, then 20 million of hybridoma cultured cells in the maintenance flask were transferred to the production flask and kept in the cell culture incubator. After three days of culturing, another 20 mL of hybridoma culture medium without FBS were added to the production flask (in total 40 mL/ production flask) and incubated for another 4-7 days (total duration is 7-10 days since starting culture in production flask). At the end of culturing, the content of production flask (~40mL) was transferred into 50 mL centrifuge tube and centrifuged at 4500 x g for 7 minutes at room temperature. The cell pellet was discarded, and the supernatant frozen at -20°C until the purification step.

8.3. Antibody purification, quantification, and qualification

After 7-10 days of hybridoma culturing with hybridoma culture medium without FBS, hybridoma culture supernatants were collected, filtered through a bottle top vacuum filter (0.22 μm), then purified using the gravity-flow purification protocol of the NAb™ Protein L Spin Kit

(Thermo Fisher Scientific, for 17D1 supernatant) and the NAb™ Protein G Spin kit (Thermo Fisher Scientific, for 1C10-1F7 supernatant) according to the manufacturer instructions. In brief, the column and buffers used in purification were equilibrated to room temperature. The hybridoma supernatant was diluted 1:1 with the binding buffer (all buffer ingredients used in the purification step are listed and described in the Materials section) and passed through a 0.22 μm vacuum filter to avoid column contamination and clogging. The column was equilibrated by adding 5mL of the binding buffer and allowed to drain the solution, then the diluted supernatant was applied to the column. A column extender (Thermo Fisher Scientific) was used to expand column capacity and accelerate the purification process. After passing the diluted supernatant, 15 mL of binding buffer were applied into the column before adding 5 mL of elution buffer to release antibodies attached to the resin column. Purified antibodies were collected as 1 mL fractions, each containing 100μL of neutralization buffer. All fractions were kept at 4 °C.

Purified antibodies were quantified using a NanoDrop^{TM} ND-1000 spectrophotometer (Thermo Fisher Scientific) at 280 nm and/or a Bio-Rad detergent compatible (DC) protein assay that is a colorimetric assay for protein concentration assessment at 750 nm. The quality and purity of the purified antibodies was determined by sodium dodecyl sulfate polyacrylamide gel electrophoresis (SDS-PAGE) and Coomassie Blue R-250 staining. All ingredients of SDS-PAGE buffers and gels, and Coomassie Blue staining and destaining solutions I & II are described in Materials section.

8.4. Conjugation of antibodies with fluorochromes

We attempted conjugating the purified mouse IgG1 anti-mouse TCR Vγ6 (clone 1C10-1F7) antibody using DyLight™ 650 (Abcam) and Alexa Fluor (AF)™ 647 (Invitrogen, Thermo Fisher Scientific) fluorochrome conjugation kits, according to the manufacturers' instructions, to decrease the background noise in the study of TCR Vγ6. The labeling quality of both kits was assessed using flow cytometry. We also attempted conjugating the purified rat IgM anti-mouse TCR Vγ6 (clone 17D1) antibody with a R-Phycoerythrin (R-PE) conjugation kit (ProZyme), according to the manufacturer's protocol, with conjugation quality measured by flow cytometry. Schematic figures below are showing the purification and labelling of rat IgM anti-mouse TCR Vγ6, (**Figure II-3**), and mouse IgG1 anti-mouse TCR Vγ6, (**Figure II-4**), antibodies.

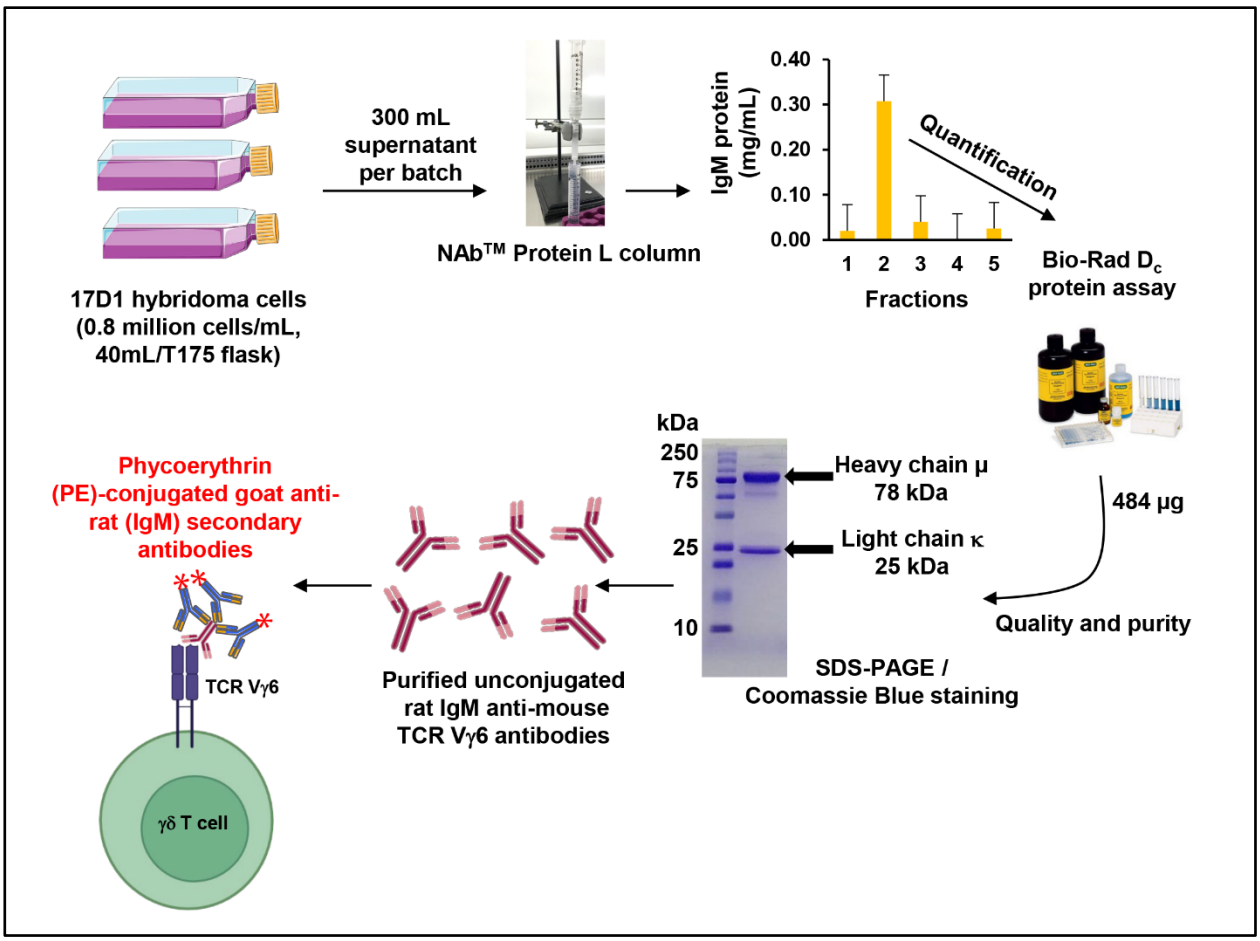

Figure II-3: Rat IgM anti-mouse TCR Vγ6 antibody purification and indirect labeling with secondary antibodies

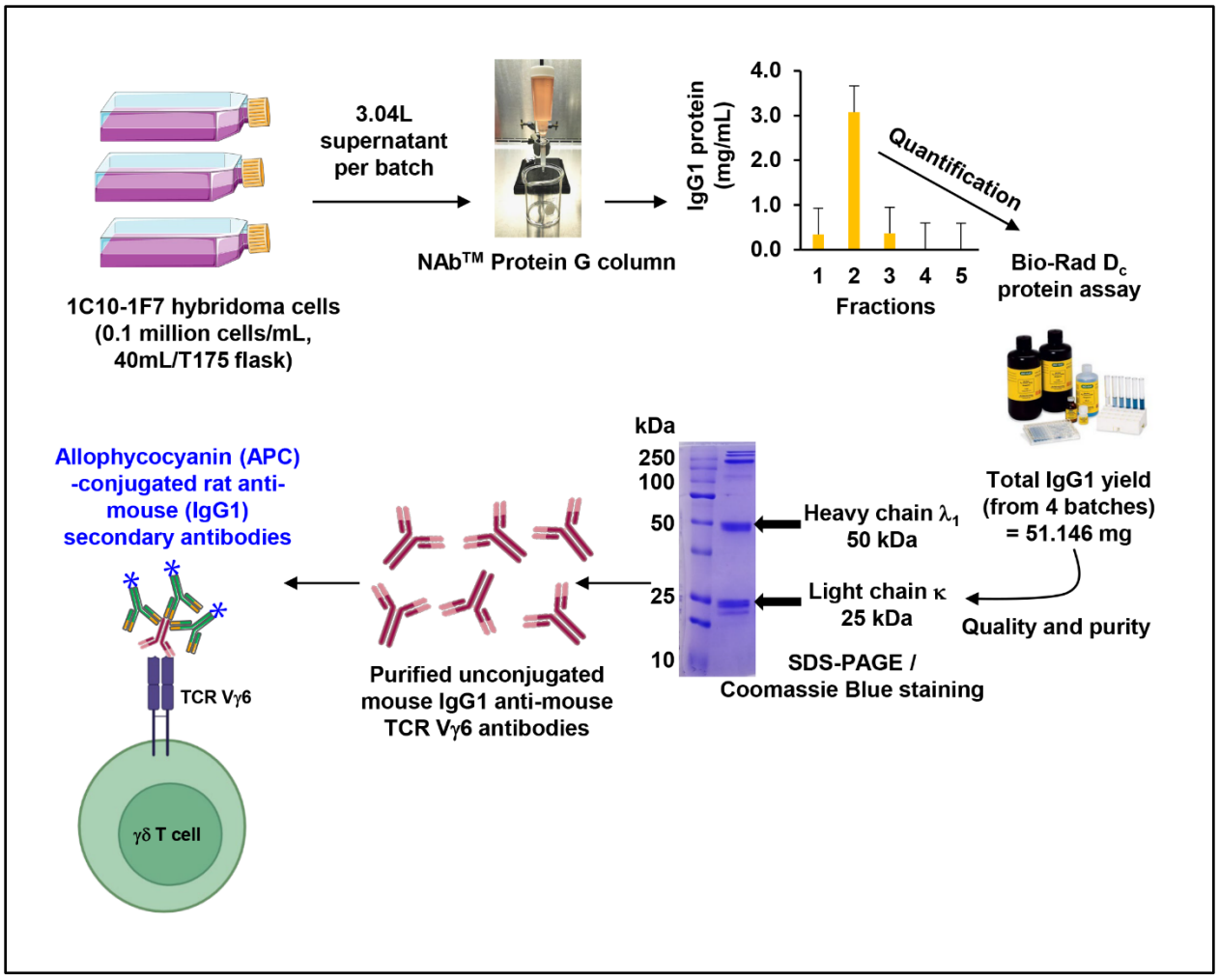

Figure II-4: Mouse IgG1 anti-mouse TCR Vγ6 antibody purification and indirect labeling with secondary antibodies

8.5. Infusion of Angiotensin II using micro-osmotic pumps

Eleven- to 13-week-old C57BL/6J male wild-type mice were anesthetized with isoflurane as above. The depth of anesthesia was confirmed by rear foot gentle squeezing. During the surgery, the mouse's eyes were covered with a lubricant eye ointment using a sterile cotton-tip applicator.

The nonsteroidal anti-inflammatory drug (NSAID) “Carprofen” (20 mg/kg) was administered subcutaneously to minimize post-operative pain. The mouse's upper back was shaved and then disinfected with Baxedin (Omega Laboratories), a sterile aqueous bactericidal antiseptic solution composed of 2% chlorhexidine gluconate and 70% Isopropyl alcohol. A surgical pocket was made with sterile surgical “Metzenbaum scissors” to facilitate the osmotic pump implantation. ALZET® micro-osmotic pumps were implanted SC to infuse Ang II (490 ng/kg/min.) for 14 days, as recommended by the manufacturer. A buffered lidocaine and bupivacaine mixture was administrated to provide additional pain relief directly at the site of surgery as a “local analgesic solution”. The surgical wound was closed with Michel suture clips. Baxedin solution was added one more time to disinfect the surgical site and prevent bacterial contamination around the surgical wound. Treated mice were then exposed to a temperature of 33-34°C for 20 minutes under monitoring until full awakening. Control mice underwent sham surgery. Carprofen was administered as above once a day for the first 3 days after pump and sham surgeries.

8.6. Tissue samples collection and enzymatic tissue digestion

At the end of the protocol, mice were weighed and then anesthetized with isoflurane as above, and blood withdrawn by cardiac puncture. The mesenteric artery vascular bed was dissected with the intestine, and spleen, and both lungs and thoracic aorta were harvested in ice-cold Roswell Park Memorial Institute Medium (RPMI) 1640 or ice-cold 1X PBS.

The mesenteric artery vascular bed was dissected to extract the MA PVAT, the mesenteric arteries, and mesenteric lymph nodes (MLNs). MA PVAT and mesenteric arteries were mechanically dissected, with a dissection blade or surgical scissors, then digested in enzyme

digestion medium composed of collagenase A (0.15 U/mL), collagenase type II (500 U/mL), elastase (2 U/mL) and soybean trypsin inhibitor (0.5 U/mL) in RPMI at 37°C for ~1.0 to 1.5h in a 1.5 or 5.0-mL conical microtube with gentle agitation in a hybridization oven. TA PVAT and lungs were mechanically dissected, then enzymatically digested at 37°C for 2h and 3h, respectively, using the same enzymatic cocktail medium as above but with addition of hyaluronidase (48 U/mL).

At the end of the digestion, the cells were filtered through a 40 µm cell strainer to obtain a single-cell suspension, then cells were collected by centrifugation at 410 x g for 5 min at 4°C. The floating fatty layers in MA PVAT and TA PVAT digested samples were gently eliminated by using a trimmed micropipette tip. Spleens and MLNs were ground by passing through a 70 µm cell strainer by using a syringe plunger, then cells were collected by centrifugation at 410 x g for 5 min at 4°C and resuspended in ice-cold RPMI.

8.7. Extracellular and intracellular immunofluorescent staining for flow cytometry and gating strategies

γδ T cell subtypes were profiled in the spleen, MLNs, TA PVAT and MA PVAT of 11-13-week-old C57BL/6J male mice infused or not with Ang II (490 ng/kg/min, SC) for 14 days using a BD LSRFortessa™ Flow Cytometer (n=5-14). Splenocytes and lymphocytes, isolated from the spleen, MLNs, TA PVAT and MA PVAT, were stained with LIVE/DEAD™ Fixable Aqua Stain, Brilliant Violet 785 (BV785)-conjugated rat anti-mouse CD45 (clone 30-F11), Alexa Fluor® 700 (AF700)-conjugated rat anti-mouse CD3 (clone 17A2), PE-CF594-conjugated hamster anti-mouse γδ-TCR (clone GL3), phycoerythrin (PE)-conjugated Armenian hamster anti-mouse TCR Vγ1 and Vγ2 (Vγ1,2, clone 4B2.9), BV605-conjugated Armenian hamster anti-mouse TCR Vγ4 (clone

UC3-10A6), Brilliant Blue 700 (BB700)-conjugated Syrian hamster anti-mouse TCR Vγ5 (clone 536), unconjugated rat anti-mouse TCR Vγ6 (clone 17D1), AF488-conjugated rabbit anti-rat IgM (secondary antibody used to reveal anti-mouse TCR Vγ6 primary antibody) and DyLight650-conjugated anti-mouse TCR Vγ7 (clone F2.67: gift from Dr. P. Pereira-Esteva, Pasteur Institute, France) antibodies. All names of TCR γ subset identifications are based on the *Heilig* and *Tonegawa* nomenclature system.[428]

The leukocytes were gated in the side scatter area (SSC-A)/forward scatter area (FSC-A) plot. Singlet lymphocytes were gated using SSC-A over SSC-wide (SSC-W). Live lymphocytes were gated in SSC-A/viability dye dot plot. $CD45^+$ immune cells were gated in SSC-A/CD45 dot plot. $CD3^+$ T cells were gated in SSC-A/CD3 dot plot. $TCR\gamma\delta^+$ T cells were gated in TCRγδ/CD3 dot plot. $V\gamma1,2^+$, $V\gamma4^+$, $V\gamma5^+$, $V\gamma6^+$ and $V\gamma7^+$ $TCR\gamma\delta^+$ T cells were gated in SSC-A/Vγ1,2, SSC-A/Vγ4, SSC-A/Vγ5, SSC-A/Vγ6 and SSC-A/Vγ7 dot plot, respectively. Since low numbers of TCR $V\gamma5^+$ and TCR $V\gamma7^+$ $TCR\gamma\delta^+$ T cells were observed in studied tissues, other tissues were used to validate these antibodies, such as the skin and intestinal intraepithelial lymphocytes (IELs), which are known to contain larger numbers of these cells, respectively.[506] FMO (fluorescent minus one) control could not be used in MLNs, TA PVAT, and MA PVAT due to low numbers of target cells. However, we used *Tcrδ* null mice as a negative control group for each tissue to check the quality of all TCR Vγ antibodies used in the study. Gated $TCR\gamma\delta^-$ $CD3^+$ T cells were used as FMO control to adjust the gates and determine the fluorescence background noise.

The phenotype of $V\gamma6^+$ γδ T cells was determined by flow cytometry in the spleen, MLNs, TA PVAT and MA PVAT of 11-13-week-old C57BL/6J male mice infused or not with Ang II (490 ng/kg/min, SC) for 14 days (n=4-14). Other groups of Ang II-treated mice were

intraperitoneally (IP) injected with 200 µg of mouse IgG1 anti-mouse TCR Vγ6-blocking antibodies or mouse IgG1 isotype control antibodies 5 times at days 0, 3, 6, 9 and 12 of Ang II infusion. Splenocytes, and lymphocytes isolated from MLNs, TA PVAT and MA PVAT, were stained with LIVE/DEAD™ Fixable Aqua Stain, BV785-conjugated rat anti-mouse CD45 (clone 30-F11), AF700-conjugated rat anti-mouse CD3 (clone 17A2), Peridinin-Chlorophyll-Protein-eFluor 710 (PerCP-eFluor™ 710)-conjugated rat anti-mouse CD4 (clone RM4-5), Allophycocyanin-eFluor 780 (APC-eFluor™ 780)-conjugated rat anti-mouse CD8a (clone 53-6.7), PE-CF594-conjugated hamster anti-mouse γδ-TCR (clone GL3), unconjugated rat anti-mouse TCR Vγ6 (clone 17D1), R-PE-conjugated goat anti-rat IgM (secondary antibody used to reveal anti-mouse TCR Vγ6 primary antibody), PE-Cy7-conjugated Armenian hamster anti-mouse C-C Chemokine Receptor type 6 (CCR6), [also known as CD196], (clone 29-2L17), APC-conjugated Armenian hamster anti-mouse C-X-C Chemokine Receptor 3 (CXCR3) ,[also known as CD183], (clone CXCR3-173), PE-Cy5-conjugated Armenian hamster anti-mouse CD69 (clone H1.2F3), BB515-conjugated rat anti-mouse CD44 (clone IM7), BV421-conjugated rat anti-mouse CD25 (clone PC61), BV605-conjugated Armenian hamster anti-mouse CD27 (clone LG.3A10), Brilliant™ Ultraviolet 395 (BUV 395)-conjugated mouse anti-mouse Ki-67 (clone B56), APC-conjugated rat anti-mouse Retinoid-related Orphan Receptor gamma t (ROR γt) (clone AFKJS-9) and PE-Cy7-conjugated mouse anti-mouse T-bet (clone 4B10), incubated with rat anti-mouse CD16/CD32 Fc receptor blocker (clone 2.4G2) and supplemented with 5% bovine serum albumin (BSA, EMD Millipore Sigma). All cells were fixed after staining with 1% Paraformaldehyde (PFA, Electron Microscopy Sciences) in PBS for 30 minutes, then washed and resuspended in 1X PBS for flow cytometry acquisition.

One in 3 spleen and lung samples were dedicated to intracellular staining to profile intracellular markers and cytokines as previously described.[536] Briefly, isolated splenocytes and lymphocytes were activated by suspending cells in T cell activation cocktail solution for 4-6 hrs at 37°C. The T cell activation cocktail solution included a combination of Phorbol 12-myristate 13-acetate (PMA) (0.05 μg/tissue sample), ionomycin (1 μg/tissue sample), monensin (1x = 1 μL/tissue sample) and RPMI 1640 to a final volume of 1 mL activation cocktail per tissue sample. After viability and extracellular staining, cells were fixed in 1% PFA for 15 minutes at 4°C, then washed in ice-cold 1X PBS. Fixed cells were then resuspended for 30 minutes at 4°C in 100 μL saponin permeabilization buffer, (0.1% Saponin, 0.1% BSA, and sterile 1X PBS), containing fluorochrome-conjugated antibodies for intracellular markers and/or cytokines. Cells were then washed and resuspended in 150μL 1X PBS for flow cytometry acquisition.

The leukocytes were gated in the SSC-A/ FSC-A plot. Singlet lymphocytes were gated using SSC-A over SSC-W. Live singlet lymphocytes were gated in the SSC-A/viability dye dot plot. $CD45^+$ immune cells were gated in the SSC-A/CD45 dot plot. $CD3^+$ T cells were gated in the SSC-A/CD3 dot plot. $TCR\gamma\delta^+$ T cells were gated in the TCRγδ/CD3 dot plot. $V\gamma6^+$ TCR $\gamma\delta^+$ T cells were gated in the SSC-A/Vγ6 dot plot. $CCR6^+$, $CXCR3^+$, $CD27^+$, $CD69^+$, $CD25^+$, $CD44^+$, Ki-67^+, ROR γt^+ and T-bet^+ $V\gamma6^+$ TCR $\gamma\delta^+$ T cells were gated in the SSC-A/CCR6, SSC-A/CXCR3, SSC-A/CD27, SSC-A/CD69, SSC-A/CD25, SSC-A/CD44, SSC-A/Ki-67, SSC-A/ROR γt and SSC-A/T-bet dot plot, respectively. FMO control was used for the spleen but could not be used for MLNs, TA PVAT, and MA PVAT due to the low numbers of target cells. However, gated $V\gamma6^-$ TCR $\gamma\delta^+$ $CD3^+$ T cells were used as FMO control.

The phenotype of Vγ4$^+$ γδ T cells was determined by flow cytometry for the spleen, MLNs, lungs, TA PVAT and MA PVAT of 11-13-week-old C57BL/6J male mice infused or not with Ang II (490 ng/kg/min, SC) for 14 days. Other groups of Ang II-treated mice were IP-injected with 200 µg of Armenian hamster IgG anti-mouse TCR Vγ4-depleting antibodies or Armenian hamster IgG isotype control antibodies 5 times at days 0, 3, 6, 9 and 12 of Ang II infusion. Splenocytes, and lymphocytes isolated from MLNs, lungs, TA PVAT and MA PVAT were stained with LIVE/DEAD™ Fixable Aqua Stain, BV785-conjugated rat anti-mouse CD45 (clone 30-F11), Brilliant Ultraviolet 395 (BUV 395)-conjugated rat anti-mouse CD3 (clone 17A2), PerCP-eFluor™ 710-conjugated rat anti-mouse CD4 (clone RM4-5), APC-eFluor™ 780-conjugated rat anti-mouse CD8a (clone 53-6.7), PE-CF594-conjugated hamster anti-mouse γδ-TCR (clone GL3), unconjugated mouse anti-mouse TCR Vγ6 (clone 1C10-1F7), APC-conjugated rat anti-mouse IgG1 (secondary antibody used to reveal anti-mouse TCR Vγ6 primary antibody), PE-conjugated Armenian hamster anti-mouse TCR Vγ4 (clone UC3-10A6), PE-Cy7-conjugated Armenian hamster anti-mouse CCR6 (clone 29-2L17), BV605-conjugated Armenian hamster anti-mouse CXCR3 (clone CXCR3-173), PE-Cy5-conjugated Armenian hamster anti-mouse CD69 (clone H1.2F3), BB515-conjugated rat anti-mouse CD44 (clone IM7), BUV 395-conjugated mouse anti-mouse Ki-67 (clone B56), APC-conjugated rat anti-mouse IL-17A (clone eBio17B7), AF488-conjugated rat anti-mouse IFNγ (clone XMG1.2), PE-Cy7-conjugated rat anti-mouse CD39 (clone Duha59), PE-conjugated rat anti-mouse CD73 (clone TY/23), Fluorescein Isothiocyanate (FITC)-conjugated rat anti-mouse FOXP3 (clone FJK-16s), APC-conjugated goat anti-mouse IL-22 (clone polyclonal) and AF488-conjugated rat anti-mouse IL-10 (clone JES5-16E3). They were incubated with rat anti-mouse CD16/CD32 Fc receptor blocker (clone 2.4G2) and supplemented with 5% bovine serum albumin. All the cells were fixed after staining with 1% PFA in PBS for 30 minutes,

then washed with 1X PBS for flow cytometry acquisition. Intracellular staining to profile intracellular markers and cytokines was done as described above.

Leukocytes were gated in the SSC-A/FSC-A plot. Singlet lymphocytes were gated using SSC-A over SSC-W. Live singlet lymphocytes were gated in the SSC-A/viability dye dot plot. $CD45^+$ immune cells were gated in the SSC-A/CD45 dot plot. $CD3^+$ T cells were gated in the SSC-A/CD3 dot plot. TCR$\gamma\delta^+$ T cells were gated in the TCR$\gamma\delta$/CD3 dot plot. V$\gamma4^+$ TCR $\gamma\delta^+$ T cells were gated in the SSC-A/Vγ4 dot plot. $CCR6^+$, $CXCR3^+$, $CD69^+$, $CD44^+$, Ki-67^+, IL-$17A^+$ and IFNγ^+ V$\gamma4^+$ TCR $\gamma\delta^+$ T cells were gated in the SSC-A/CCR6, SSC-A/CXCR3, SSC-A/CD69, SSC-A/CD44, SSC-A/Ki-67, SSC-A/IL-17A, SSC-A/IFNγ, SSC-A/CD39, SSC-A/CD73, SSC-A/FOXP3, SSC-A/IL-22 and SSC-A/IL-10 dot plot, respectively. FMO control was used for the spleen and lungs but could not be used in MLNs, TA PVAT, and MA PVAT due to the low numbers of target cells. However, gated V$\gamma4^-$ TCR $\gamma\delta^+$ $CD3^+$ T cells were used as FMO control.

8.8. Pressurized myography

Second-order mesenteric arteries were dissected and mounted on a pressurized myograph system to study vascular reactivity and mechanical properties of these vessels, as previously described.[44 537 538] At the end of protocol, mice were anesthetized using isoflurane as above, and the whole mesenteric arterial bed with surrounding intestine were gently collected and placed in ice-cold Krebs solution (pH= 7.4) containing (in mmol/L): 120 NaCl, 25 $NaHCO_3$, 4.7 KCl, 1.18 KH_2PO_4, 1.18 $MgSO_4$, 2.5 $CaCl_2$, 0.026 EDTA and 5.5 glucose, gassed continuously with 95% air and 5% CO_2.

Second-order branches of the mesenteric arterial bed (~150-250 μm lumen size, 2 mm length) were cleaned of surrounding PVAT using a stereo-dissecting microscope, mounted on glass micropipettes on a pressurized myograph chamber and perfused with Krebs solution. Mounted arteries were equilibrated at an intraluminal pressure of 45 mmHg for 45 min. with a perfusate flow of warmed (37 °C) and oxygenated Krebs solution as described above. Media and lumen diameter were measured using a computer-based video imaging system (Living Systems Instrumentation). All arteries were initially constricted by extraluminal perfusion with Krebs solution containing 10^{-5} mol/L norepinephrine (NE) and 120 mmol/L KCl. Only arteries constricting to at least 60% of the initial resting diameter were used for further studies. Vascular contractile responses to cumulative concentrations of NE (10^{-8} to 10^{-4} mol/L) were assessed. Endothelium-dependent vascular relaxation responses to cumulative concentrations of acetylcholine (Ach) (10^{-9} to 10^{-4}mol/L), and endothelium-independent sodium nitroprusside (SNP) (10^{-9} to 10^{-3}mol/L) relaxation responses were determined in arteries precontracted with NE (5 x 10^{-5} mol/L).

Thereafter, vascular mechanical and structural properties (stiffening and remodeling) were evaluated after eliminating the vascular tone by incubation in a Ca^{2+} free Krebs solution supplemented with a Ca^{2+} chelating agent, (EGTA, 10 mmol/L), for 30 min. Media thickness and lumen diameter were assessed in response to incremental augmentations of intraluminal pressure from 3 to 140 mmHg. Media cross-sectional area, media to lumen ratio and the stress-strain relationship were calculated as previously described.[539]

8.9. Implantation of radiotelemetry transmitters and blood pressure measurements

Systolic (SBP) and diastolic (DBP) blood pressure was monitored and determined by telemetry as previously described.[388] [540] Briefly, nine and half to 11-week-old mice were anesthetized with isoflurane and injected with carprofen as above, and surgically instrumented with PA-C10 radiotelemetry transmitters as recommended by the manufacturer (Data Sciences International). This radiotelemetry transmitter is designed to provide accurate and reliable measurements of systolic, diastolic, mean arterial (MAP) and pulse (PP) pressures, as well as heart rate (HR) and physical activity (PA) in freely moving mice housed in their home cages. The transmitter catheter was placed in the free-flowing blood of the systemic circulation, (inserted into the left carotid artery), and the transmitter body, (weight, 1.4g), was placed on a side of the body for long-term biocompatibility. Carprofen was administered as above once a day for the first three recovery days. Mice were allowed to recover for 7 additional days. Blood pressure parameters were determined every 5 min for 10 sec two days before Ang II micro-pump or sham surgeries, (baseline), and for the 14 following days until the mice were euthanized.

8.10. Data analysis and statistics

Results are presented as means ± standard error of the mean (SEM) or standard deviation (SD) as indicated in table or figure legends. BP and concentration-response curve data were compared by two-way analysis of variance (ANOVA) for repeated measurements with SigmaPlot version 12 (Systat Software). Comparisons between 2 groups were done using unpaired or paired Student *t*-test as indicated. Comparisons among multiple groups for other data were analyzed by

1- or 2-way ANOVA, as appropriate. All ANOVA tests were followed by a Student–Newman–Keuls *post hoc* test. $P<0.05$ was considered statistically significant.

CHAPTER III: Results

Differential distribution of γδ T cell variant γ subtypes

9.1. Mesenteric artery total RNA sequencing revealed perivascular adipose tissue γ and δ TCR subtype genes

As expected, since immune cells are underrepresented in MA RNA, γ and δ TCR variable and constant region subtype genes were expressed at low levels in the total RNA expression profile of MAs. The sum of the sequencing reads for the 24 mice studied was used to compare the expression levels of the different γ and δ TCR variants. The analysis of the total RNA expression profile of MAs revealed low expression of γ TCR variable region subtypes 2 (*Trgv2*, 60 reads), 4 (*Tcrg-v4*, 48 reads), 5 (*Tcrg-v5*, 31 reads), and 6 (*Tcrg-v6*, 65 reads). The variants 1 (*Tcrg-v1*), 3 (*Tcrg-v3*), and 7 (*Tcrg-v7*) were not detected **(Table III-1A)**. Similarly, a low expression of δ TCR variable region subtypes 2-2 (*Trdv2-2*, 12 reads), 4 (*Trdv4*, 212 reads), and 5 (*Trdv5*, 18 reads) was found, while the variants 1 (*Trdv1*), 2-1 (*Trdv2-1*), and 3 (*Trdv3*) were undetectable **(Table III-1B)**. The γ TCR constant region subtypes 1 (*Tcrg-c1*, 312 reads), 2 (*Tcrg-c2*, 110 reads), and 4 (*Tcrg-c4*, 181 reads) were expressed at low levels, and subtype 3 (*Tcrg-c3*) was not detected **(Table III-1C)**. *Trgv2*, *Tcrg-v4*, *Tcrg-v5, Tcrg-v6*, *Trdv4*, and *Tcrg-c1* were identified as potential subsets of γδ T cells contained in MA PVAT.

9.2. Validation of oligonucleotide primers for γ and δ TCR subtype genes

Trgv2 oligonucleotide primers were validated using thymus, MA with PVAT (MA+PVAT), intestine, and skin RNA. Their PCR efficiency was respectively 97%, 93%, 98%, and 96% **(Table III-2A & Figure III-1A)**. We succeeded in validating *Tcrg-v4* oligonucleotide primers using thymus, (MA+PVAT), and intestine RNA. Their PCR efficiency was respectively 106%, 102%, and 96% **(Table III-2A & Figure III-1B)**. In addition, we were able to validate

Tcrg-v5 oligonucleotide primers using skin RNA. Their PCR efficiency was 96% **(Table III-2A & Figure III-1C)**. Moreover, *Trdv4* oligonucleotide primers were validated in thymus and (MA+PVAT) RNA, with a PCR efficiency 96% and 104% respectively **(Table III-2B & Figure III-1D)**. We were able to validate *Tcrg-c1+c2* oligonucleotide primers in (MA+PVAT). Their PCR efficiency was 95% **(Table III-2C)**. Finally, *Trdc* oligonucleotide primers were successfully validated using thymus and intestine RNA. Their PCR efficiency was respectively 92% and 94% **(Table III-2D)**. Furthermore, for all of the above, one peak was detected in the dissociation curves and one band of the expected size was observed in agarose gel electrophoresis, confirming the quality of the oligonucleotide primer designs **(Figure III-1)**. The lack of success in validating some oligonucleotide primers could be due to defective design or very low expression of the genes in the studied tissues.

9.3. A differential distribution of γδ T cell variant γ subtypes was observed in lymphoid tissues compared to perivascular adipose tissues

Flow cytometry profiling revealed different proportion of γδ T cell TCRγ subtypes in the spleen, MLNs, TA PVAT, and MA PVAT.

In the spleen of sham mice, the most abundant γδ T cell variant subtypes were $V\gamma1,2^+$ (13783±1874 cells/spleen, 0.8±0.07 % of $CD3^+$ T cells) and $V\gamma4^+$ $TCR\gamma\delta^+$ T cells (11950±1590 cells/spleen, 0.7±0.06 % of $CD3^+$ T cells), followed by $V\gamma6^+$ $TCR\gamma\delta^+$ T cells (9001±1237 cells/spleen, 0.5±0.02 % of $CD3^+$ T cells), and then $V\gamma5^+$ $TCR\gamma\delta^+$ T cells (3714±925 cells/spleen, 0.2±0.06 % of $CD3^+$ T cells). $V\gamma7^+$ $TCR\gamma\delta^+$ T cells were present in very low numbers. In the spleen of Ang II-infused mice, the frequency of $V\gamma6^+$ $TCR\gamma\delta^+$ T cells was increased (0.77±0.09 % of

$CD3^+$ T cells, $P<0.01$) and tended to be greater in number (13693±3040 cells/spleen, $P=0.099$) whereas the number and frequency of other variants were unchanged **(Figure III-3)**.

A similar distribution of γδ T cell variant g subtypes was observed in another lymphoid organ, the mesenteric lymph nodes (MLNs) of sham mice. $V\gamma1,2^+$ (1632±573 cells/MLNs per mouse, 0.36±0.1% of $CD3^+$ T cells) and $V\gamma4^+$ $TCR\gamma\delta^+$ T cells (1535±303 cells/MLNs per mouse, 0.4±0.02% of $CD3^+$ T cells) were the most abundant variants followed by $V\gamma6^+$ $TCR\gamma\delta^+$ T cells (723±266 cells/MLNs per mouse, 0.17±0.06 % of $CD3^+$ T cells). The number and frequency of $V\gamma5^+$ and $V\gamma7^+$ $TCR\gamma\delta^+$ T cells were low. However, no $TCR\gamma\delta^+$ T cell g variants were affected by Ang II infusion **(Figure III-3)**.

A different distribution of γδ T cell variant γ subtypes was observed in the thoracic aortic (TA) PVAT of sham mice. $V\gamma6^+$ $TCR\gamma\delta^+$ T cells (121±29 cells/PVAT, 3.6±0.4 % of $CD3^+$ T cells) were the most abundant γδ T cell variant γ subtypes, followed by $V\gamma4^+$ $TCR\gamma\delta^+$ T cells (39±9 cells/PVAT, 1.3±0.3 % of $CD3^+$ T cells), and then $V\gamma1,2^+$ $TCR\gamma\delta^+$ T cells (15±3 cells/PVAT, 0.8±0.3 % of $CD3^+$ T cells). The number and frequency of Vγ5 and 7^+ $TCR\gamma\delta^+$ T cells were very low. The frequency of $V\gamma6^+$ $TCR\gamma\delta^+$ T cells was increased (5.9±0.8 % of $CD3^+$ T cells, $P<0.01$) whereas the number was unchanged in TA PVAT of Ang II-infused mice. The number and frequency of other variants were unaffected by Ang II infusion **(Figure III-3)**.

A similar distribution of γδ T cell variant g subtypes was observed in another PVAT, MA PVAT. The most abundant γδ T cell variant g subtypes was $V\gamma6^+$ $TCR\gamma\delta^+$ T cells (357±120 cells/PVAT, 10.2± 1.9% of $CD3^+$ T cells), followed by $V\gamma4^+$ $TCR\gamma\delta^+$ T cells (108±24 cells/PVAT, 4.02±0.6% of $CD3^+$ T cells), and then $V\gamma7^+$ $TCR\gamma\delta^+$ T cells (31±12 cells/PVAT, 1.1±0.5% of

$CD3^+$ T cells) **(Figure III-3)**. The number and frequency of $V\gamma1,2^+$ and $V\gamma5^+$ $TCR\gamma\delta^+$ T cells were very low. In MA PVAT of Ang II-infused mice, the frequency of $V\gamma6^+$ $TCR\gamma\delta^+$ T cells tended to increase (14.5±1.7 % of $CD3^+$ T cells, P=0.07) while the other variants were unchanged. The number of $TCR\gamma\delta^+$ T cell variants were unaffected by Ang II infusion.

9.4. Quality validation of anti-TCR Vγ5 and Vγ7 antibodies

Anti-TCR Vγ5 and Vγ7 antibodies were successfully validated in the skin and intestinal intraepithelial lymphocytes (IELs), respectively **(Figure III-4)**. In addition, anti-TCR Vγ1,2, Vγ4, Vγ5, Vγ6 and Vγ7 antibodies were unable to detect positive cells in the spleen, MLNs, TA PVAT, and MA PVAT of *Tcrδ* null mice, which are devoid of γδ T cells (n= 3).

9.5. Infusion of Angiotensin II increased the frequency of $CD3^{Bright}$ γδ T cells

The flow cytometry study revealed that the frequency of $CD3^{Bright}$ γδ T cells was increased significantly in the spleen (15.08±5.1% of γδT cells, P<0.05) and MA PVAT (56.7±10.9% of γδ T cells, P<0.05) of Ang II-infused mice **(Figure III-6)**.

A γ TCR variable region subtypes

Gene name	Sum of RNA seq. reads
Tcrg-v1	Not detected
Trgv2	60
Tcrg-v3	1
Tcrg-v4	48
Tcrg-v5	31
Tcrg-v6	65
Tcrg-v7	3

B δ TCR variable region subtypes

Gene name	Sum of RNA seq. reads
Trdv1	1
Trdv2-1	0
Trdv2-2	12
Trdv3	Not detected
Trdv4	212
Trdv5	18

C γ TCR constant region subtypes

Gene name	Sum of RNA seq. reads
Tcrg-c1	312
Tcrg-c2	110
Tcrg-c3	1
Tcrg-c4	181

High
Medium
Low
Not detected

Table III-1: Mesenteric artery total RNA sequencing revealed possible perivascular adipose tissue (PVAT) γ and δ TCR subtype genes. Total RNA sequencing data of mesenteric arteries (MAs) of 10-12-week-old male mice, (n=24), infused or not with Ang II (1000 ng/kg/min, SC) for 7 and 14 days. Genes encoding γ and δ TCR variable region subtypes (A and B, respectively) and γ TCR constant region subtypes (C) that are expressed in MAs were identified. *Tcrg-v* and *Trgv*,

T cell receptor γ variable region subtype gene; *Tcrg-c*, T cell receptor γ constant region subtype gene; *Trdv*, T cell receptor δ variable region subtype gene.

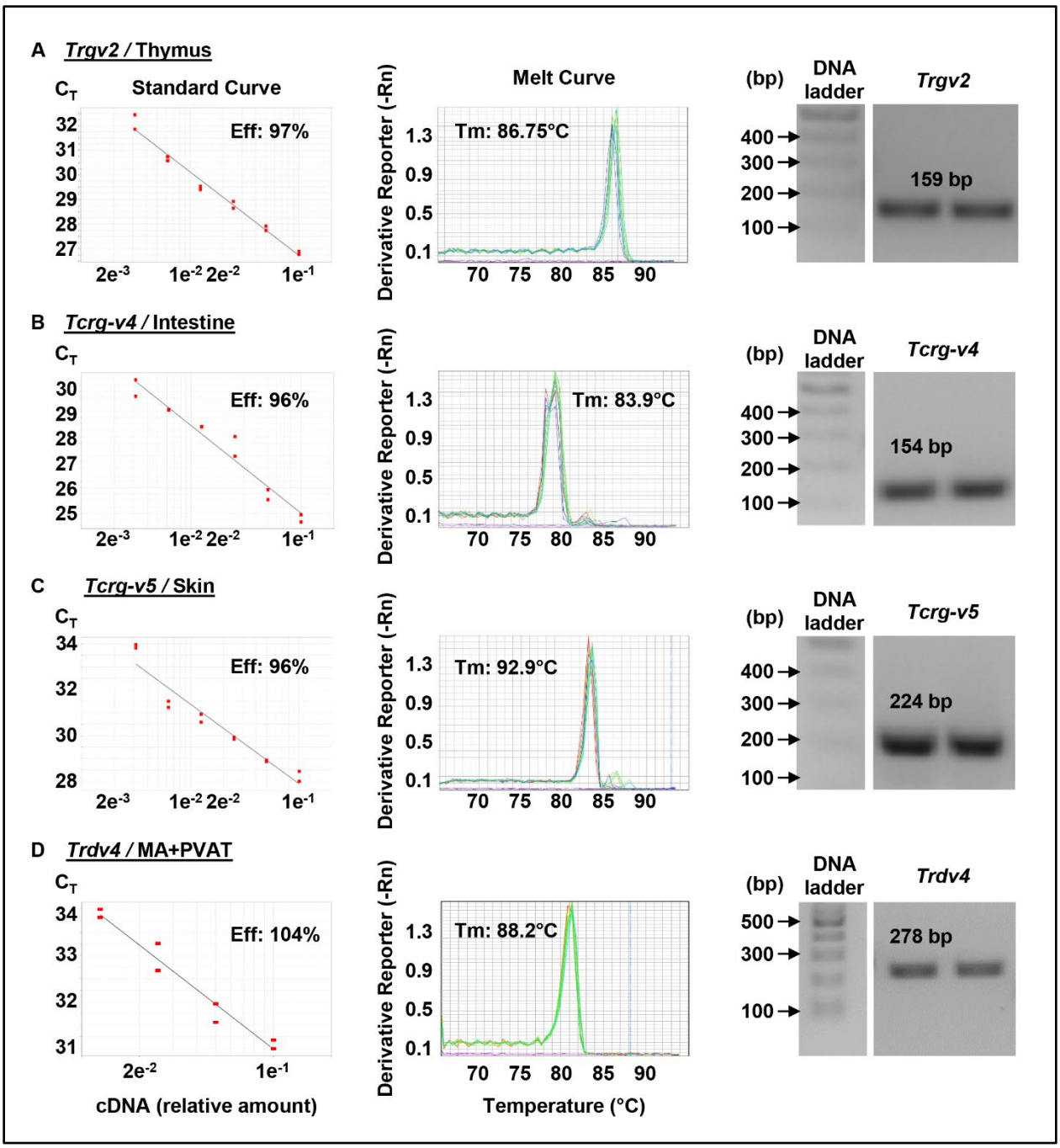

Figure III-1: Examples of oligonucleotide primer validation of γ and δ TCR variable region subtype genes in positive control tissues. Validation of oligonucleotide primers of *Trgv2* in the thymus (**A**), *Tcrg-v4* in the intestine (**B**) *Tcrg-v5* in the skin (**C**), and *Trdv4* in the mesenteric arteries with the surrounding perivascular adipose tissue (MA+PVAT) (**D**). Oligonucleotide primers were validated by RT-qPCR in positive control tissues, which are expected to express

selected genes, to have a PCR efficiency (Eff.%) between 95% and 105% and one amplicon with a Tm >80°C in the qPCR melting curve (also known as dissociation curve). Then, the right PCR product length was visualized using agarose gel electrophoresis. bp, base pair; cDNA, complementary DNA; Rn, normalized reporter; Tm, melting temperature.

TCR γ variants

Primer	MA RNA seq (reads)	Expected tissue	Tissues	Efficiency	Melting curve	Note
Tcrg-V1	Not detected	Thymus & Colon	Intestine	-	-	Not designed yet
			Skin	-	-	Not designed yet
			Thymus	-	-	Not designed yet
			MA+PVAT	-	-	Not designed yet
Trgv2	60	Thymus & Colon	Intestine	98.1%	one product	Validated
			Skin	96.0%	one product	Validated
			Thymus	97.1%	one product	Validated
			MA+PVAT	92.6%	one product	Validated
Tcrg-V3	1	Thymus	Intestine	-	-	Not tested in this tissue
			Skin	1154.0%	multiple products	Invalid
			Thymus	145.9%	one product	Low expression
			MA+PVAT	-	-	Not tested in this tissue
Tcrg-V4	48	Thymus & Colon	Intestine	95.8%	one product	Validated
			Skin	-	-	Not tested in this tissue
			Thymus	106.0%	one product	Validated
			MA+PVAT	102.4%	one product	Validated
Tcrg-V5	31	Skin & Colon	Intestine	133.9%	one product	Low expression
			Skin	96.0%	one product	Validated
			Thymus	116.6%	one product	Low expression
			MA+PVAT	99.8%	one product	Low expression
Tcrg-V6	65	Thymus & Lung	Intestine	-77.4%	multiple products	Invalid
			Skin	145.7%	multiple products	Invalid
			Thymus	682.8%	multiple products	Invalid
			MA+PVAT	-75.9%	no product	Invalid
Tcrg-V7	3	Colon & Thymus	Intestine	-	-	Not designed yet
			Skin	-	-	Not designed yet
			Thymus	-	-	Not designed yet
			MA+PVAT	-	-	Not designed yet

Table III-2A: Validation of γ TCR variable region subtype oligonucleotide primers.

TCR δ variants

Primer	MA RNA seq (reads)	Expected tissue	Tissues	Efficiency	Melting curve	Note
Trdv1	1	Thymus & Spleen	Intestine	632.4%	Multiple product	**Invalid**
			Skin	168.8%	Multiple product	**Invalid**
			Thymus	-	-	Not tested in this tissue
			MA+PVAT	119.8%	One product	Needs to be improved
Trdv2-1	0	Lung & Spleen	Intestine	-	-	Not designed yet
			Skin	-	-	Not designed yet
			Thymus	-	-	Not designed yet
			MA+PVAT	-	-	Not designed yet
Trdv2-2	12	Thymus & Spleen	Intestine	-	-	Not designed yet
			Skin	-	-	Not designed yet
			Thymus	-	-	Not designed yet
			MA+PVAT	-	-	Not designed yet
Trdv3	Pseudogene	-	Intestine	-	-	Pseudogene
			Skin	-	-	Pseudogene
			Thymus	-	-	Pseudogene
			MA+PVAT	-	-	Pseudogene
Trdv4	212	Skin & Spleen	Intestine	119.0%	One product	Needs to be improved
			Skin	-	-	Not tested in this tissue
			Thymus	95.7%	One product	**Validated**
			MA+PVAT	104.4%	One product	**Validated**
Trdv5	18	Thymus & Spleen	Intestine	-	-	Not designed yet
			Skin	-	-	Not designed yet
			Thymus	-	-	Not designed yet
			MA+PVAT	-	-	Not designed yet

Table III-2B: Validation of δ TCR variable region subtype oligonucleotide primers.

TCR γ constant regions

Primer	MA RNA seq (reads)	Expected tissue	Tissues	Efficiency	Melting curve	Note
Tcrg-C1	312	Thymus & Colon	Intestine	594.1%	Two products with huge primer dimer	**Invalid**
			Skin	-92.4%	Two products with huge primer dimer	**Invalid**
			Thymus	114.0%	Huge primer dimer formation	**Invalid**
			MA+PVAT	-	-	Not designed yet
Tcrg-C2	110	Thymus & Colon	Intestine	-	-	Not designed yet
			Skin	-	-	Not designed yet
			Thymus	-	-	Not designed yet
			MA+PVAT	-	-	Not designed yet
Tcrg-C1+C2	422	Thymus & Colon	Intestine	85.2%	One product	Needs to be improved
			Skin	307.3%	Multiple products	**Invalid**
			Thymus	77.7%	Multiple products	**Invalid**
			MA+PVAT	95.1%	One product	**Validated**
Tcrg-C3	1	Thymus	Intestine	-	-	Not designed yet
			Skin	-	-	Not designed yet
			Thymus	-	-	Not designed yet
			MA+PVAT	-	-	Not designed yet
Tcrg-C4	181	Thymus & Colon	Intestine	-	-	Not designed yet
			Skin	-	-	Not designed yet
			Thymus	-	-	Not designed yet
			MA+PVAT	-	-	Not designed yet

Table III-2C: Validation of γ TCR constant region subtype oligonucleotide primers.

TCR δ constant region

Primer	MA RNA seq (reads)	Expected tissue	Tissues	Efficiency	Melting curve	Note
Trdc	Not available	Thymus & Colon	Intestine	94.3%	One product (with minor primer dimer formation)	**Validated**
			Skin	107%	Multiple products	**Invalid**
			Thymus	92.1%	One product	**Validated**
			MA+PVAT	89%	One product and other pale band (ghost band) showed in the gel due to dimeric configuration	**Validated**

Table III-2D: Validation of δ TCR constant region subtype oligonucleotide primers.

mRNA	Primers	Product size (bp)
Trgv2	F: 5' -CACTGACTGCATTTTTCTGAGAC- 3' R: 5' -CCAAAAACCCAGAGGCAG- 3'	159
Tcrg-v4	F: 5' -GCCTCTTGACATTTGGACATG- 3' R: 5' -AAACCTTGGTTTGGTTTCTGC- 3'	154
Tcrg-v5	F: 5' -TTGCAAGCTCTCTGGGGTTC- 3' R: 5' -CCCAGCAGGCACAGTAGTAC- 3'	224
Tcrg-C1+C2	F: 5' -TCTCCATAAGACTGGGACATACC- 3' R: 5' -TGCAGCACATCATTTTTATCTTG- 3'	318
Trdv4	F: 5' -ATTCATCTTCAGTACAGGGACCTC- 3' R: 5' -TTGTTGCCTTCTGAATGTCG- 3'	278
Trdc	F: 5' -GCTGTCAAGCTTGGTCAGTATG- 3' R: 5' -ACTGTGACTCTTGGGCCATAG- 3'	182
Rps16	F: 5' -ATCTCAAAGGCCCTGGTAGC- 3' R: 5' -ACAAAGGTAAACCCCGATCC- 3'	211
Ubc	F: 5' -AGCCCAGTGTTACCACCAAG- 3' R: 5' -CCCATCACACCCAAGAACA- 3'	105

Table III-3: Oligonucleotide primers used for mouse mRNA quantitative PCR. The forward (F) and reverse (R) oligonucleotide primers used for quantitative PCR and the product sizes of mouse γ TCR variable region subtype-2, 4, and 5 (*Trgv2*, *Tcrg-v4*, and *Tcrg-v5*, respectively), γ TCR constant region subtype-1&2 (*Tcrg-c1+c2*), δ TCR variable region subtype-4 (*Trdv4*), δ TCR constant region subtype (*Trdc*), ribosomal protein S16 (*Rps16*), and Ubiquitin C (Ubc). bp, base pair.

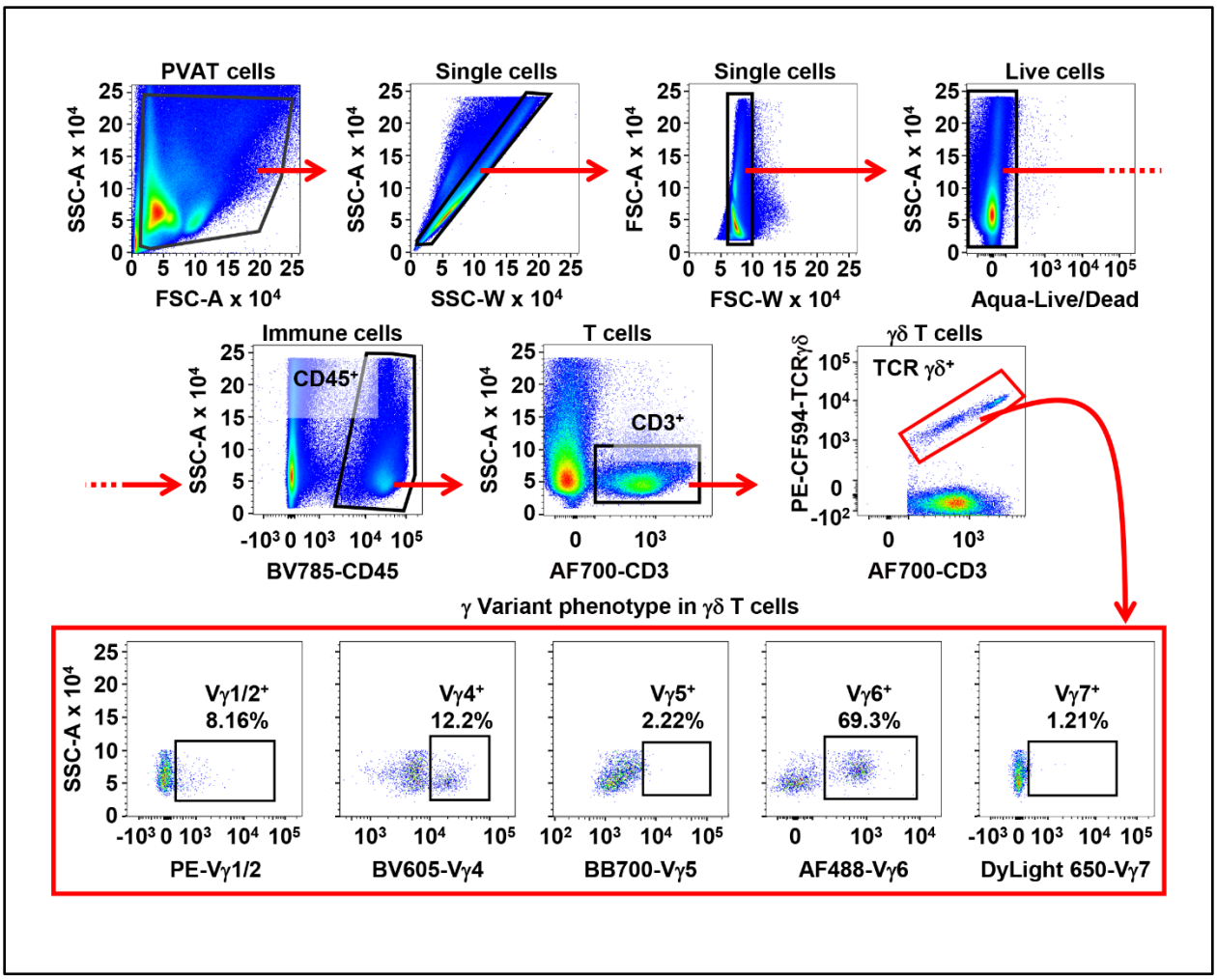

Figure III-2: Representative flow cytometry profiling gating strategy of TCR γ variant phenotyping in the thoracic aortic perivascular adipose tissue (TA PVAT) using surface markers. PVAT cells were first gated in the side scatter area (SSC-A)/forward scatter area (FSC-A) plot. Singlet cells were gated using SSC-A over SSC-wide (SSC-W). Singlet cells were gated again using FSC-A over FSC-wide (FSC-W) to further clean up the data. Live cells were gated in the SSC-A/viability dye plot, followed by gating $CD45^+$ immune cells in the SSC-A/CD45 plot. Then, $CD3^+$ T cells were gated in the SSC-A/CD3 plot. $TCR\gamma\delta^+$ T cells were gated in the TCRγδ/CD3 plot. Finally, $V\gamma1,2^+$, $V\gamma4^+$, $V\gamma5^+$, $V\gamma6^+$, and $V\gamma7^+$ $TCR\gamma\delta^+$ T cells were gated in SSC-A/Vγ1,2, SSC-A/Vγ4, SSC-A/Vγ5, SSC-A/Vγ6, and SSC-A/Vγ7 plot, respectively. AF, Alexa-

Fluor; BB, Brilliant Blue; BV, Brilliant Violet; CD, cluster of differentiation; PE, Phycoerythrin; PE-CF, PE-Cyanine-based fluorescent dye.

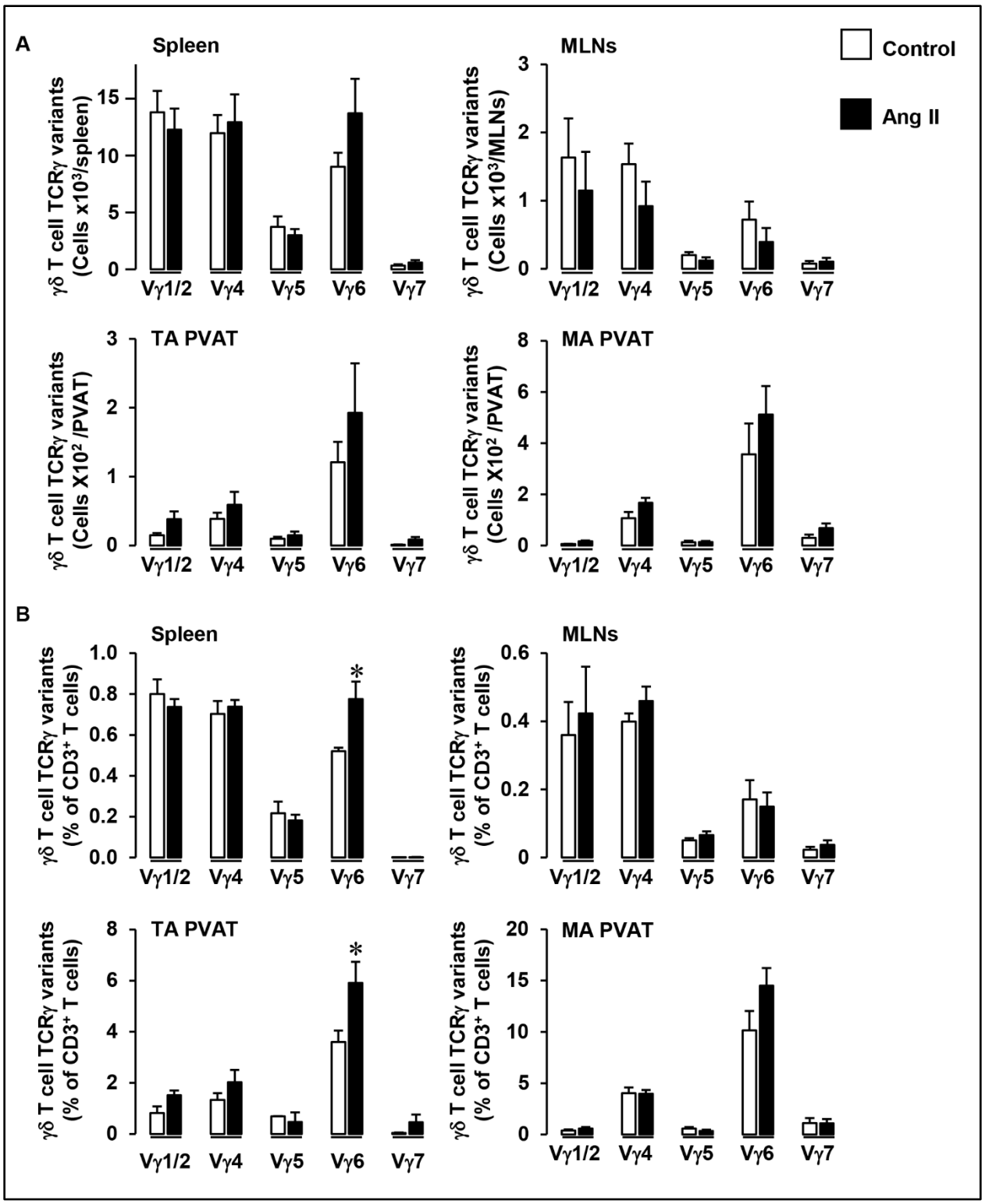

Figure III-3: Distribution of γδ T cell variant γ subtypes in lymphoid tissues compared to perivascular adipose tissues. γδ T cell γ subtypes were profiled in the spleen, mesenteric lymph

nodes (MLNs), thoracic aortic (TA) perivascular adipose tissue (PVAT), and mesenteric (MA) PVAT of 11-13-week-old wild-type (WT) C57BL/6J male mice infused or not with Ang II (490 ng/kg/min, SC) for 14 days using a BD LSRFortessa™ Flow Cytometer. The number (**A**) and frequency (**B**) of γδ T cell γ subtypes in two examples of lymphoid tissues (spleen and MLNs) and two examples of PVATs (TA and MA PVATs). Data are presented as means±SEM, n=7-8 for spleen, 5-8 for MLNs, 8-13 for TA PVAT, and 13-14 for MA PVAT. Data were analyzed using unpaired *t*-test. **P*<0.01 versus respective control.

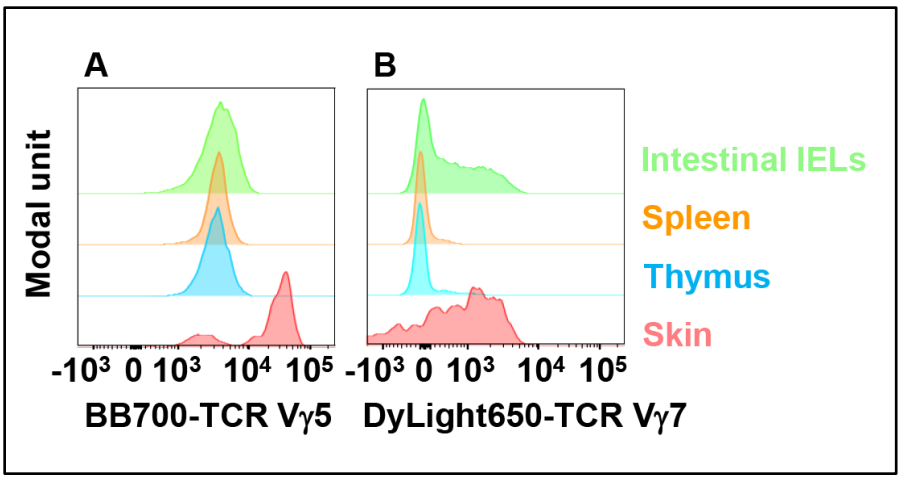

Figure III-4: Anti-TCR Vγ5 and anti-TCR Vγ7 antibody staining validation using positive control tissues. The skin and intestinal intraepithelial lymphocytes (IELs) are two postive control tissues for TCR Vγ5$^+$ (**A**) and TCR Vγ7$^+$ (**B**) γδ T cells, respectively, which are known to contain larger numbers of these cells. BB, Brilliant Blue.

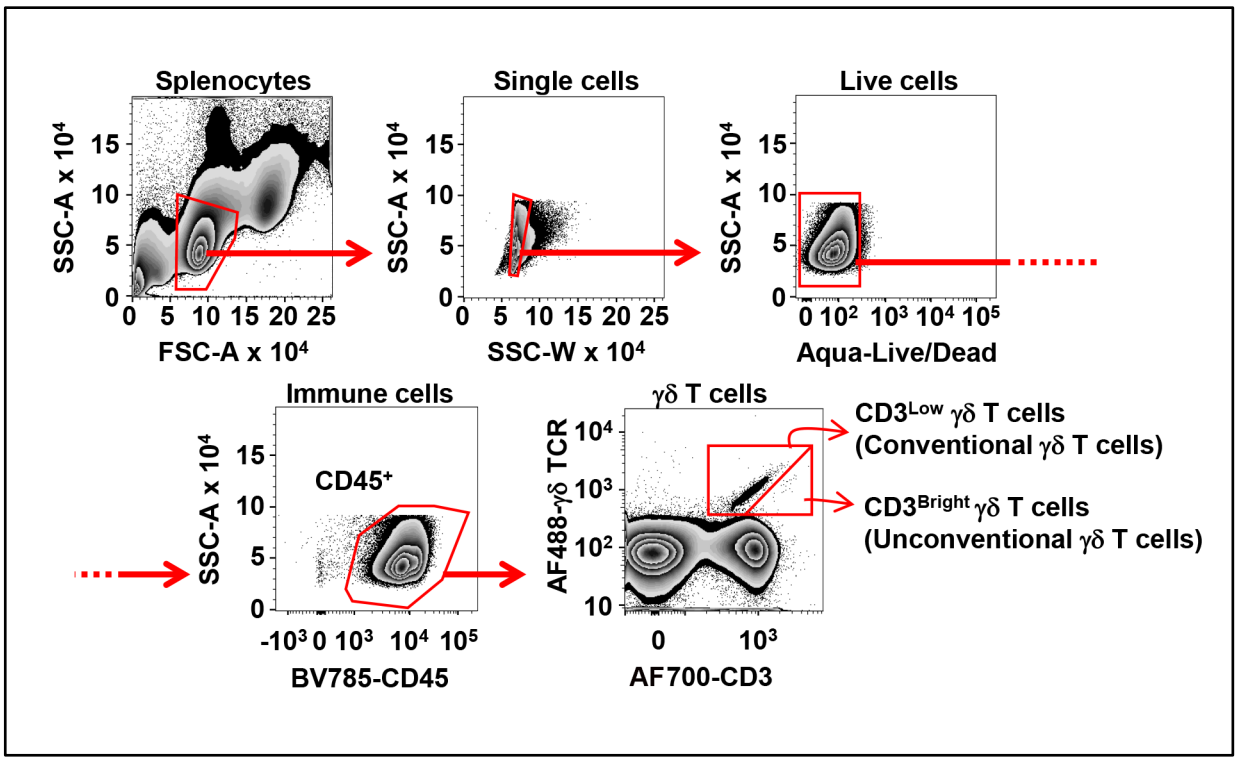

Figure III-5: Representative flow cytometry profiling gating strategy of CD3^{Bright} γδ T cells in the spleen. Splenocytes were first gated in the side scatter area (SSC-A)/forward scatter area (FSC-A) plot. Singlet cells were gated using SSC-A over SSC-wide (SSC-W). Live cells were gated in the SSC-A/viability dye plot. Then, CD45^{+} immune cells were gated in the SSC-A/CD45 plot. Finally, TCRγδ^{+} T cells were gated in the TCRγδ/CD3 plot. AF, Alexa-Fluor; BV, Brilliant Violet; CD, cluster of differentiation.

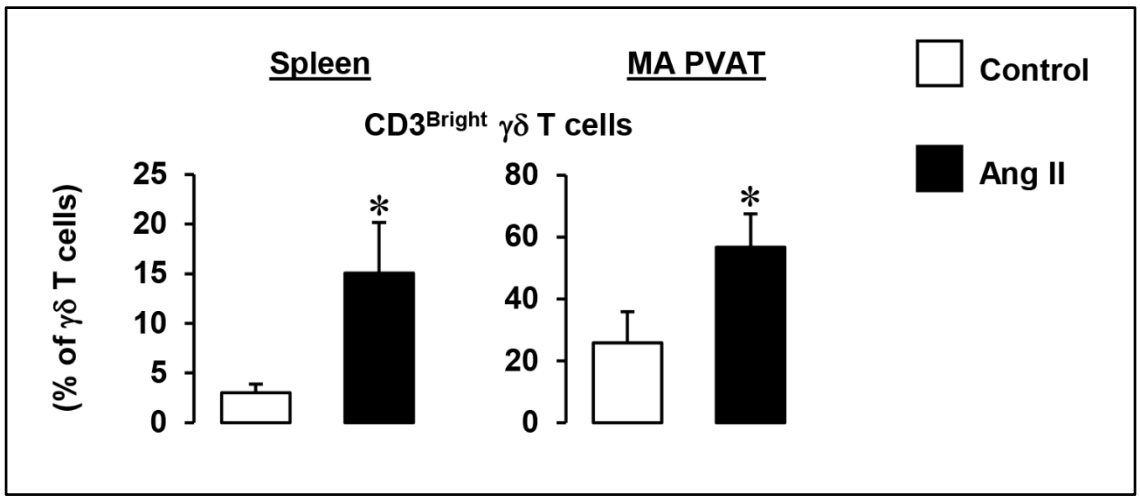

Figure III-6: CD3^{bright} γδ T cells increased in Angiotensin (Ang) II-infused mice. Infusion of Ang II (490 ng/kg/min, SC) for 14 days increased the frequency of CD3^{Bright} γδ T cells in the spleen and MA PVAT. Data are presented as means±SEM, n=6-9. Data were analyzed using unpaired *t*-test. **P*<0.05 versus respective control.

CHAPTER IV: Results

$V\gamma6^+$ γδ T cells play a protective role

in Ang II-induced hypertension and vascular injury

10.1. Profiling of Vγ6$^+$ γδ T cells in the MA PVAT, TA PVAT and spleen showed variable phenotypes in each tissue upon Ang II infusion for 14 days

Flow cytometry profiling of Vγ6$^+$ γδ T cells revealed variable expression of markers for early activation (CD69$^+$), production of IL-17 (CCR6$^+$ and ROR γt$^+$) or IFN-γ (CD27$^+$, CXCR3$^+$ and T-bet$^+$), suppression (CD25$^+$), memory (CD44$^+$), and proliferation (Ki-67$^+$) in MA PVAT, TA PVAT, and the spleen.

In MA PVAT, the phenotyping of Vγ6$^+$ γδ T cells demonstrated that 82% of cells were CCR6$^+$, 23% CXCR3$^+$, 89% CD27$^+$, 90% CD69$^+$, 22% CD25$^+$, 18% CD44^{Hi}, 16% Ki-67$^+$, 48% RORγt$^+$, and 29% T-bet$^+$. Infusion of Ang II did not cause any change in the frequency of these markers **(Figure IV-2 & Table IV-1)**.

In TA PVAT, the phenotyping of Vγ6$^+$ γδ T cells showed that 50% of cells were CCR6$^+$, 49% CXCR3$^+$, 27% CD27$^+$, 85% CD69$^+$, 72% CD25$^+$, 37% CD44^{Hi}, 65% Ki-67$^+$, 55% RORγt$^+$, and 52% T-bet$^+$. Infusion of Ang II decreased the frequency of T-bet$^+$ Vγ6$^+$ γδ T cells (from 51.8±10.7 to 14.1±5.6 % of Vγ6$^+$ γδ T cells, P<0.01) **(Figure IV-3 & Table IV-1)**.

On the other hand, in the spleen, the phenotyping of Vγ6$^+$ γδ T cells indicated that 26% of cells were CCR6$^+$, 39% CXCR3$^+$, 93% CD27$^+$, 14% CD69$^+$, 4% CD25$^+$, 60% CD44^{Hi}, 7% Ki-67$^+$, 8% RORγt$^+$, and 42% T-bet$^+$. Infusion of Ang II increased the frequency of CXCR3$^+$Vγ6$^+$ γδ T cells (from 39.2±1.4 to 44.4±0.8% of Vγ6$^+$ γδ T cells, P<0.05), CD27$^+$Vγ6$^+$ γδ T cells (from 93.1±0.7 to 94.7±0.5% of Vγ6$^+$ γδ T cells, P<0.05), and CD69$^+$Vγ6$^+$ γδ T cells (from 14.3±1.1 to 19.0±1.7 % of Vγ6$^+$ γδ T cells, P<0.05) **(Figure IV-4 & Table IV-1)**.

10.2. Infusion of Ang II increased the frequency of IL-17-producing effector memory Vγ6$^+$ γδ T cells in the spleen

Infusion of Ang II increased the frequency of IL-17-producing effector memory (CCR6$^+$CXCR3$^-$CD44$^+$CD69$^+$) Vγ6$^+$ γδ T cells in the spleen (from 15.2±1.4 to 25.5±4.3% of Vγ6$^+$ γδ T cells, P<0.05) and tended to elevate the frequency of this subset in MA PVAT (from 11.3±1.6 to 20.3±5.3% of Vγ6$^+$ γδ T cells, P=0.052) **(Figure IV-5)**.

10.3. Infusion of Ang II promoted the activation of T cell subsets and IFN-γ production in the spleen

Infusion of Ang II for 14 days increased the frequency of other T cells in the spleen, including CCR6$^+$CD4$^+$ T cells (from 2.0±0.2 to 2.8±0.3 of CD4$^+$ T cells, P<0.05), CD69$^+$CD4$^+$ T cells (from 13.0±0.8 to 16.6±1.4 of CD4$^+$ T cells, P<0.05), CXCR3$^+$CD4$^+$ T cells (from 10.7±0.8 to 12.9±0.8 of CD4$^+$ T cells, P<0.05), CD69$^+$CD8$^+$ T cells (from 4.9±0.2 to 6.6±0.4 of CD8$^+$ T cells, P<0.01), and CXCR3$^+$CD8$^+$ T cells (from 29.8±1.3 to 33.6±1.3 of CD8$^+$ T cells, P<0.05) **(Figure IV-7)**.

10.4. 1C10-1F7 monoclonal antibody is better than the 17D1 monoclonal antibody in the detection of Vγ6$^+$ γδ T cells

We compared the 1C10-1F7 mAb and the 17D1 mAb and found that the 1C10-1F7 mAb is better than the 17D1 mAb in staining Vγ6$^+$ γδ T cells. Pseudo-color density plots of flow

cytometry analysis showed a better performance for 1C10-1F7 mAb alone (detected 91.2% of Vγ6$^+$ γδ T cells) compared with 17D1 mAb alone (87.5% of Vγ6$^+$ γδ T cells) or together (84.8% of Vγ6$^+$ γδ T cells) (**Figure IV-8**).

10.5. Labeling of rat IgM anti-mouse TCR Vγ6 (17D1) and mouse IgG1 anti-mouse TCR Vγ6 (1C10-1F7) antibodies with R-PE and AF647 fluorochromes, respectively, abrogated their ability to bind to TCR Vγ6

We purified 484 µg of rat IgM anti-mouse TCR Vγ6 antibody from 300 mL of 17D1 hybridoma supernatant. The Coomassie Blue stained SDS-PAGE revealed that this was a highly purified antibody. Only two bands of 78kDa and 25 kDa referring to heavy (µ) and light (κ) chains of IgM, respectively, were observed **(Figure II-3)**. Coupling this antibody with R-PE fluorochrome reduced the ability to detect Vγ6$^+$ γδ T cells in the lungs compared with the uncoupled antibody demonstrated with a secondary antibody (0.54% vs.1.21%, respectively).

On the other hand, we also purified 51.2 mg of mouse IgG1 anti-mouse TCR Vγ6 antibody from 3.04 L of 1C10-1F7 hybridoma supernatant. The Coomassie Blue stained SDS-PAGE demonstrated that this was also a highly purified antibody. Only two bands of 50kDa and 25 kDa referring to heavy (λ_1) and light (κ) chains of IgG1, respectively, were observed **(Figure II-4)**. Coupling this antibody with AF647 fluorochrome eliminated its ability to detect Vγ6$^+$ γδ T cells in the lungs compared with the uncoupled antibody revealed with a secondary antibody (1.0% vs 26.7%, respectively) **(Figure IV-9)**.

10.6. TCR Vγ6 antibody injections robustly reduced the frequency of Vγ6$^+$ γδ T cells in MA PVAT, TA PVAT, lungs, and the spleen

A significant drop in the frequency of Vγ6$^+$ γδ T cell population was observed in mice injected with mouse IgG1 anti-mouse TCR Vγ6-blocking antibodies compared to mouse IgG1 isotype control antibodies. In MA PVAT, the frequency of Vγ6$^+$ γδ T cell population was decreased from 43.3±5.6% to 11.2±3.7 % of γδ T cells (P<0.0001). In TA PVAT, the frequency of Vγ6$^+$ γδ T cell population was reduced from 60.0±4.8% to 24.9±4.6 % of γδ T cells (P<0.001). Similarly in the lungs, the frequency of Vγ6$^+$ γδ T cell population was lowered from 50.4±3.1% to 9.5±1.4 % of γδ T cells (P<0.0001). In the spleen, the frequency of Vγ6$^+$ γδ T cell population was diminished from 9.2±1.5% to 6.3±0.7 % of γδ T cells (P<0.05) **(Figure IV-10)**.

10.7. Phenotyping of T cell subsets in the MA PVAT, TA PVAT, and spleen after Vγ6$^+$ γδ T cell blockade with anti-TCR Vγ6 (1C10-1F7) antibodies and 14 days of Ang II infusion

Flow cytometry profiling of Vγ6$^+$ γδ T cells, Vγ6$^-$ γδ T cells, CD4$^+$ T cells, and CD8$^+$ T cells showed variable expression of markers for production of IFN-γ (CXCR3$^+$ and IFN-γ$^+$) or IL-17 (CCR6$^+$ and IL-17$^+$), memory (CD44$^+$), and early activation (CD69$^+$) in MA PVAT, TA PVAT, and the spleen of Ang II-infused mice injected with IgG1 isotype control antibodies.

10.8. Blockade of Vγ6$^+$ γδ T cells decreased the frequency of other γδ T cell subsets that produce IL-17 in the MA PVAT after 14 days of Ang II infusion

In MA PVAT, the phenotyping of Vγ6$^+$ γδ T cells revealed that 0.9% of cells were CXCR3$^+$, 29.9% CCR6$^+$, 10% CD44$^+$, and 78.3% CD69$^+$. Blockade of Vγ6$^+$ γδ T cells with IP injection of TCR Vγ6 (1C10-1F7) antibodies did not cause any change in the frequency of these markers **(Figure IV-11A)**. Phenotyping of Vγ6$^-$ γδ T cells showed that 2.4% were CXCR3$^+$, 17% CCR6$^+$, 11% CD44$^+$, and 78.3% CD69$^+$. Blockade of Vγ6$^+$ γδ T cells decreased the frequency of CCR6$^+$ Vγ6$^-$ γδ T cells (from 17±5.6 to 6.7±1.9 % of Vγ6$^-$ γδ T cells, P<0.01) **(Figure IV-11B)**. Phenotyping of CD4$^+$ T cells showed that 6.9% of cells were CXCR3$^+$, 8.9% CCR6$^+$, 5.2% CD44$^+$, and 55.7% CD69$^+$. Phenotyping of CD8$^+$ T cells indicated that 6.2% were CXCR3$^+$, 4.8% CCR6$^+$, 0.5% CD44$^+$, and 30% CD69$^+$. Blockade of Vγ6$^+$ γδ T cells did not affect the frequency of these markers in CD4$^+$ or CD8$^+$ T cells **(Figures IV-11C&D)**.

10.9. Blockade of Vγ6$^+$ γδ T cells decreased the frequency of other γδ T cell subsets that produce IL-17 but increased their activation in the TA PVAT after 14 days of Ang II infusion

In TA PVAT, the phenotyping of Vγ6$^+$ γδ T cells showed that 3% of cells were CXCR3$^+$, 12% CCR6$^+$, 45.1% CD44$^+$, and 93.5% CD69$^+$. Blockade of Vγ6$^+$ γδ T cells did not cause any difference in the frequency of these markers **(Figure IV-12A)**. Phenotyping of Vγ6$^-$ γδ T cells revealed that 10.2% were CXCR3$^+$, 25.9% CCR6$^+$, 18.1% CD44$^+$, and 32.1% CD69$^+$. Blockade of Vγ6$^+$ γδ T cells decreased the frequency of CCR6$^+$ Vγ6$^-$ γδ T cells (from 25.9±4.4 to 13.2±2.6 % of Vγ6$^-$ γδ T cells, P<0.05) whereas the frequency of CD69$^+$ Vγ6$^-$ γδ T cells was increased (from

32.1±5.5 to 52.2±5.8 % of Vγ6$^-$ γδ T cells, P<0.05) **(Figure IV-12B)**. Phenotyping of CD4$^+$ T cells indicated that 2.2% were CXCR3$^+$, 7.1% CCR6$^+$, 7.2% CD44$^+$, and 38.1% CD69$^+$. Phenotyping of CD8$^+$ T cells showed that 1.4% were CXCR3$^+$, 0.5% CCR6$^+$, 1.1% CD44$^+$, and 12.7% CD69$^+$. Blockade of Vγ6$^+$ γδ T cells did not cause any change in the frequency of these markers in CD4$^+$ or CD8$^+$ T cells **(Figures IV-12C&D)**.

10.10. Vγ6$^+$ γδ T cell blockade and 14 days of Ang II infusion did not change the phenotypes of other T cell subsets in the spleen

In the spleen, the phenotyping of Vγ6$^+$ γδ T cells revealed that 29.5% of the cells were CXCR3$^+$, 12.1% CCR6$^+$, 91.2% CD44$^+$, 55% CD44^{Hi}, and 37.5% CD69$^+$. Blockade of Vγ6$^+$ γδ T cells raised the frequency of CCR6$^+$ Vγ6$^+$ γδ T cells (from 12.1±0.9 to 18.5±1.4 % of Vγ6$^+$ γδ T cells, P<0.001) whereas the frequency of CD69$^+$ Vγ6$^+$ γδ T cells was diminished (from 37.5±5.9 to 19.1±1.3 % of Vγ6$^+$ γδ T cells, P<0.001) **(Figure IV-13A)**. Phenotyping of Vγ6$^-$ γδ T cells showed that 30.7% were CXCR3$^+$, 1.7% CCR6$^+$, 79.2% CD44$^+$, 35.9% CD44^{Hi}, and 7.3% CD69$^+$ **(Figure IV-13B)**. Phenotyping of CD4$^+$ T cells demonstrated that 13.5% were CXCR3$^+$, 4.6% CCR6$^+$, 91.4% CD44$^+$, 22.8% CD44^{Hi}, 12.5% CD69$^+$, 4.6% IFN-γ$^+$, and 0.1% IL-17A$^+$ **(Figures IV-13C and IV-14B)**. Phenotyping of CD8$^+$ T cells indicated that 26% of cells were CXCR3$^+$, 0.7% CCR6$^+$, 59.2% CD44$^+$, 16.1% CD44^{Hi}, 3.9% CD69$^+$, 12% IFN-γ$^+$, and 1.1% IL-17A$^+$ **(Figures IV-13D and IV-14C)**. Blockade of Vγ6$^+$ γδ T cells did not significantly affect the frequency of these markers in Vγ6$^-$ γδ T cells, CD4$^+$ T cells or CD8$^+$ T cells **(Figures IV-13 & IV14)**.

10.11. Blockade of Vγ6$^+$ γδ T cells exacerbated the early Ang II-induced BP elevation and vascular injury

The role of Vγ6$^+$ γδ T cells in the development of hypertension and vascular injury was investigated in response to 14 days of Ang II infusion. Both groups of mice that were injected with IgG1 isotype control or anti-TCR Vγ6 (1C10-1F7) antibodies had similar increases in systolic (~42 mm Hg at daytime and ~41 mm Hg at nighttime) and diastolic BP (~33 mm Hg at daytime and ~28 mm Hg at nighttime) by the end of the 14-day Ang II. **(Figure IV-15 A and C for systolic & Figure IV-15 B and D for diastolic)**. However, anti-TCR Vγ6-injected mice had greater and earlier systolic and diastolic BP elevation during the development of hypertension, during the first week of Ang II infusion, compared to Ang II-infused mice injected with IgG1 isotype control antibodies (**Figure IV-15A-D**).

Infusion of Ang II induced an impairment in the MA endothelial relaxation response to acetylcholine in mice injected with IgG1 isotype control antibodies. Anti-TCR Vγ6 antibody injections in Ang II-infused mice reduced the MA endothelial dilatory responses to acetylcholine by ~50% compared to the control antibody injections (P<0.05) **(Figure IV-16A),** rather than decreasing the impaired response, demonstrating that Vγ6$^+$ γδ T cells exert a protective effect from deleterious effects by Ang II on the endothelium. It is noteworthy that impaired MA endothelial vasodilatory response was not the consequence of a vascular smooth muscle cell defect because endothelium-independent relaxation responses to the nitric oxide donor, sodium nitroprusside (SNP), were similar in both groups **(Figure IV-16B)**. Furthermore, blockade of Vγ6$^+$ γδ T cells in Ang II-infused mice did not induce any changes in MA mechanical and structural properties,

including vascular stiffening and remodeling, compared to Ang II-infused mice injected with IgG1 isotype control antibodies **(Figure IV-17A-C)**. Consequently, these results indicate that blockade of $V\gamma6^+$ γδ T cells has a protective rather than a deleterious effect on the initiation of Ang II-induced hypertension and vascular injury which is at least in part endothelium-dependent.

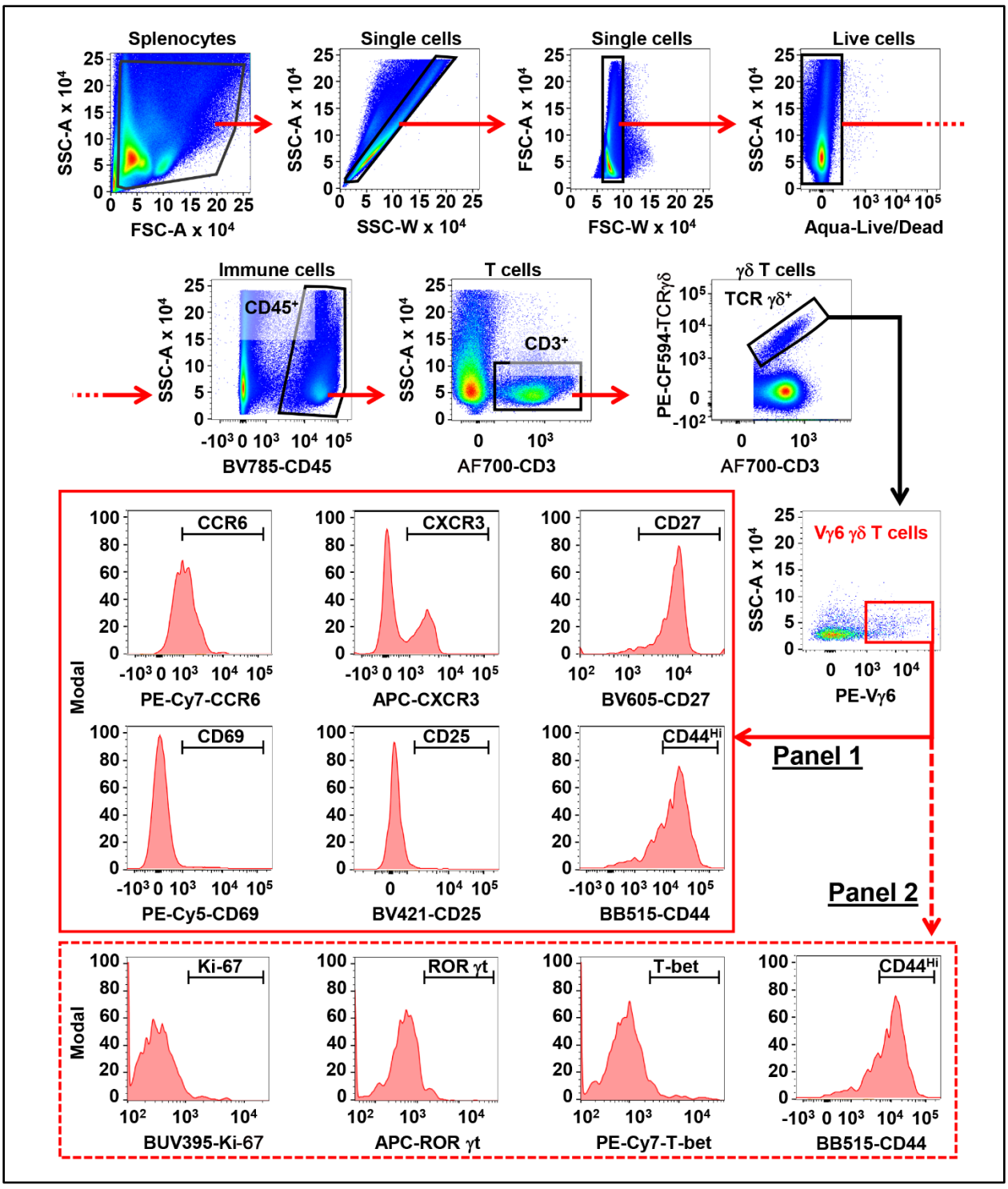

Figure IV-1: Representative flow cytometry profiling gating strategy of Vγ6⁺ γδ T cell phenotyping in the spleen. Splenocytes were first gated in the side scatter area (SSC-A)/forward scatter area (FSC-A) plot. Singlet cells were gated using SSC-A over SSC-wide (SSC-W). Singlet

cells were gated again using FSC-A over FSC-wide (FSC-W) to further clean up the data. Live cells were gated in the SSC-A/viability dye plot, followed by gating $CD45^+$ immune cells in the SSC-A/CD45 plot. Thereafter, $CD3^+$ T cells were gated in the SSC-A/CD3 plot. $TCR\gamma\delta^+$ T cells were gated in the TCRγδ/CD3 plot. $V\gamma6^+$ γδ T cells were gated in the SSC-A/Vγ6 plot. Finally, $CCR6^+$, $CXCR3^+$, $CD27^+$, $CD69^+$, $CD25^+$, $CD44^+$, $Ki\text{-}67^+$, ROR γt^+, and $T\text{-}bet^+$ $V\gamma6^+$ γδ T cells were gated in the SSC-A/CCR6, SSC-A/CXCR3, SSC-A/CD27, SSC-A/CD69, SSC-A/CD25, SSC-A/CD44, SSC-A/Ki-67, SSC-A/ROR γt, and SSC-A/T-bet plot, respectively. AF, Alexa-fluor; APC, Allophycocyanin; BB, Brilliant blue; BV, Brilliant violet; BUV, Brilliant ultraviolet; CD, Cluster of differentiation; Cy, Cyanine; PE, Phycoerythrin; PE-CF, Phycoerythrin-cyanine-based fluorescent dye; ROR, Retinoid-related orphan receptor.

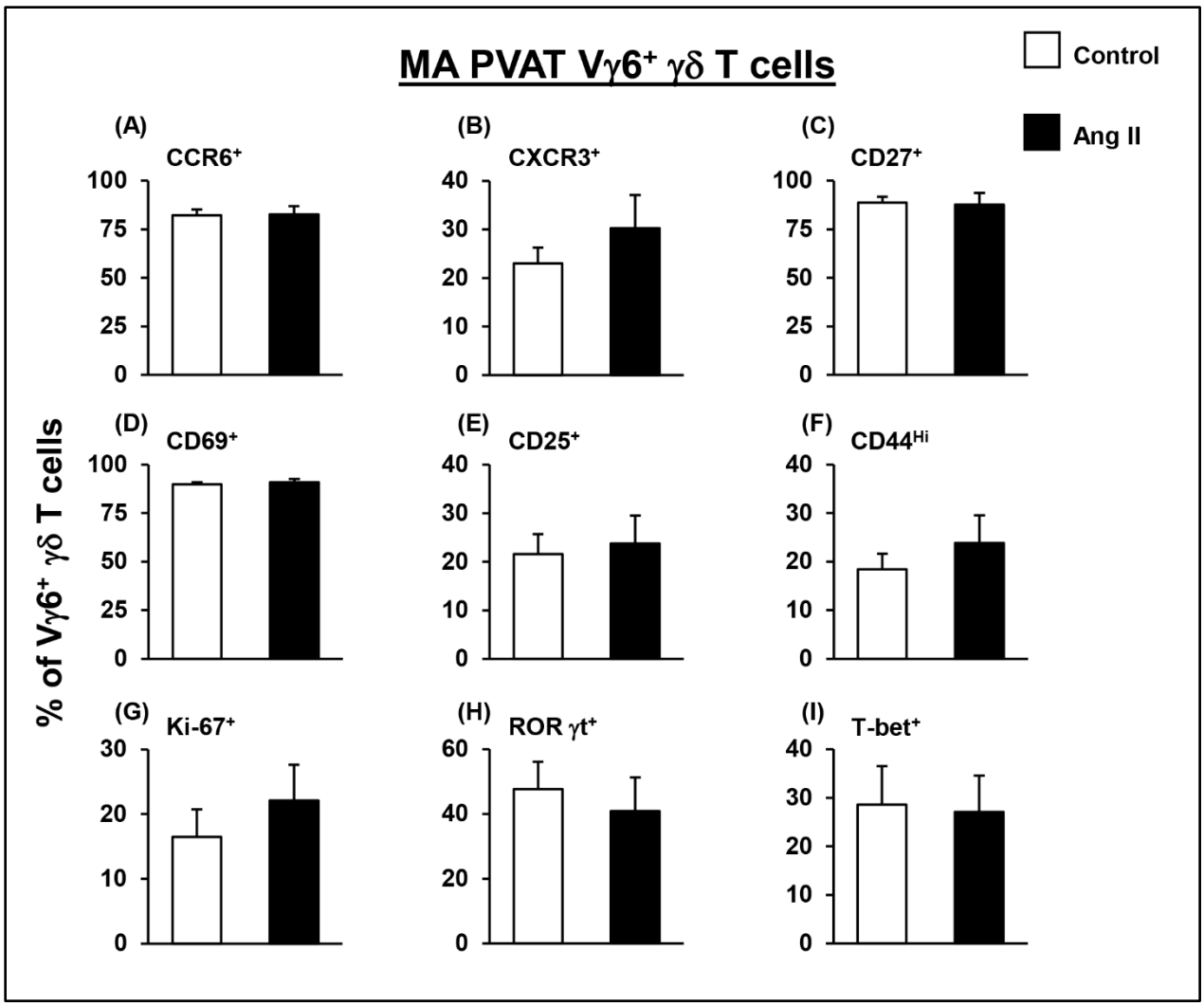

Figure IV-2: Phenotyping of Vγ6$^+$ γδ T cells in the mesenteric artery perivascular adipose tissue. The frequency (% of Vγ6$^+$ γδ T cells) of IL-17-producing (CCR6$^+$ and ROR γt$^+$) (**A** and **H**, respectively), IFN-γ-producing (CXCR3$^+$, CD27$^+$, and T-bet$^+$) (**B**, **C**, and **I**, respectively), activated (CD69$^+$) (**D**), suppressed (CD25$^+$) (**E**), memory (CD44^{Hi}) (**F**), and proliferating (Ki-67$^+$) (**G**) Vγ6$^+$ γδ T cells in the mesenteric artery with perivascular adipose tissue (MA PVAT) of wild-type (WT) mice after 14 days of Ang II infusion (490ng/kg/min) or not was determined by flow cytometry. The gating strategy is presented in Figure IV-1. Data are presented as means ± SEM, n= 10-14. CD, Cluster of differentiation; CCR, C-C motif chemokine receptor; CXCR, C-X-C motif chemokine receptor; ROR, Retinoid-related orphan receptor.

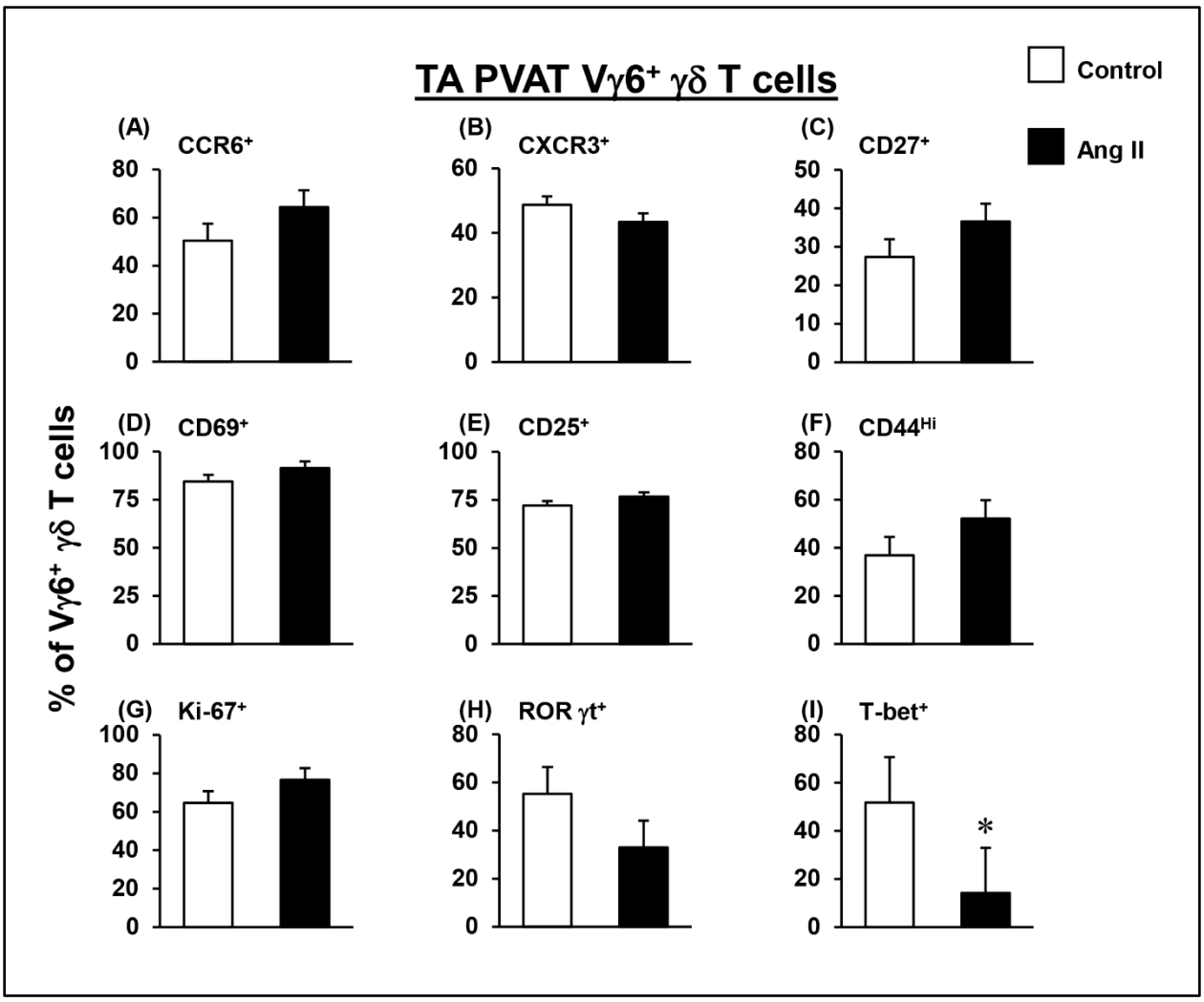

Figure IV-3: Phenotyping of Vγ6$^+$ γδ T cells in the thoracic aortic perivascular adipose tissue.

The frequency (% of Vγ6$^+$ γδ T cells) of IL-17-producing (CCR6$^+$ and ROR γt$^+$) (**A** and **H**, respectively), IFN-γ-producing (CXCR3$^+$, CD27$^+$, and T-bet$^+$) (**B**, **C**, and **I**, respectively), activated (CD69$^+$) (**D**), suppressed (CD25$^+$) (**E**), memory (CD44^{Hi}) (**F**), and proliferating (Ki-67$^+$) (**G**) Vγ6$^+$ γδ T cells in the thoracic aorta with perivascular adipose tissue (TA PVAT) of wild-type (WT) mice after 14 days of Ang II infusion (490ng/kg/min) or not was determined by flow cytometry. The gating strategy is presented in Figure IV-1. Data are presented as means ± SEM, n= 4-13. Data were analyzed using unpaired *t*-test. *P<0.01 versus respective WT control mice.

CD, Cluster of differentiation; CCR, C-C motif chemokine receptor; CXCR, C-X-C motif chemokine receptor; ROR, Retinoid-related orphan receptor.

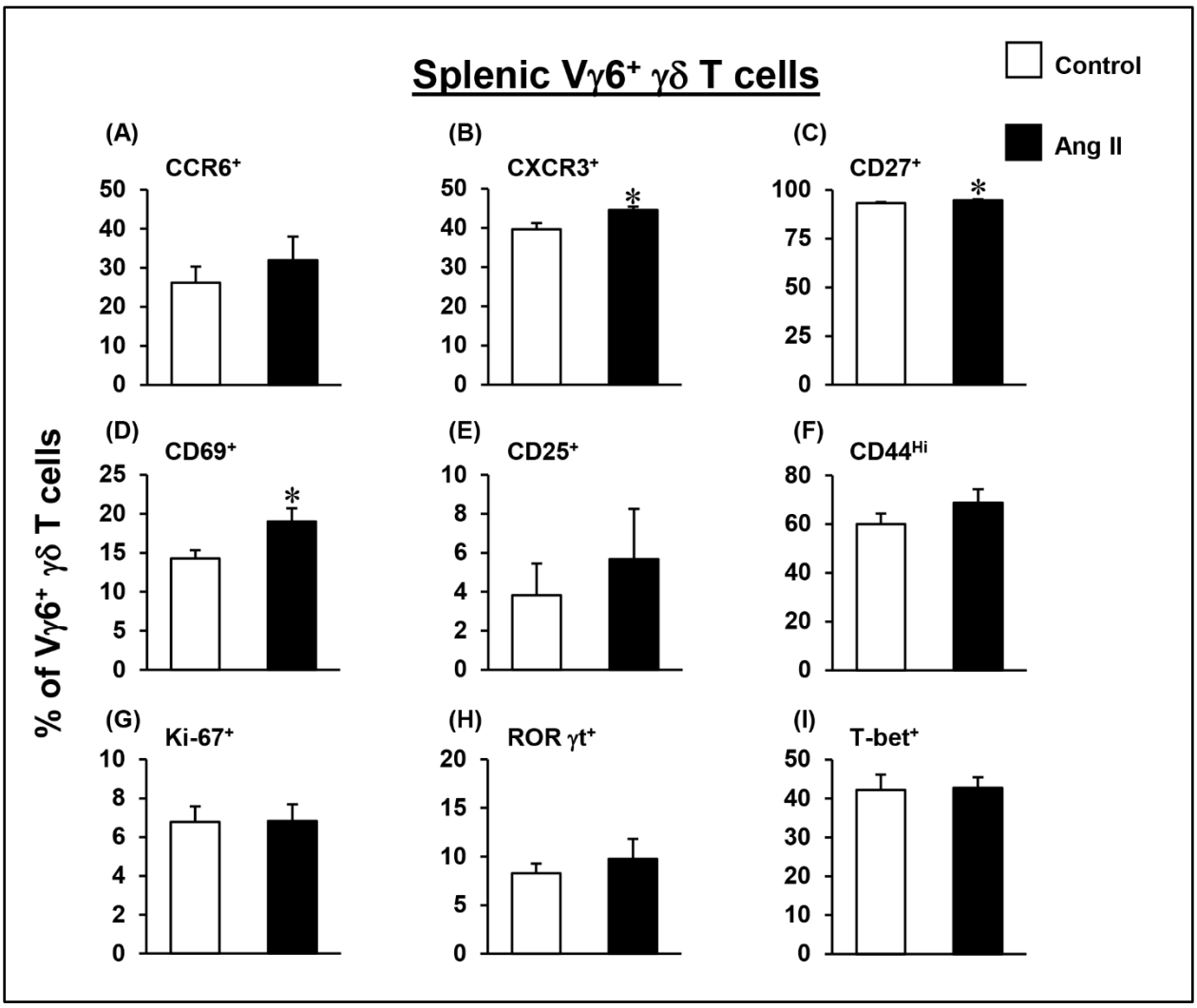

Figure IV-4: Phenotyping of Vγ6$^+$ γδ T cells in the spleen. The frequency (% of Vγ6$^+$ γδ T cells) of IL-17-producing (CCR6$^+$ and ROR γt$^+$) (**A** and **H**, respectively), IFN-γ-producing (CXCR3$^+$, CD27$^+$, and T-bet$^+$) (**B**, **C**, and **I**, respectively), activated (CD69$^+$) (**D**), suppressed (CD25$^+$) (**E**), memory (CD44^{Hi}) (**F**), and proliferating (Ki-67$^+$) (**G**) Vγ6$^+$ γδ T cells in the spleen of wild-type (WT) mice after 14 days of Ang II infusion (490ng/kg/min) or not was determined by flow cytometry. The gating strategy is presented in Figure IV-1. Data are presented as means ± SEM, n= 7-8. Data were analyzed using unpaired *t*-test. *P<0.05 versus respective WT control mice.CD, Cluster of differentiation; CCR, C-C motif chemokine receptor; CXCR, C-X-C motif chemokine receptor; ROR, Retinoid-related orphan receptor.

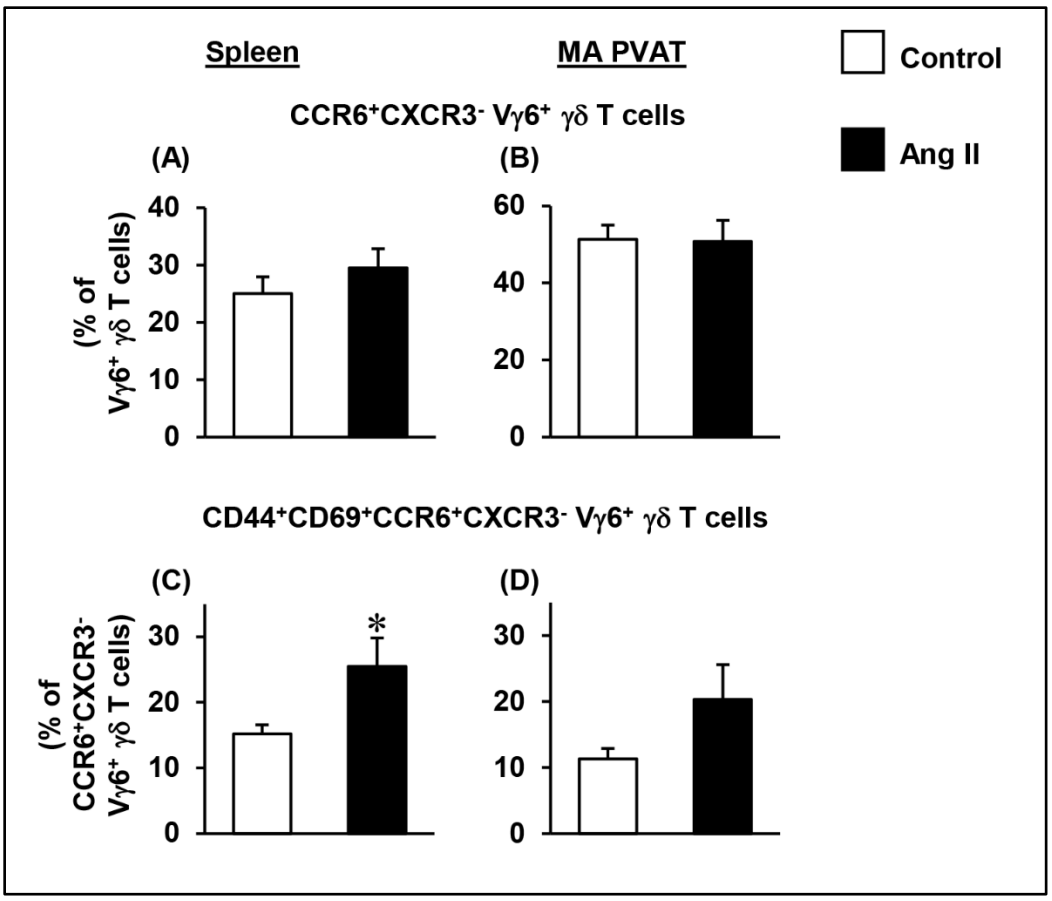

Figure IV-5: Infusion of Ang II increased the frequency of IL-17-producing effector memory Vγ6$^+$ γδ T cells in the spleen. The frequency (% of Vγ6$^+$ γδ T cells) of IL-17-producing (CCR6$^+$CXCR3$^-$) Vγ6$^+$ γδ T cells in the spleen (**A**) and mesenteric artery with perivascular adipose tissue (MA PVAT) (**B**) and the frequency (% of CCR6$^+$CXCR3$^-$ Vγ6$^+$ γδ T cells) of IL-17 producing effector memory (CD44$^+$CD69$^+$CCR6$^+$CXCR3$^-$) Vγ6$^+$ γδ T cells in the spleen (**C**) and MA PVAT (**D**) of wild-type (WT) mice after 14 days of Ang II infusion (490ng/kg/min) or not were determined by flow cytometry. Data are presented as means ± SEM, n= 7-8 in **A** and **C** and 10-14 in **B** and **D**. Data were analyzed using unpaired *t*-test. *P<0.05 versus respective WT control mice.CD, Cluster of differentiation; CCR, C-C motif chemokine receptor; CXCR, C-X-C motif chemokine receptor.

Ang II effect
↑ increase
↓ decrease

TCR Vγ6⁺ γδ T cells

	Memory		Activation		IL-17A		IFN-γ		Proliferation
	CD44^{hi}	CD25^{+}	CD69^{+}	CD27^{+}	CCR6^{+}	ROR γt^{+}	CXCR3^{+}	T-bet^{+}	Ki-67^{+}
Spleen	++	+/-	+ ↑	+++↑	+	+/-	↑++	++	+/-
MA PVAT	+	+	+++	+++	+++	++	+	+	+
TA PVAT	++	+++	+++	+	++	++	++	↓++	++

Table IV-1: Comparison of Vγ6 γδ T cell phenotype in the spleen, mesenteric artery perivascular adipose tissue, and thoracic aortic perivascular adipose tissue. The frequency (% of Vγ6^{+} γδ T cells) of memory (CD44^{Hi}), suppressed (CD25^{+}), activated (CD69^{+}), IL-17-producing (CCR6^{+} and ROR γt^{+}), IFN-γ-producing (CXCR3^{+}, CD27^{+}, and T-bet^{+}), and proliferating (Ki-67^{+}) Vγ6^{+} γδ T cells in the spleen, mesenteric artery with perivascular adipose tissue (MA PVAT), and thoiracic aorta with perivascular adipose tissue (TA PVAT) of wild-type (WT) control mice was determined by flow cytometry. +/- = 0-10%, + = 11-30%, ++ = 31-70%, and +++ = 71-100%. The effect of Ang II (490ng/kg/min) for 14 days is presented by upward arrow (increase) and downward arrow (decrease). CD, Cluster of differentiation; CCR, C-C motif chemokine receptor; CXCR, C-X-C motif chemokine receptor; ROR, Retinoid-related orphan receptor.

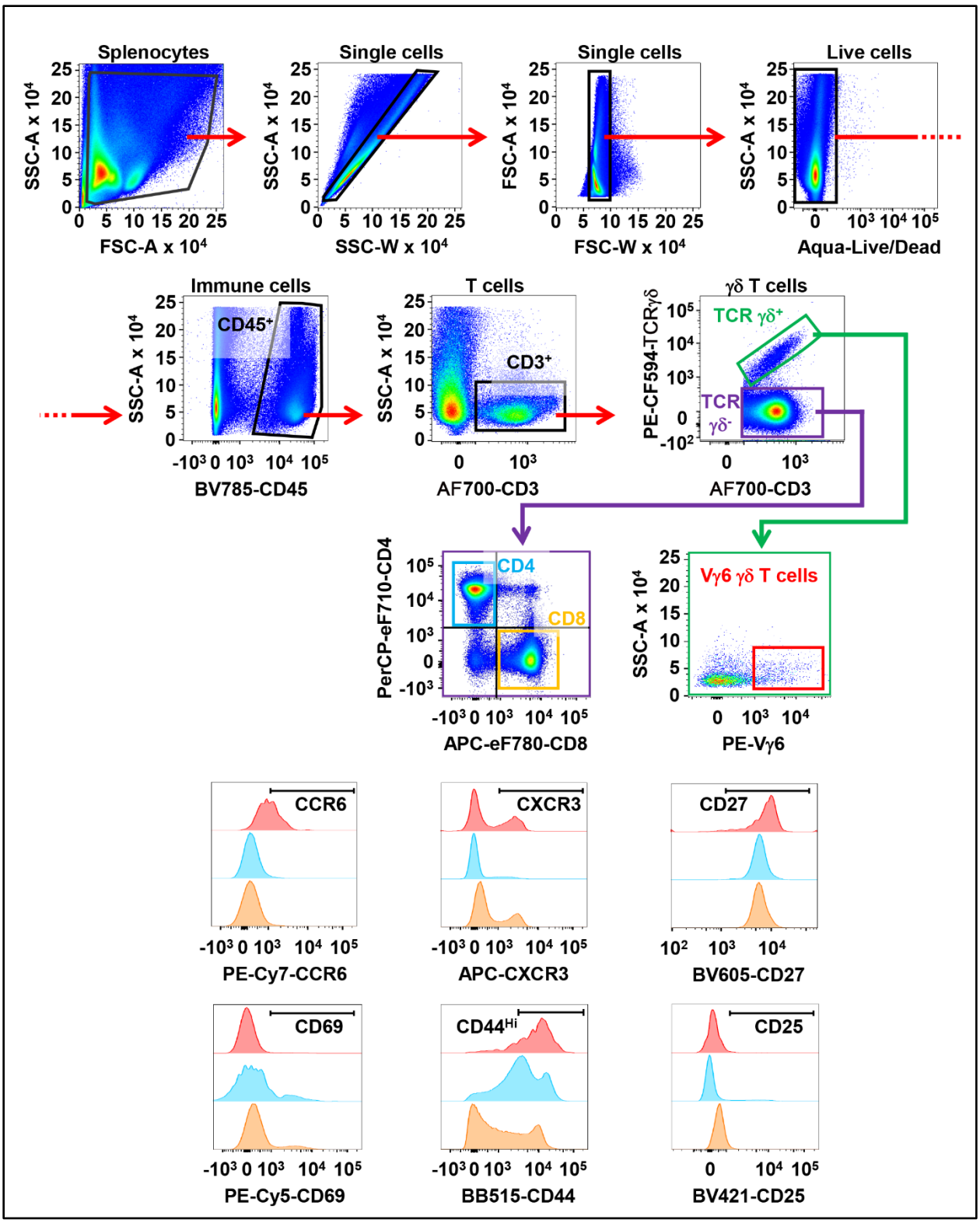

Figure IV-6: Representative flow cytometry profiling gating strategy of phenotyping of T cell subsets in the spleen. Splenocytes were first gated in the side scatter area (SSC-A)/forward

scatter area (FSC-A) plot. Singlet cells were gated using SSC-A over SSC-wide (SSC-W). Singlet cells were gated again using FSC-A over FSC-wide (FSC-W) to further clean up the data. Live cells were gated in the SSC-A/viability dye plot, followed by gating $CD45^+$ immune cells in the SSC-A/CD45 plot. $CD3^+$ T cells were gated in the SSC-A/CD3 plot. Thereafter, $CD4^+$ and $CD8^+$ T cells were gated in the CD4/CD8 plot and γδ T cells in the T cell receptor (TCR)γδ/CD3 plot. $V\gamma6^+$ γδ T cells were gated in the SSC-A/Vγ6 plot. Finally, $CCR6^+$, $CXCR3^+$, $CD27^+$, $CD69^+$, $CD44^+$, and $CD25^+$ $V\gamma6^+$ γδ T cells were gated in the Vγ6/CCR6, Vγ6/CXCR3, Vγ6/CD27, Vγ6/CD69, Vγ6/CD44, and Vγ6/CD25 plot, respectively. $CCR6^+$, $CXCR3^+$, $CD27^+$, $CD69^+$, $CD44^+$, and $CD25^+$ $CD4^+$ T cells were gated in the CD4/CCR6, CD4/CXCR3, CD4/CD27, CD4/CD69, CD4/CD44, and CD4/CD25 plot, respectively. $CCR6^+$, $CXCR3^+$, $CD27^+$, $CD69^+$, $CD44^+$, and $CD25^+$ $CD8^+$ T cells were gated in the CD8/CCR6, CD8/CXCR3, CD8/CD27, CD8/CD69, CD8/CD44, and CD8/CD25 plot, respectively. AF, Alexa-fluor; APC, Allophycocyanin; BB, Brilliant blue; BV, Brilliant violet; BUV, Brilliant ultraviolet; CD, Cluster of differentiation; CCR, C-C motif chemokine receptor; CXCR, C-X-C motif chemokine receptor; Cy, Cyanine; PE, Phycoerythrin; PE-CF, Phycoerythrin-cyanine-based fluorescent dye; PerCP, Peridinin chlorophyll-A protein; ROR, Retinoid-related orphan receptor.

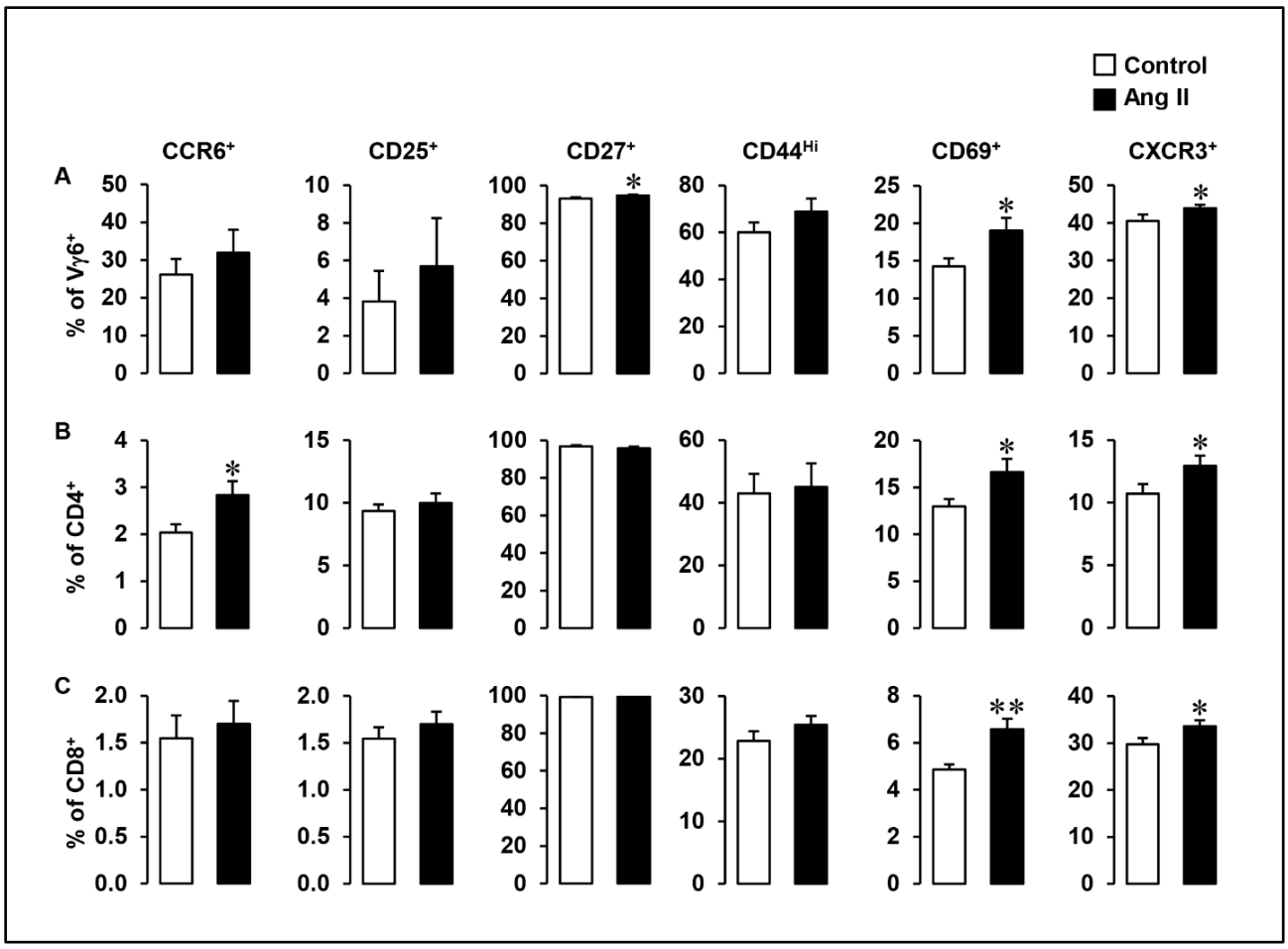

Figure IV-7: Infusion of Ang II increased the activation and IFN-γ production in T cell subsets in the spleen. The frequency (% of Vγ6$^+$ γδ T cells) of IL-17-producing (CCR6$^+$), suppressed (CD25$^+$), IFN-γ-producing (CXCR3$^+$ and CD27$^+$), memory (CD44^{Hi}), and activated (CD69$^+$) Vγ6$^+$ γδ T cells (**A**), the frequency (% of CD4$^+$ T cells) of CCR6$^+$, CD25$^+$, CD27$^+$, CD44^{Hi}, CD69$^+$, and CXCR3$^+$ CD4$^+$ T cells (**B**), and the frequency (% of CD8$^+$ T cells) of CCR6$^+$, CD25$^+$, CD27$^+$, CD44^{Hi}, CD69$^+$, and CXCR3$^+$ CD8$^+$ T cells (**C**) in the spleen of wild-type (WT) mice after 14 days of Ang II infusion (490ng/kg/min) or not were determined by flow cytometry. The gating strategy is presented in Figure IV-6. Data are presented as means ± SEM, n= 10-11. Data were analyzed using unpaired *t*-test. **P*<0.05 and ***P*<0.01 versus respective WT control

mice.CD, Cluster of differentiation; CCR, C-C motif chemokine receptor; CXCR, C-X-C motif chemokine receptor.

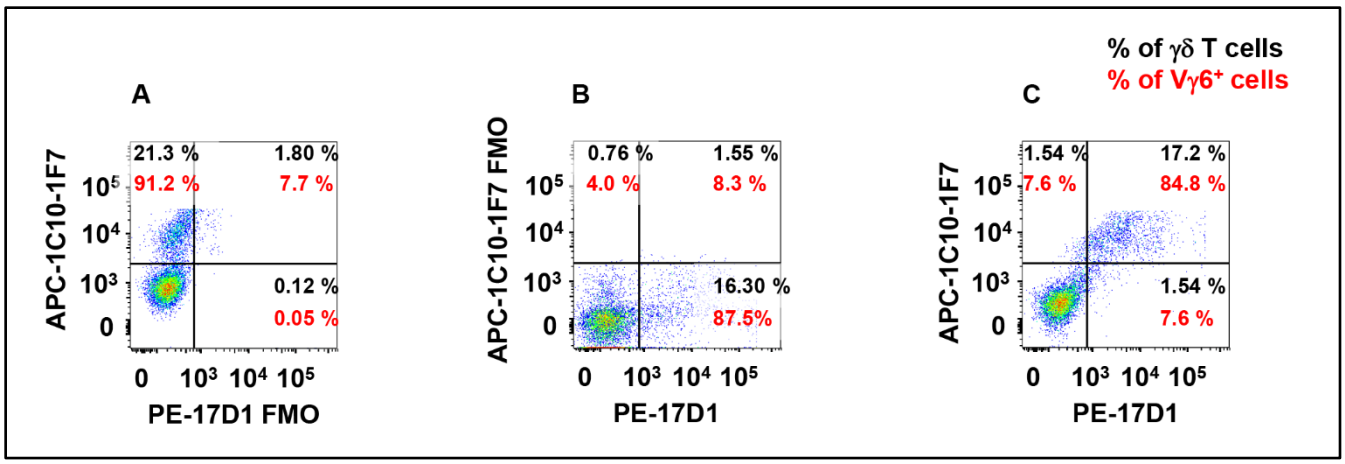

Figure IV-8: Confirmation that the 1C10-1F7 monoclonal antibody is better than the 17D1 monoclonal antibody in the detection of Vγ6$^+$ γδ T cells. Representative Vγ6$^+$ γδ T cell profiling in the presence of mouse IgG1 anti-mouse TCR Vγ6 (clone 1C10-1F7) antibodies only (**A**), rat IgM anti-mouse TCR Vγ6 (clone 17D1) antibodies only (**B**), or both types of antibodies (**C**) in the mesenteric artery with perivascular adipose tissue (MA PVAT) of wild-type (WT) mice after 14 days of Ang II infusion (490ng/kg/min). APC, Allophycocyanin; FMO, Fluorescence minus one control; PE, Phycoerythrin.

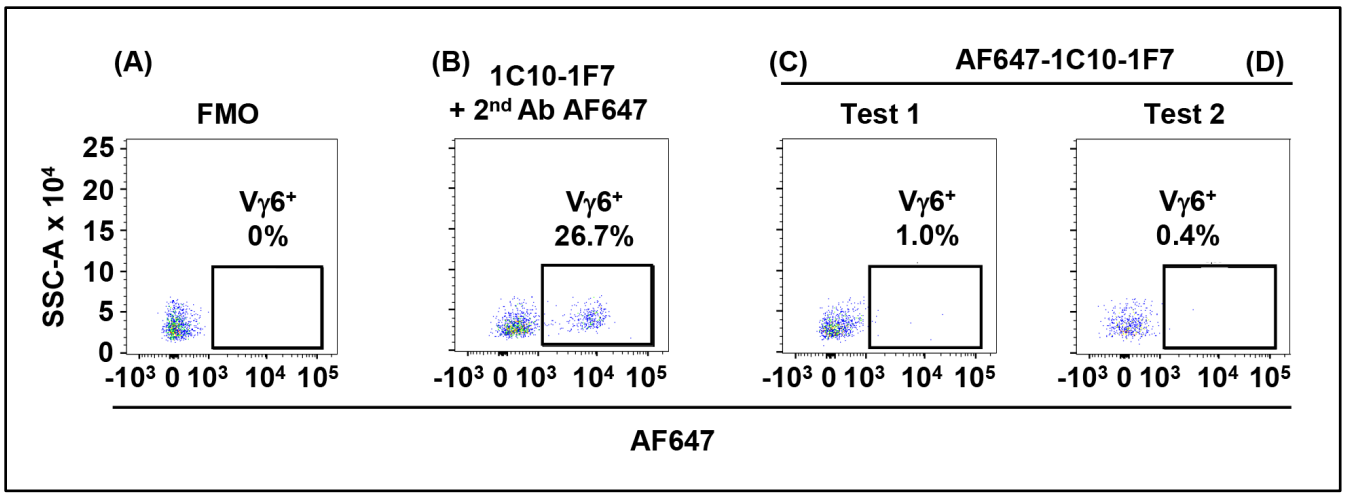

Figure IV-9: Labeling of mouse IgG1 anti-mouse TCR Vγ6 (1C10-1F7) antibodies with AF647 fluorochrome abrogated its ability to bind to TCR Vγ6. Representative $V\gamma6^+$ γδ T cell profiling in the lungs of Ang II-infused mice in the absence of mouse IgG1 anti-mouse TCR Vγ6 (clone 1C10-1F7) antibodies as a negative control gate (**A**) or in the presence of unconjugated mouse IgG1 anti-mouse TCR Vγ6 (clone 1C10-1F7) antibodies that were revealed using AF647-conjugated rat anti-mouse IgG1 secondary antibodies (**B**), or in the presence of purified mouse IgG1 anti-mouse TCR Vγ6 (clone 1C10-1F7) antibodies that were conjugated with AF647 fluorochrome (two trails, **C** and **D**). AF, Alexa-fluor; FMO, Fluorescence minus one control; SSC-A, Side scatter area.

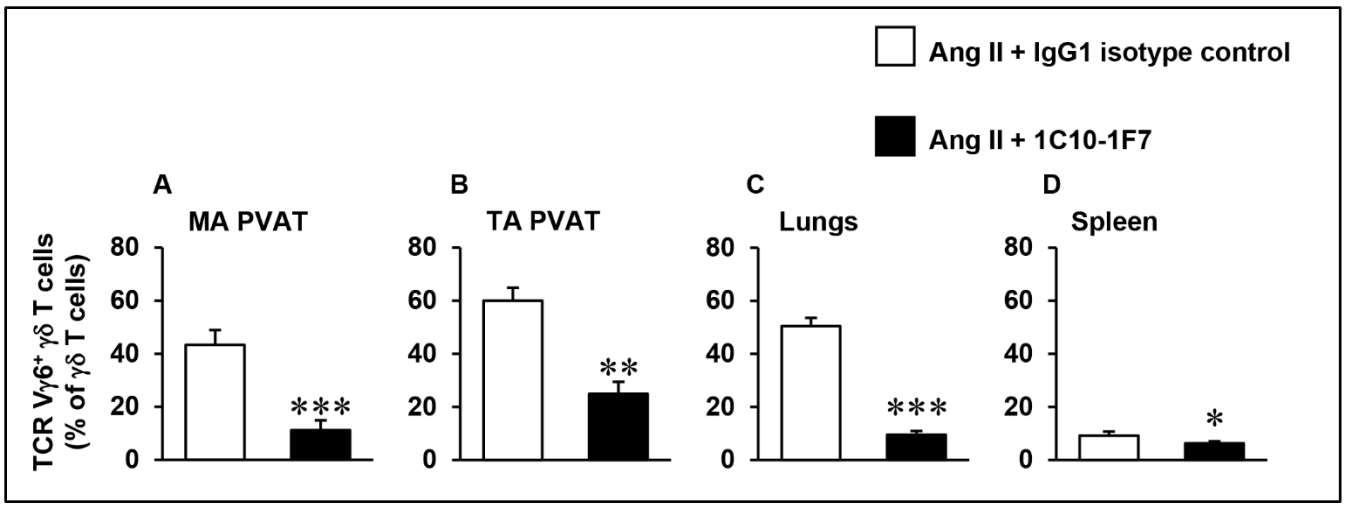

Figure IV-10: TCR Vγ6 antibody injections robustly reduced the frequency of Vγ6$^+$ γδ T cells in MA PVAT, TA PVAT, lungs, and the spleen. The frequency of Vγ6$^+$ γδ T cells in MA PVAT (**A**), TA PVAT (**B**), lungs (**C**), and the spleen (**D**) was determined in wild-type (WT) mice infused with Ang II and injected with IgG1 isotype control or anti-TCR Vγ6 (1C10-1F7) antibodies. Data are presented as means±SEM, n= 11-12 in **A**, **B**, and **D** and 9-10 in **C**. Data were analyzed using unpaired *t*-test. **P*<0.05, ***P*<0.001, and ****P*<0.0001 versus respective IgG1 isotype control antibodies.

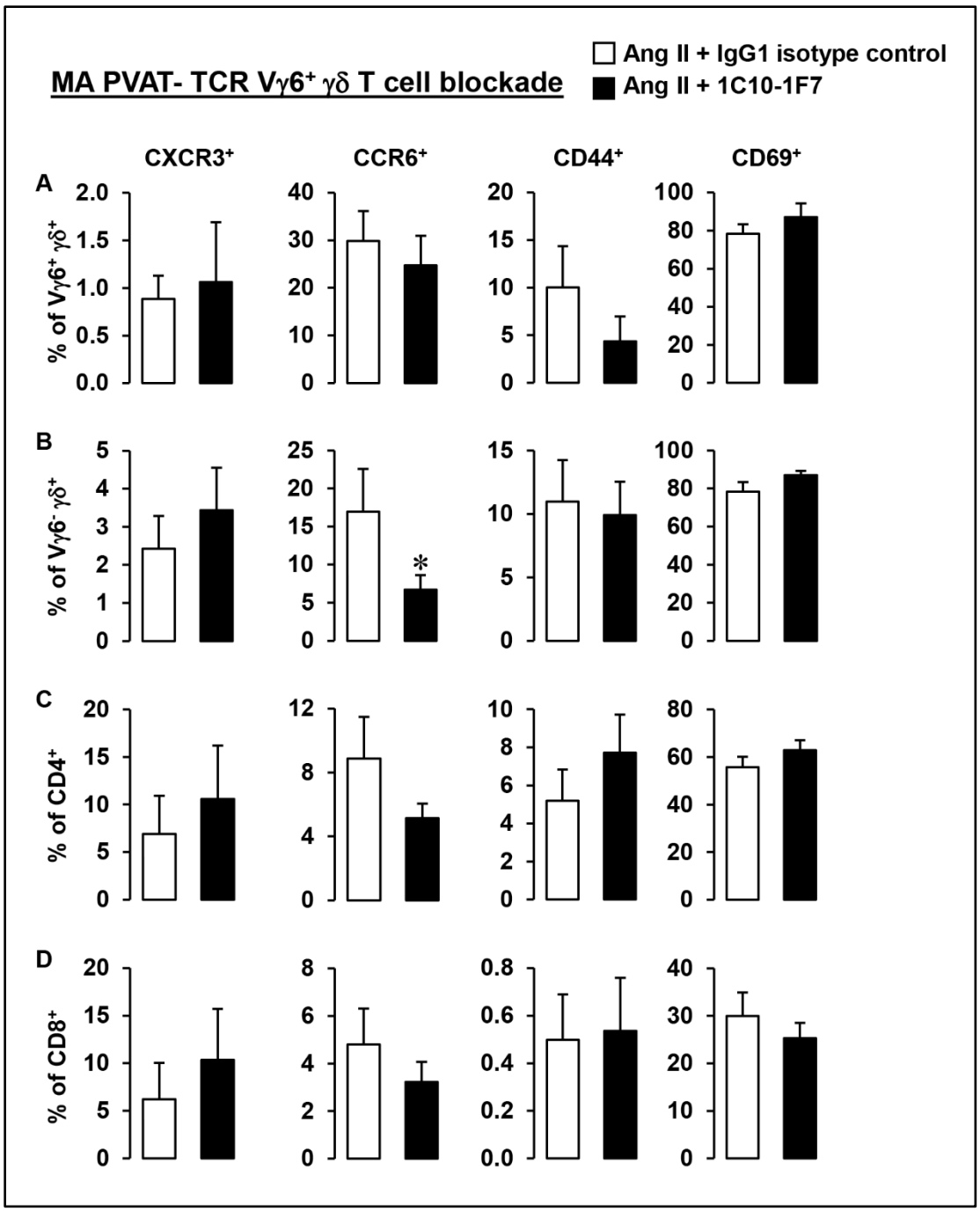

Figure IV-11: Blockade of Vγ6$^+$ γδ T cells decreased the frequency of other γδ T cell subsets that produce IL-17 in the MA PVAT after 14 days of Ang II infusion. The frequency (% of Vγ6$^+$ γδ T cells) of IFN-γ-producing (CXCR3$^+$), IL-17-producing (CCR6$^+$), memory (CD44$^+$), and activated (CD69$^+$) Vγ6$^+$ γδ T cells (**A**), the frequency (% of Vγ6$^-$ γδ T cells) of CXCR3$^+$, CCR6$^+$, CD44$^+$, and CD69$^+$ Vγ6$^-$ γδ T cells (**B**), the frequency (% of CD4$^+$ T cells) of CXCR3$^+$, CCR6$^+$,

$CD44^+$, and $CD69^+$ $CD4^+$ T cells (**C**), and the frequency (% of $CD8^+$ T cells) of $CXCR3^+$, $CCR6^+$, $CD44^+$, and $CD69^+$ $CD8^+$ T cells (**D**) in the mesenteric artery with perivascular adipose tissue (MA PVAT) of wild-type (WT) mice infused with Ang II (490ng/kg/min) and injected with IgG1 isotype control or anti-TCR Vγ6 (1C10-1F7) antibodies were determined by flow cytometry. The gating strategy is presented in **Figure IV-6**. Data are presented as means±SEM, n= 11-12. Data were analyzed using unpaired *t*-test. ***P*<0.01 versus respective IgG1 isotype control antibodies.

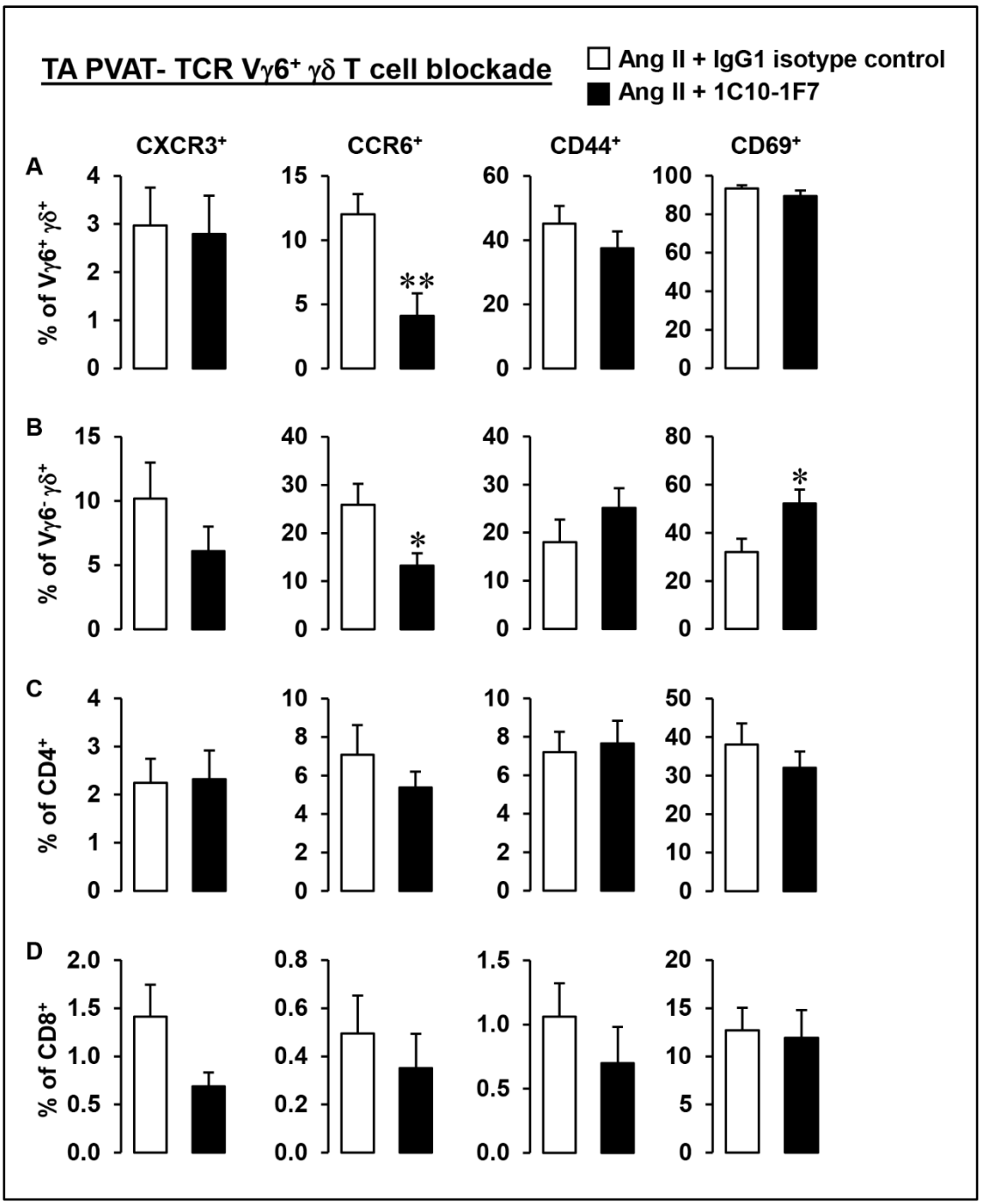

Figure IV-12: Blockade of Vγ6$^+$ γδ T cells decreased the frequency of other γδ T cell subsets that produce IL-17 but increased their activation in the TA PVAT after 14 days of Ang II infusion. The frequency (% of Vγ6$^+$ γδ T cells) of IFN-γ-producing (CXCR3$^+$), IL-17-producing (CCR6$^+$), memory (CD44$^+$), and activated (CD69$^+$) Vγ6$^+$ γδ T cells (**A**), the frequency (% of Vγ6$^-$ γδ T cells) of CXCR3$^+$, CCR6$^+$, CD44$^+$, and CD69$^+$ Vγ6$^-$ γδ T cells (**B**), the frequency (% of CD4$^+$

T cells) of CXCR3$^+$, CCR6$^+$, CD44$^+$, and CD69$^+$ CD4$^+$ T cells (**C**), and the frequency (% of CD8$^+$ T cells) of CXCR3$^+$, CCR6$^+$, CD44$^+$, and CD69$^+$ CD8$^+$ T cells (**D**) in the thoracic aorta with perivascular adipose tissue (TA PVAT) of wild-type (WT) mice infused with Ang II (490ng/kg/min) and injected with IgG1 isotype control or anti-TCR Vγ6 (1C10-1F7) antibodies were determined by flow cytometry. The gating strategy is presented in **Figure IV-6**. Data are presented as means±SEM, n= 11-12. Data were analyzed using unpaired *t*-test. **P*<0.05 and ***P*<0.01 versus respective IgG1 isotype control antibodies.

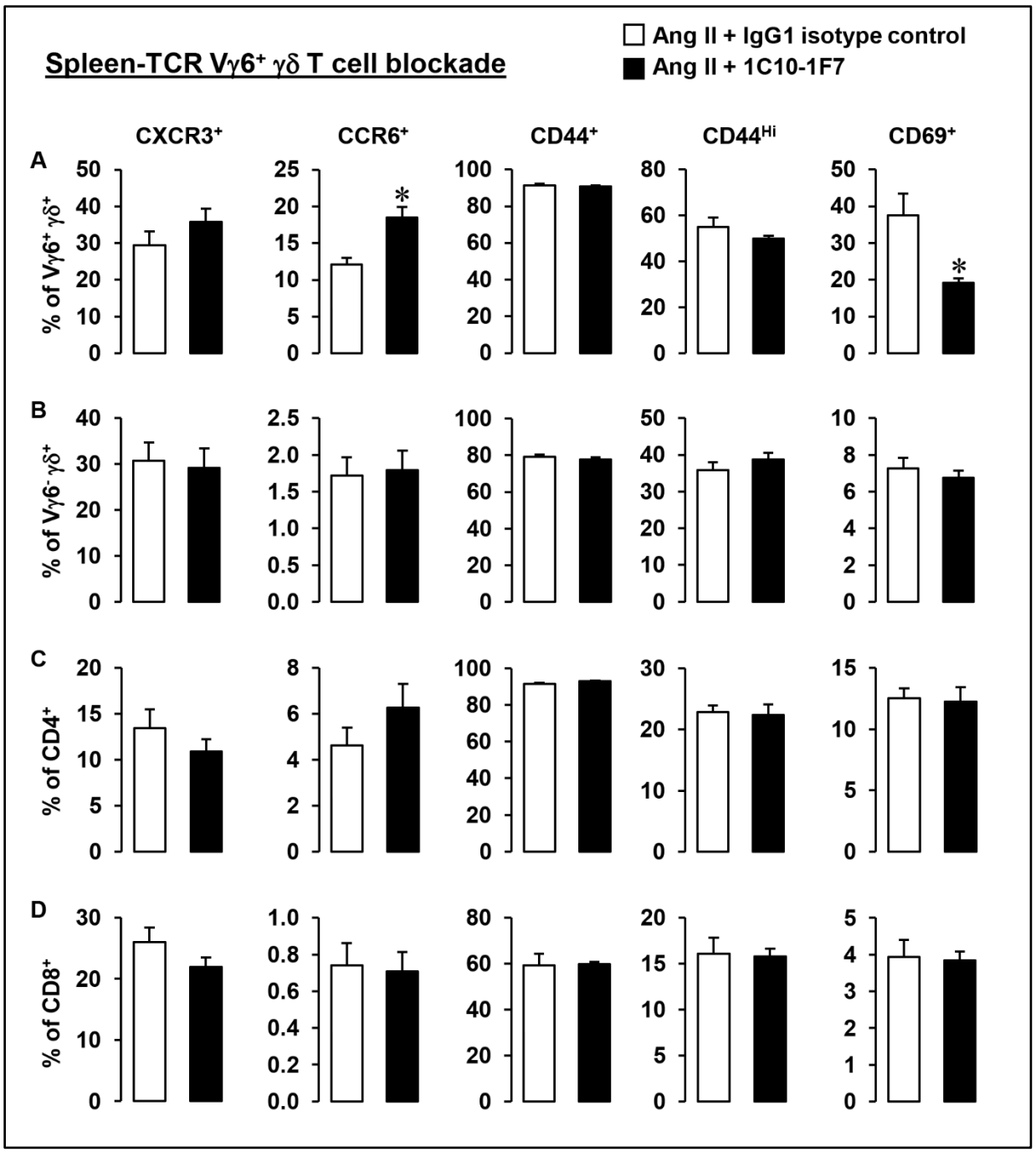

Figure IV-13: Phenotyping of T cell subsets in the spleen after Vγ6$^+$ γδ T cell blockade and 14 days of Ang II infusion using surface markers. The frequency (% of Vγ6$^+$ γδ T cells) of IFN-γ-producing (CXCR3$^+$), IL-17-producing (CCR6$^+$), memory (CD44$^+$ and CD44^{Hi}), and activated (CD69$^+$) Vγ6$^+$ γδ T cells (**A**), the frequency (% of Vγ6$^-$ γδ T cells) of CXCR3$^+$, CCR6$^+$, CD44$^+$, CD44^{Hi} and CD69$^+$ Vγ6$^-$ γδ T cells (**B**), the frequency (% of CD4$^+$ T cells) of CXCR3$^+$, CCR6$^+$,

$CD44^{+}$, $CD44^{Hi}$, and $CD69^{+}$ $CD4^{+}$ T cells (**C**), and the frequency (% of $CD8^{+}$ T cells) of $CXCR3^{+}$, $CCR6^{+}$, $CD44^{+}$, $CD44^{Hi}$, and $CD69^{+}$ $CD8^{+}$ T cells (**D**) in the spleen of wild-type (WT) mice infused with Ang II (490ng/kg/min) and injected with IgG1 isotype control or anti-TCR Vγ6 (1C10-1F7) antibodies were determined by flow cytometry. The gating strategy is presented in **Figure IV-6**. Data are presented as means±SEM, n= 11-12. Data were analyzed using unpaired *t*-test. **P*<0.001 versus respective IgG1 isotype control antibodies.

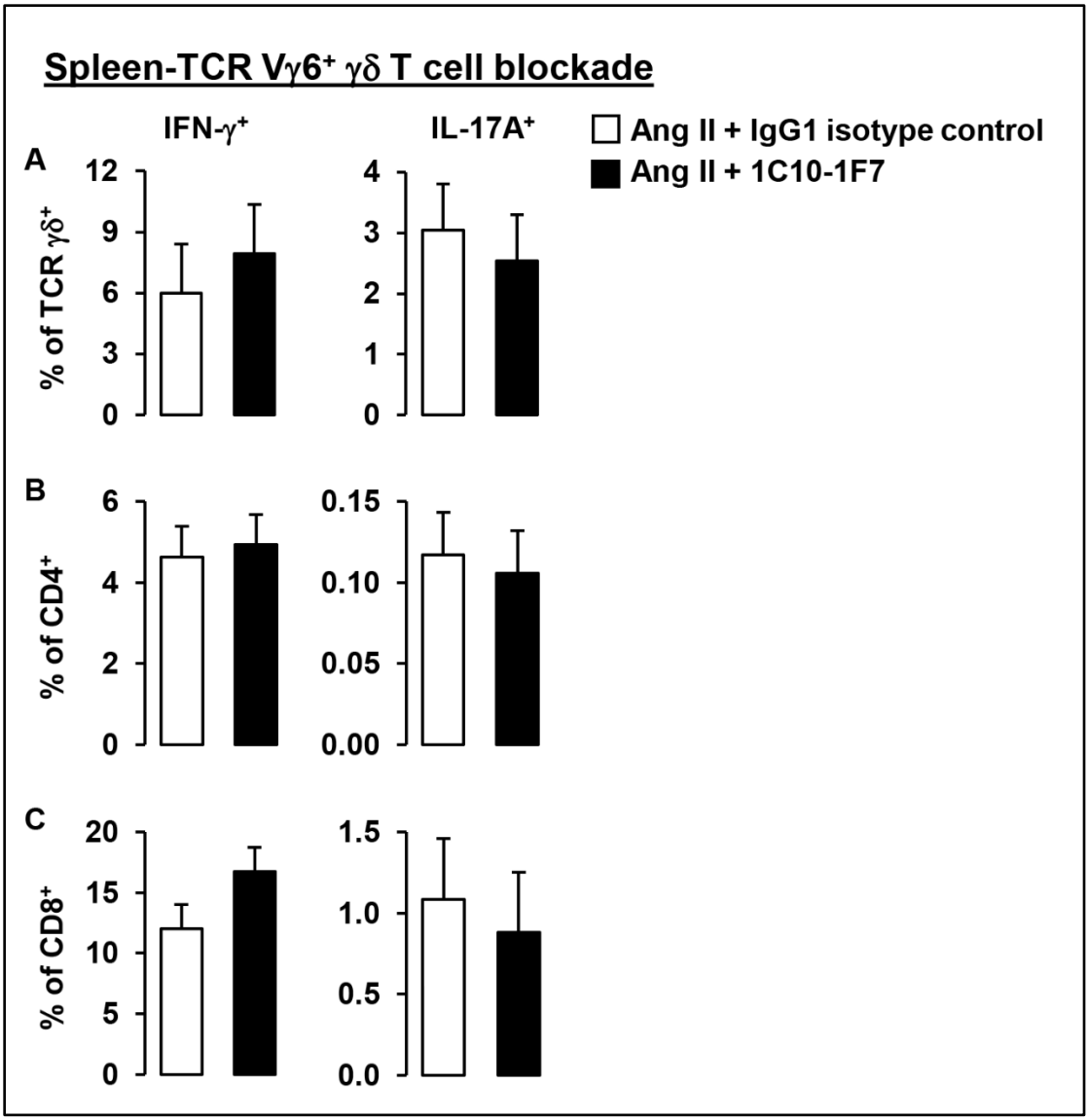

Figure IV-14: The production of IFN-γ and IL-17A in different T cell subsets did not affect by Vγ6$^+$ γδ T cell blockade in the spleen of Ang II-infused mice. The frequency (% of TCR γδ$^+$ T cells) of IFN-γ-producing (IFN-γ$^+$) and IL-17A-producing (IL-17A$^+$) γδ T cells (**A**), the frequency (% of CD4$^+$ T cells) of IFN-γ$^+$ and IL-17A$^+$ CD4$^+$ T cells (**B**), and the frequency (% of CD8$^+$ T cells) of IFN-γ$^+$ and IL-17A$^+$ CD8$^+$ T cells (**C**) in the spleen of wild-type (WT) mice infused with Ang II (490ng/kg/min) and injected with IgG1 isotype control or anti-TCR Vγ6 (1C10-1F7) antibodies were determined by flow cytometry. Data are presented as means±SEM, n= 8.

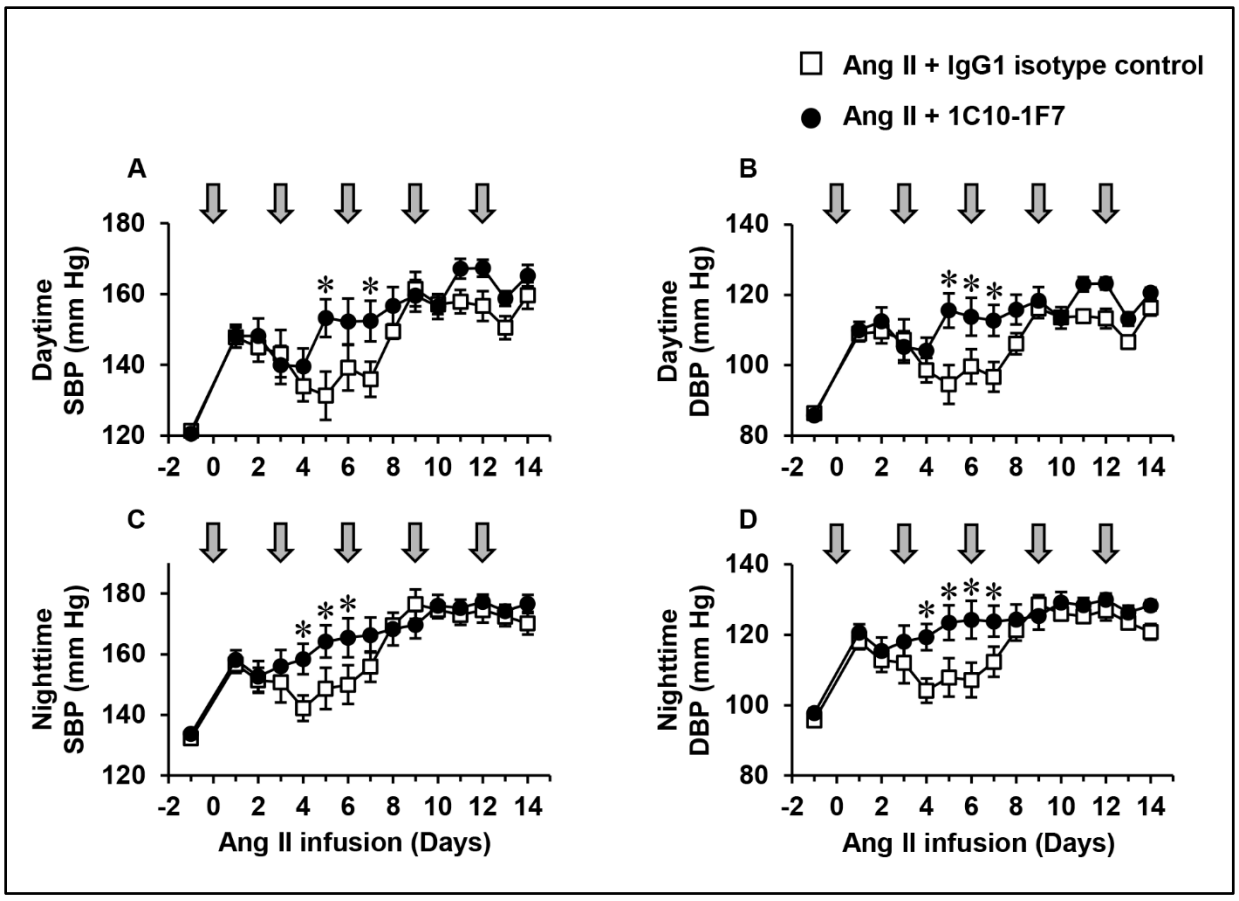

Figure IV-15: Blockade of Vγ6$^+$ γδ T cells exacerbated the early Ang II-induced BP elevation. Telemetry systolic BP (SBP, at daytime **A** and nighttime **C**) and diastolic BP (DBP, at daytime **B** and nighttime **D**) were determined in wild-type (WT) mice infused with Ang II and injected with IgG1 isotype control or anti-TCR Vγ6 (1C10-1F7) antibodies. Gray arrows indicate antibody injection days. Data are presented as means±SEM, n= 5-6. Data were analyzed using a two-way analysis of variance (ANOVA) with repeated measures followed by a Student−Newman−Keuls *post hoc* test. *P<0.05 versus respective IgG1 isotype control antibodies.

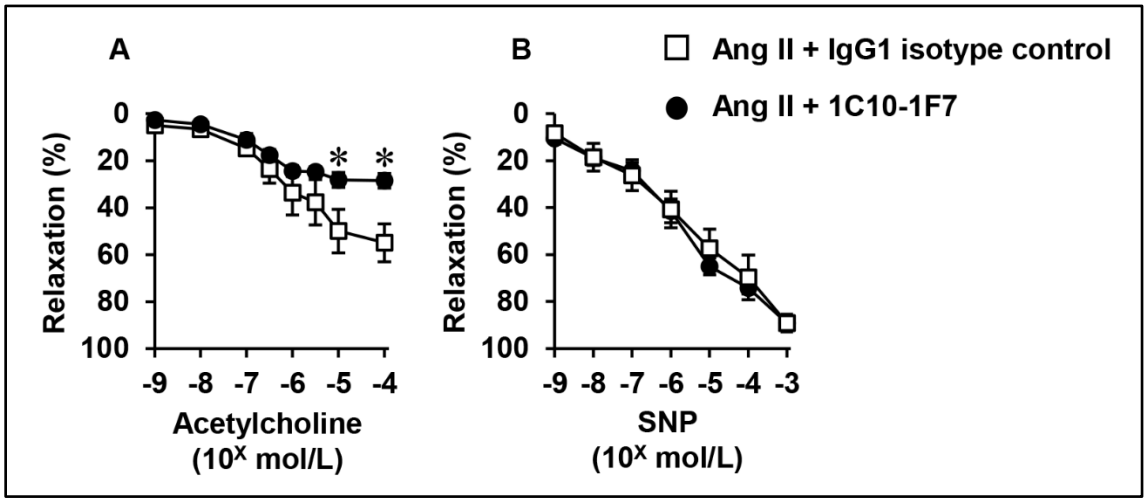

Figure IV-16: Blockade of Vγ6$^+$ γδ T cells aggravated Ang II-induced mesenteric artery (MA) endothelial dysfunction but not endothelium-independent relaxation. MA dilatory responses to acetylcholine (**A**) and to sodium nitroprusside (SNP, **B**) were determined in wild-type (WT) mice infused with Ang II and injected with IgG1 isotype control or anti-TCR Vγ6 (1C10-1F7) antibodies. Data are presented as means±SEM, n= 7-8. Data were analyzed using a two-way analysis of variance (ANOVA) with repeated measures followed by a Student−Newman−Keuls *post hoc* test. *P<0.01 versus respective IgG1 isotype control antibodies.

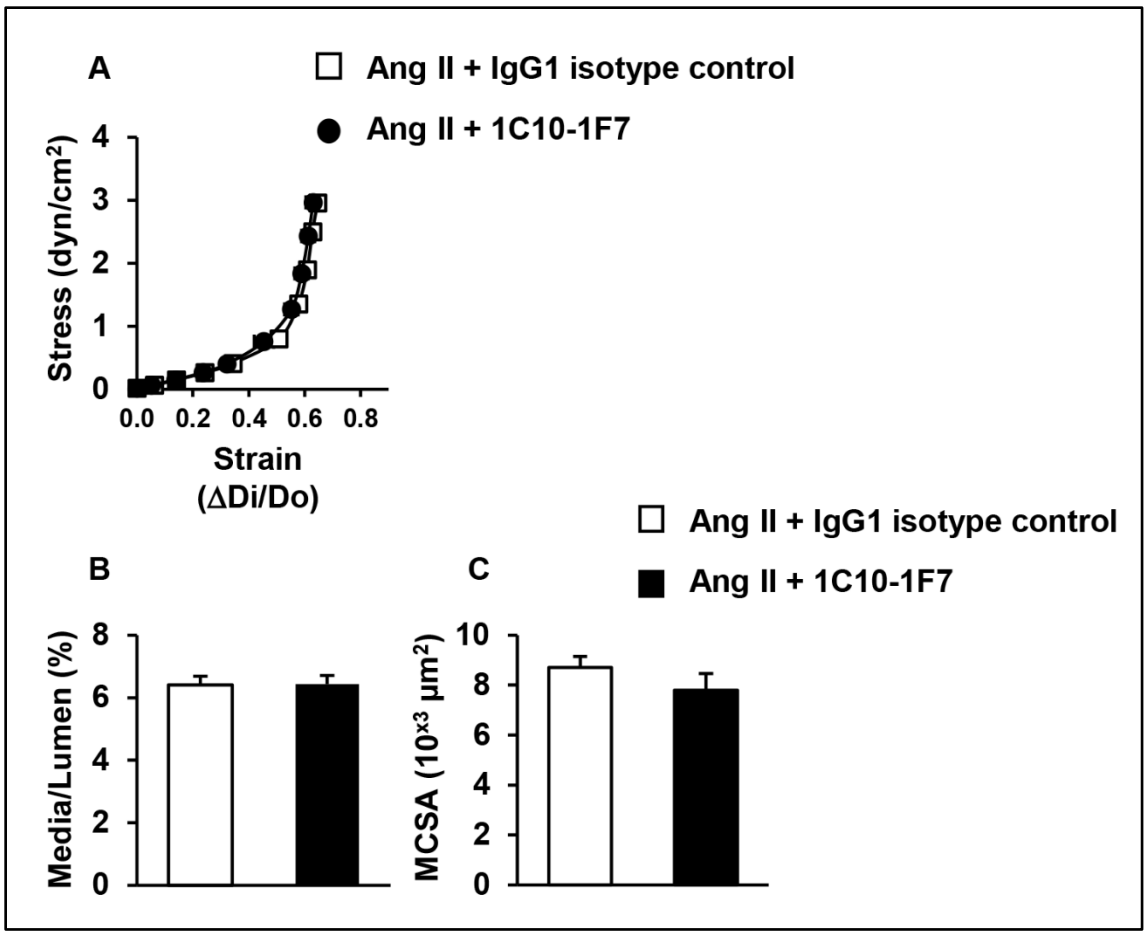

Figure IV-17: Mesenteric artery (MA) mechanical and structural properties were not affected by blockade of Vγ6$^+$ γδ T cells. MA media stress-strain relationship (**A**), media-to-lumen ratio (**B**), and media cross-sectional area (MCSA, **C**) were determined in wild-type (WT) mice infused with Ang II and injected with IgG1 isotype control or anti-TCR Vγ6 (1C10-1F7) antibodies. Data are presented as means±SEM, n= 9-10.

CHAPTER V: Results

The role of Vγ4^{+} γδ T cells

in Ang II-induced hypertension and vascular injury

11.1. TCR Vγ4 antibody injections significantly decreased the frequency of Vγ4$^+$ γδ T cells in MA PVAT, TA PVAT, and the spleen

A significant drop in the frequency of Vγ4$^+$ γδ T cell population was observed in mice injected with mouse IgG anti-mouse TCR Vγ4-depleting antibodies compared to IgG isotype control antibodies. In MA PVAT, the frequency of Vγ4$^+$ γδ T cell population was decreased from 27.1±3.8% to 4.0±2.0 % of γδ T cells (P<0.001). In TA PVAT, the frequency of Vγ4$^+$ γδ T cell population was reduced from 32.2±8.9% to 13.1±7.1 % of γδ T cells (P<0.05). Similarly in the spleen, the frequency of Vγ4$^+$ γδ T cell population was diminished from 39.5±0.7% to 1.6±0.7 % of γδ T cells (P<0.0001) **(Figure V-1)**.

11.2. Phenotyping of T cell subsets in the MA PVAT, TA PVAT, and spleen after Vγ4$^+$ γδ T cell depletion with anti-TCR Vγ4 (UC3-10A6) antibodies and 14 days of Ang II infusion

Flow cytometry profiling of Vγ6$^+$ γδ T cells, γδ T cells, CD4$^+$ T cells, and CD8$^+$ T cells revealed variable expression of markers for production of IFN-γ (CXCR3$^+$ and IFN-γ$^+$) or IL-17 (CCR6$^+$, IL-17A$^+$, and IL-22), memory (CD44$^+$), early activation (CD69$^+$), and anti-inflammatory responses (IL-10$^+$ and FOXP3$^+$) in MA PVAT, TA PVAT, and the spleen of Ang II-infused mice injected with IgG isotype control antibodies.

11.3. Depletion of Vγ4$^+$ γδ T cells with anti-TCR Vγ4 (UC3-10A6) antibodies decreased the frequency of CD44$^+$CD4$^+$ T cells in the MA PVAT after 14 days of Ang II infusion

In MA PVAT, the phenotyping of Vγ6$^+$ γδ T cells revealed that 14.8% were CXCR3$^+$, 29.6% CCR6$^+$, 16.2% CD44$^+$, and 64.5% CD69$^+$. Depletion of Vγ4$^+$ γδ T cells by IP injection of anti-TCR Vγ4 (UC3-10A6) antibodies did not cause any change in the frequency of these markers in Vγ6$^+$ γδ T cells **(Figure V-2A)**. The phenotyping of CD4$^+$ T cells showed that 6.0% were CXCR3$^+$, 2.5% CCR6$^+$, 8.1% CD44$^+$, and 59.0% CD69$^+$. Vγ4$^+$ γδ T cell depletion decreased the frequency of CD44$^+$ CD4$^+$ T cells (from 8.1±1.4 to 4.1±1.1 % of CD4$^+$ T cells, P<0.01) **(Figure V-2B)**. The phenotyping of CD8$^+$ T cells indicated that 10.6% were CXCR3$^+$, 2.1% CCR6$^+$, 2.6% CD44$^+$, and 26.7% CD69$^+$. Depletion of Vγ4$^+$ γδ T cells did not affect the frequency of these markers in CD8$^+$ T cells **(Figure V-2C)**.

11.4. Depletion of Vγ4$^+$ γδ T cells reduced the frequency of CD44$^+$CD4$^+$ and CD44$^+$CD8$^+$ T cells in the TA PVAT after 14 days of Ang II infusion

In TA PVAT, the phenotyping of Vγ6$^+$ γδ T cells revealed that 5.4% were CXCR3$^+$, 17.1% CCR6$^+$, 23.6% CD44$^+$, and 93.4% CD69$^+$. Vγ4$^+$ γδ T cell depletion did not cause any change in the frequency of these markers in Vγ6$^+$ γδ T cells **(Figure V-3A)**. Phenotyping of CD4$^+$ T cells showed that 8.4% were CXCR3$^+$, 4.8% CCR6$^+$, 10.2% CD44$^+$, and 30.2% CD69$^+$. Depletion of Vγ4$^+$ γδ T cells reduced the frequency of CD44$^+$ CD4$^+$ T cells (from 10.2±1.6 to 5.7±1.0 % of CD4$^+$ T cells, P<0.05) **(Figure V-3B)**. The phenotyping of CD8$^+$ T cells demonstrated that 12.9% were CXCR3$^+$, 3.2% CCR6$^+$, 3.1% CD44$^+$, and 16.9% CD69$^+$. Vγ4$^+$ γδ T cell depletion decreased

the frequency of $CD44^+$ $CD8^+$ T cells (from 3.1±0.5 to 1.6±0.4 % of $CD8^+$ T cells, $P<0.05$) **(Figure V-3C)**.

11.5. Vγ4$^+$ γδ T cell depletion and 14 days of Ang II infusion increased the activity of γδ T cells but did not induce changes in the phenotypes of other T cell subsets in the spleen

In the spleen, the phenotyping of Vγ6$^+$ γδ T cells revealed that 27.8% were $CXCR3^+$, 26% $CCR6^+$, 89.7% $CD44^+$, 47.5% $CD44^{Hi}$, 23.1% $CD69^+$, 6.5% IFN-γ^+, 17.8% IL-$17A^+$, 5.1% IL-22^+, 0.3% IL-10^+, and 3.1% $FOXP3^+$. Depletion of Vγ4$^+$ γδ T cells did not cause any change in the frequency of these markers in Vγ6$^+$ γδ T cells **(Figures V-4A and V-5A)**. Phenotyping of γδ T cells showed that 7.6% were $CXCR3^+$, 11.5% $CCR6^+$, 81.9% $CD44^+$, 33.8% $CD44^{Hi}$, and 8.3% $CD69^+$. Vγ4$^+$ γδ T cell depletion raised the frequency of $CD69^+$ γδ T cells (from 8.3±0.4 to 10.6±0.8 % of γδ T cells, $P<0.05$) **(Figure V-4B)**. The phenotyping of $CD4^+$ T cells demonstrated that 18.2% were $CXCR3^+$, 8% $CCR6^+$, 91.7% $CD44^+$, 21.4% $CD44^{Hi}$, 12.7% $CD69^+$, 5.3% IFN-γ^+, 3.3% IL-$17A^+$, 0.2% IL-22^+, 0.6% IL-10^+, and 3.7% $FOXP3^+$. Vγ4$^+$ γδ T cell depletion did not affect the frequency of these markers in $CD4^+$ T cells **(Figures V-4C and V-5B)**. Phenotyping of $CD8^+$ T cells indicated that 16.9% were $CXCR3^+$, 1% $CCR6^+$, 64.9% $CD44^+$, 20.5% $CD44^{Hi}$, 5.4% $CD69^+$, 13.9% IFN-γ^+, 6.2% IL-$17A^+$, 0.2% IL-22^+, 0.1% IL-10^+, and 0.04% $FOXP3^+$. Depletion of Vγ4$^+$ γδ T cells had no effect on the frequency of these markers in $CD8^+$ T cells **(Figures V-4D and V-5C)**.

11.6. Depletion of Vγ4$^+$ γδ T cells did not affect the Ang II-induced BP elevation and vascular injury

The role of Vγ4$^+$ γδ T cells in the development of hypertension and vascular injury was tested in response to 14 days of Ang II infusion. Both groups of mice that were injected with IgG isotype control or anti-TCR Vγ4 (UC3-10A6) antibodies had similar increases in systolic (~44 mm Hg at daytime and ~48 mm Hg at nighttime) and diastolic BP (~33 mm Hg at daytime and ~33 mm Hg at nighttime) by the end of the 14-day Ang II. **(Figure V-6 A and C for systolic & Figure V-6 B and D for diastolic)**. Depletion of Vγ4$^+$ γδ T cells did not cause any changes in SBP or DBP during the development of hypertension compared to Ang II-infused mice injected with IgG isotype control antibodies (**Figure V-6A-D**).

Infusion of Ang II induced a reduction in the MA endothelial relaxation response to acetylcholine in mice injected with IgG isotype control antibodies. Anti-TCR Vγ4 antibody injections in Ang II-infused mice were associated with a similar MA endothelial dilatory response to acetylcholine compared to the control antibody injections **(Figure V-7A)**. The impaired MA endothelial vasodilatory response was not the result of a vascular smooth muscle cell defect because endothelium-independent relaxation responses to the nitric oxide donor, SNP, were similar in both groups **(Figure V-7B)**. Furthermore, depletion of Vγ4$^+$ γδ T cells in Ang II-infused mice did not affect MA mechanical and structural properties, including vascular stiffening and remodeling, compared to Ang II-infused mice injected with IgG isotype control antibodies **(Figure V-8A-C)**. Accordingly, these results reveal that Vγ4$^+$ γδ T cells do not affect Ang II-induced hypertension and vascular injury.

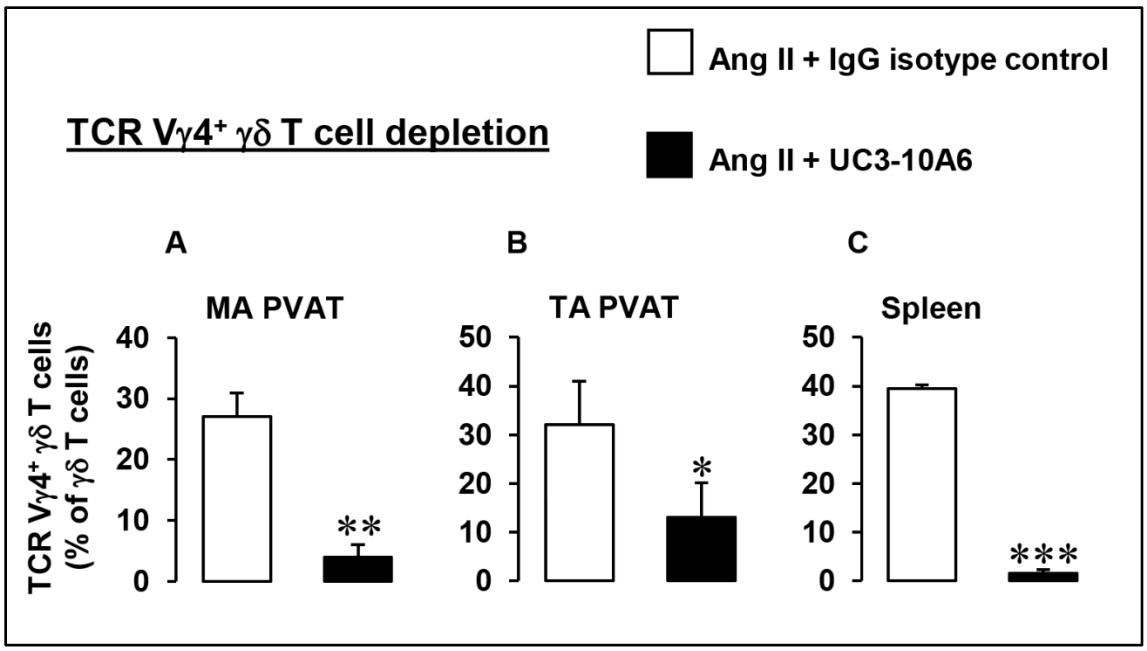

Figure V-1: TCR Vγ4 antibody injections significantly decreased the frequency of Vγ4$^+$ γδ T cells in MA PVAT, TA PVAT, and the spleen. The frequency of Vγ4$^+$ γδ T cells in MA PVAT (**A**), TA PVAT (**B**), and the spleen (**C**) was determined in wild-type (WT) mice infused with Ang II and injected with IgG isotype control or anti-TCR Vγ4 (UC3-10A6) antibodies. Data are presented as means±SEM, n= 6-7 in **A**-**C**. Data were analyzed using unpaired *t*-test. **P*<0.05, ***P*<0.001, and ****P*<0.0001 versus respective IgG1 isotype control antibodies.

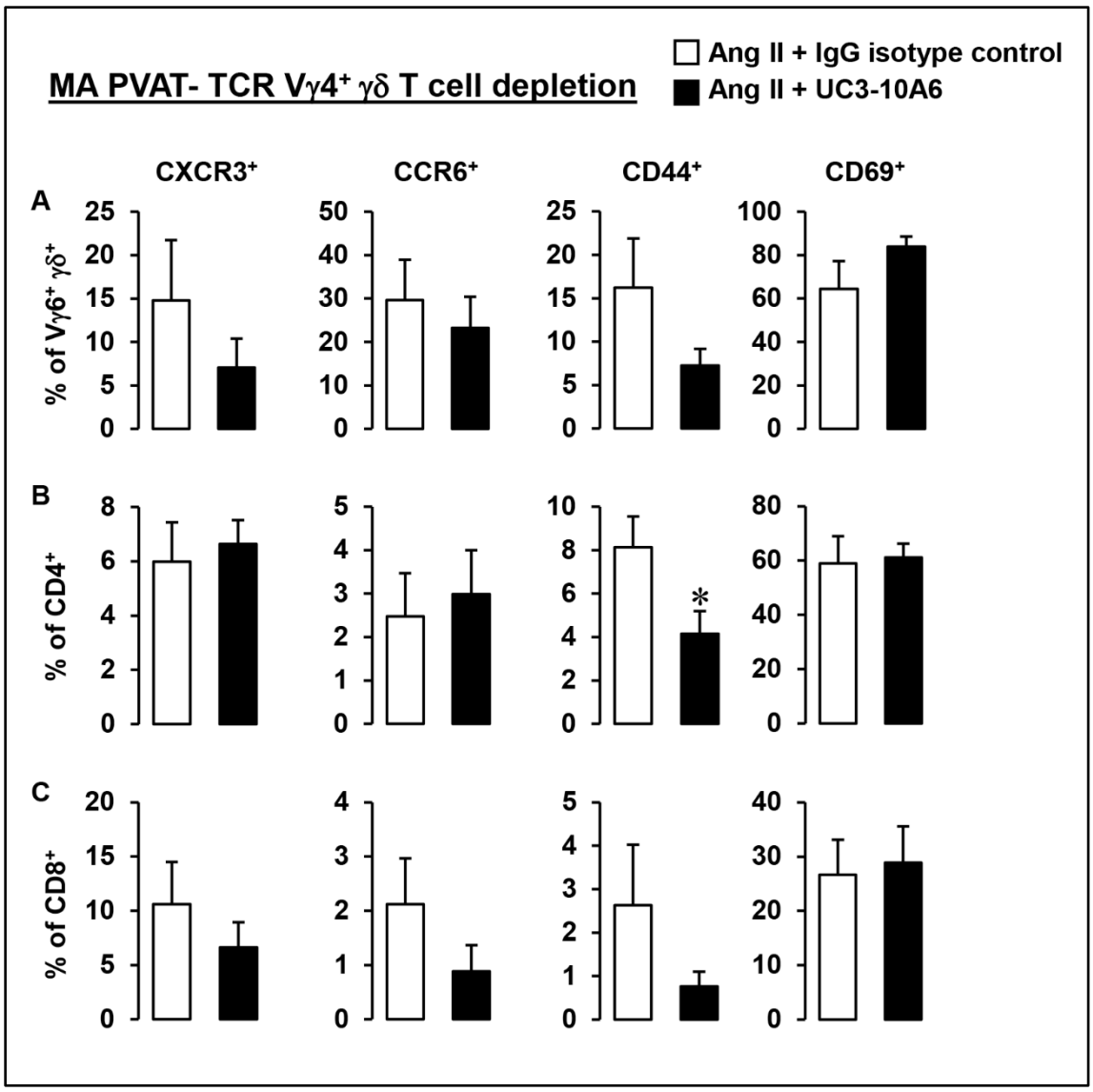

Figure V-2: Depletion of Vγ4$^+$ γδ T cells with anti-TCR Vγ4 (UC3-10A6) antibodies decreased the frequency of CD44$^+$CD4$^+$ T cells in the MA PVAT after 14 days of Ang II infusion. The frequency (% of Vγ6$^+$ γδ T cells) of IFN-γ-producing (CXCR3$^+$), IL-17-producing (CCR6$^+$), memory (CD44$^+$), and activated (CD69$^+$) Vγ6$^+$ γδ T cells (**A**) , the frequency (% of CD4$^+$ T cells) of CXCR3$^+$, CCR6$^+$, CD44$^+$, and CD69$^+$ CD4$^+$ T cells (**B**), and the frequency (% of CD8$^+$ T cells) of CXCR3$^+$, CCR6$^+$, CD44$^+$, and CD69$^+$ CD8$^+$ T cells (**C**) in the mesenteric artery with perivascular adipose tissue (MA PVAT) of wild-type (WT) mice infused with Ang II (490ng/kg/min) and injected with IgG isotype control or anti-TCR Vγ4 (UC3-10A6) antibodies

were determined by flow cytometry. Data are presented as means±SEM, n= 6-7. Data were analyzed using unpaired *t*-test. **P*<0.01 versus respective IgG isotype control antibodies.

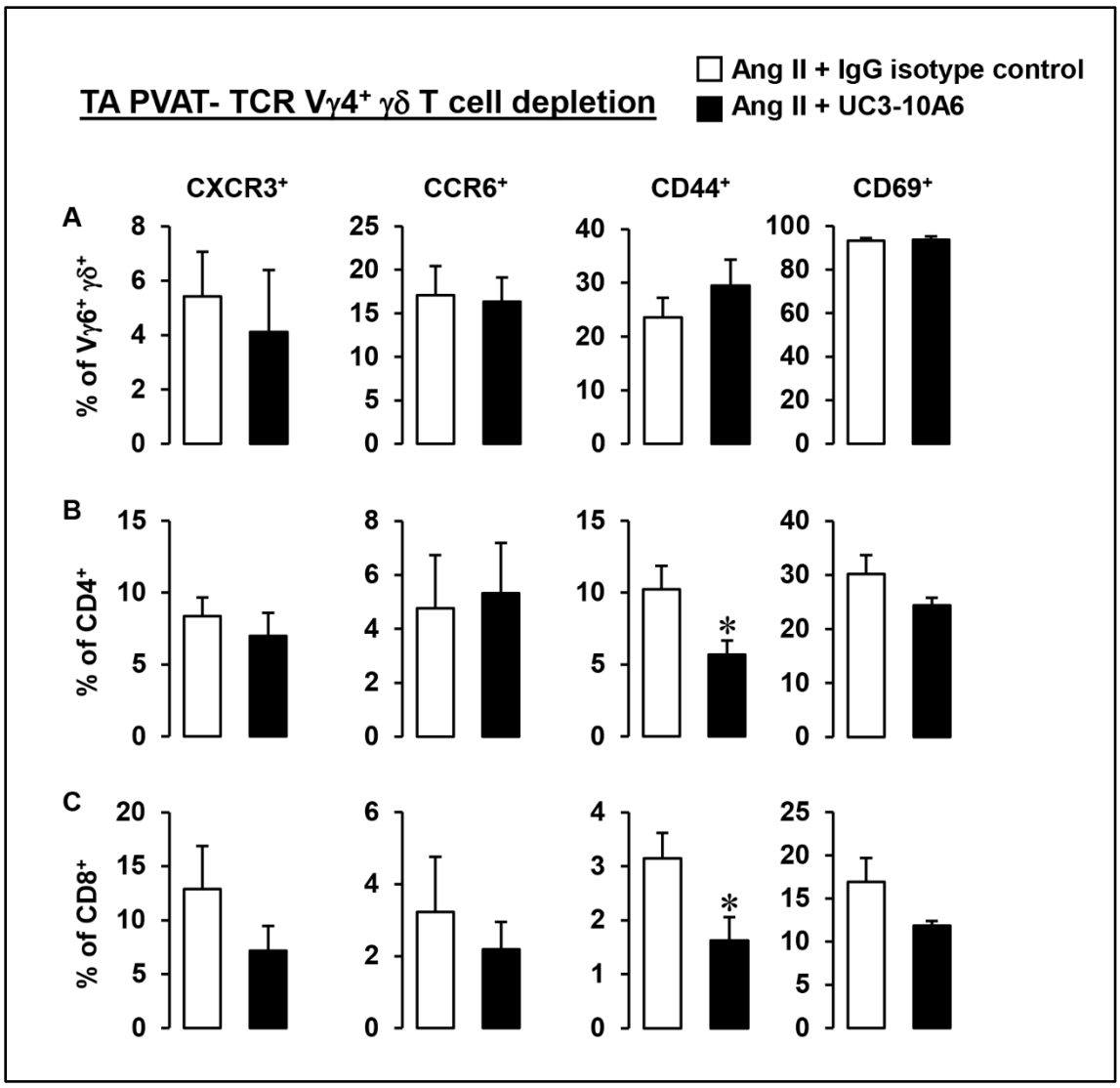

Figure V-3: Depletion of Vγ4$^+$ γδ T cells reduced the frequency of CD44$^+$CD4$^+$ and CD44$^+$CD8$^+$ T cells in the TA PVAT after 14 days of Ang II infusion. The frequency (% of Vγ6$^+$ γδ T cells) of IFN-γ-producing (CXCR3$^+$), IL-17-producing (CCR6$^+$), memory (CD44$^+$), and activated (CD69$^+$) Vγ6$^+$ γδ T cells (**A**) , the frequency (% of CD4$^+$ T cells) of CXCR3$^+$, CCR6$^+$, CD44$^+$, and CD69$^+$ CD4$^+$ T cells (**B**), and the frequency (% of CD8$^+$ T cells) of CXCR3$^+$, CCR6$^+$, CD44$^+$, and CD69$^+$ CD8$^+$ T cells (**C**) in the thoracic aorta with perivascular adipose tissue (TA PVAT) of wild-type (WT) mice infused with Ang II (490ng/kg/min) and injected with IgG isotype control or anti-TCR Vγ4 (UC3-10A6) antibodies were determined by flow cytometry. Data are

presented as means±SEM, n= 6-7. Data were analyzed using unpaired *t*-test. **P*<0.05 versus respective IgG isotype control antibodies.

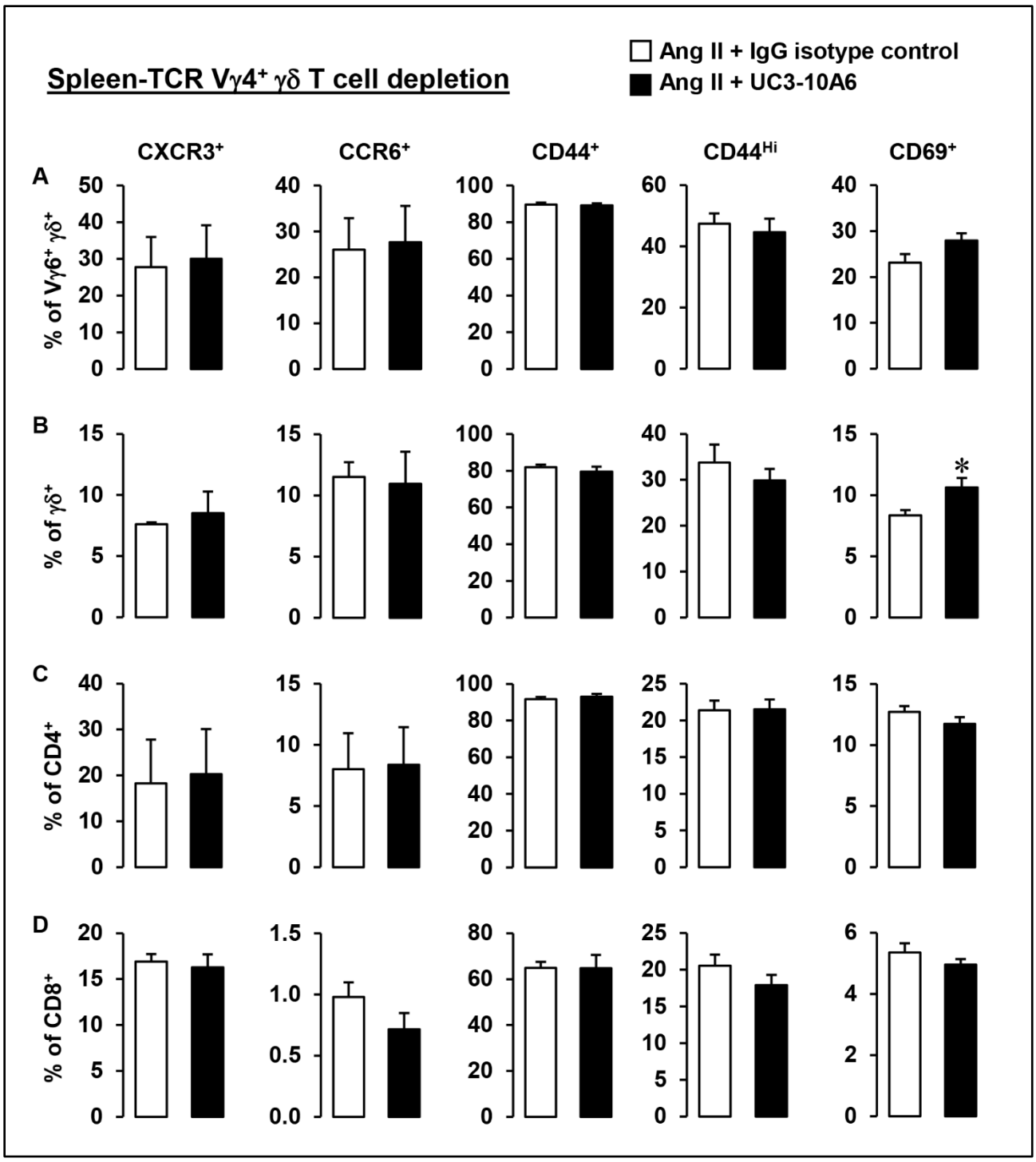

Figure V-4: Vγ4$^+$ γδ T cell depletion increased the activation of γδ T cells in the spleen of mice infused with Ang II for 14 days. The frequency (% of Vγ6$^+$ γδ T cells) of IFN-γ-producing (CXCR3$^+$), IL-17-producing (CCR6$^+$), memory (CD44$^+$ and CD44^{Hi}), and activated (CD69$^+$) Vγ6$^+$ γδ T cells (**A**), the frequency (% of γδ T cells) of CXCR3$^+$, CCR6$^+$, CD44$^+$, CD44^{Hi} and CD69$^+$ γδ

T cells (**B**), the frequency (% of $CD4^+$ T cells) of $CXCR3^+$, $CCR6^+$, $CD44^+$, $CD44^{Hi}$, and $CD69^+$ $CD4^+$ T cells (**C**), and the frequency (% of $CD8^+$ T cells) of $CXCR3^+$, $CCR6^+$, $CD44^+$, $CD44^{Hi}$, and $CD69^+$ $CD8^+$ T cells (**D**) in the spleen of wild-type (WT) mice infused with Ang II (490ng/kg/min) and injected with IgG isotype control or anti-TCR Vγ4 (UC3-10A6) antibodies were determined by flow cytometry. Data are presented as means±SEM, n= 6-7. Data were analyzed using unpaired *t*-test. **P*<0.05 versus respective IgG isotype control antibodies.

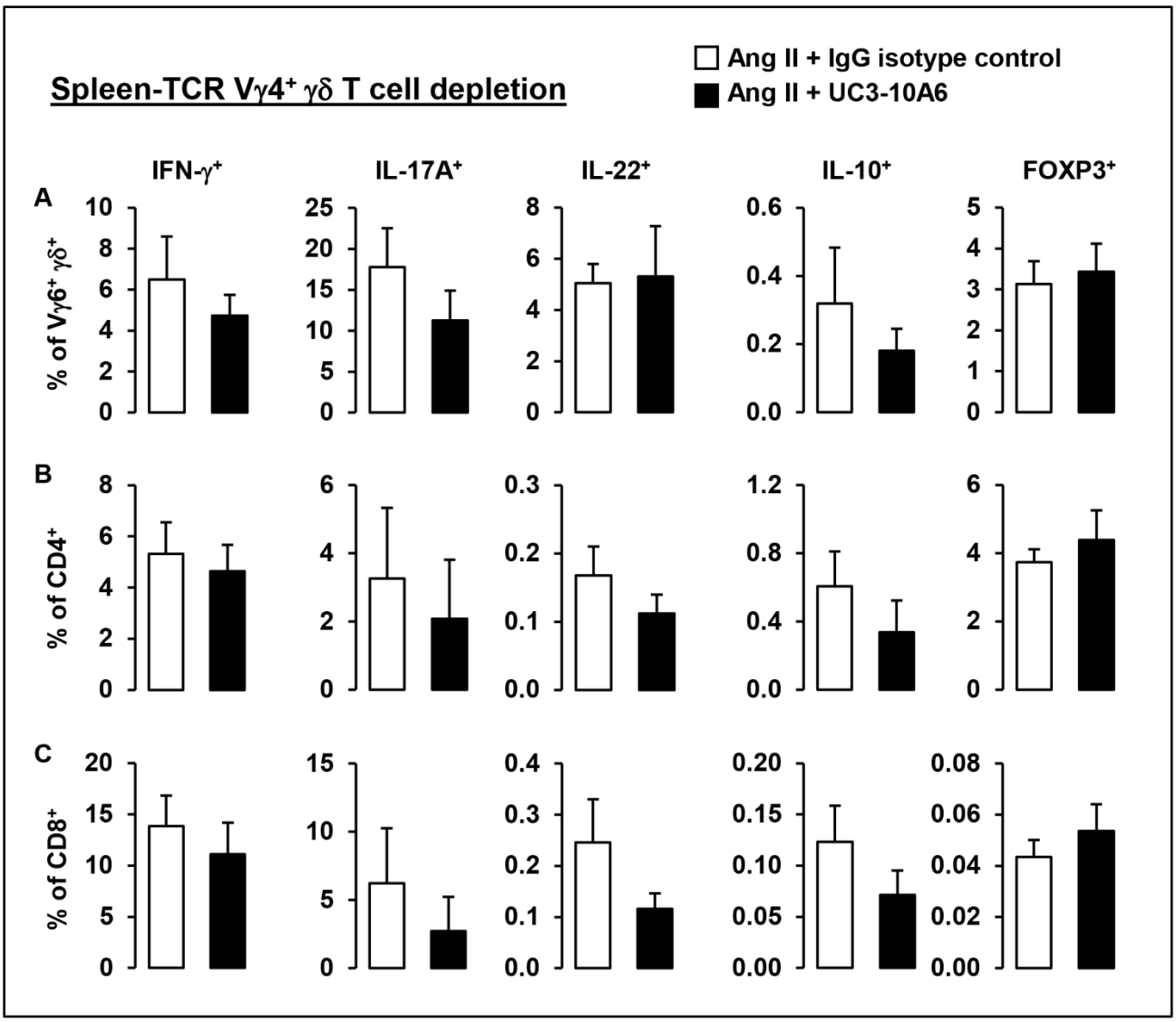

Figure V-5: Phenotyping of T cell subsets in the spleen after Vγ4$^+$ γδ T cell depletion and 14 days of Ang II infusion using intracellular markers showed no changes. The frequency (% Vγ6$^+$ γδ T cells) of IFN-γ-producing (IFN-γ$^+$) and IL-17A-producing (IL-17A$^+$ and IL-22$^+$), and anti-inflammatory (IL-10$^+$ and FOXP3$^+$) Vγ6$^+$ γδ T cells (**A**), the frequency (% of CD4$^+$ T cells) of IFN-γ$^+$, IL-17A$^+$, IL-22$^+$, IL-10$^+$, and FOXP3$^+$ CD4$^+$ T cells (**B**), and the frequency (% of CD8$^+$ T cells) of IFN-γ$^+$, IL-17A$^+$, IL-22$^+$, IL-10$^+$, and FOXP3$^+$ CD8$^+$ T cells (**C**) in the spleen of wild-type (WT) mice infused with Ang II (490ng/kg/min) and injected with IgG isotype control or anti-

TCR Vγ4 (UC3-10A6) antibodies were determined by flow cytometry. Data are presented as means±SEM, n= 7-9.

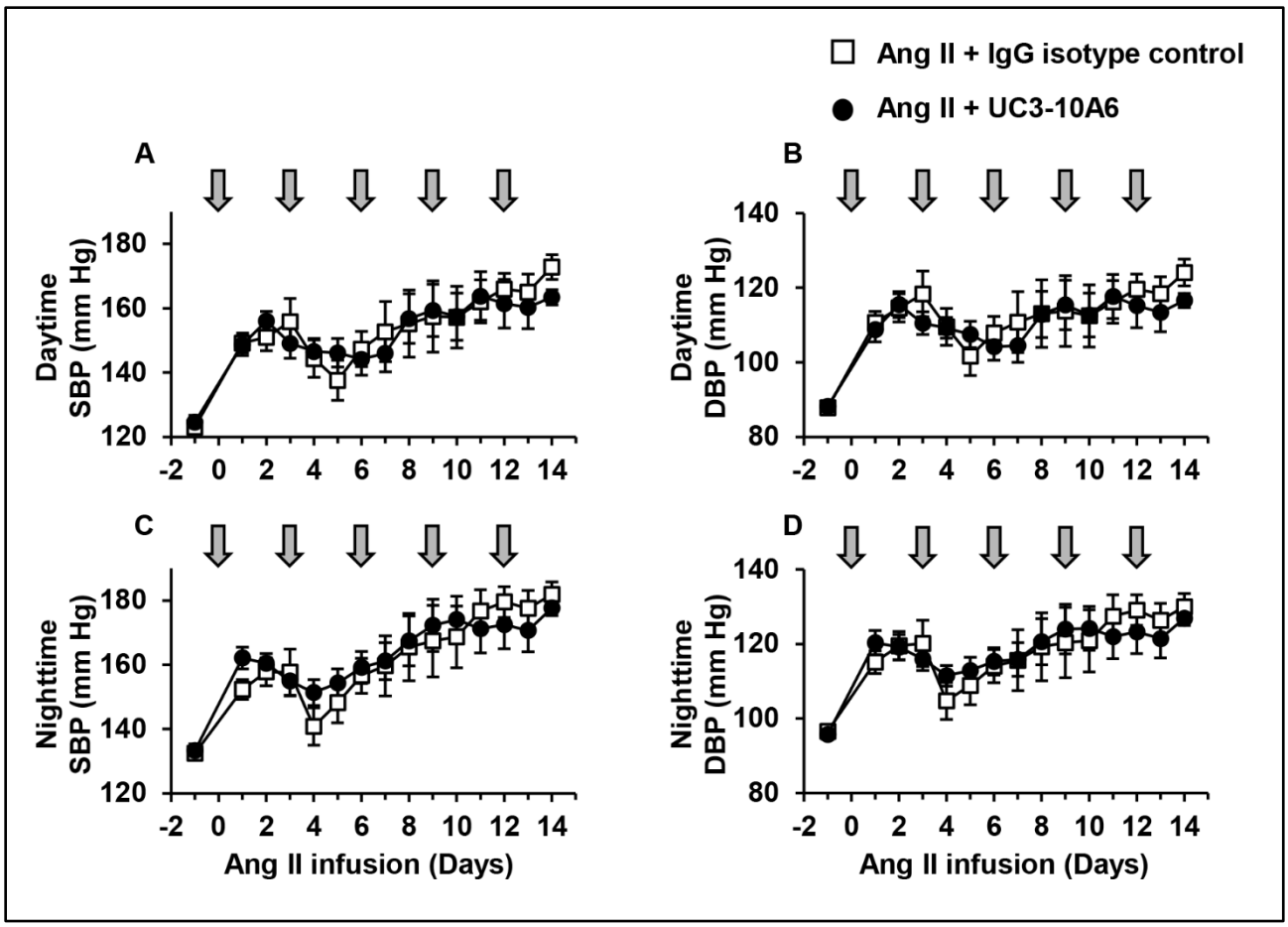

Figure V-6: Depletion of Vγ4$^+$ γδ T cells did not affect Ang II-induced BP rise. Telemetry systolic BP (SBP, at daytime **A** and nighttime **C**) and diastolic BP (DBP, at daytime **B** and nighttime **D**) were determined in wild-type (WT) mice infused with Ang II and injected with IgG isotype control or anti-TCR Vγ4 (UC3-10A6) antibodies. Gray arrows indicate antibody injection days. Data are presented as means±SEM, n= 5-6. Data were analyzed using a two-way analysis of variance (ANOVA) with repeated measures.

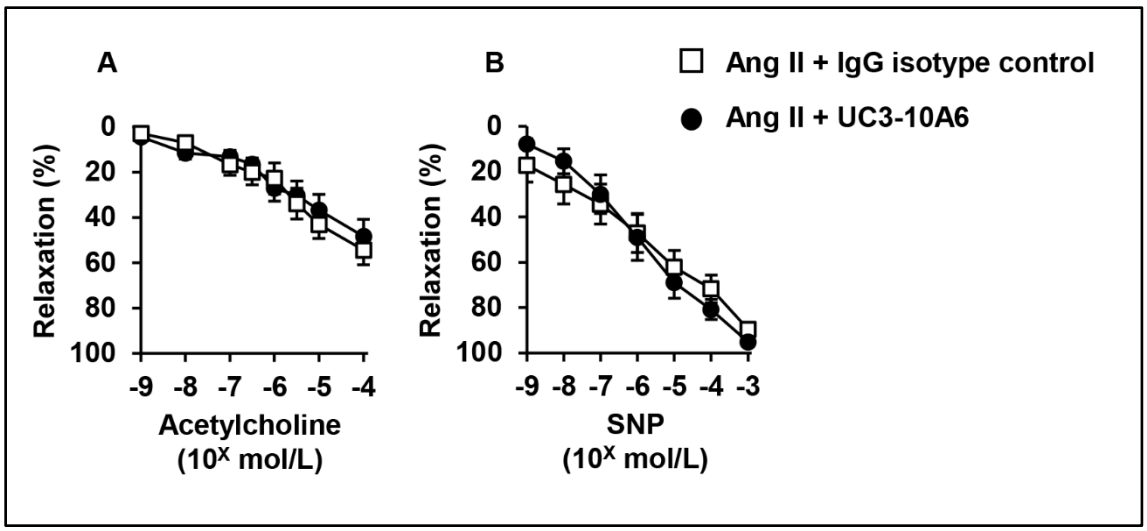

Figure V-7: Vγ4^{+} γδ T cell did not affect either Ang II-induced mesenteric artery (MA) endothelial dysfunction or endothelium-independent relaxation. MA dilatory responses to acetylcholine (**A**) and to sodium nitroprusside (SNP, **B**) were determined in wild-type (WT) mice infused with Ang II and injected with IgG isotype control or anti-TCR Vγ4 (UC3-10A6) antibodies. Data are presented as means±SEM, n= 9-10.

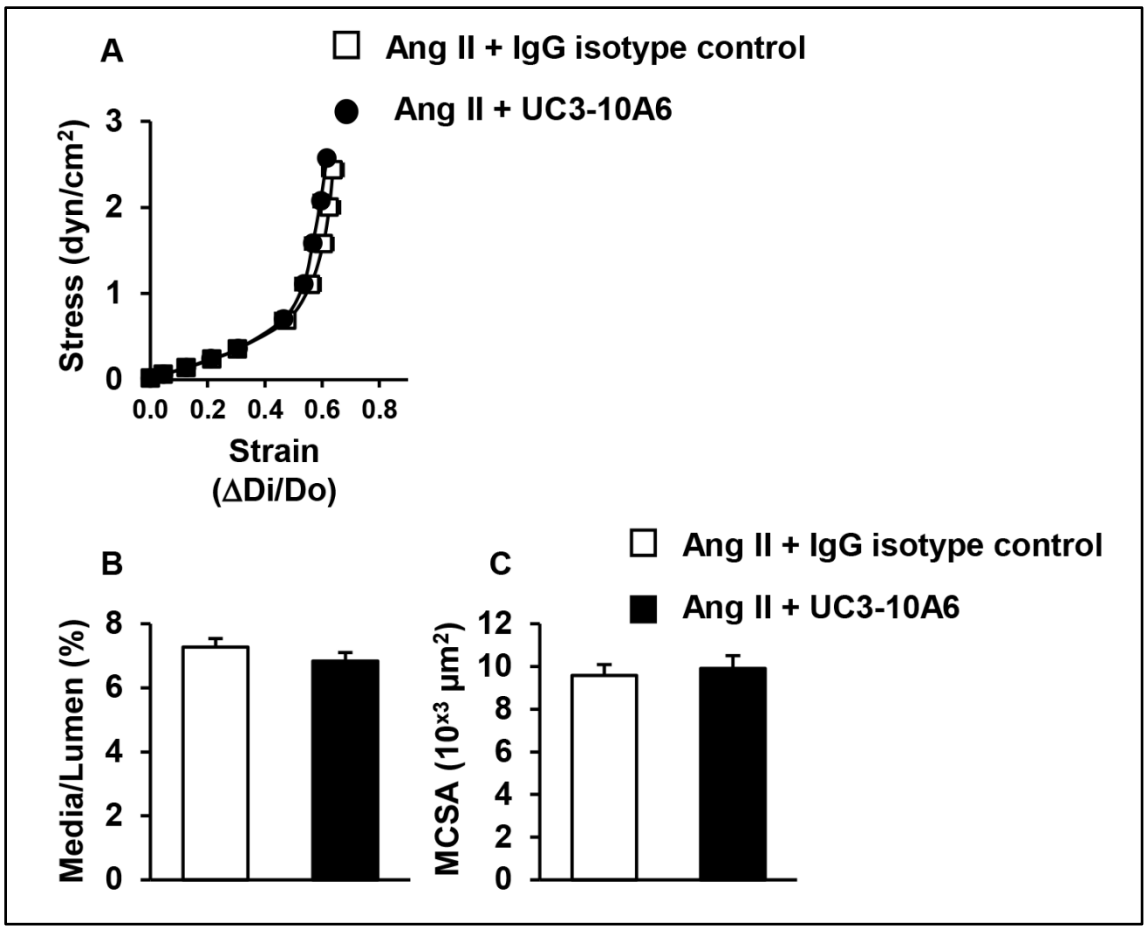

Figure V-8: Depletion of Vγ4$^+$ γδ T cells did not affect mesenteric artery (MA) mechanical and structural properties. MA media stress-strain relationship (**A**), media-to-lumen ratio (**B**), and media cross-sectional area (MCSA, **C**) were determined in wild-type (WT) mice infused with Ang II and injected with IgG isotype control or anti-TCR Vγ4 (UC3-10A6) antibodies. Data are presented as means±SEM, n= 8-10.

CHAPTER VI: Discussion

12. Discussion

The first study in this thesis demonstrated a differential distribution of γδ T cell variant γ subtypes in lymphoid tissues (spleen and MLNs) compared to PVATs (TA and MA). Vγ6$^+$ γδ T cells were the most abundant γδ T cell variant γ subtype in both MA and TA PVAT and their frequency was increased by Ang II infusion in TA PVAT and the spleen and tended to augment in MA PVAT. Extending these findings, the second study indicated that the immunophenotyping of Vγ6$^+$ γδ T cells by flow cytometry showed a different expression of markers in the spleen compared to MA and TA PVAT. In the spleen, Vγ6$^+$ γδ T cells produced mostly IFN-γ. Vγ6$^+$ γδ T cells were directed toward IL-17A production in MA PVAT, whereas they produced IFN-γ and/or IL-17A in TA PVAT. Vγ6$^+$ γδ T cells were highly activated in MA and TA PVAT compared to the spleen. Infusion of Ang II increased the activation of Vγ6$^+$ γδ T cells and the frequency of IFN-γ-producing Vγ6$^+$ γδ T cells in the spleen but reduced the frequency of IFN-γ-producing Vγ6$^+$ γδ T cells in TA PVAT. Unexpectedly, blocking of Vγ6$^+$ γδ T cells enhanced the early BP elevation and reduced the MA dilatory response to acetylcholine in Ang II-infused mice, suggesting that Vγ6$^+$ γδ T cells play a protective role in Ang II-induced HTN and vascular dysfunction. The third study revealed that depletion of Vγ4$^+$ γδ T cells did not affect Ang II-induced BP elevation or vascular injury in mice.

12.1. Distribution of γδ T cell subsets in lymphoid tissues and PVATs

At the beginning of the first study, we were unable to determine the distribution of γδ T cell variant γ subtypes that induce and expand in MA PVAT, TA PVAT, the spleen, and/or MLNs

in response to Ang II using flow cytometry because not all antibodies specific for γδ T cell variant γ subtypes were available at the time. Instead, we attempted to profile all γδ T cell variant γ subtypes using RT-qPCR. However, we were only able to validate oligonucleotide primers for 3 of 7 variant γ subtypes (*Trgv2*, *Tcrg-v4,* and *Tcrg-v5*) using RNA isolated from thymus, MA PVAT, intestine, and/or skin. The lack of success in validating some oligonucleotide primers could be due to defective design or very low levels of expression of these genes in the studied tissues. Meanwhile, we succeed in obtaining the majority of TCR Vγ antibodies except anti-TCR Vγ3 antibody (Heilig & Tonegawa's nomenclature). Anti-mouse TCR Vγ1/2^{+}, 4^{+}, and 5^{+} antibodies were commercially available. TCR Vγ6^{+} (17D1[541] and 1C10-1F7[490]) and Vγ7^{+} (F2.67[542]) antibodies were obtained from collaborators. We therefore decided to use flow cytometry to determine the distribution of γδ T cell variant γ subtypes in selected tissues.

γδ T cells are more abundant across several adipose tissues than in peripheral non-adipose tissues, including the spleen, lung, and blood.[493] In our study, the phenotyping of γδ T cell variant γ subtypes revealed a differential distribution of γδ T cell variant γ subtypes in the spleen and MLNs compared to MA and TA PVAT. In both types of PVAT, Vγ6^{+} γδ T cells were the most abundant γδ T cell variant γ subtype, followed by Vγ4^{+} γδ T cells, whereas Vγ1/2^{+} γδ T cells were the most abundant γδ T cell variant γ subtypes in the spleen and MLNs, followed by Vγ4^{+} γδ T cells. It should be noted that the antibody used to detect Vγ1/2^{+} γδ T cells was unable to distinguish between Vγ1^{+} and Vγ2^{+}γδ T cell subtypes. Vγ6^{+} γδ T cells were the only γδ T cell variant γ subtype that was increased upon Ang II infusion in TA PVAT and the spleen and tended to augment in MA PVAT.

Paget *et al*. identified a CD3^{bright} γδ T cell subset, which is a small sub-population of γδ T cells, with an effector memory phenotype. These cells rapidly produce IL-17A, but not IFN-γ, and respond promptly and strongly to pneumococcal infection and in the course of skin inflammation. They also showed by using single cell sequencing that lung CD3^{bright} γδ T cells were Vγ6^{+}Vδ1^{+} T cells.[491] In agreement with these findings, we found that CD3^{bright} γδ T cells were increased in the spleen and MA PVAT after infusion of Ang II for 14 days. Caillon *et al.* demonstrated with work in our laboratory a role for γδ T cells in Ang II induced-HTN, vascular injury, and T cell activation using *Tcrδ* null (TCRδ$^{-/-}$) mice, which are devoid of γδ T cells, and in WT mice injected with a γδ T cell-depleting antibodies.[9] However, γδ T cell subtype(s) involved in HTN is/are still unknown. Therefore, we intially hypothesized that Vγ6^{+} γδ T cells are the γδ T cell variant γ subtype that may play a role in the development of Ang II-induced HTN and vascular injury in mice.

12.2. The role of Vγ6^{+} γδ T cells in Ang II-induced HTN and vascular injury

The immunophenotyping of Vγ6^{+} γδ T cells revealed a different expression of markers in the spleen compared to MA and TA PVAT. In the spleen, Vγ6^{+} γδ T cells mostly produced IFN-γ. On the other hand, Vγ6^{+} γδ T cells were directed toward IL-17A production in MA PVAT, whereas they produced IFN-γ and/or IL-17A in TA PVAT. Furthermore, Vγ6^{+} γδ T cells were highly activated in both MA and TA PVAT compared to the spleen. Infusion of Ang II for 14 days increased the activation of Vγ6^{+} γδ T cells and the frequency of IFN-γ-producing Vγ6^{+} γδ T cells in the spleen but reduced the frequency of IFN-γ-producing Vγ6^{+} γδ T cells in TA PVAT. These

results are in agreement with the findings of Caillon *et al.* since they demonstrated that a 14-day Ang II infusion increased the frequency of activated γδ T cells in the spleen.[9] In addition, we also found that IL-17A-producing effector memory ($CCR6^+CXCR3^-CD44^+CD69^+$) $V\gamma6^+$ γδ T cell frequency was increased in the spleen and tended to be augmented in MA PVAT upon Ang II-infusion. Altogether, these results demonstrate that infusion of Ang II for two weeks has changed the activation and the expression profile of IL-17A and IFN-γ of $V\gamma6^+$ γδ T cells in lymphoid tissues and/or PVATs.

We isolated sufficient amounts of highly purified rat IgM anti-mouse TCR Vγ6 (17D1) and mouse IgG1 anti-mouse TCR Vγ6 (1C10-1F7) antibodies for flow cytometry phenotyping and blocking experiments. We tried to couple the purified antibodies with R-PE and AF647 fluorochromes, respectively, to reduce the background noise in the study of $V\gamma6^+$ γδ T cells by flow cytometry. However, the efficiency of these coupled antibodies in determining $V\gamma6^+$ γδ T cells was reduced compared with the uncoupled antibodies revealed with secondary antibodies. This could be a result of blocking the antigen binding site on the antibody surface by the fluorochrome used for coupling. Interestingly, doubling the number of washes with 1X PBS after primary and secondary antibody staining significantly improved the efficiency of both antibodies in detecting $V\gamma6^+$ γδ T cells and clearly reduced the background noise caused by the secondary antibody.

We demonstrated in the first study that $V\gamma6^+$ γδ T cells constitute the majority of the γδ T cell population in MA and TA PVAT. It has been shown that γδ T cells are an important source of IL-17A production in several adipose tissues.[493] Many studies have demonstrated that Ang II- and DOCA-salt-induced HTN and vascular dysfunction are associated with increased IL-17A

production.[348-350] [543] Madhur *et al.* have shown that IL-17A knockout mice (*IL-17a*$^{-/-}$) infused with Ang II for 4 weeks displayed a reduced maintenance of high BP, vascular dysfunction, and aortic T cell infiltration.[348] In addition, Caillon *et al.* demonstrated that Ang II-induced BP elevation, MA endothelial dysfunction, and spleen and MA PVAT T cell activation were blunted in mice deficient in γδ T cells due to *Tcrδ* knockout or injection of γδ T cell-depleting antibodies.[9] Consequently, we initially hypothesized that blockade of Vγ6^{+} γδ T cells using anti-mouse TCR Vγ6 (1C10-1F7) antibodies will blunt Ang II-induced BP elevation and vascular injury.

Unexpectedly, and contrary to our initial hypothesis, Vγ6^{+} γδ T cell blockade enhanced Ang II-induced early systolic and diastolic BP elevation. Furthermore, blocking of Vγ6^{+} γδ T cells reduced the MA dilatory response to acetylcholine compared to control Ang II-infused mice. Investigation of IL-17A and IFN-γ-producing T cells after 14 days of Ang II treatment and blockade of Vγ6^{+} γδ T cells indicated that the frequency of IL-17A-producing Vγ6^{-} γδ T cells decreased in MA and TA PVAT, whereas the frequency of IFN-γ-producing CD8^{+} T cells tended to increase in the spleen. Many studies have demonstrated a role of IFN-γ in the initiation and progression of HTN and end-organ inflammation. Kossmann *et al.* found that knockout of IFN-γ (*IFN-γ*$^{-/-}$) in mice infused for 7 days with a high dose of Ang II (1000ng/kg/min) attenuated Ang II-induced vascular dysfunction independently of BP alterations, whereas IFN-γ overexpression induced endothelial dysfunction in the absence of Ang II.[336] In another study, Han *et al.* demonstrated that IFN-γ-knockout mice infused with a higher dose of Ang II (1500ng/kg/min) for 7 days did not show any difference in BP elevation compared with WT control mice infused with the same dose of Ang II. However, these mice displayed a reduction in the cardiac infiltration of T cells and macrophages.[544] Marko *et al.* showed that deficiency of the IFN-γ receptor resulted in

protection from cardiac hypertrophy and infiltration of T cells and macrophages into the heart and a tendency to exhibit reduced mean arterial BP elevation in mice upon Ang II (1000ng/kg/min) administration for 14 days.[545] Kamat *et al.* observed that IFN-γ-deficient mice (IFN-$\gamma^{-/-}$) treated for 14 days with a moderate dose of Ang II (490ng/kg/min), which is similar to the dosage in our study, exhibited a blunted systolic BP elevation and maintained baseline renal functions in response to a saline challenge.[546] Another study done by Mikolajczyk *et al.* demonstrated endothelial dysfunction in the aorta after incubation with IFN-γ. They also reported that Ang II infusion elevated the production of IFN-γ from $CD8^+$ T cells and double-negative T cells in PVAT.[547] Accordingly, the exaggeration in Ang II-induced early BP elevation and endothelial dysfunction that was observed in our study in mice treated with anti-TCR Vγ6-blocking antibodies is likely attributable in part to the increase in IFN-γ-producing T cells, which in turn affected the balance between IFN-γ and IL-17A that is important for BP regulation. Investigation of IL-17A and IFN-γ-producing T cells after 7 days of Ang II treatment and blockade of $V\gamma6^+$ γδ T cells would provide a better insight into this paradigm because the pathophysiological effect of $V\gamma6^+$ γδ T cell blockade on BP elevation and endothelial function occurred during the first week of Ang II infusion.

12.3. The role of $V\gamma4^+$ γδ T cells in Ang II-induced HTN and vascular injury

In the first study, we showed that $V\gamma4^+$ γδ T cells were the second most abundant γδ T cell variant γ subtype in studied PVATs and lymphoid tissues. It has been demonstrated that $V\gamma4^+$ γδ T cells have the capacity to produce both IL-17A[498] and IFN-γ[548], which are key players in regulating BP elevation. However, our results revealed that depletion of $V\gamma4^+$ γδ T cells did not

affect Ang II-induced BP elevation or MA endothelial dysfunction. Depletion of $V\gamma4^+$ γδ T cells decreased the frequency of memory $CD4^+$ T cells in MA and TA PVAT, but it did not affect IL-17A- or IFN-γ-producing T cells in all studied tissues after 14 days of Ang II infusion. In mice treated with anti-TCR Vγ4-depleting antibodies, longer exposure to Ang II may be required to observe an increase in IL-17A-producing T cells in PVAT as reported in the kidney and aorta after 4 weeks of Ang II adminstration.[543] Interestingly, Mehta *et al.* demonstrated that mice deficient in all γδ T cells ($TCR\delta^{-/-}$) or only two γδ T cell variant γ subtypes, $V\gamma4^+$ and $V\gamma6^+$ γδ T cells ($V\gamma4/6^{-/-}$), are protected from obesity-induced macrophage accumulation and inflammation in PVAT.[549] Therefore, more studies are required to investigate the role of the absence of both $V\gamma4^+$ and $V\gamma6^+$ γδ T cells in Ang II-induced BP elevation and vascular injury.

13. Challenges and limitations

There were challenges and limitations that we encountered during our studies in this thesis. Dissecting MA PVAT exempt of MLNs from the mesenteric bed was challenging due to the random distribution of MLNs embedded within the PVAT and the difficulty of distinguishing them from the fat, which may be a source of contamination. Similar difficulty was also encountered with TA PVAT. The majority of MLNs are located very close to the pancreas. Damage to the pancreas could cause spreading of pancreatic digestive enzymes that may affect the intigerity of MLN cells. Another challenge, coupling rat IgM anti-mouse TCR Vγ6 and mouse IgG1 anti-mouse TCR Vγ6 antibodies with R-PE and AF647 fluorochromes, respectively, had a detrimental effect compared with the uncoupled antibodies revealed with secondary antibodies. This could be a result of blocking the antigen binding site on the antibody surface by the fluorochrome used for coupling. Increasing the number of washes with 1X PBS clearly improved the efficiency of both antibodies in detecting $V\gamma6^+$ γδ T cells by reducing the background noise caused by the secondary antibodies. Furthermore, choosing the optimal fluorochrome combinations for the multicolor flow cytometry panel with few cell numbers to reduce background noise as much as possible was challenging.

In the second study of $V\gamma6^+$ γδ T cell blockade, investigation of IL-17A- and IFN-γ-producing T cells was conducted after 14 days of Ang II infsion and $V\gamma6^+$ γδ T cell blockade. It could be more informative to investigate these phenotypes after 7 days because alterations in Ang II-induced BP elevation happened only during the first week of Ang II infusion and $V\gamma6^+$ γδ T cell blockade. Finally, in the third study of $V\gamma4^+$ γδ T cell depletion, longer exposure to Ang II may be required to observe an increase in IL-17A-producing T cells in PVAT as reported in the kidney and aorta after 4 weeks of Ang II adminstration.[543]

14. Conclusions and perspectives

We have previously demonstrated a role for γδ T cells in Ang II-induced HTN, vascular injury, and T cell activation.[9] The first study of this thesis showed a differential distribution of γδ T cell Vγ subtypes in lymphoid tissues (spleen and MLNs) compared to PVAT (TA and MA). Vγ6$^+$ γδ T cells were the most abundant γδ T cell Vγ subtype in both TA and MA PVAT and their frequency was increased by Ang II infusion in the spleen and TA PVAT and tended to augment in MA PVAT. The second study indicated that the immunophenotyping of Vγ6$^+$ γδ T cells showed that they mostly produced IFN-γ in the spleen. Vγ6$^+$ γδ T cells were directed toward IL-17A production in MA PVAT, whereas they produced IFN-γ and/or IL-17A in TA PVAT. Moreover, the frequency of IL-17A-producing effector memory Vγ6$^+$ γδ T cells was increased in the spleen and tended to be elevated in MA PVAT in Ang II-infused mice compared to control mice. Vγ6$^+$ γδ T cells were highly activated in MA and TA PVAT compared to the spleen. Infusion of Ang II increased the activation of Vγ6$^+$ γδ T cells and the frequency of IFN-γ-producing Vγ6$^+$ γδ T cells in the spleen but reduced the frequency of IFN-γ-producing Vγ6$^+$ γδ T cells in TA PVAT. Unexpectedly, the blockade of Vγ6$^+$ γδ T cells enhanced the early BP elevation and reduced the MA dilatory response to acetylcholine in Ang II-infused mice, suggesting that Vγ6$^+$ γδ T cells play a protective role in Ang II-induced HTN and vascular dysfunction. Activation of Vγ6$^+$ γδ T cells could surprisingly be a therapeutic approach to control inflammation in Ang II-induced HTN. The third study revealed that depletion of Vγ4$^+$ γδ T cells did not affect Ang II-induced BP elevation or vascular injury in mice. The studies of this thesis allowed an increased understanding of the role of immunity in experimental HTN. Understanding the role of specific subsets of γδ T cells in

modulating immune responses could help identify biomarkers of interest or design treatments to limit the progression of HTN and vascular damage.

References

1. Diseases GBD, Injuries C. Global burden of 369 diseases and injuries in 204 countries and territories, 1990-2019: a systematic analysis for the Global Burden of Disease Study 2019. *Lancet* 2020;396(10258):1204-22. doi: 10.1016/S0140-6736(20)30925-9 [published Online First: 2020/10/19]
2. Higaki A, Caillon A, Paradis P, et al. Innate and Innate-Like Immune System in Hypertension and Vascular Injury. *Curr Hypertens Rep* 2019;21(1):4. doi: 10.1007/s11906-019-0907-1 [published Online First: 2019/01/20]
3. De Ciuceis C, Amiri F, Brassard P, et al. Reduced vascular remodeling, endothelial dysfunction, and oxidative stress in resistance arteries of angiotensin II-infused macrophage colony-stimulating factor-deficient mice: evidence for a role in inflammation in angiotensin-induced vascular injury. *Arterioscler Thromb Vasc Biol* 2005;25(10):2106-13. doi: 10.1161/01.ATV.0000181743.28028.57 [published Online First: 2005/08/16]
4. Heptinstall RH. Renal biopsies in hypertension. *Br Heart J* 1954;16(2):133-41. doi: 10.1136/hrt.16.2.133 [published Online First: 1954/04/01]
5. Muller DN, Shagdarsuren E, Park JK, et al. Immunosuppressive treatment protects against angiotensin II-induced renal damage. *Am J Pathol* 2002;161(5):1679-93. doi: 10.1016/S0002-9440(10)64445-8 [published Online First: 2002/11/05]
6. Guzik TJ, Hoch NE, Brown KA, et al. Role of the T cell in the genesis of angiotensin II induced hypertension and vascular dysfunction. *J Exp Med* 2007;204(10):2449-60. doi: 10.1084/jem.20070657 [published Online First: 2007/09/19]
7. Marvar PJ, Thabet SR, Guzik TJ, et al. Central and peripheral mechanisms of T-lymphocyte activation and vascular inflammation produced by angiotensin II-induced hypertension. *Circ Res* 2010;107(2):263-70. doi: 10.1161/CIRCRESAHA.110.217299 [published Online First: 2010/06/19]
8. Marvar PJ, Vinh A, Thabet S, et al. T lymphocytes and vascular inflammation contribute to stress-dependent hypertension. *Biol Psychiatry* 2012;71(9):774-82. doi: 10.1016/j.biopsych.2012.01.017 [published Online First: 2012/03/01]

9. Caillon A, Mian MOR, Fraulob-Aquino JC, et al. gammadelta T Cells Mediate Angiotensin II-Induced Hypertension and Vascular Injury. *Circulation* 2017;135(22):2155-62. doi: 10.1161/CIRCULATIONAHA.116.027058 [published Online First: 2017/03/24]
10. Aboyans V, Lacroix P, Criqui MH. Large and small vessels atherosclerosis: similarities and differences. *Prog Cardiovasc Dis* 2007;50(2):112-25. doi: 10.1016/j.pcad.2007.04.001 [published Online First: 2007/09/04]
11. Laurent S, Boutouyrie P. The structural factor of hypertension: large and small artery alterations. *Circ Res* 2015;116(6):1007-21. doi: 10.1161/CIRCRESAHA.116.303596 [published Online First: 2015/03/15]
12. Briet M, Schiffrin EL. Treatment of arterial remodeling in essential hypertension. *Curr Hypertens Rep* 2013;15(1):3-9. doi: 10.1007/s11906-012-0325-0 [published Online First: 2012/12/20]
13. Cooke JP. The endothelium: a new target for therapy. *Vasc Med* 2000;5(1):49-53. doi: 10.1177/1358836X0000500108 [published Online First: 2000/03/29]
14. Schiffrin EL. The endothelium and control of blood vessel function in health and disease. *Clin Invest Med* 1994;17(6):602-20. [published Online First: 1994/12/01]
15. Aird WC. Phenotypic heterogeneity of the endothelium: I. Structure, function, and mechanisms. *Circ Res* 2007;100(2):158-73. doi: 10.1161/01.RES.0000255691.76142.4a [published Online First: 2007/02/03]
16. Takeda A, Sasaki N, Miyasaka M. The molecular cues regulating immune cell trafficking. *Proc Jpn Acad Ser B Phys Biol Sci* 2017;93(4):183-95. doi: 10.2183/pjab.93.012 [published Online First: 2017/04/18]
17. Thurston G, Baldwin AL, Wilson LM. Changes in endothelial actin cytoskeleton at leakage sites in the rat mesenteric microvasculature. *Am J Physiol* 1995;268(1 Pt 2):H316-29. doi: 10.1152/ajpheart.1995.268.1.H316 [published Online First: 1995/01/01]
18. Lévy BI, Tedgui A. Morphologic Aspects of the Large Artery Vascular Wall. Biology of the arterial wall. Dordrecht ; Boston: Kluwer Academic 1999:xiv, 278 p.
19. Wagenseil JE, Mecham RP. Vascular extracellular matrix and arterial mechanics. *Physiol Rev* 2009;89(3):957-89. doi: 10.1152/physrev.00041.2008 [published Online First: 2009/07/09]

20. Jackson WF. Ion channels and vascular tone. *Hypertension* 2000;35(1 Pt 2):173-8. doi: 10.1161/01.hyp.35.1.173 [published Online First: 2000/01/21]
21. Joseph BK, Thakali KM, Moore CL, et al. Ion channel remodeling in vascular smooth muscle during hypertension: Implications for novel therapeutic approaches. *Pharmacol Res* 2013;70(1):126-38. doi: 10.1016/j.phrs.2013.01.008 [published Online First: 2013/02/05]
22. Martino F, Perestrelo AR, Vinarsky V, et al. Cellular Mechanotransduction: From Tension to Function. *Front Physiol* 2018;9:824. doi: 10.3389/fphys.2018.00824 [published Online First: 2018/07/22]
23. Garoffolo G, Pesce M. Vascular dysfunction and pathology: focus on mechanical forces. *Vasc Biol* 2021;3(1):R69-R75. doi: 10.1530/VB-21-0002 [published Online First: 2021/07/23]
24. Burton AC. Relation of structure to function of the tissues of the wall of blood vessels. *Physiol Rev* 1954;34(4):619-42. doi: 10.1152/physrev.1954.34.4.619 [published Online First: 1954/10/01]
25. Thiriet M. Physiology and Pathophysiology of Arterial Flow. In: Lanzer P, SpringerLink (Online service), eds. PanVascular Medicine2014.
26. Chiang HY, Korshunov VA, Serour A, et al. Fibronectin is an important regulator of flow-induced vascular remodeling. *Arterioscler Thromb Vasc Biol* 2009;29(7):1074-9. doi: 10.1161/ATVBAHA.108.181081 [published Online First: 2009/05/02]
27. Sandoo A, van Zanten JJ, Metsios GS, et al. The endothelium and its role in regulating vascular tone. *Open Cardiovasc Med J* 2010;4:302-12. doi: 10.2174/1874192401004010302 [published Online First: 2011/02/23]
28. Jadeja RN, Rachakonda V, Bagi Z, et al. Assessing Myogenic Response and Vasoactivity In Resistance Mesenteric Arteries Using Pressure Myography. *J Vis Exp* 2015(101):e50997. doi: 10.3791/50997 [published Online First: 2015/07/15]
29. Stenmark KR, Nozik-Grayck E, Gerasimovskaya E, et al. The adventitia: Essential role in pulmonary vascular remodeling. *Compr Physiol* 2011;1(1):141-61. doi: 10.1002/cphy.c090017 [published Online First: 2011/01/01]
30. Di Wang H, Ratsep MT, Chapman A, et al. Adventitial fibroblasts in vascular structure and function: the role of oxidative stress and beyond. *Can J Physiol Pharmacol* 2010;88(3):177-86. doi: 10.1139/Y10-015 [published Online First: 2010/04/16]

31. Virdis A, Duranti E, Taddei S. Oxidative Stress and Vascular Damage in Hypertension: Role of Angiotensin II. *Int J Hypertens* 2011;2011:916310. doi: 10.4061/2011/916310 [published Online First: 2011/07/13]
32. Kuwabara JT, Tallquist MD. Tracking Adventitial Fibroblast Contribution to Disease: A Review of Current Methods to Identify Resident Fibroblasts. *Arterioscler Thromb Vasc Biol* 2017;37(9):1598-607. doi: 10.1161/ATVBAHA.117.308199 [published Online First: 2017/07/15]
33. Martinez-Lemus LA. The dynamic structure of arterioles. *Basic Clin Pharmacol Toxicol* 2012;110(1):5-11. doi: 10.1111/j.1742-7843.2011.00813.x [published Online First: 2011/10/13]
34. Eble JA, Niland S. The extracellular matrix of blood vessels. *Curr Pharm Des* 2009;15(12):1385-400. doi: 10.2174/138161209787846757 [published Online First: 2009/04/10]
35. Wang M, Kim SH, Monticone RE, et al. Matrix metalloproteinases promote arterial remodeling in aging, hypertension, and atherosclerosis. *Hypertension* 2015;65(4):698-703. doi: 10.1161/HYPERTENSIONAHA.114.03618 [published Online First: 2015/02/11]
36. Cai Z, Gong Z, Li Z, et al. Vascular Extracellular Matrix Remodeling and Hypertension. *Antioxid Redox Signal* 2021;34(10):765-83. doi: 10.1089/ars.2020.8110 [published Online First: 2020/05/29]
37. Bouvet C, Gilbert LA, Girardot D, et al. Different involvement of extracellular matrix components in small and large arteries during chronic NO synthase inhibition. *Hypertension* 2005;45(3):432-7. doi: 10.1161/01.HYP.0000154680.44184.01 [published Online First: 2005/01/19]
38. van den Akker J, Schoorl MJ, Bakker EN, et al. Small artery remodeling: current concepts and questions. *J Vasc Res* 2010;47(3):183-202. doi: 10.1159/000255962 [published Online First: 2009/11/07]
39. Intengan HD, Schiffrin EL. Structure and mechanical properties of resistance arteries in hypertension: role of adhesion molecules and extracellular matrix determinants. *Hypertension* 2000;36(3):312-8. doi: 10.1161/01.hyp.36.3.312 [published Online First: 2000/09/16]

40. Jacob MP. Extracellular matrix remodeling and matrix metalloproteinases in the vascular wall during aging and in pathological conditions. *Biomed Pharmacother* 2003;57(5-6):195-202. doi: 10.1016/s0753-3322(03)00065-9 [published Online First: 2003/07/31]
41. Gabriela Espinosa M, Catalin Staiculescu M, Kim J, et al. Elastic Fibers and Large Artery Mechanics in Animal Models of Development and Disease. *J Biomech Eng* 2018;140(2) doi: 10.1115/1.4038704 [published Online First: 2017/12/10]
42. Debelle L, Tamburro AM. Elastin: molecular description and function. *Int J Biochem Cell Biol* 1999;31(2):261-72. doi: 10.1016/s1357-2725(98)00098-3 [published Online First: 1999/04/27]
43. Rosenbloom J, Abrams WR, Mecham R. Extracellular matrix 4: the elastic fiber. *FASEB J* 1993;7(13):1208-18. [published Online First: 1993/10/01]
44. Wolinsky H, Glagov S. Structural Basis for the Static Mechanical Properties of the Aortic Media. *Circ Res* 1964;14:400-13. doi: 10.1161/01.res.14.5.400 [published Online First: 1964/05/01]
45. Chow MJ, Turcotte R, Lin CP, et al. Arterial extracellular matrix: a mechanobiological study of the contributions and interactions of elastin and collagen. *Biophys J* 2014;106(12):2684-92. doi: 10.1016/j.bpj.2014.05.014 [published Online First: 2014/06/19]
46. Barnes MJ, Farndale RW. Collagens and atherosclerosis. *Exp Gerontol* 1999;34(4):513-25. doi: 10.1016/s0531-5565(99)00038-8 [published Online First: 2000/05/19]
47. Mayne R. Collagenous proteins of blood vessels. *Arteriosclerosis* 1986;6(6):585-93. doi: 10.1161/01.atv.6.6.585 [published Online First: 1986/11/01]
48. Shekhonin BV, Domogatsky SP, Muzykantov VR, et al. Distribution of type I, III, IV and V collagen in normal and atherosclerotic human arterial wall: immunomorphological characteristics. *Coll Relat Res* 1985;5(4):355-68. doi: 10.1016/s0174-173x(85)80024-8 [published Online First: 1985/09/01]
49. Labat-Robert J. Cell-matrix interactions, alterations with aging, involvement in angiogenesis. *Pathol Biol (Paris)* 1998;46(7):527-33. [published Online First: 1998/12/08]
50. Chothia C, Jones EY. The molecular structure of cell adhesion molecules. *Annu Rev Biochem* 1997;66:823-62. doi: 10.1146/annurev.biochem.66.1.823 [published Online First: 1997/01/01]

51. Liu Y, Sun Y, Hu C, et al. Perivascular Adipose Tissue as an Indication, Contributor to, and Therapeutic Target for Atherosclerosis. *Front Physiol* 2020;11:615503. doi: 10.3389/fphys.2020.615503 [published Online First: 2021/01/05]
52. Brown NK, Zhou Z, Zhang J, et al. Perivascular adipose tissue in vascular function and disease: a review of current research and animal models. *Arterioscler Thromb Vasc Biol* 2014;34(8):1621-30. doi: 10.1161/ATVBAHA.114.303029 [published Online First: 2014/05/17]
53. Pilkington AC, Paz HA, Wankhade UD. Beige Adipose Tissue Identification and Marker Specificity-Overview. *Front Endocrinol (Lausanne)* 2021;12:599134. doi: 10.3389/fendo.2021.599134 [published Online First: 2021/03/30]
54. Soltis EE, Cassis LA. Influence of perivascular adipose tissue on rat aortic smooth muscle responsiveness. *Clin Exp Hypertens A* 1991;13(2):277-96. doi: 10.3109/10641969109042063 [published Online First: 1991/01/01]
55. Huang Cao ZF, Stoffel E, Cohen P. Role of Perivascular Adipose Tissue in Vascular Physiology and Pathology. *Hypertension* 2017;69(5):770-77. doi: 10.1161/HYPERTENSIONAHA.116.08451 [published Online First: 2017/03/23]
56. Szasz T, Webb RC. Perivascular adipose tissue: more than just structural support. *Clin Sci (Lond)* 2012;122(1):1-12. doi: 10.1042/CS20110151 [published Online First: 2011/09/14]
57. Ramirez JG, O'Malley EJ, Ho WSV. Pro-contractile effects of perivascular fat in health and disease. *Br J Pharmacol* 2017;174(20):3482-95. doi: 10.1111/bph.13767 [published Online First: 2017/03/04]
58. Villacorta L, Chang L. The role of perivascular adipose tissue in vasoconstriction, arterial stiffness, and aneurysm. *Horm Mol Biol Clin Investig* 2015;21(2):137-47. doi: 10.1515/hmbci-2014-0048 [published Online First: 2015/02/27]
59. Hu H, Garcia-Barrio M, Jiang ZS, et al. Roles of Perivascular Adipose Tissue in Hypertension and Atherosclerosis. *Antioxid Redox Signal* 2021;34(9):736-49. doi: 10.1089/ars.2020.8103 [published Online First: 2020/05/12]
60. Szasz T, Bomfim GF, Webb RC. The influence of perivascular adipose tissue on vascular homeostasis. *Vasc Health Risk Manag* 2013;9:105-16. doi: 10.2147/VHRM.S33760 [published Online First: 2013/04/12]

61. Qi XY, Qu SL, Xiong WH, et al. Perivascular adipose tissue (PVAT) in atherosclerosis: a double-edged sword. *Cardiovasc Diabetol* 2018;17(1):134. doi: 10.1186/s12933-018-0777-x [published Online First: 2018/10/12]
62. Gao YJ, Lu C, Su LY, et al. Modulation of vascular function by perivascular adipose tissue: the role of endothelium and hydrogen peroxide. *Br J Pharmacol* 2007;151(3):323-31. doi: 10.1038/sj.bjp.0707228 [published Online First: 2007/03/27]
63. Zemancikova A, Torok J. Influence of Age on Anticontractile Effect of Perivascular Adipose Tissue in Normotensive and Hypertensive Rats. *Oxid Med Cell Longev* 2019;2019:9314260. doi: 10.1155/2019/9314260 [published Online First: 2019/02/26]
64. Guzik TJ, Skiba DS, Touyz RM, et al. The role of infiltrating immune cells in dysfunctional adipose tissue. *Cardiovasc Res* 2017;113(9):1009-23. doi: 10.1093/cvr/cvx108 [published Online First: 2017/08/26]
65. Saxton SN, Withers SB, Heagerty AM. Emerging Roles of Sympathetic Nerves and Inflammation in Perivascular Adipose Tissue. *Cardiovasc Drugs Ther* 2019;33(2):245-59. doi: 10.1007/s10557-019-06862-4 [published Online First: 2019/02/13]
66. Touyz RM, Alves-Lopes R, Rios FJ, et al. Vascular smooth muscle contraction in hypertension. *Cardiovasc Res* 2018;114(4):529-39. doi: 10.1093/cvr/cvy023 [published Online First: 2018/02/03]
67. Ji Y, Liu J, Wang Z, et al. Angiotensin II induces inflammatory response partly via toll-like receptor 4-dependent signaling pathway in vascular smooth muscle cells. *Cell Physiol Biochem* 2009;23(4-6):265-76. doi: 10.1159/000218173 [published Online First: 2009/05/28]
68. Leung AS, K.; Natarajan, R. Functional Long Non-coding RNAs in Vascular Smooth Muscle Cells. In: Morris KV, SpringerLink (Online service), eds. Long Non-coding RNAs in Human Disease

1st ed2015:VIII, 262 p.

69. Bredt DS. Endogenous nitric oxide synthesis: biological functions and pathophysiology. *Free Radic Res* 1999;31(6):577-96. doi: 10.1080/10715769900301161 [published Online First: 2000/01/12]

70. Forstermann U, Sessa WC. Nitric oxide synthases: regulation and function. *Eur Heart J* 2012;33(7):829-37, 37a-37d. doi: 10.1093/eurheartj/ehr304 [published Online First: 2011/09/06]

71. Hemmrich K, Suschek CV, Lerzynski G, et al. iNOS activity is essential for endothelial stress gene expression protecting against oxidative damage. *J Appl Physiol (1985)* 2003;95(5):1937-46. doi: 10.1152/japplphysiol.00419.2003 [published Online First: 2003/07/29]

72. Steiner L, Kroncke K, Fehsel K, et al. Endothelial cells as cytotoxic effector cells: cytokine-activated rat islet endothelial cells lyse syngeneic islet cells via nitric oxide. *Diabetologia* 1997;40(2):150-5. doi: 10.1007/s001250050656 [published Online First: 1997/02/01]

73. Kroncke KD, Kolb-Bachofen V, Berschick B, et al. Activated macrophages kill pancreatic syngeneic islet cells via arginine-dependent nitric oxide generation. *Biochem Biophys Res Commun* 1991;175(3):752-8. doi: 10.1016/0006-291x(91)91630-u [published Online First: 1991/03/29]

74. Duran WN, Breslin JW, Sanchez FA. The NO cascade, eNOS location, and microvascular permeability. *Cardiovasc Res* 2010;87(2):254-61. doi: 10.1093/cvr/cvq139 [published Online First: 2010/05/14]

75. Zhao Y, Vanhoutte PM, Leung SW. Vascular nitric oxide: Beyond eNOS. *J Pharmacol Sci* 2015;129(2):83-94. doi: 10.1016/j.jphs.2015.09.002 [published Online First: 2015/10/27]

76. Boo YC, Hwang J, Sykes M, et al. Shear stress stimulates phosphorylation of eNOS at Ser(635) by a protein kinase A-dependent mechanism. *Am J Physiol Heart Circ Physiol* 2002;283(5):H1819-28. doi: 10.1152/ajpheart.00214.2002 [published Online First: 2002/10/18]

77. Heiss EH, Dirsch VM. Regulation of eNOS enzyme activity by posttranslational modification. *Curr Pharm Des* 2014;20(22):3503-13. doi: 10.2174/13816128113196660745 [published Online First: 2013/11/05]

78. Goodwin BL, Pendleton LC, Levy MM, et al. Tumor necrosis factor-alpha reduces argininosuccinate synthase expression and nitric oxide production in aortic endothelial cells. *Am J Physiol Heart Circ Physiol* 2007;293(2):H1115-21. doi: 10.1152/ajpheart.01100.2006 [published Online First: 2007/05/15]

79. Zhang J, Patel JM, Li YD, et al. Proinflammatory cytokines downregulate gene expression and activity of constitutive nitric oxide synthase in porcine pulmonary artery endothelial cells. *Res Commun Mol Pathol Pharmacol* 1997;96(1):71-87. [published Online First: 1997/04/01]

80. Zhang H, Park Y, Wu J, et al. Role of TNF-alpha in vascular dysfunction. *Clin Sci (Lond)* 2009;116(3):219-30. doi: 10.1042/CS20080196 [published Online First: 2009/01/03]

81. Schiffrin EL. Vascular endothelin in hypertension. *Vascul Pharmacol* 2005;43(1):19-29. doi: 10.1016/j.vph.2005.03.004 [published Online First: 2005/06/16]

82. Alonso D, Radomski MW. The nitric oxide-endothelin-1 connection. *Heart Fail Rev* 2003;8(1):107-15. doi: 10.1023/a:1022155206928 [published Online First: 2003/03/26]

83. Arnold WP, Mittal CK, Katsuki S, et al. Nitric oxide activates guanylate cyclase and increases guanosine 3':5'-cyclic monophosphate levels in various tissue preparations. *Proc Natl Acad Sci U S A* 1977;74(8):3203-7. doi: 10.1073/pnas.74.8.3203 [published Online First: 1977/08/01]

84. Strijdom H, Chamane N, Lochner A. Nitric oxide in the cardiovascular system: a simple molecule with complex actions. *Cardiovasc J Afr* 2009;20(5):303-10. [published Online First: 2009/11/13]

85. Loscalzo J, Welch G. Nitric oxide and its role in the cardiovascular system. *Prog Cardiovasc Dis* 1995;38(2):87-104. doi: 10.1016/s0033-0620(05)80001-5 [published Online First: 1995/09/01]

86. Dennis EA, Norris PC. Eicosanoid storm in infection and inflammation. *Nat Rev Immunol* 2015;15(8):511-23. doi: 10.1038/nri3859 [published Online First: 2015/07/04]

87. Maclouf J, Folco G, Patrono C. Eicosanoids and iso-eicosanoids: constitutive, inducible and transcellular biosynthesis in vascular disease. *Thromb Haemost* 1998;79(4):691-705. [published Online First: 1998/05/06]

88. Moncada S, Vane JR. Prostacyclin and its clinical applications. *Ann Clin Res* 1984;16(5-6):241-52. [published Online First: 1984/01/01]

89. Kawabe J, Ushikubi F, Hasebe N. Prostacyclin in vascular diseases. - Recent insights and future perspectives. *Circ J* 2010;74(5):836-43. doi: 10.1253/circj.cj-10-0195 [published Online First: 2010/04/29]

90. Imig JD. Eicosanoid blood vessel regulation in physiological and pathological states. *Clin Sci (Lond)* 2020;134(20):2707-27. doi: 10.1042/CS20191209 [published Online First: 2020/10/24]

91. Triggle CR, Dong H, Waldron GJ, et al. Endothelium-derived hyperpolarizing factor(s): species and tissue heterogeneity. *Clin Exp Pharmacol Physiol* 1999;26(2):176-9. doi: 10.1046/j.1440-1681.1999.03007.x [published Online First: 1999/03/05]

92. Triggle CR, Ding H. Endothelium-derived hyperpolarizing factor: is there a novel chemical mediator? *Clin Exp Pharmacol Physiol* 2002;29(3):153-60. doi: 10.1046/j.1440-1681.2002.03632.x [published Online First: 2002/03/22]

93. de Wit C, Griffith TM. Connexins and gap junctions in the EDHF phenomenon and conducted vasomotor responses. *Pflugers Arch* 2010;459(6):897-914. doi: 10.1007/s00424-010-0830-4 [published Online First: 2010/04/10]

94. Campbell WB, Gebremedhin D, Pratt PF, et al. Identification of epoxyeicosatrienoic acids as endothelium-derived hyperpolarizing factors. *Circ Res* 1996;78(3):415-23. doi: 10.1161/01.res.78.3.415 [published Online First: 1996/03/01]

95. Feletou M. Calcium-activated potassium channels and endothelial dysfunction: therapeutic options? *Br J Pharmacol* 2009;156(4):545-62. doi: 10.1111/j.1476-5381.2009.00052.x [published Online First: 2009/02/04]

96. Randall MD, Alexander SP, Bennett T, et al. An endogenous cannabinoid as an endothelium-derived vasorelaxant. *Biochem Biophys Res Commun* 1996;229(1):114-20. doi: 10.1006/bbrc.1996.1766 [published Online First: 1996/12/04]

97. Busse R, Edwards G, Feletou M, et al. EDHF: bringing the concepts together. *Trends Pharmacol Sci* 2002;23(8):374-80. doi: 10.1016/s0165-6147(02)02050-3 [published Online First: 2002/10/16]

98. Nieves-Cintron M, Syed AU, Nystoriak MA, et al. Regulation of voltage-gated potassium channels in vascular smooth muscle during hypertension and metabolic disorders. *Microcirculation* 2018;25(1) doi: 10.1111/micc.12423 [published Online First: 2017/10/19]

99. Nelson MT, Quayle JM. Physiological roles and properties of potassium channels in arterial smooth muscle. *Am J Physiol* 1995;268(4 Pt 1):C799-822. doi: 10.1152/ajpcell.1995.268.4.C799 [published Online First: 1995/04/01]

100. Schiffrin EL. Endothelin and endothelin antagonists in hypertension. *J Hypertens* 1998;16(12 Pt 2):1891-5. doi: 10.1097/00004872-199816121-00007 [published Online First: 1999/01/14]

101. Inoue A, Yanagisawa M, Kimura S, et al. The human endothelin family: three structurally and pharmacologically distinct isopeptides predicted by three separate genes. *Proc Natl Acad Sci U S A* 1989;86(8):2863-7. doi: 10.1073/pnas.86.8.2863 [published Online First: 1989/04/01]

102. Hong HJ, Chan P, Liu JC, et al. Angiotensin II induces endothelin-1 gene expression via extracellular signal-regulated kinase pathway in rat aortic smooth muscle cells. *Cardiovasc Res* 2004;61(1):159-68. doi: 10.1016/j.cardiores.2003.10.019 [published Online First: 2004/01/21]

103. Hu RM, Chuang MY, Prins B, et al. High density lipoproteins stimulate the production and secretion of endothelin-1 from cultured bovine aortic endothelial cells. *J Clin Invest* 1994;93(3):1056-62. doi: 10.1172/JCI117055 [published Online First: 1994/03/01]

104. Sugiura M, Inagami T, Kon V. Endotoxin stimulates endothelin-release in vivo and in vitro as determined by radioimmunoassay. *Biochem Biophys Res Commun* 1989;161(3):1220-7. doi: 10.1016/0006-291x(89)91372-7 [published Online First: 1989/06/30]

105. Matsuura A, Yamochi W, Hirata K, et al. Stimulatory interaction between vascular endothelial growth factor and endothelin-1 on each gene expression. *Hypertension* 1998;32(1):89-95. doi: 10.1161/01.hyp.32.1.89 [published Online First: 1998/07/23]

106. Bourque SL, Davidge ST, Adams MA. The interaction between endothelin-1 and nitric oxide in the vasculature: new perspectives. *Am J Physiol Regul Integr Comp Physiol* 2011;300(6):R1288-95. doi: 10.1152/ajpregu.00397.2010 [published Online First: 2011/03/04]

107. Rapoport RM. Nitric oxide inhibition of endothelin-1 release in the vasculature: in vivo relevance of in vitro findings. *Hypertension* 2014;64(5):908-14. doi: 10.1161/HYPERTENSIONAHA.114.03837 [published Online First: 2014/08/20]

108. Emori T, Hirata Y, Imai T, et al. Cellular mechanism of natriuretic peptides-induced inhibition of endothelin-1 biosynthesis in rat endothelial cells. *Endocrinology* 1993;133(6):2474-80. doi: 10.1210/endo.133.6.8243267 [published Online First: 1993/12/01]

109. Kohno M, Horio T, Yokokawa K, et al. C-type natriuretic peptide inhibits thrombin- and angiotensin II-stimulated endothelin release via cyclic guanosine 3',5'-monophosphate. *Hypertension* 1992;19(4):320-5. doi: 10.1161/01.hyp.19.4.320 [published Online First: 1992/04/01]

110. Agapitov AV, Haynes WG. Role of endothelin in cardiovascular disease. *J Renin Angiotensin Aldosterone Syst* 2002;3(1):1-15. doi: 10.3317/jraas.2002.001 [published Online First: 2002/05/02]

111. Prins BA, Hu RM, Nazario B, et al. Prostaglandin E2 and prostacyclin inhibit the production and secretion of endothelin from cultured endothelial cells. *J Biol Chem* 1994;269(16):11938-44. [published Online First: 1994/04/22]

112. Malek AM, Zhang J, Jiang J, et al. Endothelin-1 gene suppression by shear stress: pharmacological evaluation of the role of tyrosine kinase, intracellular calcium, cytoskeleton, and mechanosensitive channels. *J Mol Cell Cardiol* 1999;31(2):387-99. doi: 10.1006/jmcc.1998.0873 [published Online First: 1999/03/27]

113. Sharefkin JB, Diamond SL, Eskin SG, et al. Fluid flow decreases preproendothelin mRNA levels and suppresses endothelin-1 peptide release in cultured human endothelial cells. *J Vasc Surg* 1991;14(1):1-9. [published Online First: 1991/07/01]

114. Schiffrin EL, Touyz RM. Vascular biology of endothelin. *J Cardiovasc Pharmacol* 1998;32 Suppl 3:S2-13. [published Online First: 1999/01/12]

115. Battistini B, Woods M, O'Donnell LJ, et al. Contractile activity of endothelin precursors in the isolated gallbladder of the guinea-pig: presence of an endothelin-converting enzyme. *Br J Pharmacol* 1995;114(7):1383-90. doi: 10.1111/j.1476-5381.1995.tb13359.x [published Online First: 1995/04/01]

116. Ferro CJ, Spratt JC, Haynes WG, et al. Inhibition of neutral endopeptidase causes vasoconstriction of human resistance vessels in vivo. *Circulation* 1998;97(23):2323-30. doi: 10.1161/01.cir.97.23.2323 [published Online First: 1998/06/25]

117. Fernandez-Patron C, Radomski MW, Davidge ST. Vascular matrix metalloproteinase-2 cleaves big endothelin-1 yielding a novel vasoconstrictor. *Circ Res* 1999;85(10):906-11. doi: 10.1161/01.res.85.10.906 [published Online First: 1999/11/13]

118. Nagata N, Niwa Y, Nakaya Y. A novel 31-amino-acid-length endothelin, ET-1(1-31), can act as a biologically active peptide for vascular smooth muscle cells. *Biochem Biophys Res*

Commun 2000;275(2):595-600. doi: 10.1006/bbrc.2000.3292 [published Online First: 2000/08/31]

119. Sharmin S, Shiota M, Murata E, et al. A novel bioactive 31-amino acid ET-1 peptide stimulates eosinophil recruitment and increases the levels of eotaxin and IL-5. *Inflamm Res* 2002;51(4):195-200. doi: 10.1007/pl00000292 [published Online First: 2002/06/13]
120. Cui P, Tani K, Kitamura H, et al. A novel bioactive 31-amino acid endothelin-1 is a potent chemotactic peptide for human neutrophils and monocytes. *J Leukoc Biol* 2001;70(2):306-12. [published Online First: 2001/08/09]
121. Cui P, Sharmin S, Okumura Y, et al. Endothelin-1 peptides and IL-5 synergistically increase the expression of IL-13 in eosinophils. *Biochem Biophys Res Commun* 2004;315(4):782-7. doi: 10.1016/j.bbrc.2004.01.168 [published Online First: 2004/02/27]
122. Drawnel FM, Archer CR, Roderick HL. The role of the paracrine/autocrine mediator endothelin-1 in regulation of cardiac contractility and growth. *Br J Pharmacol* 2013;168(2):296-317. doi: 10.1111/j.1476-5381.2012.02195.x [published Online First: 2012/09/06]
123. Yoshimoto S, Ishizaki Y, Sasaki T, et al. Effect of carbon dioxide and oxygen on endothelin production by cultured porcine cerebral endothelial cells. *Stroke* 1991;22(3):378-83. doi: 10.1161/01.str.22.3.378 [published Online First: 1991/03/01]
124. Markewitz BA, Kohan DE, Michael JR. Endothelin-1 synthesis, receptors, and signal transduction in alveolar epithelium: evidence for an autocrine role. *Am J Physiol* 1995;268(2 Pt 1):L192-200. doi: 10.1152/ajplung.1995.268.2.L192 [published Online First: 1995/02/01]
125. Deng LY, Li JS, Schiffrin EL. Endothelin receptor subtypes in resistance arteries from humans and rats. *Cardiovasc Res* 1995;29(4):532-5. [published Online First: 1995/04/01]
126. Seo B, Oemar BS, Siebenmann R, et al. Both ETA and ETB receptors mediate contraction to endothelin-1 in human blood vessels. *Circulation* 1994;89(3):1203-8. doi: 10.1161/01.cir.89.3.1203 [published Online First: 1994/03/01]
127. Mencarelli M, Pecorelli A, Carbotti P, et al. Endothelin receptor A expression in human inflammatory cells. *Regul Pept* 2009;158(1-3):1-5. doi: 10.1016/j.regpep.2009.06.004 [published Online First: 2009/06/16]

128. Bacon CR, Cary NR, Davenport AP. Endothelin peptide and receptors in human atherosclerotic coronary artery and aorta. *Circ Res* 1996;79(4):794-801. doi: 10.1161/01.res.79.4.794 [published Online First: 1996/10/01]

129. Iglarz M, Clozel M. At the heart of tissue: endothelin system and end-organ damage. *Clin Sci (Lond)* 2010;119(11):453-63. doi: 10.1042/CS20100222 [published Online First: 2010/08/18]

130. Yang Z, Bauer E, von Segesser L, et al. Different mobilization of calcium in endothelin-1-induced contractions in human arteries and veins: effects of calcium antagonists. *J Cardiovasc Pharmacol* 1990;16(4):654-60. doi: 10.1097/00005344-199010000-00019 [published Online First: 1990/10/01]

131. Davie N, Haleen SJ, Upton PD, et al. ET(A) and ET(B) receptors modulate the proliferation of human pulmonary artery smooth muscle cells. *Am J Respir Crit Care Med* 2002;165(3):398-405. doi: 10.1164/ajrccm.165.3.2104059 [published Online First: 2002/01/31]

132. Oemar BS, Tschudi MR, Godoy N, et al. Reduced endothelial nitric oxide synthase expression and production in human atherosclerosis. *Circulation* 1998;97(25):2494-8. doi: 10.1161/01.cir.97.25.2494 [published Online First: 1998/07/10]

133. Hirata Y, Emori T, Eguchi S, et al. Endothelin receptor subtype B mediates synthesis of nitric oxide by cultured bovine endothelial cells. *J Clin Invest* 1993;91(4):1367-73. doi: 10.1172/JCI116338 [published Online First: 1993/04/01]

134. Schiffrin EL. Does Endothelin-1 Raise or Lower Blood Pressure in Humans? *Nephron* 2018;139(1):47-50. doi: 10.1159/000487346 [published Online First: 2018/02/16]

135. Fukuroda T, Fujikawa T, Ozaki S, et al. Clearance of circulating endothelin-1 by ETB receptors in rats. *Biochem Biophys Res Commun* 1994;199(3):1461-5. doi: 10.1006/bbrc.1994.1395 [published Online First: 1994/03/30]

136. Naomi S, Iwaoka T, Disashi T, et al. Endothelin-1 inhibits endothelin-converting enzyme-1 expression in cultured rat pulmonary endothelial cells. *Circulation* 1998;97(3):234-6. doi: 10.1161/01.cir.97.3.234 [published Online First: 1998/02/14]

137. Shichiri M, Kato H, Marumo F, et al. Endothelin-1 as an autocrine/paracrine apoptosis survival factor for endothelial cells. *Hypertension* 1997;30(5):1198-203. doi: 10.1161/01.hyp.30.5.1198 [published Online First: 1997/11/22]

138. Ozaki S, Ohwaki K, Ihara M, et al. ETB-mediated regulation of extracellular levels of endothelin-1 in cultured human endothelial cells. *Biochem Biophys Res Commun* 1995;209(2):483-9. doi: 10.1006/bbrc.1995.1527 [published Online First: 1995/04/17]

139. Komuro I, Kurihara H, Sugiyama T, et al. Endothelin stimulates c-fos and c-myc expression and proliferation of vascular smooth muscle cells. *FEBS Lett* 1988;238(2):249-52. doi: 10.1016/0014-5793(88)80489-7 [published Online First: 1988/10/10]

140. Hirata Y, Takagi Y, Fukuda Y, et al. Endothelin is a potent mitogen for rat vascular smooth muscle cells. *Atherosclerosis* 1989;78(2-3):225-8. doi: 10.1016/0021-9150(89)90227-x [published Online First: 1989/08/01]

141. Ito H, Hirata Y, Hiroe M, et al. Endothelin-1 induces hypertrophy with enhanced expression of muscle-specific genes in cultured neonatal rat cardiomyocytes. *Circ Res* 1991;69(1):209-15. doi: 10.1161/01.res.69.1.209 [published Online First: 1991/07/01]

142. Ito H, Hirata Y, Adachi S, et al. Endothelin-1 is an autocrine/paracrine factor in the mechanism of angiotensin II-induced hypertrophy in cultured rat cardiomyocytes. *J Clin Invest* 1993;92(1):398-403. doi: 10.1172/JCI116579 [published Online First: 1993/07/01]

143. Badr KF, Murray JJ, Breyer MD, et al. Mesangial cell, glomerular and renal vascular responses to endothelin in the rat kidney. Elucidation of signal transduction pathways. *J Clin Invest* 1989;83(1):336-42. doi: 10.1172/JCI113880 [published Online First: 1989/01/01]

144. Mazzocchi G, Rossi GP, Rebuffat P, et al. Endothelins stimulate deoxyribonucleic acid synthesis and cell proliferation in rat adrenal zona glomerulosa, acting through an endothelin A receptor coupled with protein kinase C- and tyrosine kinase-dependent signaling pathways. *Endocrinology* 1997;138(6):2333-7. doi: 10.1210/endo.138.6.5191 [published Online First: 1997/06/01]

145. Amiri F, Paradis P, Reudelhuber TL, et al. Vascular inflammation in absence of blood pressure elevation in transgenic murine model overexpressing endothelin-1 in endothelial cells. *J Hypertens* 2008;26(6):1102-9. doi: 10.1097/HJH.0b013e3282fc2184 [published Online First: 2008/05/14]

146. Rossi GP, Sacchetto A, Cesari M, et al. Interactions between endothelin-1 and the renin-angiotensin-aldosterone system. *Cardiovasc Res* 1999;43(2):300-7. doi: 10.1016/s0008-6363(99)00110-8 [published Online First: 1999/10/28]

147. Gunther J, Kill A, Becker MO, et al. Angiotensin receptor type 1 and endothelin receptor type A on immune cells mediate migration and the expression of IL-8 and CCL18 when stimulated by autoantibodies from systemic sclerosis patients. *Arthritis Res Ther* 2014;16(2):R65. doi: 10.1186/ar4503 [published Online First: 2014/03/13]

148. Zouki C, Baron C, Fournier A, et al. Endothelin-1 enhances neutrophil adhesion to human coronary artery endothelial cells: role of ET(A) receptors and platelet-activating factor. *Br J Pharmacol* 1999;127(4):969-79. doi: 10.1038/sj.bjp.0702593 [published Online First: 1999/08/05]

149. Lopez Farre A, Riesco A, Espinosa G, et al. Effect of endothelin-1 on neutrophil adhesion to endothelial cells and perfused heart. *Circulation* 1993;88(3):1166-71. doi: 10.1161/01.cir.88.3.1166 [published Online First: 1993/09/01]

150. Cunningham ME, Huribal M, Bala RJ, et al. Endothelin-1 and endothelin-4 stimulate monocyte production of cytokines. *Crit Care Med* 1997;25(6):958-64. doi: 10.1097/00003246-199706000-00011 [published Online First: 1997/06/01]

151. Lee RT, Kamm RD. Vascular mechanics for the cardiologist. *J Am Coll Cardiol* 1994;23(6):1289-95. doi: 10.1016/0735-1097(94)90369-7 [published Online First: 1994/05/01]

152. Kawasaki T, Sasayama S, Yagi S, et al. Non-invasive assessment of the age related changes in stiffness of major branches of the human arteries. *Cardiovasc Res* 1987;21(9):678-87. doi: 10.1093/cvr/21.9.678 [published Online First: 1987/09/01]

153. Khamdaeng T, Luo J, Vappou J, et al. Arterial stiffness identification of the human carotid artery using the stress-strain relationship in vivo. *Ultrasonics* 2012;52(3):402-11. doi: 10.1016/j.ultras.2011.09.006 [published Online First: 2011/10/28]

154. Arnett DK, Evans GW, Riley WA. Arterial stiffness: a new cardiovascular risk factor? *Am J Epidemiol* 1994;140(8):669-82. doi: 10.1093/oxfordjournals.aje.a117315 [published Online First: 1994/10/15]

155. Collaborators GBDRF. Global, regional, and national comparative risk assessment of 84 behavioural, environmental and occupational, and metabolic risks or clusters of risks for 195 countries and territories, 1990-2017: a systematic analysis for the Global Burden of Disease Study 2017. *Lancet* 2018;392(10159):1923-94. doi: 10.1016/S0140-6736(18)32225-6 [published Online First: 2018/11/30]

156. Virani SS, Alonso A, Aparicio HJ, et al. Heart Disease and Stroke Statistics-2021 Update: A Report From the American Heart Association. *Circulation* 2021;143(8):e254-e743. doi: 10.1161/CIR.0000000000000950 [published Online First: 2021/01/28]

157. Heidenreich PA, Trogdon JG, Khavjou OA, et al. Forecasting the future of cardiovascular disease in the United States: a policy statement from the American Heart Association. *Circulation* 2011;123(8):933-44. doi: 10.1161/CIR.0b013e31820a55f5 [published Online First: 2011/01/26]

158. Rabi DM, McBrien KA, Sapir-Pichhadze R, et al. Hypertension Canada's 2020 Comprehensive Guidelines for the Prevention, Diagnosis, Risk Assessment, and Treatment of Hypertension in Adults and Children. *Can J Cardiol* 2020;36(5):596-624. doi: 10.1016/j.cjca.2020.02.086 [published Online First: 2020/05/12]

159. Roerecke M, Kaczorowski J, Myers MG. Comparing Automated Office Blood Pressure Readings With Other Methods of Blood Pressure Measurement for Identifying Patients With Possible Hypertension: A Systematic Review and Meta-analysis. *JAMA Intern Med* 2019;179(3):351-62. doi: 10.1001/jamainternmed.2018.6551 [published Online First: 2019/02/05]

160. Giles TD, Materson BJ, Cohn JN, et al. Definition and classification of hypertension: an update. *J Clin Hypertens (Greenwich)* 2009;11(11):611-4. doi: 10.1111/j.1751-7176.2009.00179.x [published Online First: 2009/11/03]

161. Carretero OA, Oparil S. Essential hypertension. Part I: definition and etiology. *Circulation* 2000;101(3):329-35. doi: 10.1161/01.cir.101.3.329 [published Online First: 2000/01/25]

162. Tedla FM, Brar A, Browne R, et al. Hypertension in chronic kidney disease: navigating the evidence. *Int J Hypertens* 2011;2011:132405. doi: 10.4061/2011/132405 [published Online First: 2011/07/13]

163. Buonacera A, Stancanelli B, Malatino L. Endocrine Tumors Causing Arterial Hypertension: Pathophysiological Mechanisms and Clinical Implications. *High Blood Press Cardiovasc Prev* 2017;24(3):217-29. doi: 10.1007/s40292-017-0200-9 [published Online First: 2017/04/14]

164. Malha L, August P. Secondary Hypertension in Pregnancy. *Curr Hypertens Rep* 2015;17(7):53. doi: 10.1007/s11906-015-0563-z [published Online First: 2015/06/13]

165. Mulvany MJ. Small artery remodeling and significance in the development of hypertension. *News Physiol Sci* 2002;17:105-9. doi: 10.1152/nips.01366.2001 [published Online First: 2002/05/22]

166. Perry IJ, Whincup PH, Shaper AG. Environmental factors in the development of essential hypertension. *Br Med Bull* 1994;50(2):246-59. doi: 10.1093/oxfordjournals.bmb.a072890 [published Online First: 1994/04/01]

167. Hall JE, Granger JP, do Carmo JM, et al. Hypertension: physiology and pathophysiology. *Compr Physiol* 2012;2(4):2393-442. doi: 10.1002/cphy.c110058 [published Online First: 2013/05/31]

168. Lee RM, Dickhout JG, Sandow SL. Vascular structural and functional changes: their association with causality in hypertension: models, remodeling and relevance. *Hypertens Res* 2017;40(4):311-23. doi: 10.1038/hr.2016.145 [published Online First: 2016/10/28]

169. Buijk SE, Bruining HA. Vasopressin deficiency contributes to the vasodilation of septic shock. *Circulation* 1998;98(2):187. [published Online First: 1998/07/29]

170. Mayet J, Hughes A. Cardiac and vascular pathophysiology in hypertension. *Heart* 2003;89(9):1104-9. doi: 10.1136/heart.89.9.1104 [published Online First: 2003/08/19]

171. Haddy FJ, Overbeck HW, Daugherty RM, Jr. Peripheral vascular resistance. *Annu Rev Med* 1968;19:167-94. doi: 10.1146/annurev.me.19.020168.001123 [published Online First: 1968/01/01]

172. Schiffrin EL. Reactivity of small blood vessels in hypertension: relation with structural changes. State of the art lecture. *Hypertension* 1992;19(2 Suppl):II1-9. doi: 10.1161/01.hyp.19.2_suppl.ii1-a [published Online First: 1992/02/01]

173. Renna NF, de Las Heras N, Miatello RM. Pathophysiology of vascular remodeling in hypertension. *Int J Hypertens* 2013;2013:808353. doi: 10.1155/2013/808353 [published Online First: 2013/08/24]

174. VanLandingham LG, Gannon KP, Drummond HA. Pressure-induced constriction is inhibited in a mouse model of reduced betaENaC. *Am J Physiol Regul Integr Comp Physiol* 2009;297(3):R723-8. doi: 10.1152/ajpregu.00212.2009 [published Online First: 2009/06/26]

175. Jernigan NL, Drummond HA. Vascular ENaC proteins are required for renal myogenic constriction. *Am J Physiol Renal Physiol* 2005;289(4):F891-901. doi: 10.1152/ajprenal.00019.2005 [published Online First: 2005/05/26]

176. Nemeth Z, Hildebrandt E, Ryan MJ, et al. Pressure-induced constriction of the middle cerebral artery is abolished in TrpC6 knockout mice. *Am J Physiol Heart Circ Physiol* 2020;319(1):H42-H50. doi: 10.1152/ajpheart.00126.2020 [published Online First: 2020/05/16]

177. Jackson WF. Myogenic Tone in Peripheral Resistance Arteries and Arterioles: The Pressure Is On! *Front Physiol* 2021;12:699517. doi: 10.3389/fphys.2021.699517 [published Online First: 2021/08/10]

178. Izzard AS, Bund SJ, Heagerty AM. Myogenic tone in mesenteric arteries from spontaneously hypertensive rats. *Am J Physiol* 1996;270(1 Pt 2):H1-6. doi: 10.1152/ajpheart.1996.270.1.H1 [published Online First: 1996/01/01]

179. Schiffrin EL. Remodeling of resistance arteries in essential hypertension and effects of antihypertensive treatment. *Am J Hypertens* 2004;17(12 Pt 1):1192-200. doi: 10.1016/j.amjhyper.2004.05.023 [published Online First: 2004/12/21]

180. Laurent S. Arterial wall hypertrophy and stiffness in essential hypertensive patients. *Hypertension* 1995;26(2):355-62. doi: 10.1161/01.hyp.26.2.355 [published Online First: 1995/08/01]

181. Franklin SS. Arterial stiffness and hypertension: a two-way street? *Hypertension* 2005;45(3):349-51. doi: 10.1161/01.HYP.0000157819.31611.87 [published Online First: 2005/02/16]

182. Rizzoni D, Agabiti Rosei E. Small artery remodeling in hypertension and diabetes. *Curr Hypertens Rep* 2006;8(1):90-5. doi: 10.1007/s11906-006-0046-3 [published Online First: 2006/04/08]

183. Rizzoni D, Porteri E, Giustina A, et al. Acromegalic patients show the presence of hypertrophic remodeling of subcutaneous small resistance arteries. *Hypertension* 2004;43(3):561-5. doi: 10.1161/01.HYP.0000114604.52270.05 [published Online First: 2004/02/28]

184. Rizzoni D, Porteri E, Guefi D, et al. Cellular hypertrophy in subcutaneous small arteries of patients with renovascular hypertension. *Hypertension* 2000;35(4):931-5. doi: 10.1161/01.hyp.35.4.931 [published Online First: 2000/04/25]

185. Brown IAM, Diederich L, Good ME, et al. Vascular Smooth Muscle Remodeling in Conductive and Resistance Arteries in Hypertension. *Arterioscler Thromb Vasc Biol* 2018;38(9):1969-85. doi: 10.1161/ATVBAHA.118.311229 [published Online First: 2018/10/26]

186. Mulvany MJ, Baandrup U, Gundersen HJ. Evidence for hyperplasia in mesenteric resistance vessels of spontaneously hypertensive rats using a three-dimensional disector. *Circ Res* 1985;57(5):794-800. doi: 10.1161/01.res.57.5.794 [published Online First: 1985/11/01]

187. Lee RM, Garfield RE, Forrest JB, et al. Morphometric study of structural changes in the mesenteric blood vessels of spontaneously hypertensive rats. *Blood Vessels* 1983;20(2):57-71. doi: 10.1159/000158460 [published Online First: 1983/01/01]

188. Diep QN, Li JS, Schiffrin EL. In vivo study of AT(1) and AT(2) angiotensin receptors in apoptosis in rat blood vessels. *Hypertension* 1999;34(4 Pt 1):617-24. doi: 10.1161/01.hyp.34.4.617 [published Online First: 1999/10/16]

189. Sharifi AM, Schiffrin EL. Apoptosis in vasculature of spontaneously hypertensive rats: effect of an angiotensin converting enzyme inhibitor and a calcium channel antagonist. *Am J Hypertens* 1998;11(9):1108-16. doi: 10.1016/s0895-7061(98)00120-4 [published Online First: 1998/09/30]

190. Schiffrin EL. Vascular remodeling in hypertension: mechanisms and treatment. *Hypertension* 2012;59(2):367-74. doi: 10.1161/HYPERTENSIONAHA.111.187021 [published Online First: 2011/12/29]

191. Boumaza S, Arribas SM, Osborne-Pellegrin M, et al. Fenestrations of the carotid internal elastic lamina and structural adaptation in stroke-prone spontaneously hypertensive rats. *Hypertension* 2001;37(4):1101-7. doi: 10.1161/01.hyp.37.4.1101 [published Online First: 2001/04/17]

192. Humphrey JD. Mechanisms of Vascular Remodeling in Hypertension. *Am J Hypertens* 2021;34(5):432-41. doi: 10.1093/ajh/hpaa195 [published Online First: 2020/11/28]

193. Deanfield J, Donald A, Ferri C, et al. Endothelial function and dysfunction. Part I: Methodological issues for assessment in the different vascular beds: a statement by the

Working Group on Endothelin and Endothelial Factors of the European Society of Hypertension. *J Hypertens* 2005;23(1):7-17. doi: 10.1097/00004872-200501000-00004 [published Online First: 2005/01/12]

194. Schiffrin EL. Beyond blood pressure: the endothelium and atherosclerosis progression. *Am J Hypertens* 2002;15(10 Pt 2):115S-22S. doi: 10.1016/s0895-7061(02)03006-6 [published Online First: 2002/10/18]
195. O'Rourke MF, Nichols WW. Aortic diameter, aortic stiffness, and wave reflection increase with age and isolated systolic hypertension. *Hypertension* 2005;45(4):652-8. doi: 10.1161/01.HYP.0000153793.84859.b8 [published Online First: 2005/02/09]
196. Benetos A, Laurent S, Asmar RG, et al. Large artery stiffness in hypertension. *J Hypertens Suppl* 1997;15(2):S89-97. doi: 10.1097/00004872-199715022-00009 [published Online First: 1997/03/01]
197. Mitchell GF. Arterial Stiffness and Wave Reflection: Biomarkers of Cardiovascular Risk. *Artery Res* 2009;3(2):56-64. doi: 10.1016/j.artres.2009.02.002 [published Online First: 2010/02/18]
198. Mitchell GF, Vita JA, Larson MG, et al. Cross-sectional relations of peripheral microvascular function, cardiovascular disease risk factors, and aortic stiffness: the Framingham Heart Study. *Circulation* 2005;112(24):3722-8. doi: 10.1161/CIRCULATIONAHA.105.551168 [published Online First: 2005/12/07]
199. Zhang Y, Lacolley P, Protogerou AD, et al. Arterial Stiffness in Hypertension and Function of Large Arteries. *Am J Hypertens* 2020;33(4):291-96. doi: 10.1093/ajh/hpz193 [published Online First: 2020/02/16]
200. Safar ME, Asmar R, Benetos A, et al. Interaction Between Hypertension and Arterial Stiffness. *Hypertension* 2018;72(4):796-805. doi: 10.1161/HYPERTENSIONAHA.118.11212 [published Online First: 2018/10/26]
201. Mulvany MJ, Baumbach GL, Aalkjaer C, et al. Vascular remodeling. *Hypertension* 1996;28(3):505-6. [published Online First: 1996/09/01]
202. Heagerty AM, Aalkjaer C, Bund SJ, et al. Small artery structure in hypertension. Dual processes of remodeling and growth. *Hypertension* 1993;21(4):391-7. doi: 10.1161/01.hyp.21.4.391 [published Online First: 1993/04/01]

203. Mulvany MJ, Halpern W. Contractile properties of small arterial resistance vessels in spontaneously hypertensive and normotensive rats. *Circ Res* 1977;41(1):19-26. doi: 10.1161/01.res.41.1.19 [published Online First: 1977/07/01]

204. Brassard P, Amiri F, Schiffrin EL. Combined angiotensin II type 1 and type 2 receptor blockade on vascular remodeling and matrix metalloproteinases in resistance arteries. *Hypertension* 2005;46(3):598-606. doi: 10.1161/01.HYP.0000176744.15592.7d [published Online First: 2005/07/27]

205. Schiffrin EL, Deng LY, Larochelle P. Morphology of resistance arteries and comparison of effects of vasoconstrictors in mild essential hypertensive patients. *Clin Invest Med* 1993;16(3):177-86. [published Online First: 1993/06/01]

206. Schiffrin EL, Deng LY, Larochelle P. Effects of a beta-blocker or a converting enzyme inhibitor on resistance arteries in essential hypertension. *Hypertension* 1994;23(1):83-91. doi: 10.1161/01.hyp.23.1.83 [published Online First: 1994/01/01]

207. Schiffrin EL. The vascular phenotypes in hypertension: Relation with the natural history of hypertension. *J Am Soc Hypertens* 2007;1(1):56-67. doi: 10.1016/j.jash.2006.11.003 [published Online First: 2007/01/01]

208. Dickhout JG, Lee RM. Apoptosis in the muscular arteries from young spontaneously hypertensive rats. *J Hypertens* 1999;17(10):1413-9. doi: 10.1097/00004872-199917100-00008 [published Online First: 1999/10/20]

209. Deng LY, Schiffrin EL. Effects of endothelin on resistance arteries of DOCA-salt hypertensive rats. *Am J Physiol* 1992;262(6 Pt 2):H1782-7. doi: 10.1152/ajpheart.1992.262.6.H1782 [published Online First: 1992/06/01]

210. Deng LY, Schiffrin EL. Morphological and functional alterations of mesenteric small resistance arteries in early renal hypertension in rats. *Am J Physiol* 1991;261(4 Pt 2):H1171-7. doi: 10.1152/ajpheart.1991.261.4.H1171 [published Online First: 1991/10/01]

211. d'Uscio LV, Barton M, Shaw S, et al. Structure and function of small arteries in salt-induced hypertension: effects of chronic endothelin-subtype-A-receptor blockade. *Hypertension* 1997;30(4):905-11. doi: 10.1161/01.hyp.30.4.905 [published Online First: 1997/10/23]

212. Rizzoni D, Porteri E, Castellano M, et al. Vascular hypertrophy and remodeling in secondary hypertension. *Hypertension* 1996;28(5):785-90. doi: 10.1161/01.hyp.28.5.785 [published Online First: 1996/11/01]

213. Intengan HD, Deng LY, Li JS, et al. Mechanics and composition of human subcutaneous resistance arteries in essential hypertension. *Hypertension* 1999;33(1 Pt 2):569-74. doi: 10.1161/01.hyp.33.1.569 [published Online First: 1999/02/04]

214. Sharifi AM, Li JS, Endemann D, et al. Effects of enalapril and amlodipine on small-artery structure and composition, and on endothelial dysfunction in spontaneously hypertensive rats. *J Hypertens* 1998;16(4):457-66. doi: 10.1097/00004872-199816040-00007 [published Online First: 1998/10/31]

215. Intengan HD, Thibault G, Li JS, et al. Resistance artery mechanics, structure, and extracellular components in spontaneously hypertensive rats : effects of angiotensin receptor antagonism and converting enzyme inhibition. *Circulation* 1999;100(22):2267-75. doi: 10.1161/01.cir.100.22.2267 [published Online First: 1999/12/01]

216. Intengan HD, Schiffrin EL. Vascular remodeling in hypertension: roles of apoptosis, inflammation, and fibrosis. *Hypertension* 2001;38(3 Pt 2):581-7. doi: 10.1161/hy09t1.096249 [published Online First: 2001/09/22]

217. Saouaf R, Takasaki I, Eastman E, et al. Fibronectin biosynthesis in the rat aorta in vitro. Changes due to experimental hypertension. *J Clin Invest* 1991;88(4):1182-9. doi: 10.1172/JCI115420 [published Online First: 1991/10/01]

218. Takasaki I, Takizawa T, Sugimoto K, et al. Effects of hypertension and aging on fibronectin expression in aorta of Dahl salt-sensitive rats. *Am J Physiol* 1994;267(4 Pt 2):H1523-9. doi: 10.1152/ajpheart.1994.267.4.H1523 [published Online First: 1994/10/01]

219. Himeno H, Crawford DC, Hosoi M, et al. Angiotensin II alters aortic fibronectin independently of hypertension. *Hypertension* 1994;23(6 Pt 2):823-6. doi: 10.1161/01.hyp.23.6.823 [published Online First: 1994/06/01]

220. Heerkens EH, Shaw L, Ryding A, et al. alphaV integrins are necessary for eutrophic inward remodeling of small arteries in hypertension. *Hypertension* 2006;47(2):281-7. doi: 10.1161/01.HYP.0000198428.45132.02 [published Online First: 2005/12/29]

221. VanBavel E, Mulvany MJ. Integrins in hypertensive remodeling. *Hypertension* 2006;47(2):147-8. doi: 10.1161/01.HYP.0000198540.38872.47 [published Online First: 2005/12/29]

222. Savoia C, Schiffrin EL. Vascular inflammation in hypertension and diabetes: molecular mechanisms and therapeutic interventions. *Clin Sci (Lond)* 2007;112(7):375-84. doi: 10.1042/CS20060247 [published Online First: 2007/02/28]

223. Savoia C, Burger D, Nishigaki N, et al. Angiotensin II and the vascular phenotype in hypertension. *Expert Rev Mol Med* 2011;13:e11. doi: 10.1017/S1462399411001815 [published Online First: 2011/04/01]

224. Reaux A, Fournie-Zaluski MC, Llorens-Cortes C. Angiotensin III: a central regulator of vasopressin release and blood pressure. *Trends Endocrinol Metab* 2001;12(4):157-62. doi: 10.1016/s1043-2760(01)00381-2 [published Online First: 2001/04/11]

225. Yang R, Walther T, Gembardt F, et al. Renal vasoconstrictor and pressor responses to angiotensin IV in mice are AT1a-receptor mediated. *J Hypertens* 2010;28(3):487-94. doi: 10.1097/HJH.0b013e3283343250 [published Online First: 2009/11/13]

226. Santiago NM, Guimaraes PS, Sirvente RA, et al. Lifetime overproduction of circulating Angiotensin-(1-7) attenuates deoxycorticosterone acetate-salt hypertension-induced cardiac dysfunction and remodeling. *Hypertension* 2010;55(4):889-96. doi: 10.1161/HYPERTENSIONAHA.110.149815 [published Online First: 2010/03/10]

227. Bader M, Peters J, Baltatu O, et al. Tissue renin-angiotensin systems: new insights from experimental animal models in hypertension research. *J Mol Med (Berl)* 2001;79(2-3):76-102. doi: 10.1007/s001090100210 [published Online First: 2001/05/19]

228. Engeli S, Negrel R, Sharma AM. Physiology and pathophysiology of the adipose tissue renin-angiotensin system. *Hypertension* 2000;35(6):1270-7. doi: 10.1161/01.hyp.35.6.1270 [published Online First: 2000/06/17]

229. Geara AS, Azzi J, Jurewicz M, et al. The renin-angiotensin system: an old, newly discovered player in immunoregulation. *Transplant Rev (Orlando)* 2009;23(3):151-8. doi: 10.1016/j.trre.2009.04.002 [published Online First: 2009/06/23]

230. Dinh DT, Frauman AG, Johnston CI, et al. Angiotensin receptors: distribution, signalling and function. *Clin Sci (Lond)* 2001;100(5):481-92. [published Online First: 2001/04/11]

231. Te Riet L, van Esch JH, Roks AJ, et al. Hypertension: renin-angiotensin-aldosterone system alterations. *Circ Res* 2015;116(6):960-75. doi: 10.1161/CIRCRESAHA.116.303587 [published Online First: 2015/03/15]

232. Burson JM, Aguilera G, Gross KW, et al. Differential expression of angiotensin receptor 1A and 1B in mouse. *Am J Physiol* 1994;267(2 Pt 1):E260-7. doi: 10.1152/ajpendo.1994.267.2.E260 [published Online First: 1994/08/01]

233. Gasc JM, Shanmugam S, Sibony M, et al. Tissue-specific expression of type 1 angiotensin II receptor subtypes. An in situ hybridization study. *Hypertension* 1994;24(5):531-7. doi: 10.1161/01.hyp.24.5.531 [published Online First: 1994/11/01]

234. Llorens-Cortes C, Greenberg B, Huang H, et al. Tissular expression and regulation of type 1 angiotensin II receptor subtypes by quantitative reverse transcriptase-polymerase chain reaction analysis. *Hypertension* 1994;24(5):538-48. doi: 10.1161/01.hyp.24.5.538 [published Online First: 1994/11/01]

235. Oliverio MI, Kim HS, Ito M, et al. Reduced growth, abnormal kidney structure, and type 2 (AT2) angiotensin receptor-mediated blood pressure regulation in mice lacking both AT1A and AT1B receptors for angiotensin II. *Proc Natl Acad Sci U S A* 1998;95(26):15496-501. doi: 10.1073/pnas.95.26.15496 [published Online First: 1998/12/23]

236. Sugaya T, Nishimatsu S, Tanimoto K, et al. Angiotensin II type 1a receptor-deficient mice with hypotension and hyperreninemia. *J Biol Chem* 1995;270(32):18719-22. doi: 10.1074/jbc.270.32.18719 [published Online First: 1995/08/11]

237. Ruan X, Oliverio MI, Coffman TM, et al. Renal vascular reactivity in mice: AngII-induced vasoconstriction in AT1A receptor null mice. *J Am Soc Nephrol* 1999;10(12):2620-30. doi: 10.1681/ASN.V10122620 [published Online First: 1999/12/10]

238. Griendling KK, Ushio-Fukai M, Lassegue B, et al. Angiotensin II signaling in vascular smooth muscle. New concepts. *Hypertension* 1997;29(1 Pt 2):366-73. doi: 10.1161/01.hyp.29.1.366 [published Online First: 1997/01/01]

239. Paradis P, Dali-Youcef N, Paradis FW, et al. Overexpression of angiotensin II type I receptor in cardiomyocytes induces cardiac hypertrophy and remodeling. *Proc Natl Acad Sci U S A* 2000;97(2):931-6. doi: 10.1073/pnas.97.2.931 [published Online First: 2000/01/19]

240. Shah BH, Catt KJ. Matrix metalloproteinase-dependent EGF receptor activation in hypertension and left ventricular hypertrophy. *Trends Endocrinol Metab* 2004;15(6):241-3. doi: 10.1016/j.tem.2004.06.011 [published Online First: 2004/09/11]

241. Chen J, Chen JK, Neilson EG, et al. Role of EGF receptor activation in angiotensin II-induced renal epithelial cell hypertrophy. *J Am Soc Nephrol* 2006;17(6):1615-23. doi: 10.1681/ASN.2005111163 [published Online First: 2006/04/28]

242. Li Q, Muragaki Y, Hatamura I, et al. Stretch-induced collagen synthesis in cultured smooth muscle cells from rabbit aortic media and a possible involvement of angiotensin II and transforming growth factor-beta. *J Vasc Res* 1998;35(2):93-103. doi: 10.1159/000025570 [published Online First: 1998/05/20]

243. Schlumberger W, Thie M, Rauterberg J, et al. Collagen synthesis in cultured aortic smooth muscle cells. Modulation by collagen lattice culture, transforming growth factor-beta 1, and epidermal growth factor. *Arterioscler Thromb* 1991;11(6):1660-6. doi: 10.1161/01.atv.11.6.1660 [published Online First: 1991/11/01]

244. Nishikawa K. Angiotensin AT1 receptor antagonism and protection against cardiovascular end-organ damage. *J Hum Hypertens* 1998;12(5):301-9. doi: 10.1038/sj.jhh.1000634 [published Online First: 1998/07/09]

245. Steckelings UM, Kaschina E, Unger T. The AT2 receptor--a matter of love and hate. *Peptides* 2005;26(8):1401-9. doi: 10.1016/j.peptides.2005.03.010 [published Online First: 2005/07/27]

246. Grady EF, Sechi LA, Griffin CA, et al. Expression of AT2 receptors in the developing rat fetus. *J Clin Invest* 1991;88(3):921-33. doi: 10.1172/JCI115395 [published Online First: 1991/09/01]

247. Horiuchi M, Akishita M, Dzau VJ. Recent progress in angiotensin II type 2 receptor research in the cardiovascular system. *Hypertension* 1999;33(2):613-21. doi: 10.1161/01.hyp.33.2.613 [published Online First: 1999/02/19]

248. Lemarie CA, Schiffrin EL. The angiotensin II type 2 receptor in cardiovascular disease. *J Renin Angiotensin Aldosterone Syst* 2010;11(1):19-31. doi: 10.1177/1470320309347785 [published Online First: 2009/10/29]

249. Carey RM, Wang ZQ, Siragy HM. Role of the angiotensin type 2 receptor in the regulation of blood pressure and renal function. *Hypertension* 2000;35(1 Pt 2):155-63. doi: 10.1161/01.hyp.35.1.155 [published Online First: 2000/01/21]

250. Savoia C, Tabet F, Yao G, et al. Negative regulation of RhoA/Rho kinase by angiotensin II type 2 receptor in vascular smooth muscle cells: role in angiotensin II-induced vasodilation in stroke-prone spontaneously hypertensive rats. *J Hypertens* 2005;23(5):1037-45. doi: 10.1097/01.hjh.0000166845.49850.39 [published Online First: 2005/04/19]

251. Savoia C, Touyz RM, Volpe M, et al. Angiotensin type 2 receptor in resistance arteries of type 2 diabetic hypertensive patients. *Hypertension* 2007;49(2):341-6. doi: 10.1161/01.HYP.0000253968.95136.b8 [published Online First: 2006/12/13]

252. Yamada T, Horiuchi M, Dzau VJ. Angiotensin II type 2 receptor mediates programmed cell death. *Proc Natl Acad Sci U S A* 1996;93(1):156-60. doi: 10.1073/pnas.93.1.156 [published Online First: 1996/01/09]

253. Tea BS, Der Sarkissian S, Touyz RM, et al. Proapoptotic and growth-inhibitory role of angiotensin II type 2 receptor in vascular smooth muscle cells of spontaneously hypertensive rats in vivo. *Hypertension* 2000;35(5):1069-73. doi: 10.1161/01.hyp.35.5.1069 [published Online First: 2000/05/20]

254. Sarikonda KV, Watson RE, Opara OC, et al. Experimental animal models of hypertension. *J Am Soc Hypertens* 2009;3(3):158-65. doi: 10.1016/j.jash.2009.02.003 [published Online First: 2010/04/23]

255. Lin HY, Lee YT, Chan YW, et al. Animal models for the study of primary and secondary hypertension in humans. *Biomed Rep* 2016;5(6):653-59. doi: 10.3892/br.2016.784 [published Online First: 2017/01/21]

256. Lohmeier TE. Angiotensin II infusion model of hypertension: is there an important sympathetic component? *Hypertension* 2012;59(3):539-41. doi: 10.1161/HYPERTENSIONAHA.111.188714 [published Online First: 2012/01/26]

257. Touyz RM, Tabet F, Schiffrin EL. Redox-dependent signalling by angiotensin II and vascular remodelling in hypertension. *Clin Exp Pharmacol Physiol* 2003;30(11):860-6. doi: 10.1046/j.1440-1681.2003.03930.x [published Online First: 2003/12/18]

258. Schiffrin EL. Mechanisms of remodelling of small arteries, antihypertensive therapy and the immune system in hypertension. *Clin Invest Med* 2015;38(6):E394-402. doi: 10.25011/cim.v38i6.26202 [published Online First: 2015/12/15]

259. Xiao L, Harrison DG. Inflammation in Hypertension. *Can J Cardiol* 2020;36(5):635-47. doi: 10.1016/j.cjca.2020.01.013 [published Online First: 2020/05/12]

260. Zhang W, Wang W, Yu H, et al. Interleukin 6 underlies angiotensin II-induced hypertension and chronic renal damage. *Hypertension* 2012;59(1):136-44. doi: 10.1161/HYPERTENSIONAHA.111.173328 [published Online First: 2011/11/10]

261. Crowley SD, Gurley SB, Herrera MJ, et al. Angiotensin II causes hypertension and cardiac hypertrophy through its receptors in the kidney. *Proc Natl Acad Sci U S A* 2006;103(47):17985-90. doi: 10.1073/pnas.0605545103 [published Online First: 2006/11/09]

262. Leibowitz A, Schiffrin EL. Immune mechanisms in hypertension. *Curr Hypertens Rep* 2011;13(6):465-72. doi: 10.1007/s11906-011-0224-9 [published Online First: 2011/08/16]

263. Ferrero-Miliani L, Nielsen OH, Andersen PS, et al. Chronic inflammation: importance of NOD2 and NALP3 in interleukin-1beta generation. *Clin Exp Immunol* 2007;147(2):227-35. doi: 10.1111/j.1365-2249.2006.03261.x [published Online First: 2007/01/17]

264. Benigni A, Cassis P, Remuzzi G. Angiotensin II revisited: new roles in inflammation, immunology and aging. *EMBO Mol Med* 2010;2(7):247-57. doi: 10.1002/emmm.201000080 [published Online First: 2010/07/03]

265. Ross R. Atherosclerosis--an inflammatory disease. *N Engl J Med* 1999;340(2):115-26. doi: 10.1056/NEJM199901143400207 [published Online First: 1999/01/14]

266. Virdis A, Schiffrin EL. Vascular inflammation: a role in vascular disease in hypertension? *Curr Opin Nephrol Hypertens* 2003;12(2):181-7. doi: 10.1097/00041552-200303000-00009 [published Online First: 2003/02/18]

267. Schiffrin EL. Immune mechanisms in hypertension and vascular injury. *Clin Sci (Lond)* 2014;126(4):267-74. doi: 10.1042/CS20130407 [published Online First: 2013/10/23]

268. Dinh QN, Drummond GR, Sobey CG, et al. Roles of inflammation, oxidative stress, and vascular dysfunction in hypertension. *Biomed Res Int* 2014;2014:406960. doi: 10.1155/2014/406960 [published Online First: 2014/08/20]

269. Sprague AH, Khalil RA. Inflammatory cytokines in vascular dysfunction and vascular disease. *Biochem Pharmacol* 2009;78(6):539-52. doi: 10.1016/j.bcp.2009.04.029 [published Online First: 2009/05/06]

270. Epelman S, Liu PP, Mann DL. Role of innate and adaptive immune mechanisms in cardiac injury and repair. *Nat Rev Immunol* 2015;15(2):117-29. doi: 10.1038/nri3800 [published Online First: 2015/01/24]

271. Beutler B. Innate immunity: an overview. *Mol Immunol* 2004;40(12):845-59. doi: 10.1016/j.molimm.2003.10.005 [published Online First: 2003/12/31]

272. Lanier LL. Shades of grey--the blurring view of innate and adaptive immunity. *Nat Rev Immunol* 2013;13(2):73-4. doi: 10.1038/nri3389 [published Online First: 2013/03/08]

273. Hayday AC. [gamma][delta] cells: a right time and a right place for a conserved third way of protection. *Annu Rev Immunol* 2000;18:975-1026. doi: 10.1146/annurev.immunol.18.1.975 [published Online First: 2000/06/03]

274. Mian MO, Paradis P, Schiffrin EL. Innate immunity in hypertension. *Curr Hypertens Rep* 2014;16(2):413. doi: 10.1007/s11906-013-0413-9 [published Online First: 2014/01/11]

275. Italiani P, Boraschi D. From Monocytes to M1/M2 Macrophages: Phenotypical vs. Functional Differentiation. *Front Immunol* 2014;5:514. doi: 10.3389/fimmu.2014.00514 [published Online First: 2014/11/05]

276. Khazen W, M'Bika J P, Tomkiewicz C, et al. Expression of macrophage-selective markers in human and rodent adipocytes. *FEBS Lett* 2005;579(25):5631-4. doi: 10.1016/j.febslet.2005.09.032 [published Online First: 2005/10/11]

277. Merad M, Sathe P, Helft J, et al. The dendritic cell lineage: ontogeny and function of dendritic cells and their subsets in the steady state and the inflamed setting. *Annu Rev Immunol* 2013;31:563-604. doi: 10.1146/annurev-immunol-020711-074950 [published Online First: 2013/03/23]

278. McMaster WG, Kirabo A, Madhur MS, et al. Inflammation, immunity, and hypertensive end-organ damage. *Circ Res* 2015;116(6):1022-33. doi: 10.1161/CIRCRESAHA.116.303697 [published Online First: 2015/03/15]

279. Ginhoux F, Jung S. Monocytes and macrophages: developmental pathways and tissue homeostasis. *Nat Rev Immunol* 2014;14(6):392-404. doi: 10.1038/nri3671 [published Online First: 2014/05/24]

280. Wolf AA, Yanez A, Barman PK, et al. The Ontogeny of Monocyte Subsets. *Front Immunol* 2019;10:1642. doi: 10.3389/fimmu.2019.01642 [published Online First: 2019/08/06]

281. A complex cell. *Nat Immunol* 2016;17(1):1. doi: 10.1038/ni.3351 [published Online First: 2015/12/19]

282. Mosser DM, Edwards JP. Exploring the full spectrum of macrophage activation. *Nat Rev Immunol* 2008;8(12):958-69. doi: 10.1038/nri2448 [published Online First: 2008/11/26]

283. Stein M, Keshav S, Harris N, et al. Interleukin 4 potently enhances murine macrophage mannose receptor activity: a marker of alternative immunologic macrophage activation. *J Exp Med* 1992;176(1):287-92. doi: 10.1084/jem.176.1.287 [published Online First: 1992/07/01]

284. Doyle AG, Herbein G, Montaner LJ, et al. Interleukin-13 alters the activation state of murine macrophages in vitro: comparison with interleukin-4 and interferon-gamma. *Eur J Immunol* 1994;24(6):1441-5. doi: 10.1002/eji.1830240630 [published Online First: 1994/06/01]

285. Viola A, Munari F, Sanchez-Rodriguez R, et al. The Metabolic Signature of Macrophage Responses. *Front Immunol* 2019;10:1462. doi: 10.3389/fimmu.2019.01462 [published Online First: 2019/07/25]

286. Martinez FO, Gordon S. The M1 and M2 paradigm of macrophage activation: time for reassessment. *F1000Prime Rep* 2014;6:13. doi: 10.12703/P6-13 [published Online First: 2014/03/29]

287. Takeuch O, Akira S. Epigenetic control of macrophage polarization. *Eur J Immunol* 2011;41(9):2490-3. doi: 10.1002/eji.201141792 [published Online First: 2011/09/29]

288. Mantovani A, Biswas SK, Galdiero MR, et al. Macrophage plasticity and polarization in tissue repair and remodelling. *J Pathol* 2013;229(2):176-85. doi: 10.1002/path.4133 [published Online First: 2012/10/26]

289. Auffray C, Fogg D, Garfa M, et al. Monitoring of blood vessels and tissues by a population of monocytes with patrolling behavior. *Science* 2007;317(5838):666-70. doi: 10.1126/science.1142883 [published Online First: 2007/08/04]

290. Nahrendorf M, Swirski FK, Aikawa E, et al. The healing myocardium sequentially mobilizes two monocyte subsets with divergent and complementary functions. *J Exp Med* 2007;204(12):3037-47. doi: 10.1084/jem.20070885 [published Online First: 2007/11/21]

291. Arnold L, Henry A, Poron F, et al. Inflammatory monocytes recruited after skeletal muscle injury switch into antiinflammatory macrophages to support myogenesis. *J Exp Med* 2007;204(5):1057-69. doi: 10.1084/jem.20070075 [published Online First: 2007/05/09]

292. Crane MJ, Daley JM, van Houtte O, et al. The monocyte to macrophage transition in the murine sterile wound. *PLoS One* 2014;9(1):e86660. doi: 10.1371/journal.pone.0086660 [published Online First: 2014/01/28]

293. Wenzel P. Monocytes as immune targets in arterial hypertension. *Br J Pharmacol* 2019;176(12):1966-77. doi: 10.1111/bph.14389 [published Online First: 2018/06/10]

294. Justin Rucker A, Crowley SD. The role of macrophages in hypertension and its complications. *Pflugers Arch* 2017;469(3-4):419-30. doi: 10.1007/s00424-017-1950-x [published Online First: 2017/03/03]

295. Ko EA, Amiri F, Pandey NR, et al. Resistance artery remodeling in deoxycorticosterone acetate-salt hypertension is dependent on vascular inflammation: evidence from m-CSF-deficient mice. *Am J Physiol Heart Circ Physiol* 2007;292(4):H1789-95. doi: 10.1152/ajpheart.01118.2006 [published Online First: 2006/12/05]

296. Javeshghani D, Barhoumi T, Idris-Khodja N, et al. Reduced macrophage-dependent inflammation improves endothelin-1-induced vascular injury. *Hypertension* 2013;62(1):112-7. doi: 10.1161/HYPERTENSIONAHA.113.01298 [published Online First: 2013/05/15]

297. Wenzel P, Knorr M, Kossmann S, et al. Lysozyme M-positive monocytes mediate angiotensin II-induced arterial hypertension and vascular dysfunction. *Circulation* 2011;124(12):1370-81. doi: 10.1161/CIRCULATIONAHA.111.034470 [published Online First: 2011/08/31]

298. Ishibashi M, Hiasa K, Zhao Q, et al. Critical role of monocyte chemoattractant protein-1 receptor CCR2 on monocytes in hypertension-induced vascular inflammation and remodeling. *Circ Res* 2004;94(9):1203-10. doi: 10.1161/01.RES.0000126924.23467.A3 [published Online First: 2004/04/03]

299. Bush E, Maeda N, Kuziel WA, et al. CC chemokine receptor 2 is required for macrophage infiltration and vascular hypertrophy in angiotensin II-induced hypertension. *Hypertension* 2000;36(3):360-3. doi: 10.1161/01.hyp.36.3.360 [published Online First: 2000/09/16]

300. Liao TD, Yang XP, Liu YH, et al. Role of inflammation in the development of renal damage and dysfunction in angiotensin II-induced hypertension. *Hypertension* 2008;52(2):256-63. doi: 10.1161/HYPERTENSIONAHA.108.112706 [published Online First: 2008/06/11]

301. Kriska T, Cepura C, Magier D, et al. Mice lacking macrophage 12/15-lipoxygenase are resistant to experimental hypertension. *Am J Physiol Heart Circ Physiol* 2012;302(11):H2428-38. doi: 10.1152/ajpheart.01120.2011 [published Online First: 2012/04/03]

302. Machnik A, Neuhofer W, Jantsch J, et al. Macrophages regulate salt-dependent volume and blood pressure by a vascular endothelial growth factor-C-dependent buffering mechanism. *Nat Med* 2009;15(5):545-52. doi: 10.1038/nm.1960 [published Online First: 2009/05/05]

303. Machnik A, Dahlmann A, Kopp C, et al. Mononuclear phagocyte system depletion blocks interstitial tonicity-responsive enhancer binding protein/vascular endothelial growth factor C expression and induces salt-sensitive hypertension in rats. *Hypertension* 2010;55(3):755-61. doi: 10.1161/HYPERTENSIONAHA.109.143339 [published Online First: 2010/02/10]

304. Selvarajah V, Connolly K, McEniery C, et al. Skin Sodium and Hypertension: a Paradigm Shift? *Curr Hypertens Rep* 2018;20(11):94. doi: 10.1007/s11906-018-0892-9 [published Online First: 2018/09/15]

305. Hashimoto D, Miller J, Merad M. Dendritic cell and macrophage heterogeneity in vivo. *Immunity* 2011;35(3):323-35. doi: 10.1016/j.immuni.2011.09.007 [published Online First: 2011/09/29]

306. Lanzavecchia A, Sallusto F. Regulation of T cell immunity by dendritic cells. *Cell* 2001;106(3):263-6. doi: 10.1016/s0092-8674(01)00455-x [published Online First: 2001/08/18]

307. Kirabo A, Fontana V, de Faria AP, et al. DC isoketal-modified proteins activate T cells and promote hypertension. *J Clin Invest* 2014;124(10):4642-56. doi: 10.1172/JCI74084 [published Online First: 2014/09/23]

308. Xiao L, Patrick DM, Aden LA, et al. Mechanisms of isolevuglandin-protein adduct formation in inflammation and hypertension. *Prostaglandins Other Lipid Mediat* 2018;139:48-53. doi: 10.1016/j.prostaglandins.2018.09.008 [published Online First: 2018/10/03]

309. Barbaro NR, Foss JD, Kryshtal DO, et al. Dendritic Cell Amiloride-Sensitive Channels Mediate Sodium-Induced Inflammation and Hypertension. *Cell Rep* 2017;21(4):1009-20. doi: 10.1016/j.celrep.2017.10.002 [published Online First: 2017/10/27]

310. Xiao L, Kirabo A, Wu J, et al. Renal Denervation Prevents Immune Cell Activation and Renal Inflammation in Angiotensin II-Induced Hypertension. *Circ Res* 2015;117(6):547-57. doi: 10.1161/CIRCRESAHA.115.306010 [published Online First: 2015/07/15]

311. Vinh A, Chen W, Blinder Y, et al. Inhibition and genetic ablation of the B7/CD28 T-cell costimulation axis prevents experimental hypertension. *Circulation* 2010;122(24):2529-37. doi: 10.1161/CIRCULATIONAHA.109.930446 [published Online First: 2010/12/04]

312. Rosales C. Neutrophil: A Cell with Many Roles in Inflammation or Several Cell Types? *Front Physiol* 2018;9:113. doi: 10.3389/fphys.2018.00113 [published Online First: 2018/03/09]

313. Silvestre-Roig C, Braster Q, Ortega-Gomez A, et al. Neutrophils as regulators of cardiovascular inflammation. *Nat Rev Cardiol* 2020;17(6):327-40. doi: 10.1038/s41569-019-0326-7 [published Online First: 2020/01/31]

314. Araos P, Figueroa S, Amador CA. The Role of Neutrophils in Hypertension. *Int J Mol Sci* 2020;21(22) doi: 10.3390/ijms21228536 [published Online First: 2020/11/18]

315. Tatsukawa Y, Hsu WL, Yamada M, et al. White blood cell count, especially neutrophil count, as a predictor of hypertension in a Japanese population. *Hypertens Res* 2008;31(7):1391-7. doi: 10.1291/hypres.31.1391 [published Online First: 2008/10/30]

316. Liu X, Zhang Q, Wu H, et al. Blood Neutrophil to Lymphocyte Ratio as a Predictor of Hypertension. *Am J Hypertens* 2015;28(11):1339-46. doi: 10.1093/ajh/hpv034 [published Online First: 2015/04/01]

317. Sunbul M, Gerin F, Durmus E, et al. Neutrophil to lymphocyte and platelet to lymphocyte ratio in patients with dipper versus non-dipper hypertension. *Clin Exp Hypertens* 2014;36(4):217-21. doi: 10.3109/10641963.2013.804547 [published Online First: 2013/06/22]

318. Zhang R, Inagawa H, Kazumura K, et al. Evaluation of a Hypertensive Rat Model Using Peripheral Blood Neutrophil Activity, Phagocytic Activity and Oxidized LDL Evaluation. *Anticancer Res* 2018;38(7):4289-94. doi: 10.21873/anticanres.12726 [published Online First: 2018/07/05]

319. Morton J, Coles B, Wright K, et al. Circulating neutrophils maintain physiological blood pressure by suppressing bacteria and IFNgamma-dependent iNOS expression in the vasculature of healthy mice. *Blood* 2008;111(10):5187-94. doi: 10.1182/blood-2007-10-117283 [published Online First: 2008/02/19]

320. Chrysanthopoulou A, Gkaliagkousi E, Lazaridis A, et al. Angiotensin II triggers release of neutrophil extracellular traps, linking thromboinflammation with essential hypertension. *JCI Insight* 2021;6(18) doi: 10.1172/jci.insight.148668 [published Online First: 2021/07/30]

321. Gabrilovich DI, Nagaraj S. Myeloid-derived suppressor cells as regulators of the immune system. *Nat Rev Immunol* 2009;9(3):162-74. doi: 10.1038/nri2506 [published Online First: 2009/02/07]

322. Pan PY, Wang GX, Yin B, et al. Reversion of immune tolerance in advanced malignancy: modulation of myeloid-derived suppressor cell development by blockade of stem-cell factor function. *Blood* 2008;111(1):219-28. doi: 10.1182/blood-2007-04-086835 [published Online First: 2007/09/22]

323. Shah KH, Shi P, Giani JF, et al. Myeloid Suppressor Cells Accumulate and Regulate Blood Pressure in Hypertension. *Circ Res* 2015;117(10):858-69. doi: 10.1161/CIRCRESAHA.115.306539 [published Online First: 2015/08/22]

324. Chiasson VL, Bounds KR, Chatterjee P, et al. Myeloid-Derived Suppressor Cells Ameliorate Cyclosporine A-Induced Hypertension in Mice. *Hypertension* 2018;71(1):199-207. doi: 10.1161/HYPERTENSIONAHA.117.10306 [published Online First: 2017/11/15]

325. Caillon A, Paradis P, Schiffrin EL. Role of immune cells in hypertension. *Br J Pharmacol* 2019;176(12):1818-28. doi: 10.1111/bph.14427 [published Online First: 2018/06/29]

326. Davis MM, Bjorkman PJ. T-cell antigen receptor genes and T-cell recognition. *Nature* 1988;334(6181):395-402. doi: 10.1038/334395a0 [published Online First: 1988/08/04]

327. Wucherpfennig KW, Gagnon E, Call MJ, et al. Structural biology of the T-cell receptor: insights into receptor assembly, ligand recognition, and initiation of signaling. *Cold Spring Harb Perspect Biol* 2010;2(4):a005140. doi: 10.1101/cshperspect.a005140 [published Online First: 2010/05/11]

328. Idris-Khodja N, Mian MO, Paradis P, et al. Dual opposing roles of adaptive immunity in hypertension. *Eur Heart J* 2014;35(19):1238-44. doi: 10.1093/eurheartj/ehu119 [published Online First: 2014/04/02]

329. Zhang N, Bevan MJ. CD8(+) T cells: foot soldiers of the immune system. *Immunity* 2011;35(2):161-8. doi: 10.1016/j.immuni.2011.07.010 [published Online First: 2011/08/27]

330. Kidd P. Th1/Th2 balance: the hypothesis, its limitations, and implications for health and disease. *Altern Med Rev* 2003;8(3):223-46. [published Online First: 2003/08/30]

331. O'Shea JJ, Paul WE. Mechanisms underlying lineage commitment and plasticity of helper CD4+ T cells. *Science* 2010;327(5969):1098-102. doi: 10.1126/science.1178334 [published Online First: 2010/02/27]

332. Mitchell RE, Hassan M, Burton BR, et al. IL-4 enhances IL-10 production in Th1 cells: implications for Th1 and Th2 regulation. *Sci Rep* 2017;7(1):11315. doi: 10.1038/s41598-017-11803-y [published Online First: 2017/09/14]

333. Uyemura K, Demer LL, Castle SC, et al. Cross-regulatory roles of interleukin (IL)-12 and IL-10 in atherosclerosis. *J Clin Invest* 1996;97(9):2130-8. doi: 10.1172/JCI118650 [published Online First: 1996/05/01]

334. Shao J, Nangaku M, Miyata T, et al. Imbalance of T-cell subsets in angiotensin II-infused hypertensive rats with kidney injury. *Hypertension* 2003;42(1):31-8. doi: 10.1161/01.HYP.0000075082.06183.4E [published Online First: 2003/05/29]

335. Mazzolai L, Duchosal MA, Korber M, et al. Endogenous angiotensin II induces atherosclerotic plaque vulnerability and elicits a Th1 response in ApoE-/- mice. *Hypertension* 2004;44(3):277-82. doi: 10.1161/01.HYP.0000140269.55873.7b [published Online First: 2004/08/11]

336. Kossmann S, Schwenk M, Hausding M, et al. Angiotensin II-induced vascular dysfunction depends on interferon-gamma-driven immune cell recruitment and mutual activation of monocytes and NK-cells. *Arterioscler Thromb Vasc Biol* 2013;33(6):1313-9. doi: 10.1161/ATVBAHA.113.301437 [published Online First: 2013/03/23]

337. Xia Y, Entman ML, Wang Y. Critical role of CXCL16 in hypertensive kidney injury and fibrosis. *Hypertension* 2013;62(6):1129-37. doi: 10.1161/HYPERTENSIONAHA.113.01837 [published Online First: 2013/09/26]

338. van Heuven-Nolsen D, De Kimpe SJ, Muis T, et al. Opposite role of interferon-gamma and interleukin-4 on the regulation of blood pressure in mice. *Biochem Biophys Res Commun* 1999;254(3):816-20. doi: 10.1006/bbrc.1998.8742 [published Online First: 1999/01/28]

339. Ishimitsu T, Uehara Y, Numabe A, et al. Interferon gamma attenuates hypertensive renal injury in salt-sensitive Dahl rats. *Hypertension* 1992;19(6 Pt 2):804-8. doi: 10.1161/01.hyp.19.6.804 [published Online First: 1992/06/01]

340. Bettelli E, Carrier Y, Gao W, et al. Reciprocal developmental pathways for the generation of pathogenic effector TH17 and regulatory T cells. *Nature* 2006;441(7090):235-8. doi: 10.1038/nature04753 [published Online First: 2006/05/02]

341. Korn T, Bettelli E, Oukka M, et al. IL-17 and Th17 Cells. *Annu Rev Immunol* 2009;27:485-517. doi: 10.1146/annurev.immunol.021908.132710 [published Online First: 2009/01/10]

342. Curtis MM, Way SS. Interleukin-17 in host defence against bacterial, mycobacterial and fungal pathogens. *Immunology* 2009;126(2):177-85. doi: 10.1111/j.1365-2567.2008.03017.x [published Online First: 2009/01/08]

343. Maddur MS, Miossec P, Kaveri SV, et al. Th17 cells: biology, pathogenesis of autoimmune and inflammatory diseases, and therapeutic strategies. *Am J Pathol* 2012;181(1):8-18. doi: 10.1016/j.ajpath.2012.03.044 [published Online First: 2012/05/30]

344. Tesmer LA, Lundy SK, Sarkar S, et al. Th17 cells in human disease. *Immunol Rev* 2008;223:87-113. doi: 10.1111/j.1600-065X.2008.00628.x [published Online First: 2008/07/11]

345. Milovanovic J, Arsenijevic A, Stojanovic B, et al. Interleukin-17 in Chronic Inflammatory Neurological Diseases. *Front Immunol* 2020;11:947. doi: 10.3389/fimmu.2020.00947 [published Online First: 2020/06/26]

346. Xu S, Cao X. Interleukin-17 and its expanding biological functions. *Cell Mol Immunol* 2010;7(3):164-74. doi: 10.1038/cmi.2010.21 [published Online First: 2010/04/13]

347. Schnyder B, Schnyder-Candrian S, Pansky A, et al. IL-17 reduces TNF-induced Rantes and VCAM-1 expression. *Cytokine* 2005;31(3):191-202. doi: 10.1016/j.cyto.2005.02.012 [published Online First: 2005/06/25]

348. Madhur MS, Lob HE, McCann LA, et al. Interleukin 17 promotes angiotensin II-induced hypertension and vascular dysfunction. *Hypertension* 2010;55(2):500-7. doi: 10.1161/HYPERTENSIONAHA.109.145094 [published Online First: 2009/12/30]

349. Nguyen H, Chiasson VL, Chatterjee P, et al. Interleukin-17 causes Rho-kinase-mediated endothelial dysfunction and hypertension. *Cardiovasc Res* 2013;97(4):696-704. doi: 10.1093/cvr/cvs422 [published Online First: 2012/12/25]

350. Amador CA, Barrientos V, Pena J, et al. Spironolactone decreases DOCA-salt-induced organ damage by blocking the activation of T helper 17 and the downregulation of regulatory T lymphocytes. *Hypertension* 2014;63(4):797-803. doi: 10.1161/HYPERTENSIONAHA.113.02883 [published Online First: 2014/01/15]

351. Kleinewietfeld M, Manzel A, Titze J, et al. Sodium chloride drives autoimmune disease by the induction of pathogenic TH17 cells. *Nature* 2013;496(7446):518-22. doi: 10.1038/nature11868 [published Online First: 2013/03/08]

352. Wallace K, Richards S, Dhillon P, et al. CD4+ T-helper cells stimulated in response to placental ischemia mediate hypertension during pregnancy. *Hypertension* 2011;57(5):949-55. doi: 10.1161/HYPERTENSIONAHA.110.168344 [published Online First: 2011/04/06]

353. Cornelius DC, Hogg JP, Scott J, et al. Administration of interleukin-17 soluble receptor C suppresses TH17 cells, oxidative stress, and hypertension in response to placental ischemia during pregnancy. *Hypertension* 2013;62(6):1068-73. doi: 10.1161/HYPERTENSIONAHA.113.01514 [published Online First: 2013/09/26]

354. Freudenberg K, Lindner N, Dohnke S, et al. Critical Role of TGF-beta and IL-2 Receptor Signaling in Foxp3 Induction by an Inhibitor of DNA Methylation. *Front Immunol* 2018;9:125. doi: 10.3389/fimmu.2018.00125 [published Online First: 2018/02/20]

355. Dejaco C, Duftner C, Grubeck-Loebenstein B, et al. Imbalance of regulatory T cells in human autoimmune diseases. *Immunology* 2006;117(3):289-300. doi: 10.1111/j.1365-2567.2005.02317.x [published Online First: 2006/02/16]

356. Fehervari Z, Sakaguchi S. CD4+ Tregs and immune control. *J Clin Invest* 2004;114(9):1209-17. doi: 10.1172/JCI23395 [published Online First: 2004/11/03]

357. Lu L, Barbi J, Pan F. The regulation of immune tolerance by FOXP3. *Nat Rev Immunol* 2017;17(11):703-17. doi: 10.1038/nri.2017.75 [published Online First: 2017/08/02]

358. Cools N, Ponsaerts P, Van Tendeloo VF, et al. Regulatory T cells and human disease. *Clin Dev Immunol* 2007;2007:89195. doi: 10.1155/2007/89195 [published Online First: 2008/03/05]

359. Sakaguchi S. Naturally arising Foxp3-expressing CD25+CD4+ regulatory T cells in immunological tolerance to self and non-self. *Nat Immunol* 2005;6(4):345-52. doi: 10.1038/ni1178 [published Online First: 2005/03/24]

360. Vignali DA, Collison LW, Workman CJ. How regulatory T cells work. *Nat Rev Immunol* 2008;8(7):523-32. doi: 10.1038/nri2343 [published Online First: 2008/06/21]

361. Wu Y, Borde M, Heissmeyer V, et al. FOXP3 controls regulatory T cell function through cooperation with NFAT. *Cell* 2006;126(2):375-87. doi: 10.1016/j.cell.2006.05.042 [published Online First: 2006/07/29]

362. Ono M, Yaguchi H, Ohkura N, et al. Foxp3 controls regulatory T-cell function by interacting with AML1/Runx1. *Nature* 2007;446(7136):685-9. doi: 10.1038/nature05673 [published Online First: 2007/03/23]

363. Noble A, Giorgini A, Leggat JA. Cytokine-induced IL-10-secreting CD8 T cells represent a phenotypically distinct suppressor T-cell lineage. *Blood* 2006;107(11):4475-83. doi: 10.1182/blood-2005-10-3994 [published Online First: 2006/02/10]

364. Zou Q, Wu B, Xue J, et al. CD8+ Treg cells suppress CD8+ T cell-responses by IL-10-dependent mechanism during H5N1 influenza virus infection. *Eur J Immunol* 2014;44(1):103-14. doi: 10.1002/eji.201343583 [published Online First: 2013/10/12]

365. Mocellin S, Marincola F, Rossi CR, et al. The multifaceted relationship between IL-10 and adaptive immunity: putting together the pieces of a puzzle. *Cytokine Growth Factor Rev* 2004;15(1):61-76. doi: 10.1016/j.cytogfr.2003.11.001 [published Online First: 2004/01/30]

366. Wan YY, Flavell RA. 'Yin-Yang' functions of transforming growth factor-beta and T regulatory cells in immune regulation. *Immunol Rev* 2007;220:199-213. doi: 10.1111/j.1600-065X.2007.00565.x [published Online First: 2007/11/06]

367. Carrier Y, Yuan J, Kuchroo VK, et al. Th3 cells in peripheral tolerance. I. Induction of Foxp3-positive regulatory T cells by Th3 cells derived from TGF-beta T cell-transgenic mice. *J Immunol* 2007;178(1):179-85. doi: 10.4049/jimmunol.178.1.179 [published Online First: 2006/12/22]

368. Takahashi T, Kuniyasu Y, Toda M, et al. Immunologic self-tolerance maintained by CD25+CD4+ naturally anergic and suppressive T cells: induction of autoimmune disease

by breaking their anergic/suppressive state. *Int Immunol* 1998;10(12):1969-80. doi: 10.1093/intimm/10.12.1969 [published Online First: 1999/01/14]

369. Wahl SM, Chen W. Transforming growth factor-beta-induced regulatory T cells referee inflammatory and autoimmune diseases. *Arthritis Res Ther* 2005;7(2):62-8. doi: 10.1186/ar1504 [published Online First: 2005/03/04]
370. Gordon KJ, Blobe GC. Role of transforming growth factor-beta superfamily signaling pathways in human disease. *Biochim Biophys Acta* 2008;1782(4):197-228. doi: 10.1016/j.bbadis.2008.01.006 [published Online First: 2008/03/04]
371. Ruiz-Ortega M, Rodriguez-Vita J, Sanchez-Lopez E, et al. TGF-beta signaling in vascular fibrosis. *Cardiovasc Res* 2007;74(2):196-206. doi: 10.1016/j.cardiores.2007.02.008 [published Online First: 2007/03/23]
372. Niedbala W, Wei XQ, Cai B, et al. IL-35 is a novel cytokine with therapeutic effects against collagen-induced arthritis through the expansion of regulatory T cells and suppression of Th17 cells. *Eur J Immunol* 2007;37(11):3021-9. doi: 10.1002/eji.200737810 [published Online First: 2007/09/18]
373. Garin MI, Chu CC, Golshayan D, et al. Galectin-1: a key effector of regulation mediated by CD4+CD25+ T cells. *Blood* 2007;109(5):2058-65. doi: 10.1182/blood-2006-04-016451 [published Online First: 2006/11/18]
374. Rabinovich GA, Baum LG, Tinari N, et al. Galectins and their ligands: amplifiers, silencers or tuners of the inflammatory response? *Trends Immunol* 2002;23(6):313-20. doi: 10.1016/s1471-4906(02)02232-9 [published Online First: 2002/06/20]
375. Rabinovich GA, Ariel A, Hershkoviz R, et al. Specific inhibition of T-cell adhesion to extracellular matrix and proinflammatory cytokine secretion by human recombinant galectin-1. *Immunology* 1999;97(1):100-6. doi: 10.1046/j.1365-2567.1999.00746.x [published Online First: 1999/08/14]
376. Sojka DK, Huang YH, Fowell DJ. Mechanisms of regulatory T-cell suppression - a diverse arsenal for a moving target. *Immunology* 2008;124(1):13-22. doi: 10.1111/j.1365-2567.2008.02813.x [published Online First: 2008/03/19]
377. Gondek DC, Lu LF, Quezada SA, et al. Cutting edge: contact-mediated suppression by CD4+CD25+ regulatory cells involves a granzyme B-dependent, perforin-independent

mechanism. *J Immunol* 2005;174(4):1783-6. doi: 10.4049/jimmunol.174.4.1783 [published Online First: 2005/02/09]

378. Grossman WJ, Verbsky JW, Barchet W, et al. Human T regulatory cells can use the perforin pathway to cause autologous target cell death. *Immunity* 2004;21(4):589-601. doi: 10.1016/j.immuni.2004.09.002 [published Online First: 2004/10/16]
379. Kobie JJ, Shah PR, Yang L, et al. T regulatory and primed uncommitted CD4 T cells express CD73, which suppresses effector CD4 T cells by converting 5'-adenosine monophosphate to adenosine. *J Immunol* 2006;177(10):6780-6. doi: 10.4049/jimmunol.177.10.6780 [published Online First: 2006/11/04]
380. Deaglio S, Dwyer KM, Gao W, et al. Adenosine generation catalyzed by CD39 and CD73 expressed on regulatory T cells mediates immune suppression. *J Exp Med* 2007;204(6):1257-65. doi: 10.1084/jem.20062512 [published Online First: 2007/05/16]
381. Sakaguchi S, Yamaguchi T, Nomura T, et al. Regulatory T cells and immune tolerance. *Cell* 2008;133(5):775-87. doi: 10.1016/j.cell.2008.05.009 [published Online First: 2008/05/31]
382. Misra N, Bayry J, Lacroix-Desmazes S, et al. Cutting edge: human CD4+CD25+ T cells restrain the maturation and antigen-presenting function of dendritic cells. *J Immunol* 2004;172(8):4676-80. doi: 10.4049/jimmunol.172.8.4676 [published Online First: 2004/04/07]
383. Watanabe K, Rao VP, Poutahidis T, et al. Cytotoxic-T-lymphocyte-associated antigen 4 blockade abrogates protection by regulatory T cells in a mouse model of microbially induced innate immune-driven colitis. *Infect Immun* 2008;76(12):5834-42. doi: 10.1128/IAI.00542-08 [published Online First: 2008/10/01]
384. Sarris M, Andersen KG, Randow F, et al. Neuropilin-1 expression on regulatory T cells enhances their interactions with dendritic cells during antigen recognition. *Immunity* 2008;28(3):402-13. doi: 10.1016/j.immuni.2008.01.012 [published Online First: 2008/03/11]
385. Shalev I, Liu H, Koscik C, et al. Targeted deletion of fgl2 leads to impaired regulatory T cell activity and development of autoimmune glomerulonephritis. *J Immunol* 2008;180(1):249-60. doi: 10.4049/jimmunol.180.1.249 [published Online First: 2007/12/22]

386. Viel EC, Lemarie CA, Benkirane K, et al. Immune regulation and vascular inflammation in genetic hypertension. *Am J Physiol Heart Circ Physiol* 2010;298(3):H938-44. doi: 10.1152/ajpheart.00707.2009 [published Online First: 2010/01/02]

387. Gibbs RA, Weinstock GM, Metzker ML, et al. Genome sequence of the Brown Norway rat yields insights into mammalian evolution. *Nature* 2004;428(6982):493-521. doi: 10.1038/nature02426 [published Online First: 2004/04/02]

388. Barhoumi T, Kasal DA, Li MW, et al. T regulatory lymphocytes prevent angiotensin II-induced hypertension and vascular injury. *Hypertension* 2011;57(3):469-76. doi: 10.1161/HYPERTENSIONAHA.110.162941 [published Online First: 2011/01/26]

389. Kasal DA, Barhoumi T, Li MW, et al. T regulatory lymphocytes prevent aldosterone-induced vascular injury. *Hypertension* 2012;59(2):324-30. doi: 10.1161/HYPERTENSIONAHA.111.181123 [published Online First: 2011/12/08]

390. Kvakan H, Kleinewietfeld M, Qadri F, et al. Regulatory T cells ameliorate angiotensin II-induced cardiac damage. *Circulation* 2009;119(22):2904-12. doi: 10.1161/CIRCULATIONAHA.108.832782 [published Online First: 2009/05/28]

391. Matrougui K, Abd Elmageed Z, Kassan M, et al. Natural regulatory T cells control coronary arteriolar endothelial dysfunction in hypertensive mice. *Am J Pathol* 2011;178(1):434-41. doi: 10.1016/j.ajpath.2010.11.034 [published Online First: 2011/01/13]

392. Mian MO, Barhoumi T, Briet M, et al. Deficiency of T-regulatory cells exaggerates angiotensin II-induced microvascular injury by enhancing immune responses. *J Hypertens* 2016;34(1):97-108. doi: 10.1097/HJH.0000000000000761 [published Online First: 2015/12/03]

393. Didion SP, Kinzenbaw DA, Schrader LI, et al. Endogenous interleukin-10 inhibits angiotensin II-induced vascular dysfunction. *Hypertension* 2009;54(3):619-24. doi: 10.1161/HYPERTENSIONAHA.109.137158 [published Online First: 2009/07/22]

394. Kassan M, Galan M, Partyka M, et al. Interleukin-10 released by CD4(+)CD25(+) natural regulatory T cells improves microvascular endothelial function through inhibition of NADPH oxidase activity in hypertensive mice. *Arterioscler Thromb Vasc Biol* 2011;31(11):2534-42. doi: 10.1161/ATVBAHA.111.233262 [published Online First: 2011/08/06]

395. Cerwenka A, Carter LL, Reome JB, et al. In vivo persistence of CD8 polarized T cell subsets producing type 1 or type 2 cytokines. *J Immunol* 1998;161(1):97-105. [published Online First: 1998/07/01]

396. Mittrucker HW, Visekruna A, Huber M. Heterogeneity in the differentiation and function of CD8(+) T cells. *Arch Immunol Ther Exp (Warsz)* 2014;62(6):449-58. doi: 10.1007/s00005-014-0293-y [published Online First: 2014/06/01]

397. Bhat P, Leggatt G, Waterhouse N, et al. Interferon-gamma derived from cytotoxic lymphocytes directly enhances their motility and cytotoxicity. *Cell Death Dis* 2017;8(6):e2836. doi: 10.1038/cddis.2017.67 [published Online First: 2017/06/02]

398. He D, Wu L, Kim HK, et al. CD8+ IL-17-producing T cells are important in effector functions for the elicitation of contact hypersensitivity responses. *J Immunol* 2006;177(10):6852-8. doi: 10.4049/jimmunol.177.10.6852 [published Online First: 2006/11/04]

399. Redmond WL, Wei CH, Kreuwel HT, et al. The apoptotic pathway contributing to the deletion of naive CD8 T cells during the induction of peripheral tolerance to a cross-presented self-antigen. *J Immunol* 2008;180(8):5275-82. doi: 10.4049/jimmunol.180.8.5275 [published Online First: 2008/04/09]

400. Simon MM, Waring P, Lobigs M, et al. Cytotoxic T cells specifically induce Fas on target cells, thereby facilitating exocytosis-independent induction of apoptosis. *J Immunol* 2000;165(7):3663-72. doi: 10.4049/jimmunol.165.7.3663 [published Online First: 2000/10/18]

401. Trott DW, Thabet SR, Kirabo A, et al. Oligoclonal CD8+ T cells play a critical role in the development of hypertension. *Hypertension* 2014;64(5):1108-15. doi: 10.1161/HYPERTENSIONAHA.114.04147 [published Online First: 2014/09/27]

402. Sun XN, Li C, Liu Y, et al. T-Cell Mineralocorticoid Receptor Controls Blood Pressure by Regulating Interferon-Gamma. *Circ Res* 2017;120(10):1584-97. doi: 10.1161/CIRCRESAHA.116.310480 [published Online First: 2017/03/17]

403. Youn JC, Yu HT, Lim BJ, et al. Immunosenescent CD8+ T cells and C-X-C chemokine receptor type 3 chemokines are increased in human hypertension. *Hypertension* 2013;62(1):126-33. doi: 10.1161/HYPERTENSIONAHA.113.00689 [published Online First: 2013/05/30]

404. Shen Y, Cheng F, Sharma M, et al. Granzyme B Deficiency Protects against Angiotensin II-Induced Cardiac Fibrosis. *Am J Pathol* 2016;186(1):87-100. doi: 10.1016/j.ajpath.2015.09.010 [published Online First: 2015/11/28]

405. Bennett MS, Round JL, Leung DT. Innate-like lymphocytes in intestinal infections. *Curr Opin Infect Dis* 2015;28(5):457-63. doi: 10.1097/QCO.0000000000000189 [published Online First: 2015/08/14]

406. Godfrey DI, Uldrich AP, McCluskey J, et al. The burgeoning family of unconventional T cells. *Nat Immunol* 2015;16(11):1114-23. doi: 10.1038/ni.3298 [published Online First: 2015/10/21]

407. Brandes M, Willimann K, Moser B. Professional antigen-presentation function by human gammadelta T Cells. *Science* 2005;309(5732):264-8. doi: 10.1126/science.1110267 [published Online First: 2005/06/04]

408. Borst J, Coligan JE, Oettgen H, et al. The delta- and epsilon-chains of the human T3/T-cell receptor complex are distinct polypeptides. *Nature* 1984;312(5993):455-8. doi: 10.1038/312455a0 [published Online First: 1984/11/05]

409. Yanagi Y, Yoshikai Y, Leggett K, et al. A human T cell-specific cDNA clone encodes a protein having extensive homology to immunoglobulin chains. *Nature* 1984;308(5955):145-9. doi: 10.1038/308145a0 [published Online First: 1984/03/08]

410. Sim GK, Yague J, Nelson J, et al. Primary structure of human T-cell receptor alpha-chain. *Nature* 1984;312(5996):771-5. doi: 10.1038/312771a0 [published Online First: 1984/12/20]

411. Brenner MB, Trowbridge IS, Strominger JL. Cross-linking of human T cell receptor proteins: association between the T cell idiotype beta subunit and the T3 glycoprotein heavy subunit. *Cell* 1985;40(1):183-90. doi: 10.1016/0092-8674(85)90321-6 [published Online First: 1985/01/01]

412. Saito H, Kranz DM, Takagaki Y, et al. Complete primary structure of a heterodimeric T-cell receptor deduced from cDNA sequences. *Nature* 1984;309(5971):757-62. doi: 10.1038/309757a0 [published Online First: 1984/06/04]

413. Kranz DM, Saito H, Disteche CM, et al. Chromosomal locations of the murine T-cell receptor alpha-chain gene and the T-cell gamma gene. *Science* 1985;227(4689):941-5. doi: 10.1126/science.3918347 [published Online First: 1985/02/22]

414. Kranz DM, Saito H, Heller M, et al. Limited diversity of the rearranged T-cell gamma gene. *Nature* 1985;313(6005):752-5. doi: 10.1038/313752a0 [published Online First: 1985/02/06]

415. Chien YH, Iwashima M, Wettstein DA, et al. T-cell receptor delta gene rearrangements in early thymocytes. *Nature* 1987;330(6150):722-7. doi: 10.1038/330722a0 [published Online First: 1987/12/24]

416. Chien YH, Iwashima M, Kaplan KB, et al. A new T-cell receptor gene located within the alpha locus and expressed early in T-cell differentiation. *Nature* 1987;327(6124):677-82. doi: 10.1038/327677a0 [published Online First: 1987/06/01]

417. Brenner MB, McLean J, Dialynas DP, et al. Identification of a putative second T-cell receptor. *Nature* 1986;322(6075):145-9. doi: 10.1038/322145a0 [published Online First: 1986/07/10]

418. Bank I, DePinho RA, Brenner MB, et al. A functional T3 molecule associated with a novel heterodimer on the surface of immature human thymocytes. *Nature* 1986;322(6075):179-81. doi: 10.1038/322179a0 [published Online First: 1986/07/10]

419. Brenner MB, McLean J, Scheft H, et al. Two forms of the T-cell receptor gamma protein found on peripheral blood cytotoxic T lymphocytes. *Nature* 1987;325(6106):689-94. doi: 10.1038/325689a0 [published Online First: 1987/02/19]

420. Bluestone JA, Pardoll D, Sharrow SO, et al. Characterization of murine thymocytes with CD3-associated T-cell receptor structures. *Nature* 1987;326(6108):82-4. doi: 10.1038/326082a0 [published Online First: 1987/03/05]

421. Born WK, O'Brien RL. Discovery of the gammadelta TCR: Act II. *J Immunol* 2016;196(9):3507-8. doi: 10.4049/jimmunol.1600404 [published Online First: 2016/05/18]

422. Fowlkes BJ, Pardoll DM. Molecular and cellular events of T cell development. *Adv Immunol* 1989;44:207-64. doi: 10.1016/s0065-2776(08)60643-4 [published Online First: 1989/01/01]

423. Su C, Jakobsen I, Gu X, et al. Diversity and evolution of T-cell receptor variable region genes in mammals and birds. *Immunogenetics* 1999;50(5-6):301-8. doi: 10.1007/s002510050606 [published Online First: 2000/01/12]

424. Schatz DG, Ji Y. Recombination centres and the orchestration of V(D)J recombination. *Nat Rev Immunol* 2011;11(4):251-63. doi: 10.1038/nri2941 [published Online First: 2011/03/12]

425. Akamatsu Y, Oettinger MA. Distinct roles of RAG1 and RAG2 in binding the V(D)J recombination signal sequences. *Mol Cell Biol* 1998;18(8):4670-8. doi: 10.1128/MCB.18.8.4670 [published Online First: 1998/07/22]

426. Sewell AK. Why must T cells be cross-reactive? *Nat Rev Immunol* 2012;12(9):669-77. doi: 10.1038/nri3279 [published Online First: 2012/08/25]

427. Wilson A, de Villartay JP, MacDonald HR. T cell receptor delta gene rearrangement and T early alpha (TEA) expression in immature alpha beta lineage thymocytes: implications for alpha beta/gamma delta lineage commitment. *Immunity* 1996;4(1):37-45. doi: 10.1016/s1074-7613(00)80296-4 [published Online First: 1996/01/01]

428. Heilig JS, Tonegawa S. Diversity of murine gamma genes and expression in fetal and adult T lymphocytes. *Nature* 1986;322(6082):836-40. doi: 10.1038/322836a0 [published Online First: 1986/08/03]

429. Huck S, Dariavach P, Lefranc MP. Variable region genes in the human T-cell rearranging gamma (TRG) locus: V-J junction and homology with the mouse genes. *EMBO J* 1988;7(3):719-26. [published Online First: 1988/03/01]

430. Garman RD, Doherty PJ, Raulet DH. Diversity, rearrangement, and expression of murine T cell gamma genes. *Cell* 1986;45(5):733-42. doi: 10.1016/0092-8674(86)90787-7 [published Online First: 1986/06/06]

431. Arden B, Clark SP, Kabelitz D, et al. Mouse T-cell receptor variable gene segment families. *Immunogenetics* 1995;42(6):501-30. doi: 10.1007/BF00172177 [published Online First: 1995/01/01]

432. Elliott JF, Rock EP, Patten PA, et al. The adult T-cell receptor delta-chain is diverse and distinct from that of fetal thymocytes. *Nature* 1988;331(6157):627-31. doi: 10.1038/331627a0 [published Online First: 1988/02/18]

433. Allison TJ, Garboczi DN. Structure of gammadelta T cell receptors and their recognition of non-peptide antigens. *Mol Immunol* 2002;38(14):1051-61. doi: 10.1016/s0161-5890(02)00034-2 [published Online First: 2002/04/17]

434. Allison TJ, Winter CC, Fournie JJ, et al. Structure of a human gammadelta T-cell antigen receptor. *Nature* 2001;411(6839):820-4. doi: 10.1038/35081115 [published Online First: 2001/07/19]

435. Deseke M, Prinz I. Ligand recognition by the gammadelta TCR and discrimination between homeostasis and stress conditions. *Cell Mol Immunol* 2020;17(9):914-24. doi: 10.1038/s41423-020-0503-y [published Online First: 2020/07/28]

436. Hayday AC, Vantourout P. The Innate Biologies of Adaptive Antigen Receptors. *Annu Rev Immunol* 2020;38:487-510. doi: 10.1146/annurev-immunol-102819-023144 [published Online First: 2020/02/06]

437. Willcox BE, Willcox CR. gammadelta TCR ligands: the quest to solve a 500-million-year-old mystery. *Nat Immunol* 2019;20(2):121-28. doi: 10.1038/s41590-018-0304-y [published Online First: 2019/01/22]

438. Vermijlen D, Gatti D, Kouzeli A, et al. gammadelta T cell responses: How many ligands will it take till we know? *Semin Cell Dev Biol* 2018;84:75-86. doi: 10.1016/j.semcdb.2017.10.009 [published Online First: 2018/02/07]

439. Groh V, Steinle A, Bauer S, et al. Recognition of stress-induced MHC molecules by intestinal epithelial gammadelta T cells. *Science* 1998;279(5357):1737-40. doi: 10.1126/science.279.5357.1737 [published Online First: 1998/03/28]

440. Matis LA, Fry AM, Cron RQ, et al. Structure and specificity of a class II MHC alloreactive gamma delta T cell receptor heterodimer. *Science* 1989;245(4919):746-9. doi: 10.1126/science.2528206 [published Online First: 1989/08/18]

441. Uldrich AP, Le Nours J, Pellicci DG, et al. CD1d-lipid antigen recognition by the gammadelta TCR. *Nat Immunol* 2013;14(11):1137-45. doi: 10.1038/ni.2713 [published Online First: 2013/10/01]

442. Ito K, Van Kaer L, Bonneville M, et al. Recognition of the product of a novel MHC TL region gene (27b) by a mouse gamma delta T cell receptor. *Cell* 1990;62(3):549-61. doi: 10.1016/0092-8674(90)90019-b [published Online First: 1990/08/10]

443. Schild H, Mavaddat N, Litzenberger C, et al. The nature of major histocompatibility complex recognition by gamma delta T cells. *Cell* 1994;76(1):29-37. doi: 10.1016/0092-8674(94)90170-8 [published Online First: 1994/01/14]

444. Crowley MP, Fahrer AM, Baumgarth N, et al. A population of murine gammadelta T cells that recognize an inducible MHC class Ib molecule. *Science* 2000;287(5451):314-6. doi: 10.1126/science.287.5451.314 [published Online First: 2000/01/15]

445. Shin S, El-Diwany R, Schaffert S, et al. Antigen recognition determinants of gammadelta T cell receptors. *Science* 2005;308(5719):252-5. doi: 10.1126/science.1106480 [published Online First: 2005/04/12]

446. Dieude M, Striegl H, Tyznik AJ, et al. Cardiolipin binds to CD1d and stimulates CD1d-restricted gammadelta T cells in the normal murine repertoire. *J Immunol* 2011;186(8):4771-81. doi: 10.4049/jimmunol.1000921 [published Online First: 2011/03/11]

447. Zeng X, Wei YL, Huang J, et al. gammadelta T cells recognize a microbial encoded B cell antigen to initiate a rapid antigen-specific interleukin-17 response. *Immunity* 2012;37(3):524-34. doi: 10.1016/j.immuni.2012.06.011 [published Online First: 2012/09/11]

448. Chien YH, Zeng X, Prinz I. The natural and the inducible: interleukin (IL)-17-producing gammadelta T cells. *Trends Immunol* 2013;34(4):151-4. doi: 10.1016/j.it.2012.11.004 [published Online First: 2012/12/26]

449. Morita CT, Jin C, Sarikonda G, et al. Nonpeptide antigens, presentation mechanisms, and immunological memory of human Vgamma2Vdelta2 T cells: discriminating friend from foe through the recognition of prenyl pyrophosphate antigens. *Immunol Rev* 2007;215:59-76. doi: 10.1111/j.1600-065X.2006.00479.x [published Online First: 2007/02/13]

450. Laplagne C, Ligat L, Foote J, et al. Self-activation of Vgamma9Vdelta2 T cells by exogenous phosphoantigens involves TCR and butyrophilins. *Cell Mol Immunol* 2021;18(8):1861-70. doi: 10.1038/s41423-021-00720-w [published Online First: 2021/06/30]

451. Vavassori S, Kumar A, Wan GS, et al. Butyrophilin 3A1 binds phosphorylated antigens and stimulates human gammadelta T cells. *Nat Immunol* 2013;14(9):908-16. doi: 10.1038/ni.2665 [published Online First: 2013/07/23]

452. Harly C, Guillaume Y, Nedellec S, et al. Key implication of CD277/butyrophilin-3 (BTN3A) in cellular stress sensing by a major human gammadelta T-cell subset. *Blood* 2012;120(11):2269-79. doi: 10.1182/blood-2012-05-430470 [published Online First: 2012/07/07]

453. Belmant C, Espinosa E, Halary F, et al. A chemical basis for selective recognition of nonpeptide antigens by human delta T cells. *FASEB J* 2000;14(12):1669-70. doi: 10.1096/fj.99-0909fje [published Online First: 2000/09/07]

454. Morita CT, Lee HK, Wang H, et al. Structural features of nonpeptide prenyl pyrophosphates that determine their antigenicity for human gamma delta T cells. *J Immunol* 2001;167(1):36-41. doi: 10.4049/jimmunol.167.1.36 [published Online First: 2001/06/22]

455. Kunzmann V, Bauer E, Feurle J, et al. Stimulation of gammadelta T cells by aminobisphosphonates and induction of antiplasma cell activity in multiple myeloma. *Blood* 2000;96(2):384-92. [published Online First: 2000/07/11]

456. Gutman D, Epstein-Barash H, Tsuriel M, et al. Alendronate liposomes for antitumor therapy: activation of gammadelta T cells and inhibition of tumor growth. *Adv Exp Med Biol* 2012;733:165-79. doi: 10.1007/978-94-007-2555-3_16 [published Online First: 2011/11/22]

457. Bai L, Picard D, Anderson B, et al. The majority of CD1d-sulfatide-specific T cells in human blood use a semiinvariant Vdelta1 TCR. *Eur J Immunol* 2012;42(9):2505-10. doi: 10.1002/eji.201242531 [published Online First: 2012/07/26]

458. Luoma AM, Castro CD, Mayassi T, et al. Crystal structure of Vdelta1 T cell receptor in complex with CD1d-sulfatide shows MHC-like recognition of a self-lipid by human gammadelta T cells. *Immunity* 2013;39(6):1032-42. doi: 10.1016/j.immuni.2013.11.001 [published Online First: 2013/11/19]

459. Parker ME, Ciofani M. Regulation of gammadelta T Cell Effector Diversification in the Thymus. *Front Immunol* 2020;11:42. doi: 10.3389/fimmu.2020.00042 [published Online First: 2020/02/11]

460. Michie AM, Zuniga-Pflucker JC. Regulation of thymocyte differentiation: pre-TCR signals and beta-selection. *Semin Immunol* 2002;14(5):311-23. doi: 10.1016/s1044-5323(02)00064-7 [published Online First: 2002/09/11]

461. Fahl SP, Coffey F, Wiest DL. Origins of gammadelta T cell effector subsets: a riddle wrapped in an enigma. *J Immunol* 2014;193(9):4289-94. doi: 10.4049/jimmunol.1401813 [published Online First: 2014/10/19]

462. Livak F, Tourigny M, Schatz DG, et al. Characterization of TCR gene rearrangements during adult murine T cell development. *J Immunol* 1999;162(5):2575-80. [published Online First: 1999/03/11]

463. Muro R, Takayanagi H, Nitta T. T cell receptor signaling for gammadeltaT cell development. *Inflamm Regen* 2019;39:6. doi: 10.1186/s41232-019-0095-z [published Online First: 2019/04/13]

464. Fehling HJ, Krotkova A, Saint-Ruf C, et al. Crucial role of the pre-T-cell receptor alpha gene in development of alpha beta but not gamma delta T cells. *Nature* 1995;375(6534):795-8. doi: 10.1038/375795a0 [published Online First: 1995/06/29]

465. Pang SS, Berry R, Chen Z, et al. The structural basis for autonomous dimerization of the pre-T-cell antigen receptor. *Nature* 2010;467(7317):844-8. doi: 10.1038/nature09448 [published Online First: 2010/10/15]

466. Carpenter AC, Bosselut R. Decision checkpoints in the thymus. *Nat Immunol* 2010;11(8):666-73. doi: 10.1038/ni.1887 [published Online First: 2010/07/21]

467. Mombaerts P, Clarke AR, Rudnicki MA, et al. Mutations in T-cell antigen receptor genes alpha and beta block thymocyte development at different stages. *Nature* 1992;360(6401):225-31. doi: 10.1038/360225a0 [published Online First: 1992/11/19]

468. Qi C, Wang Y, Li P, et al. Gamma Delta T Cells and Their Pathogenic Role in Psoriasis. *Front Immunol* 2021;12:627139. doi: 10.3389/fimmu.2021.627139 [published Online First: 2021/03/19]

469. Munoz-Ruiz M, Sumaria N, Pennington DJ, et al. Thymic Determinants of gammadelta T Cell Differentiation. *Trends Immunol* 2017;38(5):336-44. doi: 10.1016/j.it.2017.01.007 [published Online First: 2017/03/14]

470. Hayes SM, Li L, Love PE. TCR signal strength influences alphabeta/gammadelta lineage fate. *Immunity* 2005;22(5):583-93. doi: 10.1016/j.immuni.2005.03.014 [published Online First: 2005/05/17]

471. Haks MC, Lefebvre JM, Lauritsen JP, et al. Attenuation of gammadeltaTCR signaling efficiently diverts thymocytes to the alphabeta lineage. *Immunity* 2005;22(5):595-606. doi: 10.1016/j.immuni.2005.04.003 [published Online First: 2005/05/17]

472. Kreslavsky T, Garbe AI, Krueger A, et al. T cell receptor-instructed alphabeta versus gammadelta lineage commitment revealed by single-cell analysis. *J Exp Med* 2008;205(5):1173-86. doi: 10.1084/jem.20072425 [published Online First: 2008/04/30]

473. Zarin P, Wong GW, Mohtashami M, et al. Enforcement of gammadelta-lineage commitment by the pre-T-cell receptor in precursors with weak gammadelta-TCR signals. *Proc Natl Acad Sci U S A* 2014;111(15):5658-63. doi: 10.1073/pnas.1312872111 [published Online First: 2014/04/08]

474. Lauritsen JP, Wong GW, Lee SY, et al. Marked induction of the helix-loop-helix protein Id3 promotes the gammadelta T cell fate and renders their functional maturation Notch independent. *Immunity* 2009;31(4):565-75. doi: 10.1016/j.immuni.2009.07.010 [published Online First: 2009/10/17]

475. Kang J, Volkmann A, Raulet DH. Evidence that gammadelta versus alphabeta T cell fate determination is initiated independently of T cell receptor signaling. *J Exp Med* 2001;193(6):689-98. doi: 10.1084/jem.193.6.689 [published Online First: 2001/03/21]

476. Melichar HJ, Narayan K, Der SD, et al. Regulation of gammadelta versus alphabeta T lymphocyte differentiation by the transcription factor SOX13. *Science* 2007;315(5809):230-3. doi: 10.1126/science.1135344 [published Online First: 2007/01/16]

477. Gray EE, Ramirez-Valle F, Xu Y, et al. Deficiency in IL-17-committed Vgamma4(+) gammadelta T cells in a spontaneous Sox13-mutant CD45.1(+) congenic mouse substrain provides protection from dermatitis. *Nat Immunol* 2013;14(6):584-92. doi: 10.1038/ni.2585 [published Online First: 2013/04/30]

478. Kang J, Coles M, Raulet DH. Defective development of gamma/delta T cells in interleukin 7 receptor-deficient mice is due to impaired expression of T cell receptor gamma genes. *J Exp Med* 1999;190(7):973-82. doi: 10.1084/jem.190.7.973 [published Online First: 1999/10/06]

479. Carding SR, Egan PJ. Gammadelta T cells: functional plasticity and heterogeneity. *Nat Rev Immunol* 2002;2(5):336-45. doi: 10.1038/nri797 [published Online First: 2002/05/30]

480. Hayday AC. gammadelta T Cell Update: Adaptate Orchestrators of Immune Surveillance. *J Immunol* 2019;203(2):311-20. doi: 10.4049/jimmunol.1800934 [published Online First: 2019/07/10]

481. Ribot JC, Lopes N, Silva-Santos B. gammadelta T cells in tissue physiology and surveillance. *Nat Rev Immunol* 2021;21(4):221-32. doi: 10.1038/s41577-020-00452-4 [published Online First: 2020/10/16]

482. Prinz I, Silva-Santos B, Pennington DJ. Functional development of gammadelta T cells. *Eur J Immunol* 2013;43(8):1988-94. doi: 10.1002/eji.201343759 [published Online First: 2013/08/10]

483. Hayday A, Gibbons D. Brokering the peace: the origin of intestinal T cells. *Mucosal Immunol* 2008;1(3):172-4. doi: 10.1038/mi.2008.8 [published Online First: 2008/12/17]

484. Carding SR, Kyes S, Jenkinson EJ, et al. Developmentally regulated fetal thymic and extrathymic T-cell receptor gamma delta gene expression. *Genes Dev* 1990;4(8):1304-15. doi: 10.1101/gad.4.8.1304 [published Online First: 1990/08/01]

485. Itohara S, Farr AG, Lafaille JJ, et al. Homing of a gamma delta thymocyte subset with homogeneous T-cell receptors to mucosal epithelia. *Nature* 1990;343(6260):754-7. doi: 10.1038/343754a0 [published Online First: 1990/02/22]

486. Havran WL, Jameson JM. Epidermal T cells and wound healing. *J Immunol* 2010;184(10):5423-8. doi: 10.4049/jimmunol.0902733 [published Online First: 2010/05/21]

487. Boismenu R, Feng L, Xia YY, et al. Chemokine expression by intraepithelial gamma delta T cells. Implications for the recruitment of inflammatory cells to damaged epithelia. *J Immunol* 1996;157(3):985-92. [published Online First: 1996/08/01]

488. Turchinovich G, Hayday AC. Skint-1 identifies a common molecular mechanism for the development of interferon-gamma-secreting versus interleukin-17-secreting gammadelta T cells. *Immunity* 2011;35(1):59-68. doi: 10.1016/j.immuni.2011.04.018 [published Online First: 2011/07/09]

489. Nielsen MM, Lovato P, MacLeod AS, et al. IL-1beta-dependent activation of dendritic epidermal T cells in contact hypersensitivity. *J Immunol* 2014;192(7):2975-83. doi: 10.4049/jimmunol.1301689 [published Online First: 2014/03/07]

490. Hatano S, Tun X, Noguchi N, et al. Development of a new monoclonal antibody specific to mouse Vgamma6 chain. *Life Sci Alliance* 2019;2(3) doi: 10.26508/lsa.201900363 [published Online First: 2019/05/09]

491. Paget C, Chow MT, Gherardin NA, et al. CD3bright signals on gammadelta T cells identify IL-17A-producing Vgamma6Vdelta1+ T cells. *Immunol Cell Biol* 2015;93(2):198-212. doi: 10.1038/icb.2014.94 [published Online First: 2014/11/12]

492. Simonian PL, Wehrmann F, Roark CL, et al. gammadelta T cells protect against lung fibrosis via IL-22. *J Exp Med* 2010;207(10):2239-53. doi: 10.1084/jem.20100061 [published Online First: 2010/09/22]

493. Kohlgruber AC, Gal-Oz ST, LaMarche NM, et al. gammadelta T cells producing interleukin-17A regulate adipose regulatory T cell homeostasis and thermogenesis. *Nat Immunol* 2018;19(5):464-74. doi: 10.1038/s41590-018-0094-2 [published Online First: 2018/04/20]

494. Hu B, Jin C, Zeng X, et al. gammadelta T cells and adipocyte IL-17RC control fat innervation and thermogenesis. *Nature* 2020;578(7796):610-14. doi: 10.1038/s41586-020-2028-z [published Online First: 2020/02/23]

495. Fiala GJ, Gomes AQ, Silva-Santos B. From thymus to periphery: Molecular basis of effector gammadelta-T cell differentiation. *Immunol Rev* 2020;298(1):47-60. doi: 10.1111/imr.12918 [published Online First: 2020/11/17]

496. Pereira P, Berthault C, Burlen-Defranoux O, et al. Critical role of TCR specificity in the development of Vgamma1Vdelta6.3+ innate NKTgammadelta cells. *J Immunol* 2013;191(4):1716-23. doi: 10.4049/jimmunol.1203168 [published Online First: 2013/07/16]

497. Wan F, Yan K, Xu D, et al. Vgamma1(+)gammadeltaT, early cardiac infiltrated innate population dominantly producing IL-4, protect mice against CVB3 myocarditis by modulating IFNgamma(+) T response. *Mol Immunol* 2017;81:16-25. doi: 10.1016/j.molimm.2016.11.006 [published Online First: 2016/11/26]

498. Dong P, Zhang S, Cai M, et al. Global characterization of differential gene expression profiles in mouse Vgamma1+ and Vgamma4+ gammadelta T cells. *PLoS One* 2014;9(11):e112964. doi: 10.1371/journal.pone.0112964 [published Online First: 2014/11/19]

499. Zheng L, Hu Y, Wang Y, et al. Recruitment of Neutrophils Mediated by Vgamma2 gammadelta T Cells Deteriorates Liver Fibrosis Induced by Schistosoma japonicum Infection in C57BL/6 Mice. *Infect Immun* 2017;85(8) doi: 10.1128/IAI.01020-16 [published Online First: 2017/05/17]

500. Spidale NA, Sylvia K, Narayan K, et al. Interleukin-17-Producing gammadelta T Cells Originate from SOX13(+) Progenitors that Are Independent of gammadeltaTCR Signaling. *Immunity* 2018;49(5):857-72 e5. doi: 10.1016/j.immuni.2018.09.010 [published Online First: 2018/11/11]

501. Murphy AG, O'Keeffe KM, Lalor SJ, et al. Staphylococcus aureus infection of mice expands a population of memory gammadelta T cells that are protective against subsequent infection. *J Immunol* 2014;192(8):3697-708. doi: 10.4049/jimmunol.1303420 [published Online First: 2014/03/14]

502. Shibata K, Yamada H, Nakamura M, et al. IFN-gamma-producing and IL-17-producing gammadelta T cells differentiate at distinct developmental stages in murine fetal thymus. *J Immunol* 2014;192(5):2210-8. doi: 10.4049/jimmunol.1302145 [published Online First: 2014/02/04]

503. Haas JD, Gonzalez FH, Schmitz S, et al. CCR6 and NK1.1 distinguish between IL-17A and IFN-gamma-producing gammadelta effector T cells. *Eur J Immunol* 2009;39(12):3488-97. doi: 10.1002/eji.200939922 [published Online First: 2009/10/16]

504. Sumaria N, Grandjean CL, Silva-Santos B, et al. Strong TCRgammadelta Signaling Prohibits Thymic Development of IL-17A-Secreting gammadelta T Cells. *Cell Rep* 2017;19(12):2469-76. doi: 10.1016/j.celrep.2017.05.071 [published Online First: 2017/06/22]

505. Buus TB, Odum N, Geisler C, et al. Three distinct developmental pathways for adaptive and two IFN-gamma-producing gammadelta T subsets in adult thymus. *Nat Commun* 2017;8(1):1911. doi: 10.1038/s41467-017-01963-w [published Online First: 2017/12/06]

506. Vantourout P, Hayday A. Six-of-the-best: unique contributions of gammadelta T cells to immunology. *Nat Rev Immunol* 2013;13(2):88-100. doi: 10.1038/nri3384 [published Online First: 2013/01/26]

507. Lombes A, Durand A, Charvet C, et al. Adaptive Immune-like gamma/delta T Lymphocytes Share Many Common Features with Their alpha/beta T Cell Counterparts. *J Immunol* 2015;195(4):1449-58. doi: 10.4049/jimmunol.1500375 [published Online First: 2015/07/01]

508. Haas JD, Ravens S, Duber S, et al. Development of interleukin-17-producing gammadelta T cells is restricted to a functional embryonic wave. *Immunity* 2012;37(1):48-59. doi: 10.1016/j.immuni.2012.06.003 [published Online First: 2012/07/10]

509. Pantelyushin S, Haak S, Ingold B, et al. Rorgammat+ innate lymphocytes and gammadelta T cells initiate psoriasiform plaque formation in mice. *J Clin Invest* 2012;122(6):2252-6. doi: 10.1172/JCI61862 [published Online First: 2012/05/02]

510. Papotto PH, Ribot JC, Silva-Santos B. IL-17(+) gammadelta T cells as kick-starters of inflammation. *Nat Immunol* 2017;18(6):604-11. doi: 10.1038/ni.3726 [published Online First: 2017/05/19]

511. Cai Y, Xue F, Fleming C, et al. Differential developmental requirement and peripheral regulation for dermal Vgamma4 and Vgamma6T17 cells in health and inflammation. *Nat Commun* 2014;5:3986. doi: 10.1038/ncomms4986 [published Online First: 2014/06/10]

512. Cai Y, Shen X, Ding C, et al. Pivotal role of dermal IL-17-producing gammadelta T cells in skin inflammation. *Immunity* 2011;35(4):596-610. doi: 10.1016/j.immuni.2011.08.001 [published Online First: 2011/10/11]

513. Pinget GV, Corpuz TM, Stolp J, et al. The majority of murine gammadelta T cells at the maternal-fetal interface in pregnancy produce IL-17. *Immunol Cell Biol* 2016;94(7):623-30. doi: 10.1038/icb.2016.48 [published Online First: 2016/06/01]

514. Gomez-Lopez N, StLouis D, Lehr MA, et al. Immune cells in term and preterm labor. *Cell Mol Immunol* 2014;11(6):571-81. doi: 10.1038/cmi.2014.46 [published Online First: 2014/06/24]

515. Nakasone C, Yamamoto N, Nakamatsu M, et al. Accumulation of gamma/delta T cells in the lungs and their roles in neutrophil-mediated host defense against pneumococcal infection. *Microbes Infect* 2007;9(3):251-8. doi: 10.1016/j.micinf.2006.11.015 [published Online First: 2007/02/20]

516. Lockhart E, Green AM, Flynn JL. IL-17 production is dominated by gammadelta T cells rather than CD4 T cells during Mycobacterium tuberculosis infection. *J Immunol* 2006;177(7):4662-9. doi: 10.4049/jimmunol.177.7.4662 [published Online First: 2006/09/20]

517. Misiak A, Wilk MM, Raverdeau M, et al. IL-17-Producing Innate and Pathogen-Specific Tissue Resident Memory gammadelta T Cells Expand in the Lungs of Bordetella pertussis-

Infected Mice. *J Immunol* 2017;198(1):363-74. doi: 10.4049/jimmunol.1601024 [published Online First: 2016/11/20]

518. Olivares-Villagomez D, Van Kaer L. Intestinal Intraepithelial Lymphocytes: Sentinels of the Mucosal Barrier. *Trends Immunol* 2018;39(4):264-75. doi: 10.1016/j.it.2017.11.003 [published Online First: 2017/12/10]
519. Shires J, Theodoridis E, Hayday AC. Biological insights into TCRgammadelta+ and TCRalphabeta+ intraepithelial lymphocytes provided by serial analysis of gene expression (SAGE). *Immunity* 2001;15(3):419-34. doi: 10.1016/s1074-7613(01)00192-3 [published Online First: 2001/09/25]
520. Ismail AS, Severson KM, Vaishnava S, et al. Gammadelta intraepithelial lymphocytes are essential mediators of host-microbial homeostasis at the intestinal mucosal surface. *Proc Natl Acad Sci U S A* 2011;108(21):8743-8. doi: 10.1073/pnas.1019574108 [published Online First: 2011/05/11]
521. Fichtner AS, Ravens S, Prinz I. Human gammadelta TCR Repertoires in Health and Disease. *Cells* 2020;9(4) doi: 10.3390/cells9040800 [published Online First: 2020/04/01]
522. Davey MS, Willcox CR, Joyce SP, et al. Clonal selection in the human Vdelta1 T cell repertoire indicates gammadelta TCR-dependent adaptive immune surveillance. *Nat Commun* 2017;8:14760. doi: 10.1038/ncomms14760 [published Online First: 2017/03/02]
523. Mao Y, Yin S, Zhang J, et al. A new effect of IL-4 on human gammadelta T cells: promoting regulatory Vdelta1 T cells via IL-10 production and inhibiting function of Vdelta2 T cells. *Cell Mol Immunol* 2016;13(2):217-28. doi: 10.1038/cmi.2015.07 [published Online First: 2015/05/06]
524. Singh AK, Novakova L, Axelsson M, et al. High Interferon-gamma Uniquely in Vdelta1 T Cells Correlates with Markers of Inflammation and Axonal Damage in Early Multiple Sclerosis. *Front Immunol* 2017;8:260. doi: 10.3389/fimmu.2017.00260 [published Online First: 2017/03/25]
525. Dunne PJ, Maher CO, Freeley M, et al. CD3epsilon Expression Defines Functionally Distinct Subsets of Vdelta1 T Cells in Patients With Human Immunodeficiency Virus Infection. *Front Immunol* 2018;9:940. doi: 10.3389/fimmu.2018.00940 [published Online First: 2018/05/18]

526. Hviid L, Smith-Togobo C, Willcox BE. Human Vdelta1(+) T Cells in the Immune Response to Plasmodium falciparum Infection. *Front Immunol* 2019;10:259. doi: 10.3389/fimmu.2019.00259 [published Online First: 2019/03/07]

527. Lo Presti E, Di Mitri R, Mocciaro F, et al. Characterization of gammadelta T Cells in Intestinal Mucosa From Patients With Early-Onset or Long-Standing Inflammatory Bowel Disease and Their Correlation With Clinical Status. *J Crohns Colitis* 2019;13(7):873-83. doi: 10.1093/ecco-jcc/jjz015 [published Online First: 2019/01/29]

528. Dimova T, Brouwer M, Gosselin F, et al. Effector Vgamma9Vdelta2 T cells dominate the human fetal gammadelta T-cell repertoire. *Proc Natl Acad Sci U S A* 2015;112(6):E556-65. doi: 10.1073/pnas.1412058112 [published Online First: 2015/01/27]

529. Davey MS, Willcox CR, Hunter S, et al. The human Vdelta2(+) T-cell compartment comprises distinct innate-like Vgamma9(+) and adaptive Vgamma9(-) subsets. *Nat Commun* 2018;9(1):1760. doi: 10.1038/s41467-018-04076-0 [published Online First: 2018/05/04]

530. Dieli F, Poccia F, Lipp M, et al. Differentiation of effector/memory Vdelta2 T cells and migratory routes in lymph nodes or inflammatory sites. *J Exp Med* 2003;198(3):391-7. doi: 10.1084/jem.20030235 [published Online First: 2003/08/06]

531. Wang H, Sarikonda G, Puan KJ, et al. Indirect stimulation of human Vgamma2Vdelta2 T cells through alterations in isoprenoid metabolism. *J Immunol* 2011;187(10):5099-113. doi: 10.4049/jimmunol.1002697 [published Online First: 2011/10/21]

532. Hintz M, Reichenberg A, Altincicek B, et al. Identification of (E)-4-hydroxy-3-methyl-but-2-enyl pyrophosphate as a major activator for human gammadelta T cells in Escherichia coli. *FEBS Lett* 2001;509(2):317-22. doi: 10.1016/s0014-5793(01)03191-x [published Online First: 2001/12/14]

533. Moens E, Brouwer M, Dimova T, et al. IL-23R and TCR signaling drives the generation of neonatal Vgamma9Vdelta2 T cells expressing high levels of cytotoxic mediators and producing IFN-gamma and IL-17. *J Leukoc Biol* 2011;89(5):743-52. doi: 10.1189/jlb.0910501 [published Online First: 2011/02/19]

534. Mangan BA, Dunne MR, O'Reilly VP, et al. Cutting edge: CD1d restriction and Th1/Th2/Th17 cytokine secretion by human Vdelta3 T cells. *J Immunol* 2013;191(1):30-4. doi: 10.4049/jimmunol.1300121 [published Online First: 2013/06/07]

535. Petrasca A, Melo AM, Breen EP, et al. Human Vdelta3(+) gammadelta T cells induce maturation and IgM secretion by B cells. *Immunol Lett* 2018;196:126-34. doi: 10.1016/j.imlet.2018.02.002 [published Online First: 2018/02/14]

536. Foster B, Prussin C, Liu F, et al. Detection of intracellular cytokines by flow cytometry. *Curr Protoc Immunol* 2007;Chapter 6:Unit 6 24. doi: 10.1002/0471142735.im0624s78 [published Online First: 2008/04/25]

537. Leibovitz E, Ebrahimian T, Paradis P, et al. Aldosterone induces arterial stiffness in absence of oxidative stress and endothelial dysfunction. *J Hypertens* 2009;27(11):2192-200. doi: 10.1097/HJH.0b013e328330a963 [published Online First: 2009/08/06]

538. Roach MR, Burton AC. The reason for the shape of the distensibility curves of arteries. *Can J Biochem Physiol* 1957;35(8):681-90. [published Online First: 1957/08/01]

539. Neves MF, Endemann D, Amiri F, et al. Small artery mechanics in hyperhomocysteinemic mice: effects of angiotensin II. *J Hypertens* 2004;22(5):959-66. doi: 10.1097/00004872-200405000-00018 [published Online First: 2004/04/21]

540. Wang Y, Thatcher SE, Cassis LA. Blood Pressure Monitoring Using Radio Telemetry Method in Mice. *Methods Mol Biol* 2017;1614:75-85. doi: 10.1007/978-1-4939-7030-8_7 [published Online First: 2017/05/14]

541. Roark CL, Aydintug MK, Lewis J, et al. Subset-specific, uniform activation among V gamma 6/V delta 1+ gamma delta T cells elicited by inflammation. *J Leukoc Biol* 2004;75(1):68-75. doi: 10.1189/jlb.0703326 [published Online First: 2003/10/04]

542. Grigoriadou K, Boucontet L, Pereira P. T cell receptor-gamma allele-specific selection of V gamma 1/V delta 4 cells in the intestinal epithelium. *J Immunol* 2002;169(7):3736-43. doi: 10.4049/jimmunol.169.7.3736 [published Online First: 2002/09/24]

543. Saleh MA, Norlander AE, Madhur MS. Inhibition of Interleukin 17-A but not Interleukin-17F Signaling Lowers Blood Pressure and Reduces End-organ Inflammation in Angiotensin II-induced Hypertension. *JACC Basic Transl Sci* 2016;1(7):606-16. doi: 10.1016/j.jacbts.2016.07.009 [published Online First: 2017/03/11]

544. Han YL, Li YL, Jia LX, et al. Reciprocal interaction between macrophages and T cells stimulates IFN-gamma and MCP-1 production in Ang II-induced cardiac inflammation and fibrosis. *PLoS One* 2012;7(5):e35506. doi: 10.1371/journal.pone.0035506 [published Online First: 2012/05/09]

545. Marko L, Kvakan H, Park JK, et al. Interferon-gamma signaling inhibition ameliorates angiotensin II-induced cardiac damage. *Hypertension* 2012;60(6):1430-6. doi: 10.1161/HYPERTENSIONAHA.112.199265 [published Online First: 2012/10/31]

546. Kamat NV, Thabet SR, Xiao L, et al. Renal transporter activation during angiotensin-II hypertension is blunted in interferon-gamma-/- and interleukin-17A-/- mice. *Hypertension* 2015;65(3):569-76. doi: 10.1161/HYPERTENSIONAHA.114.04975 [published Online First: 2015/01/21]

547. Mikolajczyk TP, Nosalski R, Szczepaniak P, et al. Role of chemokine RANTES in the regulation of perivascular inflammation, T-cell accumulation, and vascular dysfunction in hypertension. *FASEB J* 2016;30(5):1987-99. doi: 10.1096/fj.201500088R [published Online First: 2016/02/14]

548. Huber SA, Born W, O'Brien R. Dual functions of murine gammadelta cells in inflammation and autoimmunity in coxsackievirus B3-induced myocarditis: role of Vgamma1+ and Vgamma4+ cells. *Microbes Infect* 2005;7(3):537-43. doi: 10.1016/j.micinf.2004.12.011 [published Online First: 2005/03/22]

549. Mehta P, Nuotio-Antar AM, Smith CW. gammadelta T cells promote inflammation and insulin resistance during high fat diet-induced obesity in mice. *J Leukoc Biol* 2015;97(1):121-34. doi: 10.1189/jlb.3A0414-211RR [published Online First: 2014/11/15]